

**Antitumor Activities of Ergosterol Peroxide and 9,11-
dehydroergosterol Peroxide from *Ganoderma lucidum*
Mycelia**

ZHENG Lin

**A Thesis Submitted in Partial Fulfillment
of the Requirements for the Degree of
Doctor of Philosophy
in
Biology**

March 2009

UMI Number: 3392267

All rights reserved

INFORMATION TO ALL USERS

The quality of this reproduction is dependent upon the quality of the copy submitted.

In the unlikely event that the author did not send a complete manuscript and there are missing pages, these will be noted. Also, if material had to be removed, a note will indicate the deletion.



UMI 3392267

Copyright 2010 by ProQuest LLC.

All rights reserved. This edition of the work is protected against unauthorized copying under Title 17, United States Code.



ProQuest LLC
789 East Eisenhower Parkway
P.O. Box 1346
Ann Arbor, MI 48106-1346

Thesis/Assessment Committee

Professor Peter Chi Keung Cheung (Chair)

Professor Yum Shing Wong (Supervisor)

Professor Anthony Hau Yin Chung (Committee Member)

Professor Nai Ki Mak (External Examiner)

Abstract

Ganoderma lucidum is one of most popular medicinal mushrooms in oriental countries. The medicinal properties of *Ganoderma lucidum* in the treatment of various diseases have been documented for hundreds of years. In recent years, more and more attentions are paid on the studies of the action mechanisms of bioactive compounds purified from this mushroom.

Triterpenes and steroids are two important classes of *Ganoderma lucidum* metabolites of low molecular mass that are responsible for the antitumor activities of the mushroom. In this study, two fungal steroids, namely, 5 α ,8 α -epidioxy-22*E*-ergosta-6,22-dien-3 β -ol (ergosterol peroxide (EP)) and 5 α ,8 α -epidioxy-22*E*-ergosta-6,9(11),22-trien-3 β -ol (9,11-dehydroergosterol peroxide (9(11)-DHEP)) were purified from the mycelia of *Ganoderma lucidum* grown under submerged culture using activity-guided purification procedures against human breast adenocarcinoma MCF-7 cells. In addition to MCF-7 cells, both of these two fungal steroids showed antiproliferative activities against other human cancer cells including hepatocellular carcinoma HepG2 cells, colorectal carcinoma Colo201 cells, esophageal squamous carcinoma KYSE cells and malignant melanoma A375 cells. However, EP and 9(11)-DHEP were less toxic to MCF-10-2A, non-tumorigenic human epithelial cells, and the normal human skin fibroblast Hs68 cells.

The antiproliferative activities of EP and 9(11)-DHEP were studied by flow cytometry. Exposure of cancer cells with these two fungal steroids resulted in an accumulation of cell population at the subG1 phase in a dosage- and time-dependent manner, indicating the induction of apoptotic cell death. Morphological apoptotic changes in HepG2 cells and A375 cells were observed using TUNEL assay and Annexin-V-FLUOS assay. The signaling pathway in apoptotic cell death induced by



EP and 9(11)-DHEP involved the activation of caspase 3, 7 and 9, followed by the cleavage of PARP. In Colo201 cells, a change in the ratio of expression levels of Bcl-2/Bax was observed in cells treated with EP and 9(11)-DHEP. In A375 cells, exposure to EP and 9(11)-DHEP resulted in the release of mitochondrial cytochrome *c*, the down-regulation of Mcl-1 and a slight up-regulation of Bak in a dosage-dependent manner. All these results indicated that apoptotic cell death in susceptible cancer cells induced by EP and 9(11)-DHEP was via the mitochondria-mediated pathway.

The *in vivo* antitumor activity of EP was demonstrated. EP was shown to suppress the growth of A375 cells in a nude mice xenograft model. Further studies showed that EP induced the cleavage of PARP and enhanced the total caspase 7 gene expression in the tumor cells.

In conclusion, the *Ganoderma* steroids EP and 9(11)-DHEP can induce caspase-dependent apoptosis in susceptible cancer cells via the mitochondria-mediated pathway. *In vitro* and *in vivo* studies suggested that these two fungal steroids have the potential to be used as natural chemopreventive agents.

Keywords: Ergosterol peroxide, 9(11)-dehydroergosterol peroxide, *Ganoderma lucidum*, Mycelia, Antitumor activity, Apoptosis

中文摘要

靈芝是中國最著名的藥用真菌之一。幾千年的臨床實踐歷史表明它對多種疾病都具有治療效果。近年來從靈芝中提取的各種活性物質的研究應用得到了越來越多的關注。

三萜和甾醇是在靈芝抗癌活性中起重要作用的活性小分子物質。我們從靈芝菌絲體中成功地通過抗癌活性引導提取出了麥角甾醇過氧化物 (ergosterol peroxide) 和 9(11) 脫氫麥角甾醇過氧化物 (9, 11-dehydroergosterol peroxide) 兩個靈芝甾醇。體外實驗結果顯示，這兩個靈芝甾醇對於不同的人癌細胞株都有劑量依賴和時間依賴性的抑制作用。粗篩選的結果顯示兩個靈芝甾醇對人腸癌細胞 Colo201 和人皮膚癌細胞 A375 有極為顯著的抗癌活性。但兩個靈芝甾醇對非癌上皮細胞株 MCF-10-2A 和人皮膚正常纖維細胞株 Hs68 卻沒有顯著毒性。

細胞週期分析顯示兩個靈芝甾醇能將不同癌細胞株都停止在 G1 前期，應用末端轉移酶標記技術 (TUNEL) 和 Annexin-V-FLUOS 法觀察兩個靈芝甾醇對肝癌細胞 HepG2 和皮膚癌細胞 A375 凋亡的影響，結果發現這兩個靈芝甾醇能引起顯著的癌細胞凋亡形態變化。對其凋亡的分子機制研究表明，兩個靈芝甾醇能啟動 caspase 3, 7 和 9 活性，從而導致多聚 ADP 核糖聚合酶 (PARP) 的裂解，引起癌細胞的凋亡。兩個靈芝甾醇能引起腸癌細胞 Colo201 中促凋亡分子 Bax 和抑凋亡分子 Bcl-2 比例的變化；在惡性皮膚癌細胞 A375 中也證實，該靈芝甾醇還能導致細胞色素 c 向細胞質轉移，從而引起 Mcl-1 蛋白表達的下降和 Bak 蛋白表達的略微提高，以上結果顯示該靈芝甾醇引起的細胞凋亡是經線粒體引導通路。

另外，在人皮膚癌細胞 A375 裸鼠體內實驗模型中，麥角甾醇過氧化物能顯著地縮小腫瘤體積，減少腫瘤的重量，抑制率與對照組相比達 52%。進一步的研究表明麥角甾醇過氧化物引起腫瘤中多聚 ADP 核糖聚合酶(PARP)的裂解和總 caspase 7 基因轉錄的提高。

綜上所述，體內外實驗證明麥角甾醇過氧化物和 9(11) 脫氫麥角甾醇過氧化物能誘導線粒體通路引起的 caspase 家族依賴性細胞凋亡，從而有效抑制癌細胞的生長，是有效的抗癌候選化合物。

關鍵字：麥角甾醇過氧化物，9(11) 脫氫麥角甾醇過氧化物，靈芝菌絲體，細胞凋亡

Acknowledgements

I would like to express my sincere gratitude to my supervisor, Prof. Y. S. Wong for his patience, continuing encouragement and elaborate guidance. Besides giving me pinpoint, he is also kind and considerate during my study and research.

I am sincerely grateful to my internal examiners, Prof. Cheung Chi Keung Peter and Prof. Chung Hau Yin Anthony for their invaluable advice and criticisms in my research project and thesis. I am indebted to Prof. Mak Nai Ki of Hong Kong Baptist University, for being my external examiner and for his expert advice.

We are grateful to Dr. Mingfang He of our department for the chemicals purification technique instruction. We thank Dr. Yan Wang of Chinese medicine institution for providing the advice on analysis of mass spectrum. In addition, great thanks are given to Dr. Xin Hong of Medicine Department in the Chinese University of Hong Kong, Dr. Tianfeng Chen of my lab and Dr. Qi Chang, Dr. Jianyong Si of Institute of medicinal plant development Chinese academy of medical sciences& Peking union medical college for their help in identifications of the chemical structures of the two steroids.

I am delighted the help of Ms. Iris Tong for her valuable technical support, assistant and encouragement. Thanks also give to Miss Rita Foo, Mr. Freddie Kwok, Mr. Wilson Lau for their technical support and assistance and Mr. K.H. Man for his assistance in Animal House.

I am deeply thanking my laboratory collaborators including Mr. Enoch Wong, Dr. Qi Chang, Mr. Tianfeng Chen, Ms Karry Nai, Ms Ava Yeung, Ms Natalie Lau, Ms Junyi Xue, Ms Yudong Wang, Ms Daisy Choi, Ms Carrier Kong, Ms Jenny Ho, Ms Tina Wong and Ms Ceci Wong, without their help and encouragement this project could not be completed. Thanks also give to Dr. Lin Liu and Mr. Kai Yao for their kindly assistance. In addition, gratitude is presented to Dr. Yurong Bi for her greatly recommendation.

Finally, special thanks to my parents and good friends for their patient and continuous guidance during my four-year PhD study in Hong Kong.

List of Abbreviations

AIF	apoptosis inducing factor
Akt	protein kinase B
APAF-1	apoptotic protease-activating factor-1
ASG	acylated steryl glycosides
ATP	adenosine triphosphate
BrdU	5-bromo-2'-deoxyuridine
BSA	bovine serum albumin
CAM	chorioallantoic membrane
CBG	cytosolic β -glycosidase
Cdks	cyclin-dependent kinases
CKIs	cdk inhibitors
CLSM	confocal laser scanning microscope
CR3	complement receptor 3
9(11)-DHEP	9(11)-dehydroergosterol peroxide
DEPC	diethyl pyrocarbonate
DMEM	Dulbecco's modified Eagle's medium
DMBA	7,12-dimethylbenz(α)-anthracene
DMSO	dimethylsulfoxide
EA	ethyl acetate
EC ₅₀	50 % effective concentration values
EDTA	ethylenediaminetetraacetic acid
ER	endoplasmic reticulum
ERK	extracellular signal-regulated protein kinase
EP	ergosterol peroxide
FADD	Fas-associated death domain
FAK	focal adhesion kinase
FBS	fetal bovine serum
FGF	fibroblast growth factor
FS	free alcohol
GA	Ganoderic acid
GPCRs	G-protein couple receptors
GPx	glutathione peroxidase
GSH	glutathione
GSSG	oxidized glutathione
GST	glutathione S-transferase
HEPES	N-(2-hydroxyethyl)piperazine-N'-(2-ethansulfonic acid) hemisodium

	salts
HPLC	high performance liquid chromatography
HRP	horseradish peroxidase
IC ₅₀	50% inhibition concentration values
IMM	inner mitochondrial membrane
IMS	intermembrane space
INT	(2-[4-iodophenyl]-3-[4-nitrophenyl]- 5-phenyltetrazoium chloride)
JNK	c-Jun N-terminal kinase
LA	lucidenic acid
LDH	lactate dehydrogenase
LDL	low density lipoprotein
LPH	lactase phloridzin hydrolase
LPO	lipid peroxidation
LPS	lipopolysaccharide
MAPK	mitogen-activated protein kinase
MMP	matrix metalloproteinase
MOMP	mitochondrial outer membrane permeabilization;
MTT	3-(4,5-dimethylthiazol-2-yl)-2,5-diphenyl tetrazolium bromide
NF- κ B	nuclear factor κ B
NK	natural killer
NO	nitric oxide
NOS	nitric oxide synthase
OMM	outer mitochondrial membrane
P _{app}	apparent permeability coefficient
PBL	peripheral blood lymphocytes
PBS	phosphate buffered saline
PE	petroleum ether
PI	propidium iodide
PI3K	phosphatidylinositol 3-kinase
PKC	protein kinase C
PMA	phorbol-12-myristate-13-acetate
POD	peroxidase
PS	phosphatidylserine
PTK	protein tyrosine kinase
PTPC	permeability transition pore complex
ROS	reactive oxygen species
SAPK	stress-activated protein kinases
SAR	structure-activity relationships
SE	fatty-acid esters

SG	steryl glycosides
SOD	superoxide dismutase
TCM	traditional Chinese medicine
TdT	terminal deoxynucleotidyl transferase
TLR4	toll-like receptor 4
TPA	12- <i>O</i> -tetradecanoyl-phorbol-13-acetate
TUNEL	TdT-mediated X-dUTP nick end labeling
UDP	uridine-diphosphate
VEGF	vascular endothelial growth factor

Table of Contents

Abstract	i
中文摘要	iii
Acknowledgement	v
List of Abbreviations	vii
List of Tables	xv
List of Figures	xv
Chapter I General Introduction	1
1.1 Cancer	1
1.2 Medicinal mushroom and cancer	2
1.3 <i>Ganoderma lucidum</i>	3
1.4 Antitumor activities of <i>Ganoderma lucidum</i>	4
1.4.1 <i>Ganoderma</i> peptide and polysaccharide	4
1.4.2 <i>Ganoderma</i> triterpene	7
1.4.2.1 Triterpene	7
1.4.2.2 Biological function of <i>Ganoderma</i> triterpene	8
1.4.2.3 Antitumor activities of <i>Ganoderma</i> triterpene	9
1.4.3 <i>Ganoderma</i> steroid	13
1.4.3.1 Phytosterol	13
1.4.3.2 Biological activities of phytosterol	14
1.4.3.3 Antitumor activities of <i>Ganoderma</i> steroids	15
1.5 Apoptosis	17
1.5.1 Mechanisms of apoptosis	18
1.5.2 Apoptosis components	19
1.5.2.1 Caspase family	19
1.5.2.2 Mitochondria and apoptosis	20
1.5.2.3 Bcl-2 family	20
1.6 Research objectives	22
Chapter II Purification and identification of ergosterol peroxide and 9,11-dehydroergosterol peroxide from <i>Ganoderma lucidum</i> mycelia	

2.1	Introduction	32
2.2	Materials and methods	34
2.2.1	Chemicals and reagents	34
2.2.2	Submerged Culture of <i>Ganoderma lucidum</i>	34
2.2.3	Preliminary screening of antitumor fractions from <i>Ganoderma lucidum</i>	35
2.2.4	The purification of antitumor compounds from <i>Ganoderma lucidum</i> mycelia	35
2.2.5	High performance liquid chromatography (HPLC) analysis	36
2.2.6	Studies on the anti-proliferation activities of crude fractions	37
2.2.6.1	Cell culture	37
2.2.6.2	Sample preparation	38
2.2.6.3	MTT assay	38
2.2.6.4	Determination of 50% effective concentration (IC ₅₀)	39
2.2.6.5	Statistical analysis	39
2.3	Results	41
2.3.1	Preliminary screening of antitumor activities of crude fractions from <i>Ganoderma lucidum</i>	41
2.3.2	Purification and identification of EP and 9(11)-DHEP from <i>Ganoderma lucidum</i> mycelia	41
2.4	Discussion	48
Chapter III <i>In vitro</i> antitumor activities of ergosterol peroxide and 9(11)-dehydroergosterol peroxide from <i>Ganoderma lucidum</i> in different human cancer cell lines		
3.1	Introduction	50
3.2	Materials and methods	53
3.2.1	Chemicals and reagents	53
3.2.2	Sample preparation	54
3.2.3	Cell culture	54
3.2.4	Studies on the anti-proliferation activities of EP and 9(11)-DHEP on different cancer cell lines	55
3.2.4.1	MTT assay	55
3.2.4.2	Cell proliferation ELISA-BrdU (chemiluminescence) assay	55

3.2.4.3	Determination of 50% inhibitory concentration (IC ₅₀)	55
3.2.5	Apoptosis detection	56
3.2.5.1	TUNEL enzymatic labeling assay	56
3.2.5.2	Annexin-V-FLUOS labeling assay	57
3.2.6	Analysis of cell cycle progression by flow cytometry	58
3.2.7	Western immunoblotting and detection	58
3.2.7.1	Preparation of protein lysates	58
3.2.7.2	SDS-polyacrylamide gel (SDS-PAGE)	59
3.2.7.3	Western blot analysis	59
3.2.8	Statistical analysis	60
3.3	Results	61
3.3.1	9(11)-DHEP and EP inhibited the cell proliferation of different cancer cells	61
3.3.2	Flow cytometry analysis on the different cancer cells treated with 9(11)-DHEP and EP	62
3.3.3	Analysis of apoptotic morphology in HepG2 cancer cells treated with 9(11)-DHEP and EP	63
3.3.4	9(11)-DHEP and EP induced apoptosis of Colo201 cancer cells via mitochondria-mediated pathway	64
3.4	Discussion	92
Chapter IV Mechanisms studies on the <i>in vitro</i> and <i>in vivo</i> antitumor activities of ergosterol peroxide and 9(11)-dehydro ergosterol peroxide from <i>Ganoderma lucidum</i> mycelia against human A375 malignant melanoma		
4.1	Introduction	97
4.2	Materials and methods	100
4.2.1	Chemicals and reagents	100
4.2.2	Sample preparation	101
4.2.3	Cell culture	101
4.2.4	Study on the anti-proliferation activities of EP and 9(11)-DHEP on A375 cancer cell line	102
4.2.4.1	MTT assay	102
4.2.4.2	Cell proliferation ELISA-BrdU (chemiluminescence)	102

assay	
4.2.4.3	Determination of 50% inhibitory concentration (IC ₅₀) 102
4.2.5	Cytotoxicity detection 102
4.2.5.1	Lactate dehydrogenase (LDH) assay 102
4.2.5.2	Optimal of cell density for LDH assay 103
4.2.5.3	Detection of LDH activity 104
4.2.5.4	Determination of 50% effective concentration (EC ₅₀) 104
4.2.6	Apoptosis detection 105
4.2.6.1	TUNEL enzymatic labeling assay 105
4.2.6.2	Annexin-V-FLUOS labeling assay 105
4.2.7	Analysis of cell cycle progression by flow cytometry 106
4.2.8	Western immunoblotting and detection 106
4.2.8.1	Preparation of protein lysates 106
4.2.8.2	Preparation of mitochondria-free cytosolic fraction and mitochondria fraction 107
4.2.8.2	Tricine-SDS-polyacrylamide gel (Tricine-SDS-PAGE) 107
4.2.8.3	Western blot analysis 108
4.2.9	<i>In vivo</i> studies on the xenograft mice 108
4.2.9.1	Chemicals and reagents 108
4.2.9.2	Animals 109
4.2.9.3	Analysis of protein expression in the tumor 109
4.2.9.4	Analysis of gene expression in the tumor 110
4.2.10	Statistical analysis 111
4.3	Results 113
4.3.1	9(11)-DHEP and EP inhibited the A375 malignant melanoma cells proliferation 113
4.3.2	The cytotoxicity of 9(11)-DHEP and EP on the A375 malignant melanoma cells and Hs68 normal fibroblast cells 114
4.3.3	Cell cycle analysis on the A375 malignant melanoma cells by flow cytometry 114
4.3.4	Analysis of apoptotic morphology in A375 malignant melanoma cells treated with 9(11)-DHEP and EP 115
4.3.5	9(11)-DHEP and EP induced apoptosis of A375 malignant melanoma cells 116

melanoma cells via mitochondria-mediated pathway	
4.3.6 EP inhibited tumor growth in xenograft tumor-bearing nude mice	117
4.4 Discussion	141
Chapter V Conclusion	147
References	153
Appendix 1. Two dimensions NMR analysis of 9(11)-DHEP: C-H relation in CDCl₃, 500MHz	178
Appendix 2. C-NMR analysis of 9(11)-DHEP in CDCl₃, 500MHz	179
Appendix 3. Two dimensions NMR analysis of 9(11)-DHEP: H-H relation in CDCl₃, 500MHz	180
Appendix 4. H-NMR analysis of 9(11)-DHEP in CDCl₃, 500MHz	181
Appendix 5. DEPT analysis of 9(11)-DHEP in CDCl₃, 500MHz	182
Appendix 6. C-NMR analysis of EP in CDCl₃, 500MHz	183
Appendix 7. H-NMR analysis of EP in CDCl₃, 500MHz	184
Appendix 8. Two dimensions NMR analysis of EP: C-H relation in CDCl₃, 500MHz	185
Appendix 9. Two dimensions NMR analysis of EP: H-H relation in CDCl₃, 500MHz	186
Appendix 10. DEPT analysis of EP in CDCl₃, 500MHz	187
Appendix 11. UV analysis of 9(11)-DHEP and EP in CDCl₃, 500MHz	188
Appendix 12. IR spectrum analysis of 9(11)-DHEP and EP in CDCl₃, 500MHz	189

List of Tables

Table 1.1	Different biological activities of <i>Ganoderma lucidum</i> triterpenes	27
Table 1.2	Anti-proliferation and apoptosis inducing mechanisms of <i>Ganoderma lucidum</i> extracts on cancer cells	28
Table 1.3	Overview of caspases family function	30
Table 2.1	The antitumor activities of different crude extracts of <i>Ganoderma lucidum</i> mycelia and culture medium on MCF-7 cancer cells by MTT assay	43
Table 2.2	The antitumor activities of different fractions purified from chloroform extract of <i>Ganoderma lucidum</i> mycelia on MCF-7 cancer cells by MTT assay	43
Table 2.3	Preliminary antitumor activity screening on different cell lines	44
Table 2.4	¹ H and ¹³ C spectral data of compound A and B isolated from <i>G. lucidum</i> mycelia.	47
Table 3.1	Preliminary antitumor activity screening of 9(11)-DHEP and EP on different cell lines by MTT assay	66
Table 3.2	Anti-proliferation activity screening of 9(11)-DHEP and EP on different cancer cells by BrdU assay	71
Table 4.1	Overview of the experimental setup of cytotoxicity (LDH) assay	112
Table 4.2	The EC ₅₀ values of 9(11)-DHEP and EP on different cell lines after 72hr incubation as determined by LDH assay	122
Table 5.1	Inhibitory effects of EP and 9(11)-DHEP extracted from different mushroom on different cancer cells	151

List of Figures

Figure 1.1	Biosynthesis of triterpenes and phytosterols	25
Figure 1.2	Skeleton structure of <i>Ganoderma</i> triterpenes	26
Figure 1.3	The chemical structure of steroids	29
Figure 1.4	Overview of death receptor-mediated and mitochondria-mediated apoptosis pathway	31
Figure 2.1	The procedure of antitumor substance purification from <i>Ganoderma lucidum</i> mycelia (a) and culture media (b)	40

Figure 2.2	The extraction procedure of major compound detected by HPLC analysis.	45
Figure 2.3	The structure of the two steroids isolated from <i>G lucidum</i> mycelia	46
Figure 3.1	Inhibitory effects of 9(11)-DHEP and EP on HepG2 cancer cells in a time-dependent manner.	67
Figure 3.2	Inhibitory effects of 9(11)-DHEP and EP on Colo201 cancer cells in a time-dependent manner.	68
Figure 3.3	Inhibitory effects of 9(11)-DHEP and EP on SW620 cancer cells in a time-dependent manner.	69
Figure 3.4	Inhibitory effects of 9(11)-DHEP and EP on KYSE cancer cells in a time-dependent manner.	70
Figure 3.5	Inhibitory effects of 9(11)-DHEP and EP on different cancer cells in a dosage-dependent manner by BrdU assay.	72
Figure 3.6	Effects of 9(11)-DHEP and EP treatment on the morphological changes of MCF-7 cells.	73
Figure 3.7	Fluorescence-activated cell sorting analysis of MCF-7 cancer cells after 72hr treatment with 9(11)-DHEP and EP at different concentration.	74
Figure 3.8	Effects of 9(11)-DHEP and EP treatment on the morphological changes of HepG2 cells.	75
Figure 3.9	Fluorescence-activated cell sorting analysis of HepG2 cancer cells after 72hr treatment with 9(11)-DHEP and EP at different concentration.	76
Figure 3.10	Effects of 20ug/ml 9(11)-DHEP (a) or EP (b) on cell cycle phase distribution in HepG ₂ cancer cells at different incubation times.	77
Figure 3.11	Effects of 9(11)-DHEP and EP treatment on the morphological changes of Colo201 cells.	78
Figure 3.12	Fluorescence-activated cell sorting analysis of Colo201 cancer cells after 72hr treatment with 9(11)-DHEP and EP at different concentration.	79
Figure 3.13	Effects of 20ug/ml 9(11)-DHEP (a) or EP (b) on cell cycle phase distribution in Colo201 cancer cells at different incubation times.	80
Figure 3.14	Effects of 9(11)-DHEP and EP treatment on the morphological changes of KYSE cells.	81

Figure 3.15	Fluorescence-activated cell sorting analysis of KYSE cancer cells after 72hr treatment with 9(11)-DHEP and EP at different concentration.	82
Figure 3.16	Effects of 20ug/ml 9(11)-DHEP (a) or EP (b) on cell cycle phase distribution in KYSE cancer cells at different incubation times.	83
Figure 3.17	Effects of 9(11)-DHEP and EP on HepG2 cancer cells by confocal laser scanning microscope using TUNEL assay.	84
Figure 3.18	Effects of 9(11)-DHEP on HepG2 cancer cells by confocal laser scanning microscope after staining with Annexin-V-FLUOS and propidium iodide.	85
Figure 3.19	Effects of EP on HepG2 cancer cells by confocal laser scanning microscope after staining with Annexin-V-FLUOS and propidium iodide.	86
Figure 3.20	Dose-dependent effects of 9(11)-DHEP and EP on Colo201 cancer cells by Western blotting analysis using cleaved PARP(Asp214) antibody (human specific) 89Kb.	87
Figure 3.21	Dose-dependent effects of 9(11)-DHEP and EP on Colo201 cancer cells by Western blotting analysis using cleaved caspase 3 antibody, cleaved caspase 7 antibody (human specific), cleaved caspase 6, caspase 9, caspase 8.	87
Figure 3.22	Dose-dependent effects of 9(11)-DHEP and EP on Colo201 cancer cells by Western blotting analysis using Bad, Bax, Bak, Puma, Mcl-1, Bcl-2 and Bcl-xl antibodies.	88
Figure 3.23	Dose-dependent effects of 9(11)-DHEP and EP on Bax/Bcl-2 expression in Colo201 cancer cells.	89
Figure 3.24	Dose-dependent effects of 9(11)-DHEP and EP on Bax/Bcl-2 expression ratio in Colo201 cancer cells.	90
Figure 3.25	Dose-dependent effects of 9(11)-DHEP and EP on Mcl-1 expression in Colo201 cancer cells.	90
Figure 3.26	Dose-dependent effects of 9(11)-DHEP and EP on Puma expression in Colo201 cancer cells.	91

Figure 3.27	Mitochondria-mediated apoptosis induced by 9(11)-DHEP and EP in Colo201 cancer cells	96
Figure 4.1	The chemical structure of natural triterpenes	99
Figure 4.2	Inhibitory activities of different natural compounds on A375 malignant melanoma cells growth.	119
Figure 4.3	Inhibitory effects of natural compounds on A375 malignant melanoma cells in a time-dependent manner.	120
Figure 4.4	Inhibitory effects of 9(11)-DHEP and EP on A375 malignant melanoma cells in a dosage-dependent manner by BrdU assay.	121
Figure 4.5	The cytotoxicity of 9(11)-DHEP and EP on different cells as determined by LDH assay after 72h incubation.	123
Figure 4.6	Effects of 9(11)-DHEP and EP treatment on the morphological changes of A375 cells.	124
Figure 4.7	Fluorescence-activated cell sorting analysis of A375 malignant melanoma cells after 72hr treatment with 9(11)-DHEP and EP at different concentration.	125
Figure 4.8	Effects of 20ug/ml 9(11)-DHEP and EP on cell cycle phase distribution in A375 cancer cells at different incubation times.	126
Figure 4.9	Fluorescence-activated cell sorting analysis of A375 malignant melanoma cells after 72hr treatment with natural triterpenes at different concentration.	127
Figure 4.10	Effects of 9(11)-DHEP and EP on A375 malignant melanoma cells by confocal laser scanning microscopy using TUNEL assay.	128
Figure 4.11	Effects of 9(11)-DHEP on A375 malignant melanoma cells by confocal laser scanning microscopy after staining with Annexin-V-FLOUS and propidium iodide.	129
Figure 4.12	Effects of EP on A375 malignant melanoma cells by confocal laser scanning microscopy after staining with Annexin-V-FLOUS and propidium iodide.	130
Figure 4.13	Dose-dependent effects of 9(11)-DHEP and EP on A375 malignant melanoma cells by Western blotting analysis using total PARP antibody (human specific).	131

Figure 4.14	Dose-dependent effects of 9(11)-DHEP and EP on A375 malignant melanoma cells by Western blotting analysis using anti-cytochrome <i>c</i> antibody.	131
Figure 4.15	Dose-dependent effects of 9(11)-DHEP and EP on A375 malignant melanoma cells by Western blotting analysis using cleaved caspase 3 antibody, cleaved caspase 7 antibody (human specific), cleaved caspase 6, caspase 9, caspase 8 and caspase 10.	132
Figure 4.16	Dose-dependent effects of 9(11)-DHEP and EP on A375 malignant melanoma cells by Western blotting analysis using Bad, Bax, Bak, Puma, Mcl-1, Bcl-2 and Bcl-xl antibodies.	133
Figure 4.17	Dose-dependent effects of 9(11)-DHEP and EP on Mcl-1 expression in A375 malignant melanoma cells.	134
Figure 4.18	Dose-dependent effects of 9(11)-DHEP and EP on Bak expression in A375 malignant melanoma cells.	135
Figure 4.19	Nude mice with A375 malignant melanoma solid tumor.	136
Figure 4.20	A375 malignant melanoma solid tumor excised from EP-treated and control group of xenograft tumor-bearing nude mice.	137
Figure 4.21	The inhibitory effect of EP on A375 malignant melanoma cells in xenograft tumor-bearing nude mice.	138
Figure 4.22	Effect of EP on A375 malignant melanoma solid tumor by Western blotting analysis using cleaved PARP (Asp214) antibody 89Kb.	139
Figure 4.23	EP induced gene expression change in A375 malignant melanoma tumor.	140
Figure 4.24	Mitochondria-mediated apoptosis induced by EP and 9(11)-DHEP in A375 cancer cells	146

Chapter I General Introduction

1.1 Cancer

Cancer is one of the lethal diseases in the world. It arises because of genetic alternations that are responsible for inappropriate growth. Cancer may occur spontaneously as a result of mistakes in DNA replication and repair, or after the exposure of cells to environmental mutagens. Cancer is a malignant disease. One defining feature of cancer is the rapid accumulation of abnormal cells which grow beyond their usual boundaries, and which can invade adjoining parts of the body, enter the bloodstream or lymphatic system and spread to other organs, a process referred to as metastasis. It differs from benign tumors, cells from which do not spread to other parts of the body. Metastases are the major cause of death from cancer.

Cancers are classified according to their origin. In general, they are classified into the following categories: a). **Carcinoma**: Malignant tumors derived from epithelial cells. This group represents the most common cancers, including the common forms of breast, prostate, skin, lung and colon cancer. b). **Sarcoma**: Malignant tumors derived from connective tissue, or mesenchymal cells. c). **Lymphoma and leukemia**: Malignancies derived from hematopoietic (blood-forming) cells. d). **Germ cell tumor**: Tumors derived from totipotent cells. In adults, germ cell tumors are often found in the testicle and ovary. In fetuses, babies, and young children, these tumors are often found on the body midline, particularly at the tip of the tailbone. e). **Blastic tumor**: A tumor (usually malignant) which resembles to immature or embryonic tissue. Many of these tumors are common in children.

Up to now, many methods such as surgery, chemotherapy, radiation therapy and immunotherapy are developed for cancer therapy. The choice of therapy depends

upon the location and grade of the tumor and the stage of the disease, as well as the general state of the patient (performance status).

In theory, cancers can be cured if it is entirely removed by surgery. But it's impossible for a complete surgical excision when the cancer has metastasized to other sites in the body. Radiation therapy (also called radiotherapy, X-ray therapy, or irradiation) is the use of ionizing radiation to kill cancer cells and shrink tumors. However, radiation usually has a great side effect on normal tissue. Cancer immunotherapy refers to a diverse set of therapeutic strategies designed to induce the patient's own immune system to attack the malignant tumor. But many kinds of cancer cell are more tolerated by the patient's own immune system.

Chemotherapy usually refers to the treatment with cytotoxic drugs which affect rapidly dividing cells in general. While surgery and radiation therapy are used to treat localized cancers, chemotherapy is used to treat cancer cells that have metastasized (spread) to other parts of the body. In spite of the many advances in cancer treatment, chemotherapy of solid tumors is still greatly limited by the lack of selectivity of anticancer drugs and by the recurrence of drug-resistant tumors. Most chemotherapeutic drugs target on all rapidly dividing cells and are not specific for cancer cells. Development of novel chemotherapeutics continues to be a focus of effort.

1.2 Medicinal mushroom and cancer

Studies showed that many causes have been found to contribute to cancer genesis. Inappropriate diet is one of the major reasons linked to cancer development. This suggests that there maybe something important in the diet for the cancer prevention. People try to find some new special anticancer drugs with lower side effect. Recent interest attentions are found on the natural products in the dietary.

Mushrooms have long been valued as highly tasty and nutritional foods containing digestible proteins, dietary fiber, crude fat, vitamins and mineral. Mushrooms rise out of the mycelium when the right nutrients are amassed and the right environmental conditions are present. Mushrooms release spores at maturity. When spores land on the right spot, the cycle starts over again. The fruiting bodies, mycelia, and spores have been used not only as home remedies but also as new drug sources.

Medicinal properties have been attributed to mushrooms for hundreds of years. Searching for new antitumor and other medicinal substances from mushrooms and to study the medicinal value of these mushrooms have become a matter of great significance. Moreover, it is estimated that there are about 14,000 species of mushrooms in the world and only 10% are now known. Mushrooms are considered to be a largely source of powerful new pharmaceutical products. Many of these mushroom extracts have been proven to be efficacy against various cancers and showed clinical potency (Wasser & Weis, 1999). Chemopreventive effects of mushroom polysaccharides [*Lentinus edodes* (LPS), *Ganoderma lucidum* (GPS) and *Coriolus versicolor* (CPS)] were assessed in both initiation and promotion processes in carcinogenesis. However, most of the active components in mushroom have not been clearly defined (Zaidman BZ, et al., 2005).

1.3 *Ganoderma lucidum*

Ganoderma lucidum (Leyss. ex Fr.) Karst., a medicinal fungus called “Lingzhi” in China, is a basidiomycete, lamellaless fungus belonging to the family of polyporaceae. In nature, it is rarely found since it flourishes mainly on the dried trunks of dead plum, guercus serrata or pasonia trees. It is considered as a natural medicine that can promote longevity and maintains the vitality of human beings and has been used in traditional Chinese medicine for centuries.

Since the mushroom is very rare in nature, fruiting bodies are artificially cultivated on wood logs and on sawdust in plastic bags or bottles. Biotechnological cultivation of *Ganoderma lucidum* mycelia in bioreactors has also been established, both on solid substrates and in liquid media by submerged cultivation of fungal biomass.

There are lots of bioactive agents identified from the *Ganoderma lucidum*, which have recently received more and more attention not only as dietary supplement but also as new drug sources, such as protein, nucleosides (Yuan JP, et al., 2008), polysaccharides, triterpene and steroid. They have been used to treat various human diseases such as allergy, arthritis, bronchitis, gastric ulcer, hyperglycemia, hypertension, chronic hepatitis, hepatopathy, insomnia, nephritis, neurasthenia, scleroderma, inflammation and cancer (Sliva D, 2003). Antitumor activities of *Ganoderma lucidum* are explored in more detail below.

1.4 Antitumor activities of *Ganoderma lucidum*

1.4.1 *Ganoderma* peptide and polysaccharides

Polysaccharides and proteins are two important classes of *Ganoderma lucidum* metabolites of high molecular mass with a variety of biological activities such as hepatoprotective effect (Zhang GL, et al., 2002) and antioxidant activity (Zhang HN, et al., 2003; Yuen JWM, et al., 2008). All of these metabolites are proteins, β -D-glucans, β -D-glucans linked to proteins. Previous studies showed that they could not kill the cancer cell directly, but exhibited their antitumor activities through activating host immune response. They are used as biological response modifiers to strengthen the cancer patient's immunological defenses (Lin ZB, 2005; Lin ZB and Zhang HN, 2004; Boh B, et al., 2007).

An immuno-modulatory protein, Ling Zhi-8 (LZ-8) isolated from *Ganoderma*

lucidum was found to exhibit potent mitogenic effects upon human peripheral blood lymphocytes (PBL). rLZ-8 was found to induce IL-2 gene expression via the Src-family protein tyrosine kinase (PTK), reactive oxygen species (ROS), and differential protein kinase-dependent pathways in human primary T cells and cultured Jurkat T cells (Hsu HY, et al., 2008; Tong MH, et al., 2008).

Ganoderma lucidum polysaccharides exert immunomodulatory activities by stimulating the expression of inflammatory cytokines from mouse spleen cells (Wang et al., 2002; Chen et al., 2004; Ma C, et al., 2008), human whole blood (Kuo MC, et al., 2006) and human monocytic leukemia cells (Cheng KC, et al., 2007); enhancing inflammatory response in mouse macrophage (Hsu HY, et al., 2004); enhancing NK-cell-mediated cytotoxicity (Chien CM, et al., 2004); promoting the maturation and function of dendritic cell (Cao LZ and Lin ZB, 1992); regulating cytotoxic T-lymphocytes (Cao LZ and Lin ZB, 2003).

In the *in vivo* study, Ganopoly significantly reduced the tumor weight of sarcoma-180 with a broad spectrum of immuno-modulating activities (Gao Y et al., 2005). Low-dose *GI-PS* treatment was found to enhance the activity of immunological effector cells in immunosuppressed mice (Zhu XL et al., 2007). The antlered form of *Ganoderma lucidum* enhanced the anti-tumor and anti-metastatic effects by inhibiting the decrease in NK activity and stimulating the recovery of T cell functions in cyclophosphamide-treated mice (Nonaka Y, et al., 2008). This herb was applied as an efficacious adjacent immunopotentiating therapy against cancer chemotherapy-induced immunosuppression.

The biochemical mechanisms that mediate antitumor activities of polysaccharides are still not clearly understood until CR3 was identified as the major leukocyte membrane receptor for β -glucans (Zhu XL and Lin ZB, 2005). When During bacterial or yeast infection, the complement component iC3b was activated.

The cleaved fragment of iC3b bind onto the surface of pathogens and form pores on pathogen membranes. Opsonification through the binding with polysaccharide on the bacterial surface with iC3b would stimulate the phagocytosis of the pathogens. The lack of similar CR3-binding polysaccharides on human cells explains why the tumor cell can escape from the CR3-mediated phagocytosis or extracellular cytotoxicity opsonized with iC3b. Small soluble β -1-3-glucan polysaccharides isolated from fungi cannot penetrate cells due to their large molecular mass, so they modulate cellular activity through binding to the lectin site of CR3 with high affinity and prime the receptor for subsequent cytotoxic activation by iC3b-tumor cells. The receptor binds specific structures of the β -glucan chains, and the success of the β -glucan as an immunostimulant is determined by the ability of the β -glucan to mediate binding to this receptor. β -glucans with few binding sites are thus less potent as immunostimulants.

Mechanistic studies showed that many pathways and molecule are involved in the immuno-modulation activities of *Ganoderma lucidum* polysaccharides. Induction of Erk1/2 activity by *Ganoderma lucidum* polysaccharide extract was demonstrated in tumor cell (Xie YZ, et al., 2006). PS-G enhanced neutrophil function in phagocytosis and chemotaxis via the activities of phosphatidylinositol 3-kinase (PI3K), p38 MAPK, Src tyrosine kinases and protein kinase C (PKC) (Hsu MJ, et al., 2003). Increase of toll-like receptor 4 (TLR4) by *Ganoderma lucidum* polysaccharide extract was observed in macrophages, and the effect was associated with the up-regulation of expression of inflammatory cytokine IL-1 (Hua KF, et al., 2007; Shao BM., et al., 2004). Polysaccharide fraction Reishi-F3 caused mouse splenic B cell activation and differentiation to IgM-secreting plasma cells, and the process depended on induction of Blimp-1, a master regulator capable of triggering the changes of a cascade of gene expression during plasmacytic differentiation (Lin KI,

et al., 2006).

1.4.2 Ganoderma triterpene

1.4.2.1 Triterpene

Triterpene and steroid are unique phytochemicals with very similar chemical structure. They share a common biosynthetic pathway. In plants the reduced HMG-CoA (six carbons) can be arranged in ring form, which leading to the cyclization of squalene (30 carbons or “three terpenes”) (Wendt KU, et al., 2000). Enzymatic ring closure steps then form cycloartenol (also 30 carbons), and additional enzymatic reactions form common plant triterpenes such as phytosterols, triterpene alcohols, and brassinosteroids (Figure 1.1) (Ostlund RE Jr. 2002).

Triterpene refers to a particular type of molecular structure that has a four- or five-ring, planar-base molecule containing 30 carbon atoms. The triterpenes are subdivided into about 20 groups, depending on their particular structures. The base structure that is found in the largest variety of medicinal plants is the oleanane triterpene. Most triterpenes exist in glycoside form in nature. Glycoside refers to the attachment of various sugar molecules to the triterpene unit, which is known as the aglycone or genin when the sugar component is removed. When glycosides are consumed, the sugar molecule is usually cleaved off by enzymatic action either in the gut or in the blood stream. The triterpenes and the plant steroids are broadly described as saponins; the term refers to their ability to form a soapy material when concentrated. Saponins can enter into fatty materials and, in large enough quantity, break them up (just as soap can dissolve fat). Indeed, a well-known toxic effect of these plant compounds, when given in high dosage, is to break up red blood cells by disrupting their membranes (hemolytic effect) (Dharmananda S, 2000).

The triterpenes produced by *Ganoderma lucidum* contain oxygenated functional

groups in a lanostane skeleton, which are species-specific and thought to contribute to the bitter taste of the fungi. In addition, more and more new members in this family were identified (Li C, et al., 2005; LIY C, et al., 2006; Guan SH, et al., 2007). In the past two decades, over 130 highly oxygenated triterpenes and related compounds have been isolated from the fruiting bodies, mycelia, and spores. According to their chemical structure, the *Ganoderma* triterpene are divided into 10 groups, such as ganoderic acid, ganoderiol, ganolucidic acid, lucidenic acid and so on (Figure 1.2).

The patterns of oxygenated triterpenoids vary in a predictable manner during the formation of the fruiting bodies and culture conditions. Strain specificity of *Ganoderma* triterpenoids has also been reported. The pattern is useful in distinguishing *Ganoderma lucidum* from other taxonomically related species, such as *Ganoderma tsugae*, which is frequently used as a substitute for *Ganoderma lucidum*. According to the squalene synthase gene expression analysis, steroid and triterpene were relatively low in mycelia and reached a relatively high level in the mushroom primordial (Zhao MW, et al., 2007).

1.4.2.2 Biological function of *Ganoderma* triterpene

Interestingly triterpenoids play a key role in the plant's survival. They have an acidic quality and contribute to the bitter taste of plant. Some triterpenes exhibit antibiotic properties and they are used to protect plant from herbivores. Many plants also use triterpenes to establish territoriality. Triterpenes released from their leaves or roots may be toxic to their botanical competitors.

A lot of highly oxidized lanostane triterpenoids are thought to contribute to the bitterness of the fruiting body of the fungus *Ganoderma lucidum* (Nishitoba T, et al., 1986) that cannot be found in any other mushroom. The bitterness varies in quality

depending on the place of production, cultivation conditions and the strains of *Ganoderma* mushroom. Though relationship between the bitterness and the pharmacological effect has not fully been revealed yet, the bitterness attracts attention as a marker substance for pharmacological evaluation and chemical quality judgment of *Ganoderma lucidum* and chemical classification of *Ganoderma* (Gao JJ, et al., 2004).

While the relationship between the chemical structure and bitterness has not so far been clarified, it was pointed out that the oxygen functional groups (Kubota T *et al.*, 1969) and the hydrophobic moieties played significant roles in generating bitterness (Kumazawa T, et al., 1985). In the case of *Ganoderma lucidum* bitterness, it was revealed that they have a similarity in their chemical structures and the spatial distances among three oxygen atoms and the hydrophobic methyl groups played an important role. For example, lucidenic acid A and lucidone A have the similar structure, both of which showed almost the same bitterness.

1.4.2.3 Antitumor activities of *Ganoderma* triterpene

Most of *Ganoderma* triterpenes were proven to have cytotoxic, anti-angiogenesis, anti-HIV protease and cholesterol synthetic inhibiting effects (Table 1.1).

Previous studies found that the triterpene of *Ganoderma lucidum* have great antitumor activities. Obviously different from that of polysaccharides and glycoprotein complexes which can enhance tumoricidal activity by the activation of host immune responses *in vivo* (Wang SY *et al.*, 1997; Won *et al.*, 1989), *Ganoderma* triterpene exert their effects by inhibiting cancer cell proliferation, inducing cell apoptosis, suppressing angiogenesis activities and cancer cell migration (Table 1.2).

1.4.2.3.1 Anti-proliferation activity

The antitumor activities of different crude triterpenes (organic solvent extracts, such as ethanol, methanol and chloroform) have been well documented.

In breast cancer cells MCF-7 and MDA-MB-231, extracts of *Ganoderma lucidum* were shown to inhibit cell proliferation by down-regulating the expression of Akt and *NF-κB* and up-regulating p21/Waf1 (Hu H *et al.*, 2002), which were followed by arresting cell cycle at G0/G1, suppressing the expression of *NF-κB*-regulated cyclin D1 and cdk4 (Jiang JH (a) *et al.*, 2004)

Zhu *et al* reported that alcohol extracts from *Ganoderma lucidum* spores strongly inhibited the growth of HeLa cells by blocking the G1/S cell cycle transition and inducing a marked decrease of intracellular calcium level. (Zhu HS *et al.* 2000).

The triterpene enriched fraction, WEES-G6, prepared from mycelia of *Ganoderma lucidum* inhibited the growth of human hepatoma Huh-7 cells. Treatment with WEES-G6 caused a rapid decrease in the activity of cell growth regulative protein, PKC, and the activation of JNK and p38 MAP kinases, which resulted in a prolonged G2 cell cycle phase and strong growth inhibition of the hepatoma cells (Lin SB *et al.*, 2003).

In human prostate cancer cells PC-3 results demonstrated that *Ganoderma lucidum* (commercial product, contains 13.5% polysaccharides and 6% triterpenes) inhibited cell proliferation by the down-regulation of expression of cyclin B and Cdc2 and the up-regulation of p21 expression. The inhibition of cell growth was also demonstrated by cell cycle arrest at G2/M phase. (Jiang JH, *et al.* 2004 b)

Ethanol extracts of *Ganoderma lucidum* showed greatly growth inhibitory effects on human bladder cancer cell (HUC-PC), which was associated with G2/M arrest (Lu QY *et al.*, 2004).

1.4.2.3.2 Induction of apoptosis

Induction of apoptosis is another major anticancer activity mechanism of *Ganoderma lucidum*. The alcohol extract of *Ganoderma lucidum* can up regulate a pro-apoptotic Bax protein in human breast cancer MCF-7 cells (Hu H, *et al.*, 2002). Furthermore, *Ganoderma lucidum* (commercial product, contains 13.5% polysaccharides and 6% triterpenes) decreased slightly the expression of NF- κ B-regulated Bcl-2 and Bcl-xl in human prostate cancer PC-3 cells. However, the expression of proapoptotic Bax protein was markedly up-regulated, resulting in the enhancement of the ratio of Bax/Bcl-2 and Bax/Bcl-xl (Jiang JH, *et al.*, 2004 b). The ethanol extract also increased caspase-3 activity in HT-29 human colonic carcinoma cells (Hong KJ *et al.*, 2004).

Ganoderma acid X and lucidenic acid B were also found to induce apoptosis by activating the intrinsic pathway. The early activation of JNK by Ganoderma acid X in the apoptotic hepatoma cancer cells decreased Bcl-xL level and disrupted mitochondrial membrane, cytosolic release of cytochrome c and activation of caspase-3 and degradation of chromosomal DNA (Li CH *et al.*, 2005; Hsu CL, *et al.*, 2008)

1.4.2.3.3 Anti-angiogenic activity

It was recently found that the triterpenoid fraction (mainly ganoderic acid F) isolated from the fruiting bodies of *Ganoderma lucidum* could inhibit angiogenesis induced by Matrigel (a soluble basement membrane extract of the Engelbreth-Holm-Swarm (EHS) tumor) supplemented with vascular endothelial growth factor (VEGF) and heparin in an *in vivo* model (Kimura *et al.* 2002).

The 70% ethanol extract of *Ganoderma lucidum* fresh fruit bodies also showed a significant anti-angiogenic activity in the chick embryo chorioallantoic membrane

(CAM) assay. The extract also had inhibitory activity on lipopolysaccharide-induced nitric oxide (NO) production in RAW 264.7 macrophages. Because nitric oxide synthase (NOS) is essential for NO synthesis (Kwon *et al.* 1990), angiogenesis could be enhanced via the VEGF-NOS signaling pathway (Kao *et al.* 2003). The inhibition of NO production by *Ganoderma lucidum* further supported its anti-angiogenic activity (Song YS *et al.*, 2004).

Extract of *Ganoderma lucidum* can modulate the phosphorylation of Erk1/2 and Akt in PC-3 cell, which in turn inhibited the activity of AP-1 and resulted in the down-regulation of secretion of VEGF and FGF (Stanley G *et al.*, 2005).

These observation support the notion that the anti-tumor effect of *Ganoderma lucidum* may be linked to the inhibition of angiogenesis.

1.4.2.3.4 Inhibition of migration activity

Studies indicated that *Ganoderma lucidum* extracts were capable of inhibiting human cancer cell migration *in vitro* (Lu QY *et al.*, 2004; Thyagarajan A, *et al.*, 2006). The ethanol extracts induced actin polymerization, which in turn inhibited carcinogen 4-aminobiphenyl induced migration in the bladder cancer cell (HUC-PC cells). The increased actin polymerization was associated with increased stress fibers and focal adhesion complex formation. However, expression of matrix metalloproteinase-2 (MMP-2) and focal adhesion kinase (FAK, total and phospholated) were unchanged (Lu QY *et al.*, 2004).

Lucidenic acids A, B, C and N isolated from *Ganoderma lucidum* were found to have potential anti-invasive activity on phorbol-12-myristate-13-acetate (PMA)-induced HepG2 cells by suppressing the MMP-9 activity (Weng CJ, *et al.*, 2007; Weng CJ, *et al.*, 2008). Ganoderic acid A and Ganoderic acid H suppressed growth and invasive behavior of MDA-MB-231 cells through the down-regulation of

expression of Cdk4 and the suppression of secretion of uPA, respectively. (Jiang J, et al., 2008). In these studies, the inhibitory effects on cancer cells migration were attributed to the suppression of the phosphorylation of Erk1/2 and the reduction of AP-1 and NF- κ B DNA-binding activities

1.4.2.3.5 *In vivo* immunomodulatory effect

Ganoderic acid Me (GA-Me) is a lanostane triterpenoid purified from *Ganoderma lucidum* mycelia. GA-Me could inhibit both tumor growth and lung metastasis of Lewis lung carcinoma in C57BL/6 mice. The natural killer (NK) cell activity was significantly enhanced by intraperitoneal administration of GA-Me. the expression of Nuclear Factor- κ B (NF- κ B) was up-regulated after the treatment with GA-Me, which might be involved in the production of IL-2 and Interferon- γ (IFN- γ). In conclusion, the findings of this study implied that GA-Me could effectively inhibit tumor growth and lung metastasis through increasing immune function (Wang G, et al., 2007).

1.4.3 Ganoderma steroid

1.4.3.1 Phytosterol

Phytosterols (plant sterols) are members of the “triterpene” family of natural products. Most phytosterols contain 28 or 29 carbons and one or two carbon-carbon double bonds, typically one in the sterol nucleus and sometimes a second in the alkyl side chain. They are specific phytochemicals that are structurally very similar to cholesterol except that they contain an extra methyl or ethyl group, or double bond; the side chains of most phytosterol contain 9–10 carbon atoms, instead of 8 as found in cholesterol (Ling WH and Jones PJH, 1995).

More than 200 different types of phytosterols have been reported in plant

species. In all plant tissues, phytosterols occur in four common forms: as the free alcohol (FS), as fatty-acid esters (SE), as steryl glycosides (SG), and as acylated steryl glycosides (ASG), all of which have double bonds at the C-5 position of the ring. The last three forms (SE, SG, and ASG) are generically called “phytosterol conjugates” in which the 3 β -hydroxyl group is esterified to a fatty acid or a hydroxycinnamic acid, or glycosylated with a hexose (usually glucose) or a 6-fatty acyl hexose. Free phytosterols serve to stabilize phospholipid bilayers in plant cell membranes just as cholesterol does in animal cell membranes. Sterol molecules are essential for maintaining the proper structure and function of eukaryotic cell membranes (Czub J and Baginski MJ, 2006).

1.4.3.2 Biological activities of phytosterols

Phytosterols are enriched in high lipid content plant foods such as nuts, legumes including peanuts, and seeds such as sesame seeds (Bradford PG and Awad AB, 2007). Phytosterols are proposed to have a wide spectrum of biological effects including anti-inflammatory, anti-oxidative, and anti-carcinogenic activities, one of their most studied and outstanding properties is their cholesterol-lowering activity. They are absorbed only in trace amounts but inhibit the absorption of intestinal cholesterol including recirculating endogenous biliary cholesterol, a key step in cholesterol elimination, which has been the most extensively research. (Ryan E, et al., 2007).

Cholesterol is the predominant sterol found in humans—a constituent of all cell membranes and plasma lipoproteins, especially low-density lipoprotein (LDL). Serum LDL cholesterol-lowering effect of plant stanols/sterols originates from the reduced intestinal cholesterol absorption. Because of their structural similarity to cholesterol, hence they act by competing with cholesterol at the luminal absorption

site, thereby lowering total plasma cholesterol and low-density lipoprotein (LDL) levels (Lagarda MJ, et al., 2006). It is suggested that natural food phytosterols may be clinically important (Ostlund RE Jr. 2002). Phytosterols are absorbed from the diet in small but significant amounts. Phytosterols are now being added to an increasing variety of foodstuffs (Kritchevsky D and Chen SC, 2005). Their potency in decreasing serum cholesterol levels has led to the development of functional foods enriched with plant sterols in protecting against cardiovascular diseases (Ostlund RE Jr. 2002; Thompson GR and Grundy SM, 2005; Plat J and Mensink RP, 2005).

These oxygenated sterols from *Ganoderma lucidum* inhibited cholesterol biosynthesis via the conversion of acetate or mevalonate as a precursor of cholesterol. The lanosterol 14 α -demethylase, which converts 24,25-dihydrolanosterol to cholesterol, can be inhibited by the 26-oxygenosterols from *Ganoderma lucidum*. These 26-oxygenosterols could lead to the development of novel therapeutic agents that lower blood cholesterol (Hajjaj H, et al., 2005).

In addition, there are a variety of final phytosterol metabolic products in plant, and each species has a characteristic distribution of sterols that has sometimes been used as a chemical fingerprint for identification of food product sources. (Ostlund RE Jr. 2002).

1.4.3.3 Antitumor activities of *Ganoderma* steroids

Ganoderma steroid is other major group low molecular secondary metabolites of this fungus. There are 20 steroids isolated from this fungus so far. They abundantly present in the cholesterol type and ergosterol type. Results showed that *Ganoderma lucidum* contained both free and esterified ergosterols and their distribution varied in different parts of *Ganoderma lucidum*. The contents of

esterified ergosterol were much higher in the tubes and the spores than the pileus and stipe.

Ergosterol, also called (22E)-ergosta-5,7,22-trien-3 β -ol, is a principal sterol of the cell membrane in fungi (Figure 1.3a) (Czub J and Baginski M, 2006). It is a major fungal steroid and has been reported in concentrations of 0.3-0.4% in *Ganoderma lucidum*. The content of ergosterol has been widely used as an estimate of fungal biomass in various environments because a strong correlation has been found between ergosterol content and fungal dry mass. Ergosterol content may be a suitable marker for evaluating the quality of Ganoderma spore and Ganoderma spore lipid (GSL) products (Yuan JP, et al., 2006; Yuan JP, et al., 2007). It is able to activate expression of a number of defense genes and increase the resistance of plants against the pathogens (Lochman J and Mikes V, 2005).

Ergosterol and its derivatives were tested to have great antitumor activity. When ergosterol enter into the human body, it can be metabolized to generate newer bioactive products, such as 17R, 24-dihydroxyergosterol, which has been found to inhibit the proliferation of skin cells in culture, as demonstrated in human keratinocytes and melanoma cell lines (Slominski A, et al., 2005).

Peroxide of ergosterol, 5 α , 8 α -epidioxy-22E-ergosta-6, 22-dien-3 β -ol (Figure 1.3b) is also widely distributed in mushrooms such as *Hypsizigus marmoreus*, *Pleurotus eringii*, *Russula cyanoxantha* and *Ganoderma lipsiense* (Lee SH, et al., 2006; Fujimoto H, et al., 1994; Yang Kuo LM, et al., 2005; Gao JM, et al., 2000). Studies showed that ergosterol peroxide suppress LPS or TPA-induced inflammatory responses through inhibition of NF- κ B and C/EBP β transcriptional activity, and phosphorylation of MAPKs in RAW264.7 macrophage-like cells, or STAT1 mediated inflammatory responses by altering the redox state in HT29 cells

(Yasukawa K, et al., 1996; Kobori M, et al., 2007). Ergosterol peroxide (EP) inhibited the growth of some cancer cells and decreases lipid peroxidation of rat liver microsomes. It can also enhance the inhibitory effect of linoleic acid on DNA polymerase β (Mizushina Y *et al.*, 1998).

9(11)-DHEP, which possesses one more double bond than EP, is also found in several edible mushrooms and fungi used in medicine (Figure 1.3c). The steroid was found in mushroom *Polyporus ellissi* (Gao JM, *et al.*, 2003), *Pisolithus tinctorius*, *Microporus flabelliformis* and *Lenzites betulina* (Fujimoto H, *et al.*, 1994)

Ergosterol and its derivatives were tested to have great antitumor activity. EP and 9(11)-DHEP are major antitumor steroids produced by edible or medicinal mushrooms. EP and 9(11)-DHEP can inhibit human myeloid leukemia HL60 cells and HT29 colon cancer cells by inducing apoptosis (Takei T, et al., 2005; Kobori M, et al., 2007). However, their molecular mechanisms of action have not yet to be determined.

1.5 Apoptosis

Apoptosis (programmed cell death) is the physiological process by which unwanted or useless cells are eliminated. It is most often found during normal cell turnover and tissue homeostasis, embryogenesis, induction and maintenance of immune tolerance, development of the nervous system and endocrine-dependent tissue atrophy. Apoptosis is characterized by a precise sequence of morphological changes which result in the swallow of the dying cell by macrophages in the absence of inflammation. These changes include cell shrinkage, plasma membrane blebbing, chromatin condensation, nuclear segmentation and the formation of apoptotic bodies (Saikumar P, et al., 1999).

Tumor cells can acquire resistance to apoptosis by the expression of anti-apoptotic proteins or by the down-regulation or mutation of pro-apoptotic proteins. So induction of apoptosis is an important cancer treatment strategy.

1.5.1 Mechanisms of apoptosis

Two major apoptosis pathways have been defined in mammalian cells. One involves extracellular signals transmitted via the tumor necrosis factor receptor 1, whereas the second, the mitochondrial pathway, is triggered by intrinsic pro-apoptotic stimuli such as DNA-damage and by extracellular and/or environmental stressors. The two pathways share the common final step of caspase 3 activation, which catalyzes PARP and result in apoptosis (Figure 1.4) (Igney FH, et al., 2002).

In death receptor-mediated pathway, the cell death receptor acquire extracellular stress signal, and recruits signalling proteins such as FADD (Fas-associated death domain), which trigger the binding of procaspase 8. This results in the auto-activation of caspase 8. The active caspase 8 is involved in the cleavage and activation of effector caspase 3, which trigger the downstream caspase cascade and cell apoptosis.

In mitochondria-mediated pathway, the mitochondria stress will reduce the mitochondria membrane potential, which results in the release of cytochrome C from the intermembrane space of the mitochondria into the cytosol. In turn, it binds to cytosolic procaspase-9 and APAF-1 to form apoptosome complex, a multi-protein complex consisting of cytochrome C, Apaf-1, pro-caspase 9 and ATP, resulting in autoactivation and release of mature caspase-9. The latter enzyme activates caspase 3 and caspase 7, which in turn activate a downstream caspase cascade.

1.5.2 Apoptosis components

1.5.2.1 Caspase family

Caspases are a ubiquitous family of aspartate specific cystein-dependent proteases with central functions in apoptotic pathway. For structure, certain caspases have large prodomains that contain related homotypic oligomerization motifs such as the caspase recruitment domain (CARD, caspase-1, -2, -4, -5, -9, -11, -12) and the death effector domain (DED, caspase-8 and -10). The short prodomain caspases (caspase-3, -6, -7, -14) are activated by proteolytic maturation by large prodomain caspases or other proteases.

Of the 14 known human caspases, six (caspase 3, 6, 7, 8, 9 and 10) are definitely involved in apoptosis in various model systems. Based on their prodomains and roles in cell death, these apoptotic caspases are divided into two classes, namely effector (or 'downstream') caspases, which are responsible for most of the cleavages that disassemble the cell, and initiator (or 'upstream') caspases, which initiate the proteolytic cascade. These caspases are responsible for the cleavage of the key cellular proteins, such as cytoskeletal proteins, that lead to the typical morphological changes observed in cells undergoing apoptosis.

Recent data indicated that caspases are involved in cell differentiation, proliferation and NF- κ B activation besides apoptosis (Lamkanfi M, et al., 2007). Caspase-1 is the prototypical member of a subclass of caspases involved in cytokine maturation termed inflammatory caspases that also include caspase-4, caspase -5, caspase -11 and caspase -12 (Martinon F and Tschopp J, 2007) (Table 1.3).

1.5.2.2 Mitochondria and apoptosis

Mitochondria are critical organelle because they generate most of the cell's supply of ATP that is used as a source of chemical energy in a series of life activities.

Mitochondria are involved in a range of life processes, such as signaling, cellular differentiation, cell death, as well as the control of the cell cycle and cell growth. Studies showed that mitochondria have been implicated in several human diseases and may play a role in the aging process.

Mitochondria play a crucial role in apoptosis. Mitochondrial membrane permeabilization (MMP) is the critical event responsible for caspase activation in the intrinsic pathway of apoptosis. Several intracellular stress, such as DNA damage and ER stress, free radical damage and growth factor deprivation converge on mitochondria to induce MMP, which causes the release of proapoptotic factors from the intermembrane space (IMS) such as AIF, Smac/DIABLO and cytochrome C from permeability transition pore. Cytochrome C is important molecular in the mitochondria-mediated pathway, which localized to the intermembrane space of mitochondria. It needs special process to across the outer membrane into cytosol. These pores are thought to form through the action of the pro-apoptotic members of the Bcl-2 family of proteins. (Chipuk JE, et al., 2006).

1.5.2.3 Bcl-2 family

Bcl-2 and the related cytoplasmic proteins are other key regulators of apoptosis. They can be divided into a) pro-apoptotic members (Bax, BAD, Bak and Bok among others); b) anti-apoptotic members (including Bcl-2 proper, Bcl-xl, and Bcl-w,); and c) the BH3 domain-only proteins (*e.g.*, Bad, Bim and Bid). Bcl-2 family proteins govern mitochondrial outer membrane permeabilisation (MOMP). Normal cellular homeostasis requires the suppression of proapoptotic players by various mechanisms, including phosphorylation, intracellular localization and heterodimerization with prosurvival Bcl-2 family proteins. Disruption of the balance between pro- and antiapoptotic Bcl-2 family members is suggested to be fundamental to the

development of many diseases (Adams JM and Cory S, 1998; 2002; Gross A, et al., 1999).

The anti-apoptotic proteins include Bcl-2, Bcl-xl and Mcl-1(myeloid cell leukaemia-1) which reside in the out mitochondria membrane (OMM) and the membrane of the endoplasmic reticulum. It has been implicated in modulating mitochondrial calcium homeostasis and proton flux. They prevent apoptosis through two different mechanisms: by heterodimerization with and neutralisation of pro-apoptotic Bcl-2 family proteins, for example, Bim or Bak (Michels J, et al., 2005) and by its direct pore-forming effect on the outer membrane of mitochondria to help maintaining a normal membrane state under stress conditions which result in the suppression of cytochrome *c* release from mitochondria.

The pro-apoptotic Bcl-2 proteins are often found in the cytosol where they act as sensors of cellular damage or stress. Following cellular stress they relocate to the surface of the mitochondria where the anti-apoptotic proteins are located. This interaction between pro- and anti-apoptotic proteins disrupts the normal function of the anti-apoptotic Bcl-2 proteins and lead to the formation of pores in the mitochondria and the release of cytochrome *c* and other pro-apoptotic molecules from the intermembrane space. This in turn leads to the formation of the apoptosome and the activation of the caspase cascade.

Multidomain proapoptotic members Bax and Bak are key components for cellular induced apoptosis, which possess the BH1, BH2, and BH3 domains. In healthy cells, the protein Bak is associated with the outer mitochondria membrane, whereas the other protein Bax resides in the cytosol. Bax and Bak are in an inactive conformation in which their NH₂ and COOH termini are folded into a hydrophobic pocket (Borner C. 2003; Kaufmann T, et al., 2004; Schinzel A, et al., 2004). Upon apoptotic stimulation, an upstream stimulator like truncated BID (tBID) induces a

conformational change of Bax or Bak (with exposure of their NH₂ terminus), their full insertion into mitochondrial membranes as homooligomerized multimers, and formation of giant protein-permeable pores by binding to components of the permeability transition pore complex (PTPC). The resulting hetero-oligomers may allow IMS proteins (cytochrome C etc.) to release from mitochondria, and the subsequent activation of caspase-9 and the downstream caspase activation pathway for apoptosis (Kroemer G, et al., 2007; Kuwana T, et al., 2002; Nechushtan A, et al., 2001;).

The BH3-only proteins are a group of pro-apoptotic proteins of the Bcl-2 family that share the conserved BH3 domain, including Bad, Bmf (Bcl-2-modifying factor), Bid, Bik/Nbk (Bcl-2-interacting killer/natural born killer), Bim, and Puma (p53 upregulated modulator of apoptosis). This short BH3 domain is essential for interaction with pro-survival members of the Bcl-2 family and allows for their pro-apoptotic activities. BH3-only molecule functions as upstream sentinels that sense cellular abnormalities, such as lack of survival signals or DNA damage. Many of these proteins appear to display distinct roles in apoptosis through tissue-specific expression. Most of them localize in the cytosolic fraction of cells as an inactive precursor. They are able to translocate to mitochondria, bind to and antagonize anti-apoptotic Bcl-2 family members including Bcl-2, Bcl-xL after certain damage signals triggering, and induces cytochrome c release and mitochondrial damage, which relay an apoptotic signal from the cell surface to mitochondria.

1.6 Research objectives

The pharmacologically activities of herbal medicines result from the interaction of “active” ingredients. The major obstacle for the acceptance of the extracts from natural products in western medicine is their complexity and absence of

standardization of biologically active compounds. The amount of biologically active compounds in *G lucidum* extract may vary and depends on the strain of *G lucidum*, place of production, cultivation conditions, and extraction procedures. In the search for active compounds from Ganoderma species, the majority of research has been performed on extracts from the fruiting body and there have been fewer studies on extracts from the liquid cultivated mycelia (Tang YJ and Zhong JJ, 2002 and 2003; Fang QH and Zhong JJ, 2002). In fact, one of the most important reasons that some of the Ganoderma bioactive preparations are not yet available as medicines may be due to the mass production (Smith et al., 2002).

Submerged culture appears to have potential advantages for their higher mycelial production in a compact space and shorter time with lesser chances of contamination. Submerged culture for Ganoderma mycelia product production is thought to be an alternative to meet the more and more increasing demands in the international markets. But most sample studied was extracted from the fruiting body and spore of *G lucidum*, few are reported from the mycelia. In addition, most reports about the submerged culture production are focused on the polysaccharides of *G lucidum* mycelia (Yang FC, et al., 2000); there were little documents on the low molecular weight metabolites.

Now the major feature of the traditional medicine is the use of herb mixtures. Modern pure compound research is necessary to advance our knowledge of their structure–activity relationships and the mechanism of their biological actions. Most of the past studies focused on crude extracts of Ganoderma, few are about the pure compounds except for Ganoderic acid X (Li CH, et al., 2005), Ganoderic acid T (Tang W, et al., 2006), Ganoderic acid A and Ganoderic acid H (Jiang J, et al., 2008), Lucidenic acid B (Hsu CL, et al., 2008; Weng CJ, et al., 2007). Moreover, the antitumor mechanisms of these phytochemicals are still not fully elucidated.

The aims of this study are (1) to purify and characterize bioactive compounds from *Ganoderma lucidum* mycelia; (2) and to determine their possible antitumor mechanism *in vitro*; (3) to study their antitumor activities *in vivo*.

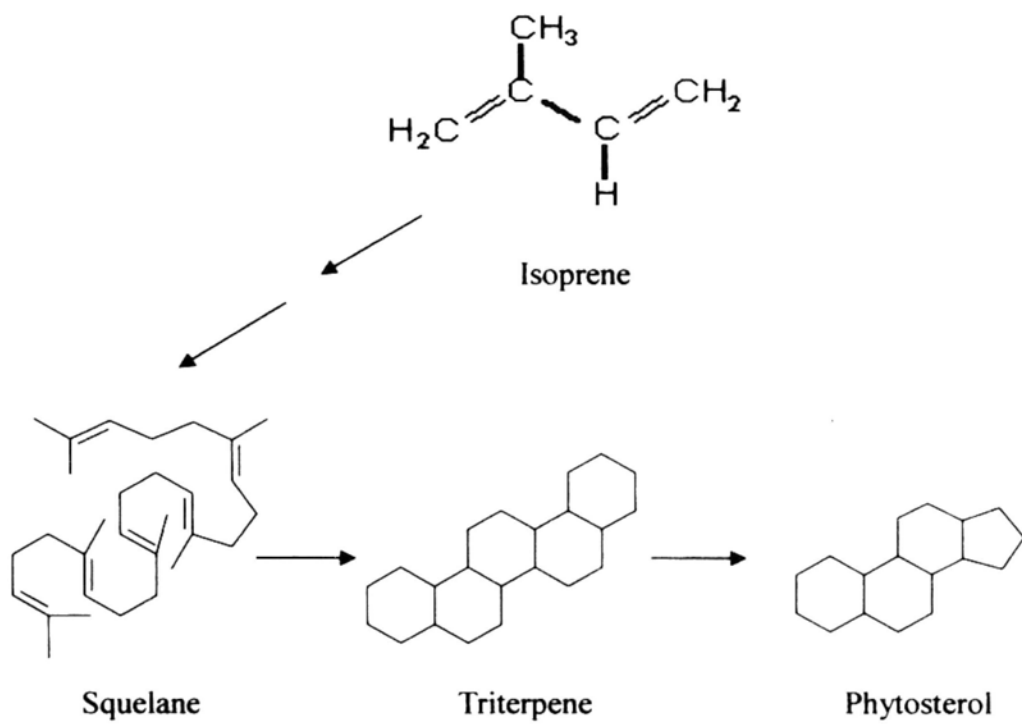
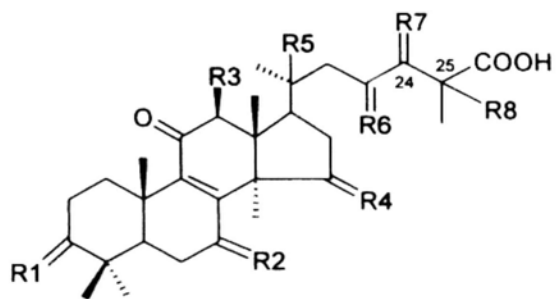
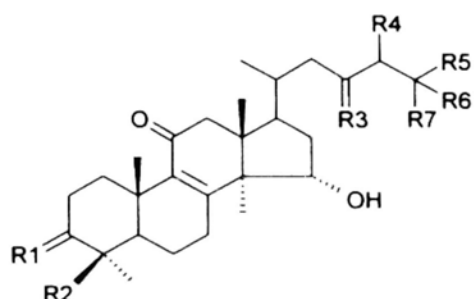


Figure 1.1. Biosynthesis of triterpenes and phyosterols

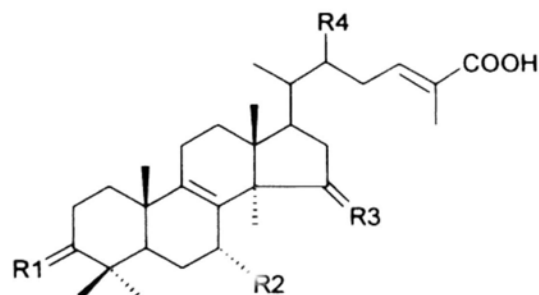
Ganoderic acid:



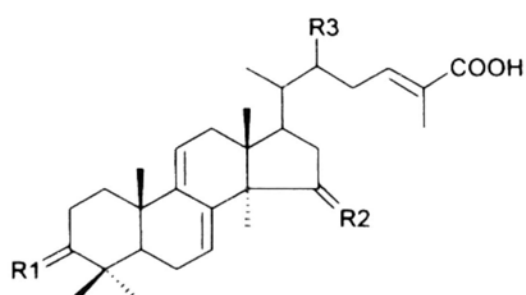
Ganolucidic acid:



Ganoderic acid from mycelium:

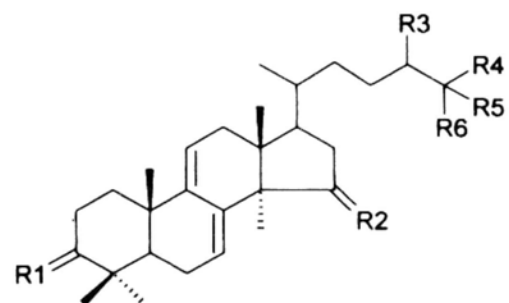


(I)

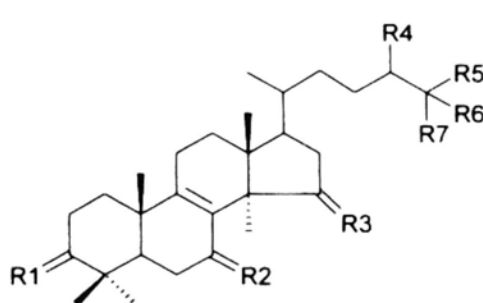


(II)

Ganoderiol:

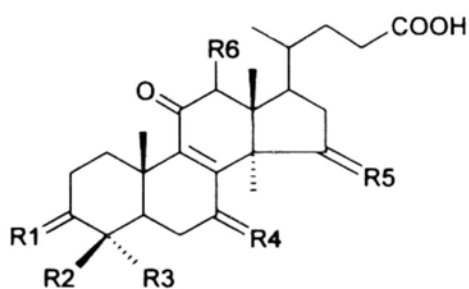


(I)



(II)

Lucidenic acid:



Lucidone:

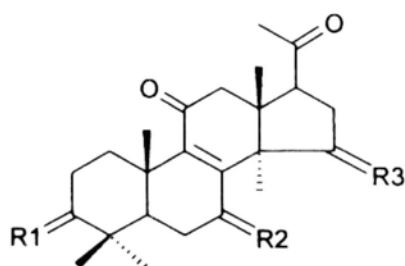


Figure 1.2 Skeleton structure of Ganoderma triterpenes

Table 1.1 Different biological activities of *Ganoderma lucidum* triterpenes

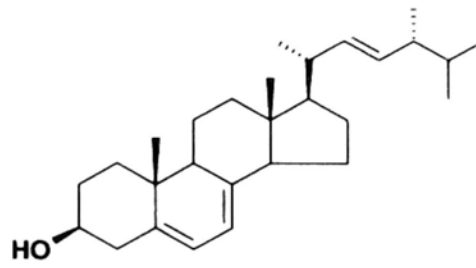
<i>Activities</i>	<i>Triterpene</i>	<i>Reference</i>
anti-HIV-1	ganoderiol F and ganodermanontriol	El-Mekkawy S <i>et al.</i> , 1998
anti-HIV-1 protease	Lucidumol B and ganodermanontriol	Min BS <i>et al.</i> , 1998
anticholesterol	ganoderic acids B and C	Sonoda Y <i>et al.</i> , 1988; Komoda Y <i>et al.</i> , 1989
antinociceptive	ganoderic acids A, B, and G and compound C6	Koyama K <i>et al.</i> , 1997
antihistamine	ganoderic acids C1 and C2	Kohoda H <i>et al.</i> , 1985
anticomplement	ganoderiol F, ganodermanondiol, and ganodermanontriol	Min BS <i>et al.</i> , 2001
cytotoxic effects	Ganodermanondiol, lucidunols A and B, lucialdehyde C, lucidenic acids A and N	Min BS <i>et al.</i> , 2000; Gao JJ <i>et al.</i> , 2002 ; Wu TS <i>et al.</i> , 2001
Inhibition of 5 α -reductase activity	ethanol extracts and ganoderol B	Liu J, <i>et al.</i> , 2006; Liu J a, <i>et al.</i> , 2007; Liu J b, <i>et al.</i> , 2007
platelet anti-aggregation	ganodermic acid S	Su CY <i>et al.</i> , 1999 & 2000
antioxidant properties	ganoderic acid A	Paterson RR, 2006

Table 1.2. Anti-proliferation and apoptosis inducing mechanisms of *Ganoderma lucidum* extracts on cancer cells

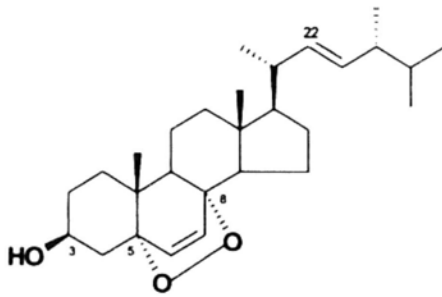
<i>Target Molecule</i>		<i>Biological Effect</i>	<i>Cell Type</i>	<i>Reference</i>
NF- κ B	↓	G2 cell cycle arrest	Prostate cancer	Jiang JH (b) <i>et al.</i> , 2004
Akt	↓			
Cyclin B	↓			
Cdc2	↓			
p21/Waf-1	↑	G1 cell cycle arrest	Breast cancer	Hu H <i>et al.</i> , 2002; Jiang JH (a) <i>et al.</i> , 2004
Cyclin D1	↓			
Cdk4	↓			
Bax	↑	Induction of apoptosis		
Caspase-7	↑			
Caspase-3	↑		Colon cancer	Hong KJ <i>et al.</i> , 2004
PKC	↓	G2 cell cycle arrest	Hepatoma	Lin SB <i>et al.</i> , 2003
JNK	↑			
P38 MAPK	↑			

“↑” means up-regulation; “↓” means down-regulation.

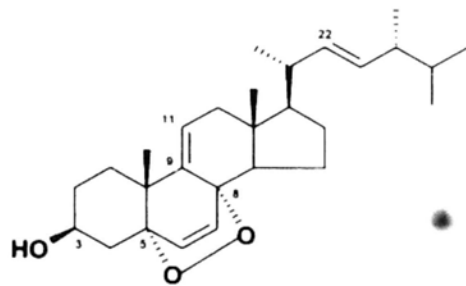
NF- κ B = nuclear factor κ B; PKC= protein kinase C; JNK = c-Jun N-terminal kinase; MAPK = mitogen-activated protein kinase. Akt = protein kinase B (PKB)



a.



b



c

Figure 1.3. The chemical structure of steroids: a is ergosterol; b is ergosterol peroxide (EP); c is 9(11)-dehydroergosterol peroxide (9(11)-DHEP)

Table 1.3. Overview of caspases family function

<i>Name of caspase</i>	<i>Function</i>	<i>Molecular Weight(kD)</i>	<i>Reference</i>
Caspase 1	Inflammation, Cytokine maturation	45	Ghayur T, et al., 1997; Li P, et al., 1995; Franchi L, et al., 2006; Mariathasan S, et al., 2005; Lamkanfi M, et al., 2004.
Caspase 2	NF-kB activation, Apoptosis induction	51	Lamkanfi M, et al., 2005; Zhivotovsky B, 2005; Bergeron L, et al., 1998.
Caspase 3	Apoptosis induction, Immuno-modulatory activity, Cell differentiation	32	De Botton S, et al., 2002; Woo M, et al., 2003; Fernando P, et al., 2005; Miura M, et al., 2004; Santambrogio L, et al., 2005.
Caspase 4	Apoptosis induction Cytokine production	43	Hitomi J, et al., 2004; Lakshmanan U, 2007
Caspase 5	Cytokine maturation	48	Martinon F, et al., 2002
Caspase 6	Apoptosis induction	34	Eguchi R, et al., 2009
Caspase 7	Apoptosis induction	35	Eguchi R, et al., 2009
Caspase 8	Apoptosis induction, NF-kB activation, Immunity cell proliferation and differentiation	55	Su H, et al., 2005; Salmena L, et al., 2003; Jun JI, et al., 2005; Chaudhary PM, et al., 2000; Kang TB, et al., 2004; Black S, et al., 2004
Caspase 9	Apoptosis induction	46	Pajak B, et al., 2009
Caspase 10	NF-kB activation Apoptosis induction	55	Takahashi K, et al., 2006
Caspase 11	Cytokine maturation	43	Wang S, et al., 1998
Caspase 12	Attenuation of inflammation and susceptibility to sepsis	50	Saleh M, et al, 2004; 2006. Roy S, et al., 2008
Caspase 13	Apoptosis induction	43	Evans AC, et al., 2004
Caspase 14	Cell differentiation	30	Lippens S, et al., 2000; Eckhart L, et al., 2000

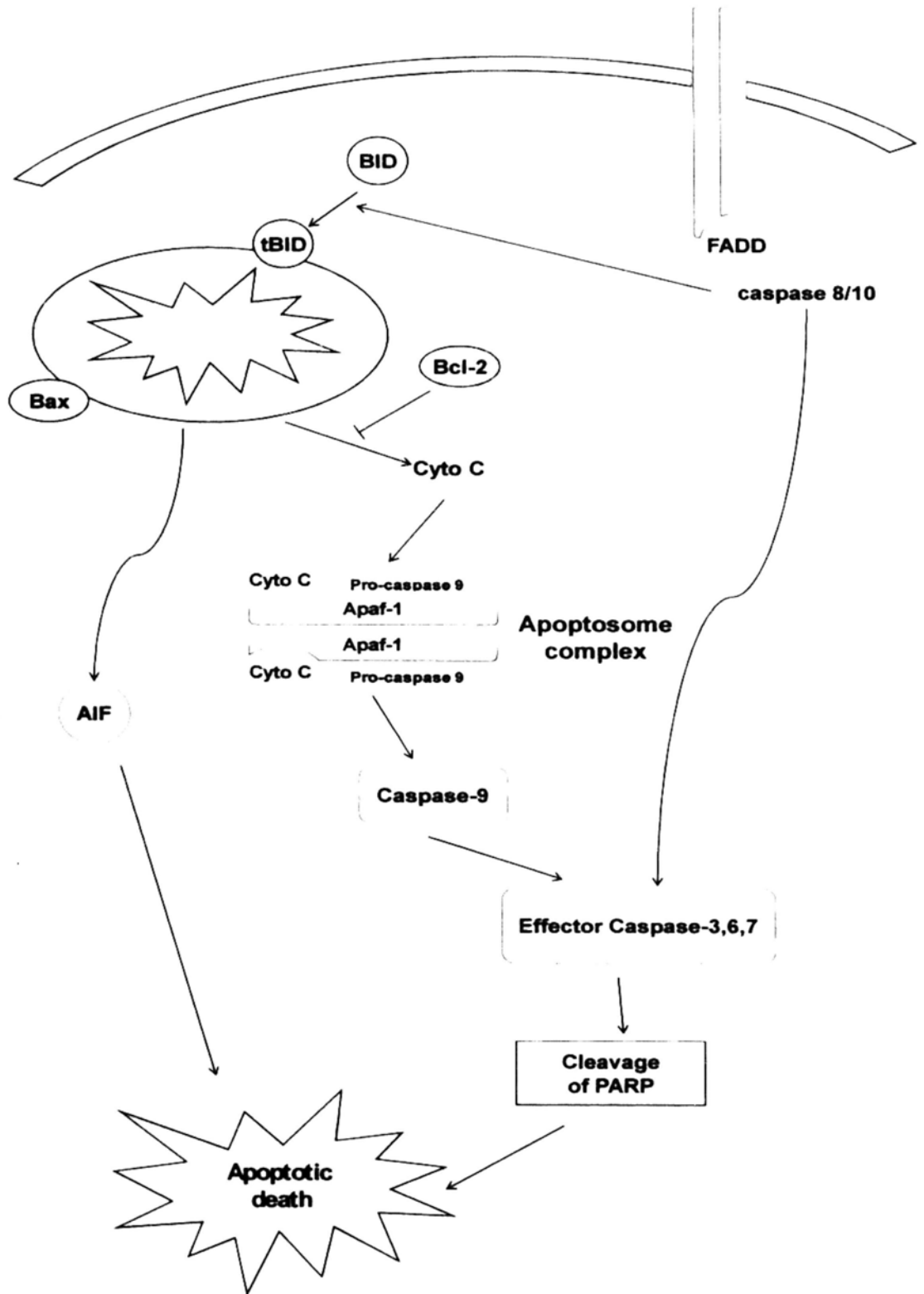


Figure 1.4 Overview of death receptor-mediated and mitochondria-mediated apoptosis pathway

Chapter II Purification and identification of ergosterol peroxide and 9,11-dehydroergosterol peroxide from *Ganoderma lucidum* mycelia

2.1 Introduction

Increasing evidence of health benefits of phytochemicals with expanding applications has prompted research on development for the production of phytochemicals on a commercial-scale from natural sources. Isolation methods of phytochemical differ from each other according to the characteristics of different chemicals. Traditional solvent extraction methods are commonly used for the production of crude extracts. Water, methanol and ethanol, or water: alcohol mixtures have been widely used for extraction of all sterol lipid classes from plant matrices (Akihisa T, et al., 2007). In recent years, microwave and ultrasound methods are developed into new techniques for natural product extraction.

Once a lipid extract has been prepared it is often necessary to separate (fractionate) one or more of the sterol lipid classes. Traditionally, column chromatography (CC) and thin layer chromatography (TLC) are accessible and affordable separation techniques (Lagarda MJ, et al., 2006). A common method for the preliminary purification of phytosterol and triterpenoids after the extraction step involves the partitioning of them between aqueous phase and a water immiscible solvent such as *n*-butanol. Further purification can be carried out using solvent precipitation, adsorption, ultrafiltration, and/or chromatography. While chromatographic procedures such as open column chromatography, thin layer chromatography, flash chromatography, liquid chromatography (low, medium and high pressure), and countercurrent chromatography have been well established and widely used for analytical scale purification of saponins (Güçlü-Ustündağ Ö and

Mazza G, 2007). The determination of phytosterols in plant material is usually performed by capillary gas chromatography (GC), with flame ionization detection (FID) or mass spectrometry (MS) to confirm peak identity, although HPLC can also be used (Moreau RA, et al., 2002).

Phytosterols and triterpenoids in *Ganoderma lucidum* can be isolated by solvent extraction with chloroform–methanol, chloroform–methanol–water, hexane, methylene chloride or acetone followed by alkaline hydrolysis and chromatographic purification to obtain enriched total sterols. For the isolation of *Ganoderma* steroid, fruit bodies were chipped and extracted with CHCl_3 . The CHCl_3 extracts were individually subjected to silica gel column chromatography and eluted with hexane and C_6H_6 –EtOAc (Ko HH, et al., 2008; Ziegenbein FC, et al., 2006). The isolation of *Ganoderma* triterpenoids was quite different from that of *Ganoderma* steroids. Alkaline saponification (NaHCO_3) and acid hydrolysis (HCl) are essential for the *Ganoderma* triterpene purification (Tang YJ and Zhong JJ, 2002).

In my study, two steroids were purified from the mycelia of *Ganoderma lucidum* grown under submerged culture using activity-guided purification procedures against human breast adenocarcinoma MCF-7 cells. TLC and HPLC were used for the determination of the two steroids. NMR and MS results suggested the two steroids were ergosterol peroxide (EP) and 9(11)-dehydroergosterol peroxide (9(11)-DHEP).

2.2 Materials and Methods

2.2.1 Chemicals and reagents

Sodium bicarbonate, sodium pyruvate, trypsin, ethylenediaminetetraacetic acid (EDTA), Vitamin B and dimethylsulfoxide (DMSO) were purchased from Sigma. Yeast extract and peptone were obtained from BD Co.. Fetal bovine serum (FBS), fungizone (amphotericin B 250 μ g/ml), Triton X-100, phosphate buffered saline (PBS), penicillin (10,000unit/ml)-streptomycin (10,000 μ g/ml) were obtained from Invitrogen Chemical Co. 3-(4,5-dimethyl-thiazoly-2-yl)-2,5-diphenyl tetrazolium bromide (MTT) and RPMI-1640 medium were obtained from ICN. Glucose and acetone were bought from BDH. Sequit-blot PVDF membrane (0.2 μ m) was bought from Bio-Rad. Culture flasks (25cm² and 75cm²) and 96-well tissue culture plate were obtained from Falcon. Ethanol, methanol, hydrochloric acid (HCl) and isopropanol were obtained from Merck. Petroleum ether, ethyl acetate and sulfuric acid (H₂SO₄) were obtained from Ajax Co. Hexane was obtained from Tedia Co.

2.2.2 Submerged culture of *Ganoderma lucidum*

Ganoderma lucidum (Leyss. ex Fr.) Karst was a gift from the Centre for International Services on Mushroom Biotechnology. During experimental work, the strain was maintained on petri dishes on potato dextrose agar (PDA) at 28°C. A shake flask culture was incubated in 500ml culture bottles, which contained 250ml of the medium. One liter of the medium consists of g/l: 35 g glucose, 5 g yeast extract, 5 g peptone, 1 g KH₂PO₄, 0.5 g MgSO₄·7H₂O and 0.05 g thiamin hydrochloride (Vitamin B₁); pH5.5 (Wagnera R, 2004). The inoculum for a liquid substrate consisted of eight agar block (about 1 cm²) of a 7 days old culture from PDA. The flasks were incubated on rotary shaker under the conditions of 150 rpm/min and 30°C for 7 days.

2.2.3 Preliminary screening of antitumor fractions from *Ganoderma lucidum*

The *Ganoderma lucidum* mycelia were separated from culture medium by vacuum filtration after the incubation period, washed with distilled water several times. The mycelia and culture media of *Ganoderma lucidum* were freeze-dried at -80°C and then extracted as the following procedure (Figure 2.1).

Fresh mycelia of *Ganoderma lucidum* were lyophilized and milled using a vibration mill. The powder (413g) was extracted with 70% EtOH. Then we made the EtOH crude extracts partitioned with chloroform and water. After concentration, two crude fractions were extracted from the mycelia: the chloroform fraction and the water fraction.

For the culture medium, lyophilized culture medium was resolved in some water. By adding 3 times volume 100% EtOH, the polysaccharide was precipitated from the medium. The non-polysaccharide fraction was further partitioned with petroleum ether (PE) and ethyl acetate (EA) in turn. Finally, we got four crude fractions from the culture medium: the polysaccharide fraction, the PE fraction, the EA fraction and the non-polysaccharide water fraction.

The antitumor activities of all the crude fractions were assessed in the human breast cancer cells (MCF-7) by MTT assay.

2.2.4 The purification of antitumor compound from *Ganoderma lucidum* mycelia

Then the chloroform extracts were chromatographed on a column of normal phase silica gel column. Elution was started with hexane-acetone (50:1, 8:1, 4:1 to 2:1) and then acetone-methanol (2:1) yielded 7 fractions. The antitumor activities of

all the fractions were assessed in the human breast cancer cells (MCF-7) by MTT assay. The crude extracts showing potency in preliminary antitumor screening procedures are selected for antitumor activity-guided fractionation to isolate the active metabolites. Analytical thin-layer and high-pressure liquid chromatography (HPLC) techniques are used to help determine optimal solvent systems for the maximal separation of active components of fraction.

According to the results of the preliminary antitumor screening, fraction IV showed the most antitumor activities of the all fractions. So fraction IV was rechromatographed on LiChroprep® RP-18 pre-packed column (40-63 μ m) (310mm length, 25mm diameter) (Merck Corporation, German). Finally EP and 9(11)-DHEP were identified as following steps. Measurements of ¹H-NMR spectra, including two-dimensional NMR experiments, *i.e.* double quantum filtered-correlation spectroscopy (DQF-COSY), heteronuclear multiple bond correlation (HMBC), were performed on superconducting Fourier transform nuclear magnetic resonance spectrometry (Varian^{INOVA} 500NB, USA). Mass spectrum was obtained on LC/MS 4000QTrap system (Applied Biosystems Cor. USA). IR spectrum was obtained on EQUINO \times 55. UV absorbance was performed on UV530 (Thermo Electron Cor., USA).

2.2.5 High performance liquid chromatography (HPLC) analysis

Chromatographic separation was achieved on a reversed-phase C₁₈ column (Symmetry shieldTM RP₁₈, 5 μ m, 2.1x150mm I.D., Water Incorporation). The liquid chromatographic system (Waters 2695 Separation Module system) consisted of a Waters 2695 system, PDA and equipped with an autosampler and a Waters model 996 photodiode array detector.

The mobile phase consisted of ACN (eluant A) and water (eluant B). It was

continuously started at 75% ACN from time 0 to 15min. The flow rate was 0.5ml/min. The two steroids were eluted by gradient 75%--80% acetonitrile in mill-Q water at 0.5ml/min flow rate. UV-VIS absorbance spectra from 200 to 400nm were collected continuously during the course of each chromatogram. Analysis was performed at room temperature.

2.2.6 Studies on the anti-proliferation activities of the crude fractions

2.2.6.1 Cell culture

The human cell lines selected for this study included colorectal adenocarcinoma Colo201 cells and SW620 cells, hepatocellular carcinoma HepG2 cells, breast adenocarcinoma MCF-7 cells, fibrocystic disease MCF-10-2A cells, esophageal squamous cell carcinoma KYSE cell and malignant melanoma A375 cells. The cells of MCF-10-2A, KYSE and A375 were obtained from American Type Culture Collection (ATCC), while the cells of Colo201, HepG2 and MCF-7 were kindly provided by Dr. Ooi of Biology Department in CUHK.

HepG2 and MCF-7 cells were cultured in RPMI-1640 supplemented with 2.01g/L sodium bicarbonate and 2mM L-glutamine. Colo201 cells were cultured in RPMI-1640 medium supplemented with 1.5g/L sodium bicarbonate, 4.5g/L glucose, 2mM L-glutamine, 10mM HEPES buffer and 1mM sodium pyruvate. A375 malignant melanoma cells and esophageal squamous cell carcinoma KYSE cells were cultured in DMEM medium supplemented with 2.01g/L sodium bicarbonate and 2mM L-glutamine. MCF-10-2A cells were cultured in Ham's F12 medium supplemented with 20 ng/ml epidermal growth factor, 0.01 mg/ml insulin and 5% horse serum. Cells were routinely cultured in an appropriate essential medium supplemented with 10% heat-inactivated FBS, 1% penicillin and streptomycin solution and 0.1% fungizone. They were grown at 37°C in a humidified atmosphere

with 5% CO₂. The cultured cells were propagated in cell culture flasks at desired density with three times a week.

Before each subsequent assay, cultured cells were seeded with desired cell density and pre-incubated for 24 hours at 37°C in a humidified atmosphere with 5% CO₂.

2.2.6.2 Sample preparation

EP and 9(11)-DHEP were freshly dissolved in and filtered by a syringe filter with a 0.20µm PVDF membrane (Gelman Laboratory). In the subsequent assays, the two steroids were further diluted to desired concentrations. The final concentration of EtOH was 0.05% (v/v).

2.2.6.3 MTT assay

MTT assay is based on the ability of mitochondrial dehydrogenases in viable cells to convert soluble yellow tetrazolium salt (MTT) to form a dark blue formazan product. According to the method of Son *et al.* (2003) with some modifications, cells undergoing exponential growth were suspended in fresh medium at a concentration of 1.25×10^4 cells/ml and were seeded onto 96-multiwell plate (100µl/well). After 24h pre-incubation, exponentially growing cells were treated with a final concentration of 0-50ug/ml steroids for additional 24, 48 and 72h. In the negative control, cells were treated in 0.05% EtOH (v/v) instead of steroids. After treatment, 20µl/well of MTT solution (5mg/ml in PBS) was added and further incubated for 5h. The culture medium was then discarded and 150µl acidic isopropanol (0.04M HCl in isopropanol) was added to dissolve the formazan crystals. Absorbance at 570nm was taken by 96-well microplate spectrophotometer (SpectroAmax™ 250). The growth inhibitory activity was expressed as percentage (%) of inhibition in treatment group relative to

the control group (Equation 2.1).

$$\% \text{ inhibition} = \left(1 - \frac{A_{\text{treatment}}}{A_{\text{control}}}\right) \times 100\% \quad (2.1)$$

where $A_{\text{treatment}}$: absorbance of treatment group

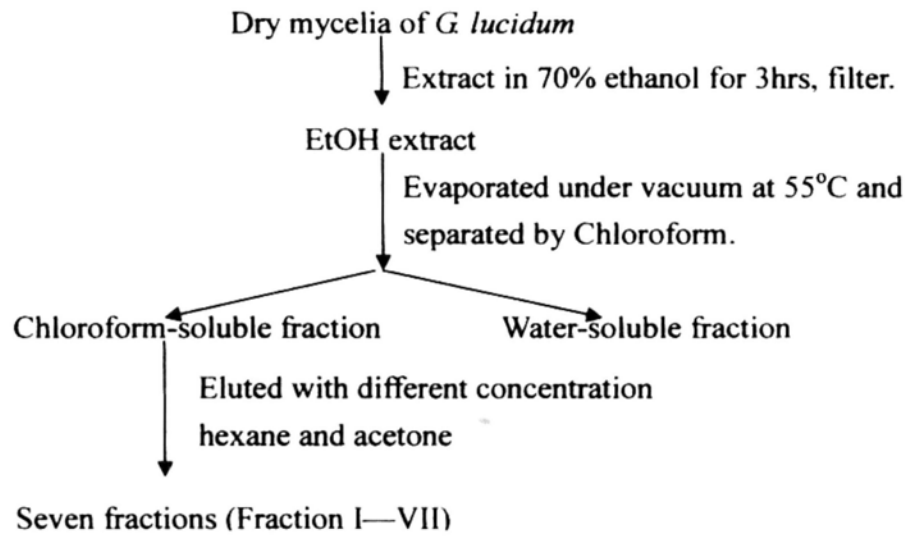
A_{control} : absorbance of control group

2.2.6.4 Determination of 50% effective concentration (IC₅₀)

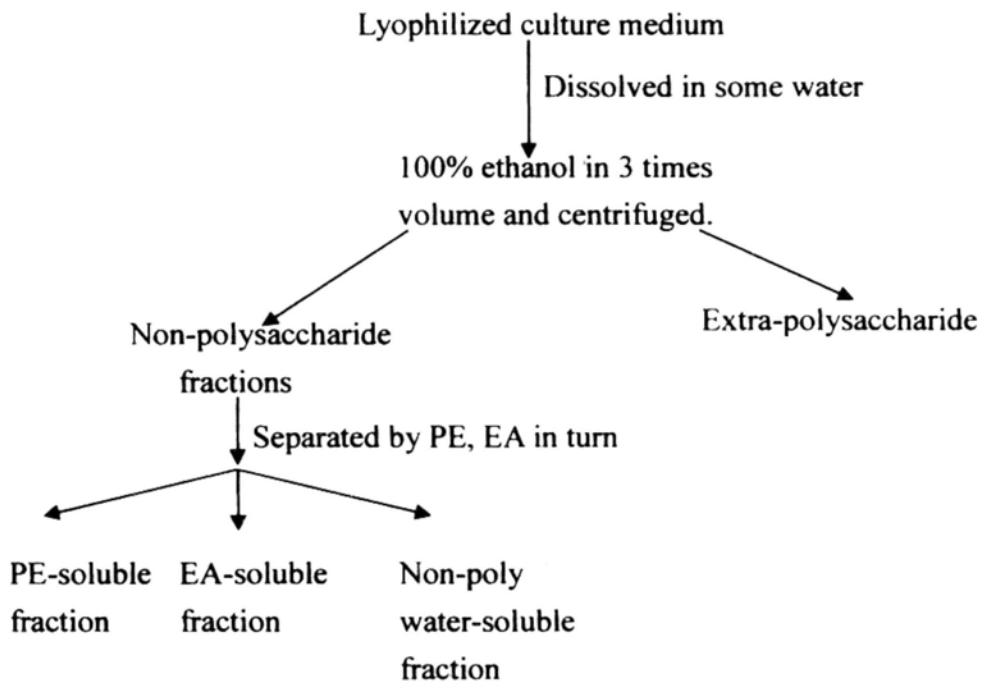
Colo201, A375, HepG2 and MCF-7 cells were treated with the different crude fractions of different concentrations. The IC₅₀ was determined in MTT assay and was defined as 50% of the maximum cytotoxic response as compared with control group. The IC₅₀ concentration was obtained from linear regression of analysis ($r^2 > 0.95$).

2.2.6.5 Statistical analysis

All samples were determined in triplicate and results were expressed as mean \pm standard deviation (SD). Statistical analysis was performed using a two-tailed Student's *t*-test. Differences with $P < 0.05$ were considered statistically significant.



(a)



(b)

Figure 2.1 The procedure of antitumor substance purification from *Ganoderma lucidum* mycelia (a) and culture media (b)

2.3 Results

2.3.1 Preliminary screening of antitumor activities of crude fractions from *Ganoderma lucidum*

In a typical experiment, *G. lucidum* mycelia powder (413g) and lyophilized medium was extracted as described in Materials and Methods. We investigated the effects of the crude extracts on the proliferation of human cancer cells and normal cells evaluated by MTT assay. IC_{50} were used to express the result after 72h treatment with the sample. The antitumor activities of different crude extracts of *Ganoderma lucidum* showed that the solvent extracts of the mycelia and medium were most effective (Table 2.1), suggesting that small molecular compounds such as triterpenes, steroid, may play a key role in antitumor activities of *Ganoderma lucidum in vitro*. The water fraction and polysaccharide of *Ganoderma lucidum* exhibited no *in vitro* antitumor activity (Table 2.1). However, the amount of the PE fraction extracted from culture medium was too low to be purified. Finally we have chosen the chloroform fraction of mycelia for the further purification.

In preliminary screening studies against a panel of human cancer cells, all the human cancer cells were found susceptible to the chloroform extract of *Ganoderma* mycelia except for the non-tumorigenic MCF-10A-2 cells (Table 2.3).

2.3.2 Purification and identification of EP and 9(11)-DHEP from *Ganoderma lucidum* mycelia

Based on the preliminary antitumor fraction screening, we managed to purify the antitumor metabolite from the solvent extract of the mycelia. Seven fractions were collected from silica gel chromatographic separation of the chloroform extract (31.76g). We obtained a fraction with great antitumor activity on human breast cancer MCF-7 cells from the chloroform extract of *Ganoderma lucidum* mycelia as

previous described. As the Table 2.2 shown, fraction IV has the highest antitumor activity against MCF-7 cells with IC_{50} at about $20.12\mu\text{g/ml}$. The fraction IV, which eluted with hexane/acetone 8:1, was applied to a RP-18 pre-packed column for further purification. This fraction was further subjected to reversed-phase chromatographic separation and two compounds (A and B) with antitumor activities against MCF-7 cells were obtained with a yield of 101.2mg (0.025%) and 69.1 mg (0.017%) respectively. The purity of these two compounds was analyzed by HPLC (Figure 2.2).

The molecular formula of compound A was $C_{28}H_{44}O_3$; positive ion electrospray mass spectrometry was observed at m/z : $451.3(M + Na)^+$, $429.3(M + H)^+$, $410(M - H_2O)^+$, 393 , 375.5 , 265.4 , 249 . The pattern of the mass spectrum was similar to that of 9(11)-DHEP: $427.5(M + H)^+$, $409(M - H_2O)^+$, $391.4(M - O_2)^+$, $375.2(M - O_2 - H_2O)^+$, 251.4 . The lower of 2 mass units in the molecular weight of compound B suggested the presence of an additional double bond in the molecular. Table 2.4 showed the NMR analysis results of compound A and B.

Based on the results above, we proposed the two steroids are ergosterol peroxide (compound A) and 9(11)-dehydroergosterol peroxide (compound B).

Table 2.1. The antitumor activities of different crude extracts of *Ganoderma lucidum* mycelia and culture medium on MCF-7 cancer cells by MTT assay

	<i>Fractions</i>	<i>IC₅₀(ug/ml)</i>
Mycelia	Chloroform	71.06±4.31
	Water	>200
Culture medium	PE	16.43±4.31
	EA	>200
	Polysaccharide	>200
	Non-polysaccharide	>200

The IC₅₀ concentrations represented the concentration which results in 50% inhibition of cell growth after incubation. Results are expressed as mean value of three independent experiments.

Table 2.2. The antitumor activities of different fractions purified from chloroform extract of *Ganoderma lucidum* mycelia on MCF-7 cancer cells by MTT assay

<i>Solvent system</i>			<i>IC₅₀(ug/ml)</i>	
Hexane/acetone	50:1	Fraction I	119.50±8.02	
		Fraction II	30.45±4.57	
		Fraction III	55.09±2.51	
	8:1	Fraction IV	20.22±2.81	
		4:1	Fraction V	93.29±3.03
			Fraction VI	>200
Acetone/methanol	2:1	Fraction VII	>200	

The IC₅₀ concentrations represented the concentration which results in 50% inhibition of cell growth after incubation. Results are expressed as mean value of three independent experiments.

Table 2.3. Preliminary antitumor activity screening on different cell lines

	<i>IC₅₀</i> (ug/ml)	
	Chloroform fraction	Fraction IV
MCF-7	71.06±4.31	20.22±2.81
HepG2	40.26±3.26	13.57±2.30
Colo201	63.83±5.01	18.09±1.31
A375	56.19±2.17	12.68±1.03
MCF-10A-2	> 100	> 100

The IC_{50} concentrations represented the concentration which results in 50% inhibition of cell growth after incubation. Results are expressed as mean value of three independent experiments.

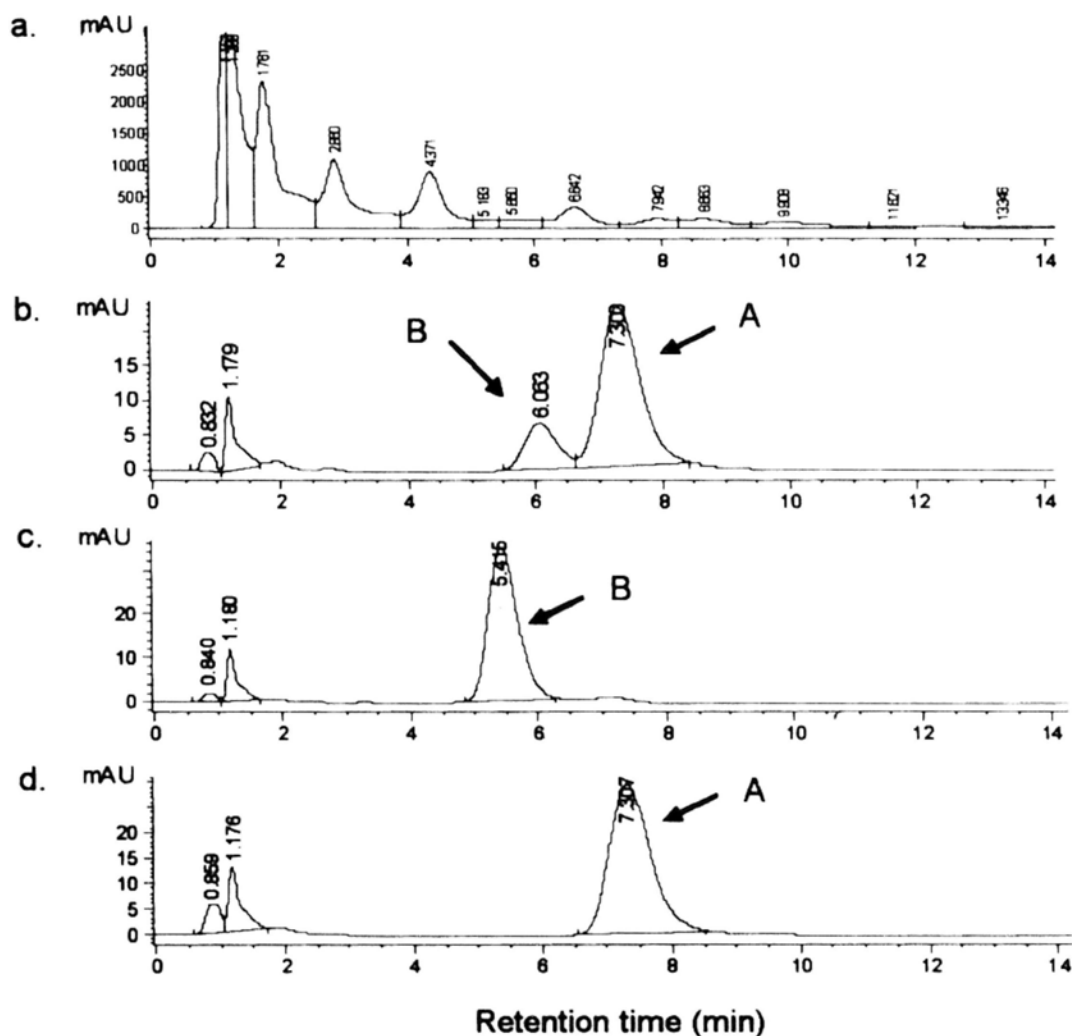
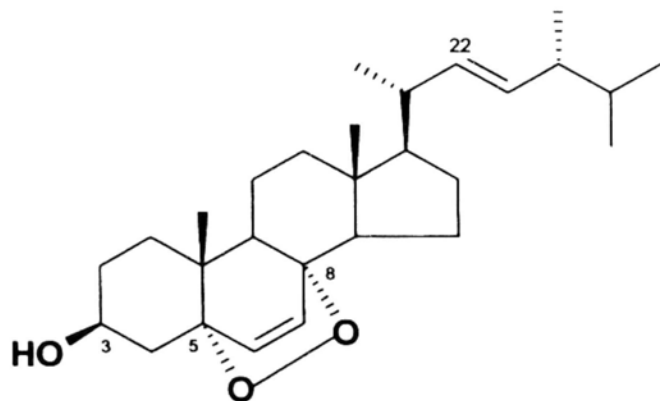
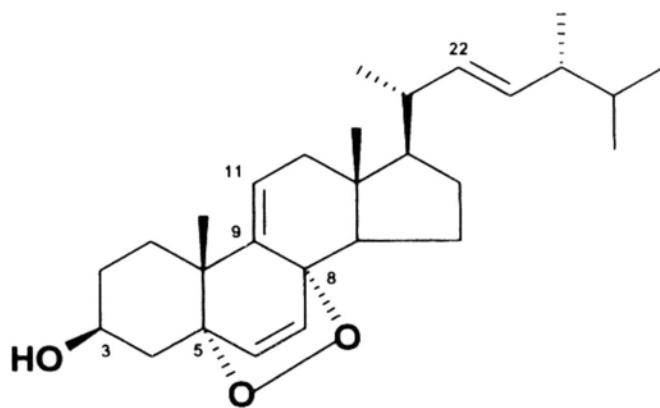


Figure 2.2. The extraction procedure of major compounds detected by HPLC analysis. Different fractions were analyzed by C-18 reverse silica column (Waters) and were eluted by gradient 75%--80% acetonitrile in mill-Q water at 0.5ml/min flow rate. a. Chloroform crude extract; b. Fraction IV of first silica gel chromatography; c. Compound B purified from fraction IV, it was eluted at 5.476min; d. Compound A purified from fraction IV, it was eluted at 7.303min



A



B

Figure 2.3. The structures of the two steroids isolated from *G lucidum* mycelia : **A**,[†] ergosterol peroxide (EP); **B**, 9(11)-dehydroergosterol peroxide (9(11)-DHEP).

Table 2.4. ^1H and ^{13}C spectral data of compound A and B isolated from *G. lucidum* mycelia.

Position	Compound A (in CDCl_3)		Compound B (in CDCl_3)	
	^1H (δ , multiplicity, J (Hz))	^{13}C (δ)	^1H (δ , multiplicity, J (Hz))	^{13}C (δ)
1		34.7		33.1
2		30.0		32.5
3	3.96 m	66.4	4.01 m	66.3
4		36.9		36.1
5		82.1		82.7
6	6.24 d 8.5	135.4	6.29 d 8.5	135.4
7	6.50 d 8.5	130.7	6.60 d 8.5	130.7
8		79.4		78.4
9		51.1		142.6
10		36.8		37.9
11		23.4	5.41 dd 6.0 2.0	119.7
12		39.3	2.03 m 2.27 dd 17.0 6.0	41.2
13		44.5		43.6
14		51.7		48.2
15		20.6		29.1
16		28.6		20.9
17		56.2		55.9
18	0.82 s	12.9	0.74 s	12.9
19	0.88 s	18.1	1.10 s	25.5
20		39.7	1.96 m	39.9
21	1.00 d 6.5	20.9	1.01 d 6.5	20.7
22	5.14 dd 15.0 8.5	135.2	5.16 dd 15.3 8.3	135.1
23	5.22 dd 15.0 7.5	132.3	5.25 dd 15.3 8.0	132.4
24		42.8		42.8
25		33.0		33.0
26 or 27		19.6		19.6
26 or 27		19.9		19.9
28	0.91 d 7.0	17.5	0.92 d 6.5	17.5

All the data were referred to the Appendix 1-10.

2.4 Discussion

Ganoderma steroid is another major group of low molecular weight secondary metabolites of this fungus except for triterpenes. There are 20 steroids isolated from this fungus so far. They abundantly present in the cholesterol type and ergosterol type. Ergosterol is a membrane component of fungal cell. It is a major fungal steroid and has been reported in concentrations of 0.3-0.4% in Reishi. Ergosterol peroxide, a presumed product of the H₂O₂-dependent enzymatic oxidation of ergosterol, may play a role in the detoxication reaction of reactive oxygen species (Bates ML, *et al.*, 1976) and in the host infection by pathogenic fungi (Sgarbi DB, *et al.*, 1997).

In the ¹³C-NMR spectrum of compound A (Table 2.4), two of four olefinic carbon signals at δ 135.4, 135.2, 132.3 and 130.7 ppm showed the presence of two olefins in its structure. The simple doublet olefin protons at δ 6.50 ($J = 8.5$ Hz) and 6.24 ($J = 8.5$ Hz) showed further *cis* olefin couplings by protons. The relative down-field shifted carbon signals at δ 82.1 and 79.4 ppm suggested the peroxide residue was related to the above olefin. The doublets of doublet olefin protons at δ 5.22 ($J = 7.5, 15.0$ Hz) and 5.14 ($J = 8.5, 15.0$ Hz) implied *trans* olefin coupled with a methyl proton, respectively. In accordance with the presence of six methyls and the molecular formula, the structure of compound A was identified as ergosterol peroxide (EP). The compound B showed a proton signal at 5.41 ppm except for coupled H6-H7 and H22-H23 pairs in the lower field region, which suggested that there may be an additional double bond in its structure. The lower field shift of C9 to δ 142.6 ppm and the olefinic carbon signals at C11 (δ 119.7 ppm) revealed that the extra double bond was at C9-C11. A comparison of ¹H- and ¹³C-NMR spectral data of compound B with that of compound A indicated that compound B was 9(11)-dehydroergosterol peroxide (9(11)-DHEP). Figure 2.3 shows the chemical structures of EP and 9(11)-DHEP.

EP is one of the nine rare sterols which were previously isolated from marine invertebrates such as tunicate, common pillar coral, sponge and sea hare (Gunatilaka AA Leslie, *et al.*, 1981). It has been reported that 8g ergosterol and 150mg ergosterol peroxide were extracted from 8kg fruiting bodies of *Ganoderma lucidum* (Arisawa M, *et al.*, 1986). In our study, EP and 9(11)-DHEP were purified from the *Ganoderma mycelia* and found to reach 0.024% and 0.017% in *Ganoderma lucidum mycelia*, respectively. The extraction rate of EP were 245ug/g dried weight mycelia, greatly higher than the yield reported above of it extracted from fruiting bodies of *G lucidum* (18.75ug/g).

In my study, EP and 9,11-DHEP are extracted from *Ganoderma lucidum mycelia* for the first time. Our result also showed that the two compounds are the major fractions of the mycelia, which were responsible for the antitumor activities of *Ganoderma lucidum mycelia*.

Chapter III *In vitro* antitumor activities of ergosterol peroxide and 9(11)-dehydroergosterol peroxide from *Ganoderma lucidum* in different human cancer cell lines

3.1 Introduction

Ganoderma lucidum is considered as a natural medicine that promotes longevity and maintains the vitality of human beings. *Ganoderma lucidum* are widely sold as nutritional supplements in combination with conventional chemo/radiotherapies for cancer treatment. It is documented that *Ganoderma lucidum* have antitumor activities on different cancer.

Breast cancer is the second leading cause of cancer deaths in women today (after lung cancer) and is the most common cancer among women, excluding nonmelanoma skin cancers. Studies showed that *Ganoderma lucidum* extracts could significantly inhibit human breast cancer cell proliferation and invasion, which were regulated by the NF- κ B signaling pathway. (Yue GG, et al., 2006; Jiang JH, et al., 2006; Thyagarajan A, et al., 2007). For liver cancer, *Ganoderma lucidum* has been widely used for the treatment of chronic hepatopathy. The hepatoprotective activity of peptides from *Ganoderma lucidum* (GLP) was evaluated against d-galactosamine (d-GalN)-induced hepatic injury in mice (Shia YL, et al., 2008). Previous studies indicated that polysaccharides of *Ganoderma lucidum* could effectively prevent ethanol induced hepatic damage in mice (Zhou et al., 2002). The triterpenoids isolated from *Ganoderma lucidum* also showed protective effects against liver injury induced by CCl₄, d-GalN and Bacillus Calmette-Guerin (BCG) plus lipopolysaccharide (LPS) *in vivo* (Wang et al., 2000). Ganoderenic acid A, one of the

triterpenoids found in *Ganoderma lucidum*, was proven to be a potent inhibitor of β -glucuronidase activity, an indicator of hepatic damage (Kim et al., 1999). For colon cancer, both polysaccharide and triterpene of *Ganoderma lucidum* significantly inhibited the proliferation of colon cancer SW 480 cells (Xie JT, et al., 2006)

Substantial attention has been given to primary cancer prevention in daily life. Dietary factors are thought to contribute to as much as one-third of the factors influencing the development of cancer. Phytosterol are one of important chemipreventive compounds in nature. They were found to act at various stages of tumor development, including inhibition of tumorigenesis, tumor promotion, invasion of tumor cells and metastasis (Ovesná Z, et al., 2004). One of the bioactive components of *Ganoderma lucidum* is Ganoderma steroids, which attract our specific attention. Our interest has been focused especially on their anti-tumor and chemopreventive activity. In the present study, 9(11)-DHEP and EP are purified from *Ganoderma lucidum* mycelia. Both of the two Ganoderma steroids are important derivatives of ergosterol. Ergosterol is the basic building block of vitamin D in plants. When ultraviolet light from the sun hits the leaf of a plant, ergosterol is converted into ergocalciferol, or vitamin D₂. Vitamin D is one of well-studied steroids. Vitamin D, its active form, 1,25-dihydroxyvitamin D₃ [1,25(OH)₂D₃] and analogs have important antitumoral properties (Townsend K, et al., 2005), which might be explored in chemopreventive as well as in therapeutic cancer approaches. (Bortman P, et al., 2002). Induction of apoptotic features in response to vitamin D has been demonstrated in breast, colon, and prostate cancer cells as well as in melanoma, myeloma, and glioblastoma cells *in vitro* (Hansen CM, et al., 2001). Besides having antiproliferative properties, vitamin D might also reduce the invasiveness of cancer cells and act as an anti-angiogenesis agent. The similarities of chemical structure of

these steroids predict their similar biological activities. EP and 9(11)-DHEP can inhibit HL60 cancer cells and HT29 colon cancer cells by inducing apoptosis (Takei T, et al., 2005; Kobori M, et al., 2006b). However, their molecular mechanisms of action have not yet to be determined.

In the following study, our results showed that both of the two steroids could induce apoptosis on different cancer cell lines, including breast cancer MCF-7 cells, liver cancer HepG2 cells, colon cancer Colo201 cells, esophageal squamous cell carcinoma KYSE cells.

3.2 Materials and Methods

3.2.1 Chemicals and reagents

N-(2-Hydroxyethyl)piperazine-N'-(2-ethansulfonic acid) hemisodium salts (HEPES) solution, sodium bicarbonate, sodium pyruvate, trypsin, ethylenediaminetetraacetic acid (EDTA), ribonuclease A (Type I-A), bovine serum albumin (BSA), propidium iodide (PI), dimethylsulfoxide (DMSO), β -mercaptoethanol, glycerol, bromophenol blue, glycine and paraformaldehyde were purchased from Sigma. Dulbecco's modified Eagle's (DMEM) medium, Leibovitz's L-15 medium, fetal bovine serum (FBS), fungizone (amphotericin B 250 μ g/ml), Triton X-100, phosphate buffered saline (PBS), penicillin (10,000unit/ml)-streptomycin (10,000 μ g/ml) and DNase (grade 1) were obtained from Invitrogen Chemical Co. 3-(4,5-dimethyl-thiazoly-2-yl)-2,5-diphenyl tetrazolium bromide (MTT) and RPMI-1640 medium were obtained from ICN. Glucose was bought from BDH. SDS was bought from Bio-Rad. Culture flasks (25cm² and 75cm²) and 8-chamber polystyrene vessels (tissue culture treated glass slide) were obtained from Falcon. The lumi-film chemiluminescent detection film, cell proliferation ELISA-BrdU (chemiluminescence) assay kit, *in situ* cell death detection kit (fluorescein) and annexin-V-FLUOS staining kit were bought from Roche Molecular Biochemicals. Ethanol, methanol, hydrochloric acid (HCl) and isopropanol were obtained from Merck. Sodium citrate, Tris-HCl and acrylamide/bis (37.5:1, 40%) solutions were purchased from JT Baker. Antibody of β -actin was purchased from BD Biosciences PharMingen, USA. Antibodies for anti-cleaved PARP (Asp214), anti-PARP, anti-Bax, anti-Bad, anti-Bak, anti-puma, anti-Bcl-2, anti-Bcl-xl, anti-Mcl-1 and anti-cleaved caspase 3 (Asp175), anti-caspase 6, anti-cleaved caspase 7 (Asp198), anti-caspase 8 and anti-caspase 9 were obtained from Cell signaling Co. (USA). Goat anti-rabbit IgG-conjugated to horseradish peroxidase (HRP) and goat

anti-mouse IgG-conjugated to HRP were purchased from Biovision (Mountain View, CA). Phototope[®]-HRP Western blot detection system was purchased from Cell Signaling Technology.

3.2.2 Sample preparation

EP and 9(11)-DHEP were freshly dissolved and filtered by a syringe filter with a 0.20µm PVDF membrane (Gelman Laboratory). The two steroids were further diluted to desired concentrations. The final concentration of EtOH was 0.05% (v/v).

3.2.3 Cell culture

Human colorectal adenocarcinoma Colo201, hepatocellular carcinoma HepG2, breast adenocarcinoma MCF-7 and esophageal squamous cell carcinoma KYSE cell lines were used in this study. KYSE cells were obtained from American Type Culture Collection (ATCC), while Colo201, HepG2 and MCF-7 cells were kindly provided by Dr. Ooi.

HepG2 and MCF-7 cells were cultured in RPMI-1640 supplemented with 2.01g/L sodium bicarbonate and 2mM L-glutamine. Colo201 cells were cultured in RPMI-1640 medium supplemented with 1.5g/L sodium bicarbonate, 4.5g/L glucose, 2mM L-glutamine, 10mM HEPES buffer and 1mM sodium pyruvate.

Cells were routinely cultured in appropriate essential medium supplemented with 10% heat-inactivated FBS, 1% penicillin and streptomycin solution and 0.1% fungizone. They were grown at 37°C in a humidified atmosphere with 5% CO₂. The cultured cells were propagated in cell culture flasks at desired density with three times a week.

Before each assay, cultured cells were seeded with desired cell density and pre-incubated for 24 hours at 37°C in a humidified atmosphere with 5% CO₂.

3.2.4 Studies on the anti-proliferation activities of EP and 9(11)- DHEP on different cancer cell lines

3.2.4.1 MTT assay

According to the method of Son *et al.* (2003) with some modifications, 100ul 1×10^5 human cancer cells/ml were plated in 96-well tissue culture plate and incubated for 24 h, then treated with different concentrations of EP and 9(11)-DHEP for different hours. Details were referred to Chapter II.

3.2.4.2 Cell proliferation ELISA-BrdU (chemiluminescence) assay

The 5-bromo-2'-deoxyuridine (BrdU) assay is a chemiluminescence immunoassay for the quantification of cell proliferation (Huong *et al.*, 1991; Porstmann *et al.*, 1985). For the BrdU assay, the first step is the same as MTT assay. After incubation at 37°C for 72h, 20µl BrdU was added to the cells and incubated again for 2h. The procedures were followed according to the manufacturer's instructions; finally, the chemiluminescence readings were measured by a microliter plate luminometer (ML3000). Results were expressed as the percentage (%) of inhibition in treatment group as compared to control: Inhibition (%) = $(1 - A_{\text{treatment}} / A_{\text{control}}) \times 100\%$, where $A_{\text{treatment}}$ means the absorbance of treatment group; A_{control} means the absorbance of control group.

3.2.4.3 Determination of 50% inhibitory concentration (IC₅₀)

Colo201, HepG2, KYSE and MCF-7 cells were treated with the two steroids of different concentrations. The IC₅₀ was determined in MTT and BrdU assays. IC₅₀ was defined as the microgram concentration of the two steroids, at which 50% of cell growth or cell proliferation was inhibited in relation to control, respectively. The IC₅₀

values were obtained from linear regression of analysis ($r^2 > 0.97$).

3.2.5 Apoptosis detection

3.2.5.1 TUNEL enzymatic labeling assay

DNA fragmentation can be directly determined with the *In Situ* Cell Death Detection Kit, Fluorescein (Roche Molecular Biochemicals) using fluorescence microscopy (Gold *et al.*, 2003; Sgonc *et al.*, 1994). The TUNEL (TdT-mediated dUTP nick end labeling) reaction is designed to detect and quantify apoptotic cell death at single cell level in cells and tissues, since TUNEL preferentially labels DNA strand breaks generated during apoptosis. According to manufacturer's instructions, Cells density of 6×10^3 cells/chamber was suspended in fresh medium and then seeded onto chamber slide. After 24h pre-incubation, cells were treated with 0-20ug/ml 9(11)-DHEP or EP. For the control group (negative control and positive control), 0.05% EtOH (v/v) was used instead of sample. After additional 72h incubation, cells were air dried and fixed with freshly prepared fixation solution (4% paraformaldehyde in PBS, pH 7.4) for 1h at room temperature. Slides were then rinsed with PBS (pH7.4) and were re-incubated in permeabilisation solution (0.1% Triton X-100 in 0.1% sodium citrate) for 2min at 2-8°C. Slides were further rinsed twice with PBS. Finally, the fixed and permeabilized cells were incubated with TUNEL reaction mixture containing nucleotide mixture and terminal deoxynucleotidyl transferase (TdT) for 60min in a humidified atmosphere at 37°C in darkness. In each experimental setup, both the negative control and the positive control were included. For the negative control, the fixed and permeabilized cells were incubated with nucleotide mixture in reaction buffer (without terminal transferase) instead of TUNEL reaction mixture. Prior to labeling procedures, DNA strand breaks were induced in positive control by incubating the fixed and

permeabilized cells with DNase I, grade 1 (1U/ml in 10mM Tris-HCl, pH7.5 containing 1mM magnesium chloride and 1mg/ml BSA) for 10min at room temperature. After labeling, slides were rinsed three times with PBS. The fluorescein labels incorporated in nucleotide polymers were directly analyzed under confocal laser scanning microscope (CLSM) (Bio-Rad). For the evaluation of fluorescence microscopy, an excitation wavelength at 488nm and emission wavelength at 515nm were used. Fluorescence images were collected using a Bio-Rad Radiance 2100 system with LaserShape2000 software (Bio-Rad).

3.2.5.2 Annexin-V-FLUOS labeling assay

Annexin-V-FLUOS labeling assay was performed by using Annexin-V-FLUOS staining kit (Roche Molecular Biochemicals) (Martin SJ, et al., 1995). According to manufacturer's instruction, 6×10^3 cells were suspended in fresh medium and the cells were seeded onto chamber slide for pre-incubation at 37°C. Cells were then treated with 0-20ug/ml 9(11)-DHEP or EP. In the negative control, cells were treated in 0.05% EtOH (v/v) instead of the steroids. After 72h re-incubation, medium was removed. Slides were rinsed with PBS (pH7.4) and were covered with 100 μ l/chamber of Annexin-V-FLUOS labeling solution (annexin-V-fluorescein in a HEPES buffer containing PI). Slides were further incubated for 10-15min at room temperature. After labeling, slides were directly analyzed under confocal laser scanning microscope (CLSM) (Bio-Rad). Fluorescence images were collected using a Bio-Rad Radiance 2100 system with the LaserShape2000 software (Bio-Rad). In order to evaluate annexin-V-fluorescein, an excitation wavelength at 488nm and emission wavelength at 515nm were used. On the other hand, an excitation wavelength at 488nm and emission wavelength at 617nm were used for PI.

3.2.6 Analysis of cell cycle progression by flow cytometry

With the use of flow cytometer and DNA specific fluorescence dye, DNA content can be measured at single cell level. Cells at different phases in cell cycle (G_0/G_1 , S, G_2/M) with difference of DNA content can be displayed in a flow cytometric diagram, these patterns give information on the cell cycle distribution and therefore the changes in cell cycle of a cell population can be analyzed. The DNA staining pattern can also be employed to confirm apoptosis.

Cell cycle distribution of Colo201, HepG2, KYSE and MCF-7 cells after treatment with 9(11)-DHEP or EP was monitored by flow cytometry. 6×10^5 cells were seeded onto 75cm^2 culture flask. After pre-incubation for 24h, cells were treated in the absent or presence of 9(11)-DHEP or EP at the concentrations between 0--30ug/ml and were incubated at desired time. 2×10^6 cells were harvested and fixed overnight at -20°C with 70%. Fixed cells were followed by washing twice with PBS (pH7.4) and centrifuge at 1500rpm for 5min to remove ethanol. Cells were further washed with 1% BSA and incubated in the dark at 4°C with propidium iodide (PI) staining mixture (1.21mg/ml Tris, 700U/ml RNase, $50.1\mu\text{g/ml}$ PI, pH8.0) overnight. Finally, stained cells were measured using Beckman Coulter Epics XL-MCL flow cytometer (Miami, FL). Cell cycle distribution profile was analyzed using MultiCycle software (Phoenix Flow Systems, San Diego, CA). The proportion of cells in G_0/G_1 , S, G_2/M phases was represented as DNA histogram. Apoptotic cells with hypodiploid DNA content were observed in cell cycle pattern.

3.2.7 Western immunoblotting and detection

3.2.7.1 Preparation of protein lysates

6×10^5 cells were seeded in 75cm^2 culture flask. After pre-incubation for 24h, exponentially growing cells were treated with 0--30ug/ml 9(11)-DHEP or EP for

additional desired incubation times. Cell number of 2×10^6 cells was harvested and was centrifuged at 1500rpm for 5min. Cell pellets were then resuspended with 50 μ l ice-cold lysis buffer (20mM Tris-HCl, pH8.0, 150mM NaCl, 5mM EDTA, 0.2% BSA and 1% Triton X-100) and incubated for 45min on ice. After centrifugation at 4°C for 15min at 14,000rpm, cell lysates were collected as supernatant and stored at -20°C until analysis.

3.2.7.2 SDS-polyacrylamide gel (SDS-PAGE)

Total cellular protein was determined by using the BCA assay kit (Sigma). Equal amounts of protein (50-100 μ g) were mixed with 2X sample loading buffer (0.0625M Tris-HCl, pH6.8, 2% SDS, 1% β -mercaptoethanol, 10% glycerol and 0.01% bromophenol blue) and heated at 95°C for 5min. The samples were resolved in 13% SDS-PAGE in electrode buffer (25mM Tris, 0.19M glycine and 0.1% SDS, pH 8.3) at 50V for 30min and followed at 100V for 90min. After electrophoresis, the gel was stained in colloidal coomassie solution (0.1% coomassie brilliant blue G-250, 34% methanol, 17% ammonium sulfate and 3% phosphoric acid) for 24h or further proceed the procedure of Western blot analysis in section 3.2.7.3.

3.2.7.3 Western blot analysis

The protein samples (in the gel) were blotted onto nitrocellulose membrane (Amesham bioscience, USA) using Mini Trans-Blot cell (Bio-Rad) and then transferred in Towbin buffer (25mM Tris, 0.2M Glycine and 20% methanol) at 100V for 90min. After transfer, the blotted membrane was first blocked in 0.2% Aurora blocking (w/v) with TBS/T (0.1% Tween-20, 20mM Tris, 137mM NaCl, and 1M HCl) for 1hr and incubated with primary monoclonal antibody (anti-cleaved PARP (Asp214), anti-Bax, anti-Bad, anti-Bak, anti-BID, anti-Bmf, anti-Bim, anti-puma,

anti-Bcl-2, anti-Bcl-xl anti-Mcl-1 and anti-cleaved caspase 3 (Asp175), anti-caspase 6, anti-cleaved caspase 7 (Asp198), anti-caspase 8 and anti-caspase 9 antibody (Cell signaling)) in desired dilution for 3hr at room temperature. The membranes were also probed with β -actin antibody in 1:5000 dilution to verify uniform protein loading across samples. This was followed by washing in TBS-T and then incubating with horseradish peroxidase (HRP)-conjugated secondary antibody (1:2000) and HRP-conjugated anti-biotin antibody (1:1000) (Cell signaling, Inc.) to detect biotinylated protein markers with gentle agitation for 1 hr at room temperature. After several washings, membranes were subjected to chemiluminescent Western detection with LumiGLO[®] reagent as described in the manual of Phototope[®]-HRP Western Blot detection system (Cell Signaling Technology, Inc.). The membranes were visualized by Digital Imaging System (Bio-Gene Technology Ltd.). Quantification was performed by densitometric analysis (Model GS-690 Imaging Densitometer) (Bio-Rad).

3.2.8 Statistical analysis

Dates were expressed as mean \pm standard deviation (SD) in three independently experiments. β -Actin was used as the internal control in Western blot. The amount of protein was expressed as arbitrary densitometric units of β -actin. The data were expressed as the relative density compared to their respective controls (untreated cells), taken as 1.0. Statistical analysis was performed using a two-tailed Student's *t*-test. Differences with $p < 0.05$ were considered statistically significant.

3.3 Results

3.3.1 9(11)-DHEP and EP inhibited the cell proliferation of different cancer cells

Effects of various concentrations of 9(11)-DHEP or EP on cancer cells growth were examined in different cancer cells by MTT assay. IC_{50} were used to express the result after 72h treatment with the sample. The IC_{50} (concentration causing 50% inhibition) of steroids on different cancer cell lines were determined and listed in Table 3.1. The results showed that 9(11)-DHEP selectively mediated growth inhibition on different cancer cells in a dose-dependent manner. For EP, it can greatly decrease all cancer cells growth. The rank of inhibitory activity with regard to IC_{50} was 4.42ug/ml in KYSE cells > 10.77ug/ml in SW620 cells > 12.93ug/ml in Colo201 cells > 14.04ug/ml in HepG2 cells > 16.80ug/ml in MCF-7 cells. In contrast, they were less toxic to the MCF-10A-2, a non-tumorigenic cell line. At the concentrations up to more than 50 μ g/ml, the two steroids did not significantly inhibit the growth of MCF-10A-2 cells.

Meanwhile, the inhibitory effects of the two steroids on different cancer cells also behaved in a time-dependent manner (Figure 3.1-3.4). Significant inhibition of both the two steroids on cell growth was started at 24h for all the observed cancer cell lines and after 48h treatment the viability of the cancer cells was suppressed above 50%.

To illustrate the antiproliferative effect of the two steroids, we investigated the inhibitory effects of the two steroids on the DNA synthesis of selected human cancer cells evaluated by BrdU assay. This is based on the measurement of 5-bromo-2'-deoxyuridine-labeled dUTP incorporation during DNA synthesis in proliferating cells. The maximum anti-proliferative response of EP and 9(11)-DHEP was observed after 72h of treatment. IC_{50} were used to interpret the result of the

sample (Table 3.2). The result suggested that both the two steroids could inhibit DNA synthesis in all the cancer cell lines (Figure 3.5). Results of MTT assay and BrdU assay showed that both of two steroids have the strongest inhibition on the Colo201 cancer cells. The concentration of EP and 9(11)-DHEP required inhibiting 50% of Colo201 cancer cells proliferation (IC_{50}) is $12.93\mu\text{g/ml}$ and $13.02\mu\text{g/ml}$ in MTT assay, and is about for $12.39\mu\text{g/ml}$ and $16.55\mu\text{g/ml}$ in BrdU assay, respectively.

3.3.2 Flow cytometry analysis on the different cancer cells treated with 9(11)-DHEP and EP

To investigate the mechanism by which the two steroids inhibited cancer cells growth, cell cycle analysis was performed with flow cytometry. The cancer cell line MCF-7 (Figure 3.6), HepG2 (Figure 3.8), Colo201 (Figure 3.11) and KYSE (Figure 3.14) were treated with different concentrations of 9(11)-DHEP and EP for 72hrs. The number of the cells in subG1 phase increased gradually in a dosage-dependent manner after 72hr treatment with the steroids in different cancer cells (Figure 3.7, Figure 3.9, Figure 3.12, and Figure 3.15). The total number of cells in subG₁ was increasing from the treatment of $10\mu\text{g/ml}$ EP; this percentage significantly rose to above 80% with the $20\mu\text{g/ml}$ EP treatment. These results suggested that the two steroids inhibit the cancer cell by inducing apoptosis. In addition, subG1 distribution results of HepG2 and Colo201 cancer cells treated with 9(11)-DHEP and EP showed that the cancer cells seemed to more sensitive to EP than them to 9(11)-DHEP.

The different cancer cells were treated with $20\mu\text{g/ml}$ 9(11)-DHEP or EP for 24h, 48h, and 72h. Results showed that both the two steroids could induce apoptosis of cancer cells in a time-dependent manner (Figure 3.10, Figure 3.13, and Figure 3.16). A significant increase on subG1 phase appeared in Colo201, HepG2 and KYSE cells

treated with 20ug/ml EP for 24h or treated with 20ug/ml 9(11)-DHEP for 48h. After 24h inhibition, the apoptotic cells of EP-treated increased dramatically. The subG1 cells increased from $5.09 \pm 0.69\%$ to $51.33 \pm 0.31\%$ on HepG2 cells, $2.92 \pm 0.52\%$ to $22.45 \pm 3.39\%$ on Colo201 cells and $6.66 \pm 0.67\%$ to $15.48 \pm 1.94\%$ on KYSE cells. The inhibition on different cancer cells was over 50% after 48h treatment with 9(11)-DHEP and EP.

3.3.3 Analysis of apoptotic morphology in HepG2 cancer cells treated with 9(11)-DHEP and EP

To understand characteristic of the apoptotic effect, human hepatoma HepG2 cancer cells were subjected to apoptosis assays, including TUNEL enzymatic labeling assay (*In situ* Cell Death Detection Kit, Fluorescein) and Annexin-V-FLUOS assay. Cells were cultivated with 9(11)-DHEP and EP in concentration of 0ug/ml, 10ug/ml, 20ug/ml for 72h. The results were represented as image under the confocal laser scanning microscope (CLSM).

The TUNEL enzymatic labeling assay measures apoptosis by direct labeling and detection of DNA strand breaks in individual cells. Those apoptotic cells are intensely stained green and are easily visible under fluorescence microscopy. This allows discrimination of apoptosis from necrosis and from primary DNA strand breaks induced by antitumor drugs and irradiation (Gorczyca *et al.*, 1993; Gavrieli Y, *et al.*, 1992). Compared with the negative control, apoptotic bodies were seen in the HepG2 cells by TUNEL staining treated with the two steroids above 10ug/ml as the Figure 3.17 showed. The results suggested that exposure to the two steroids caused cell death by apoptosis in HepG2 cancer cells.

Annexin V staining and propidium iodide (PI) accumulation were used to

determine the percentage of apoptotic cells as well as the morphological changes characteristic of this process. Early events in the apoptotic process are loss of plasma membrane asymmetry accompanied by translocation of phosphatidylserine (PS) from the inner to the outer membrane leaflet, thereby exposing PS to the external environment. The phospholipid-binding protein annexin V has a high affinity for PS and binds to cells labelled with fluorescence. In this research of Annexin-V-FLUOS assay, the green dye, Annexin-V, is used and serves as a marker for apoptotic cells. Simultaneously, the red dye, propidium iodide, is used for DNA staining. This can help to discriminate between early phase, late phase apoptosis and necrosis at single cell level (Vermes I, et al., 1995; Koopman G, et al., 1994). The Annexin V-/PI- population was regarded as normal healthy cells, while Annexin V+/PI- cells were taken as a measure of early apoptosis, Annexin V+/PI+ as late apoptosis, and Annexin V-/PI+ as necrosis. These results showed that the number of apoptotic cells increased concomitantly with dosage and that annexin V/PI double-positive cells also increased at 20µg/ml steroids. At 10ug/ml 9(11)-DHEP or EP, HepG2 cells were living and observed with low staining of annexin and PI (Figure 3.18 and Figure 3.19). Nevertheless, late apoptotic cells with high annexin and high PI staining were shown at 20µg/ml 9(11)-DHEP or EP (Figure 3.18 and Figure 3.19), which suggested that apoptosis was the major reason of the cancer cells death.

3.3.4 9(11)-DHEP and EP induced apoptosis of Colo201 cancer cells by mitochondria-mediated pathway

To investigate how the two steroids induce apoptosis of Colo201 cancer cells, the expressions of PARP, caspase family and Bcl-2 family were investigated in our work. Colo201 cancer cells were treated with EP for 24h or 9(11)-DHEP for 48h. The proteins were extracted and separated by 12% SDS-PAGE.

Our results indicated that the increase expression of cleaved PARP fragments (89kb) were observed in both the steroids treated cancer cells in a dosage-dependent manner (Figure 3.20). The PARP is the downstream product of caspase 3 and its cleavage suggested that the two Ganoderma steroids could induce apoptosis on Colo201 cancer cells.

Caspases, a family of cysteine acid proteases, are central regulators of apoptosis. Several caspase proteins were detected in Colo201 cancer cells treated by the two steroids. Results showed the effect of EP and 9(11)-DHEP on the expression of caspase-3, caspase-6, caspase-7, caspase-9 in Colo201 cancer cells. Both the two steroids noticeably stimulated the cleavage of caspase 3, 7, 9 in tumor cells in a dosage-dependent manner but not the caspase 8 (Figure 3.21). In addition, 9(11)-DHEP can also induce the cleavage of caspase 6. The result suggested that the apoptosis induced by the two steroids is caspase-dependent.

Meanwhile, the expressions of the Bcl-2 family of Colo201 cancer cells under the two Ganoderma steroids treatment were detected. Our result showed that the Bcl-2 protein was down-regulated in a dosage-dependent manner, whereas the expressions of Bcl-xl, Bad, Bax, Bak were not changed (Figure 3.22). The ratio of Bax and Bcl-2 was significant shift after EP and 9(11)-DHEP treatment (Figure 3.23 and Figure 3.24). In addition, 9(11)-DHEP could also induce the decrease expression of Mcl-1 (Figure 3.25) and the increase expression of Puma (Figure 3.26).

Table 3.1. Preliminary antitumor activity screening of 9(11)-DHEP and EP on different cell lines by MTT assay

	IC ₅₀ (ug/ml)	
	9(11)-DHEP	EP
HepG2	13.99±2.55	14.04±1.32
SW620	32.87±0.76	10.77±0.83
Colo201	13.02±0.34	12.93±0.57
MCF-7	16.89±1.40	17.22±1.31
KYSE	7.89±0.94	4.42±1.65
MCF-10-2A	67.89±2.64	72.69±2.70

The IC₅₀ concentrations represented the concentration which results in 50% inhibition of cell growth after incubation. Results are expressed as mean value ± SD of three independent experiments (p<0.05)

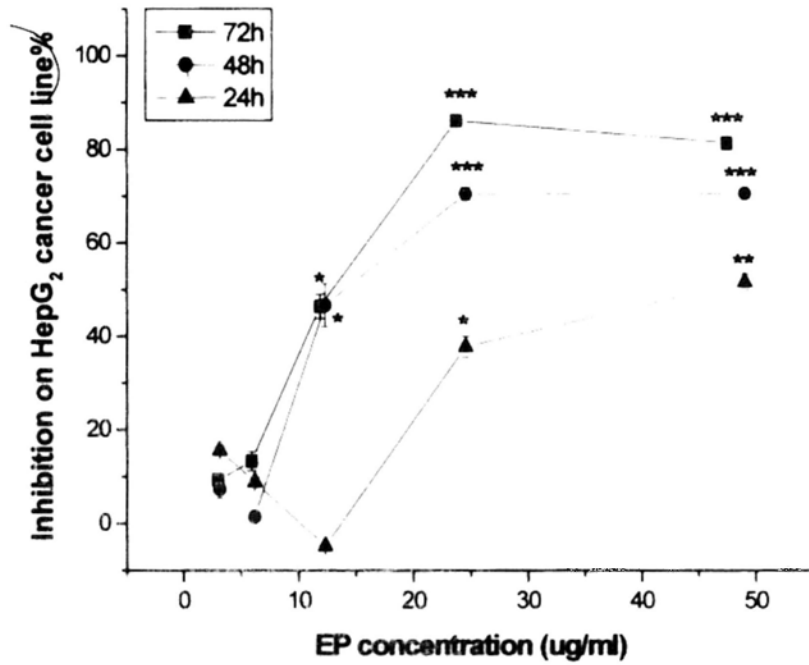
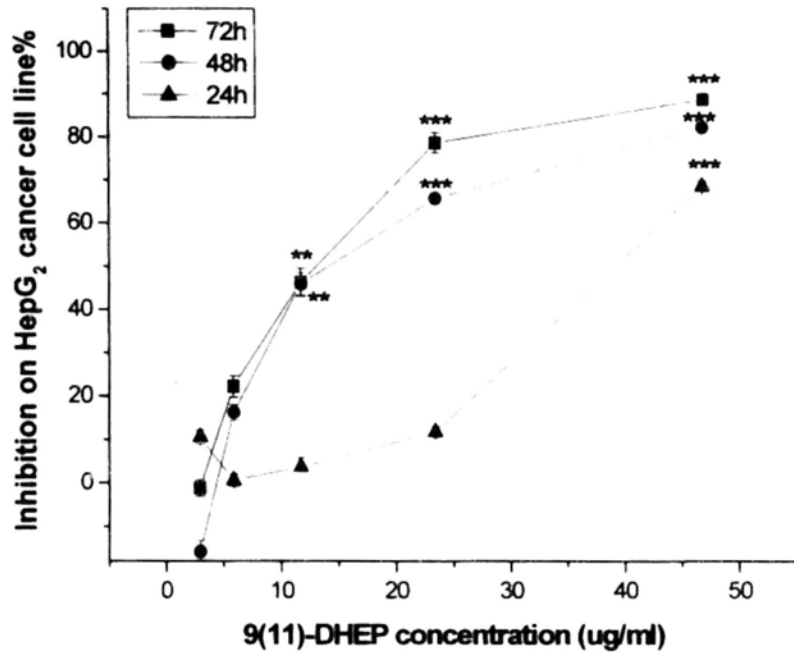


Figure 3.1. Inhibitory effects of 9(11)-DHEP and EP on HepG2 cancer cells in a time-dependent manner. Cells were treated with various concentrations of the two steroids for 72h; and cell viability was determined by the MTT assay. Results are expressed as percentages of proliferation compared to the control (mean \pm SD, n=3). Differences with $P<0.05$ (*), $P<0.01$ (**), $P<0.001$ (***) were considered significantly different.

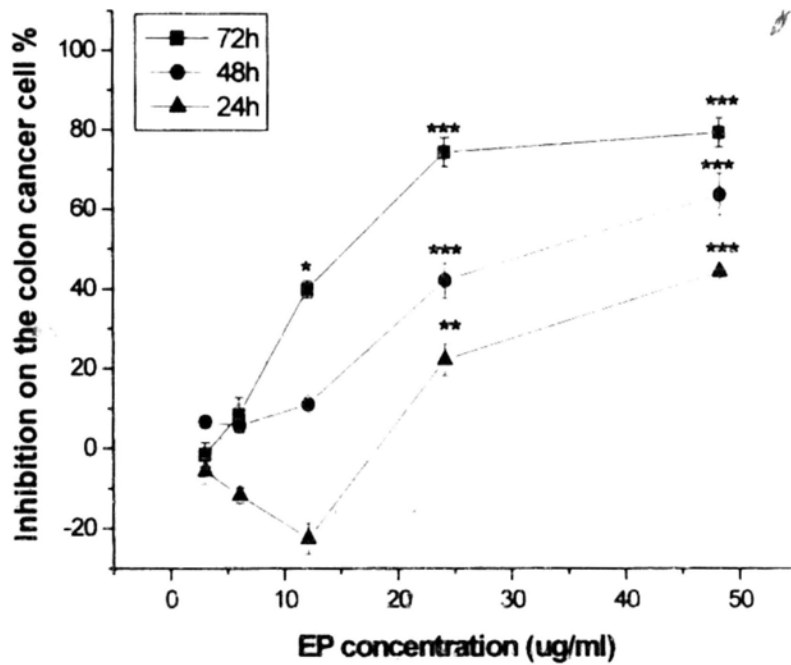
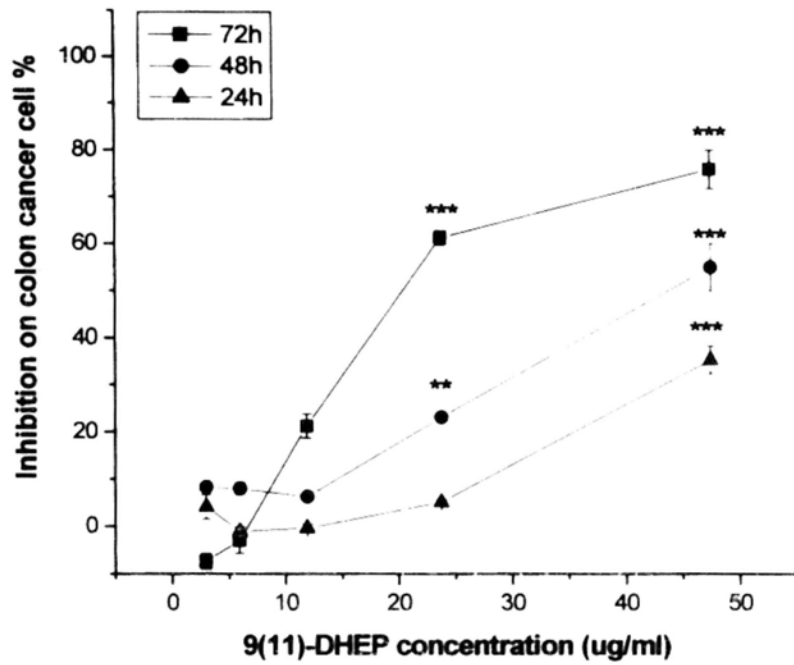


Figure 3.2. Inhibitory effects of 9(11)-DHEP and EP on Colo201 cancer cells in a time-dependent manner. Cells were treated with various concentrations of the two steroids for 72h; and cell viability was determined by the MTT assay. Results are expressed as percentages of proliferation compared to the control (mean \pm SD, n=3). Differences with $P < 0.05$ (*), $P < 0.01$ (**), $P < 0.001$ (***) were considered significantly different.

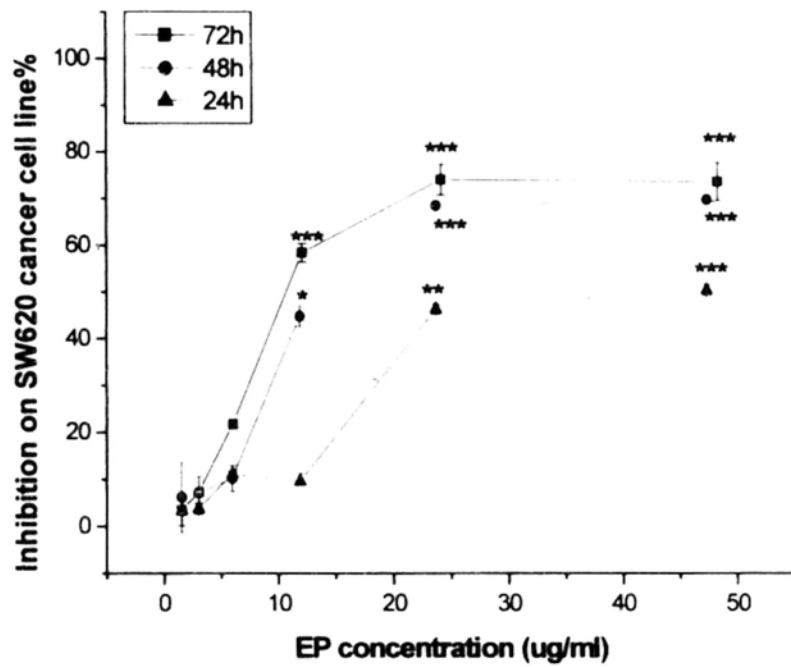
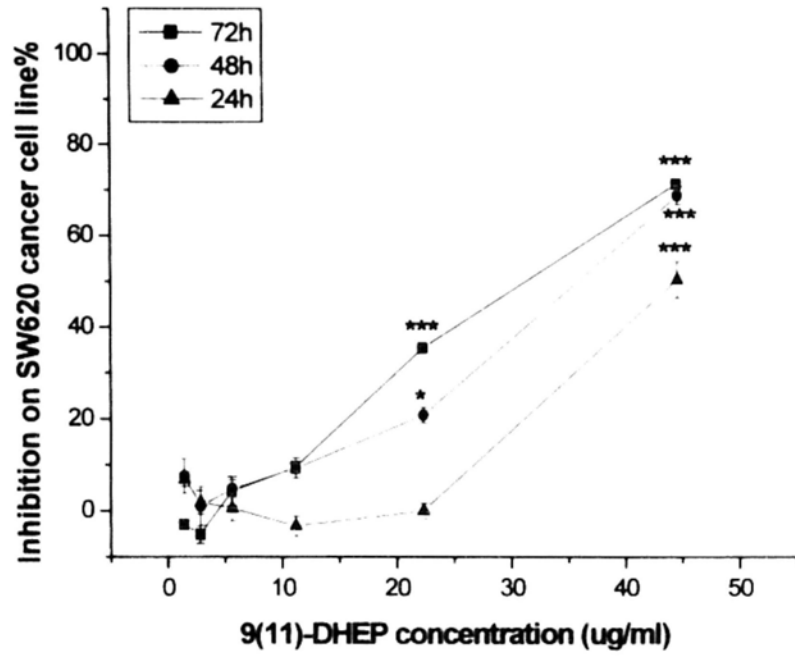


Figure 3.3. Inhibitory effects of 9(11)-DHEP and EP on SW620 cancer cells in a time-dependent manner. Cells were treated with various concentrations of the two steroids for 72h; and cell viability was determined by the MTT assay. Results are expressed as percentages of proliferation compared to the control (mean \pm SD, n=3). Differences with $P < 0.05$ (*), $P < 0.01$ (**), $P < 0.001$ (***) were considered significantly different.

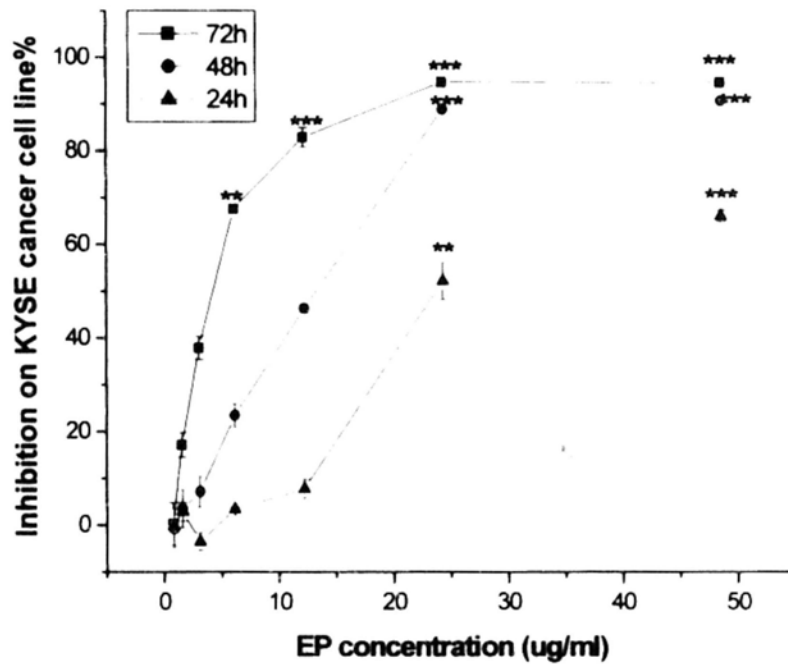
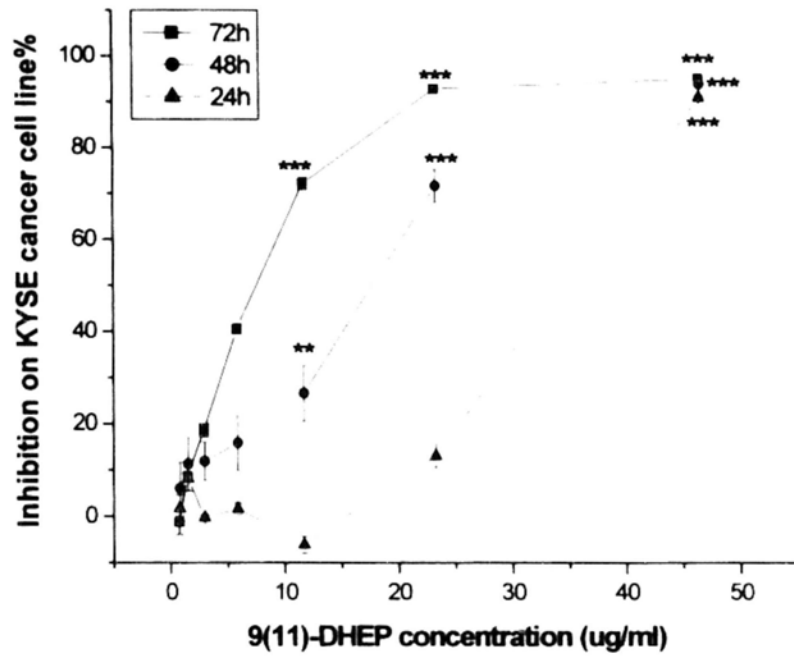


Figure 3.4. Inhibitory effects of 9(11)-DHEP and EP on KYSE cancer cells in a time-dependent manner. Cells were treated with various concentrations of the two steroids for 72h; and cell viability was determined by the MTT assay. Results are expressed as percentages of proliferation compared to the control (mean \pm SD, n=3). Differences with $P < 0.05$ (*), $P < 0.01$ (**), $P < 0.001$ (***) were considered significantly different.

Table 3.2. Anti-proliferation activity screening of 9(11)-DHEP and EP on different cancer cells by BrdU assay

	IC₅₀ (ug/ml)	
	9(11)-DHEP	EP
MCF-7	30.31±2.13	40.43±1.86
HepG2	27.01±1.09	36.22±0.98
Colo201	16.55±1.21	12.39±0.77
KYSE	21.75±1.14	13.87±2.17

The IC₅₀ concentrations represented the concentration which results in 50% inhibition of cell growth after incubation. Results are expressed as mean value ± SD of three independent experiments (p<0.05)

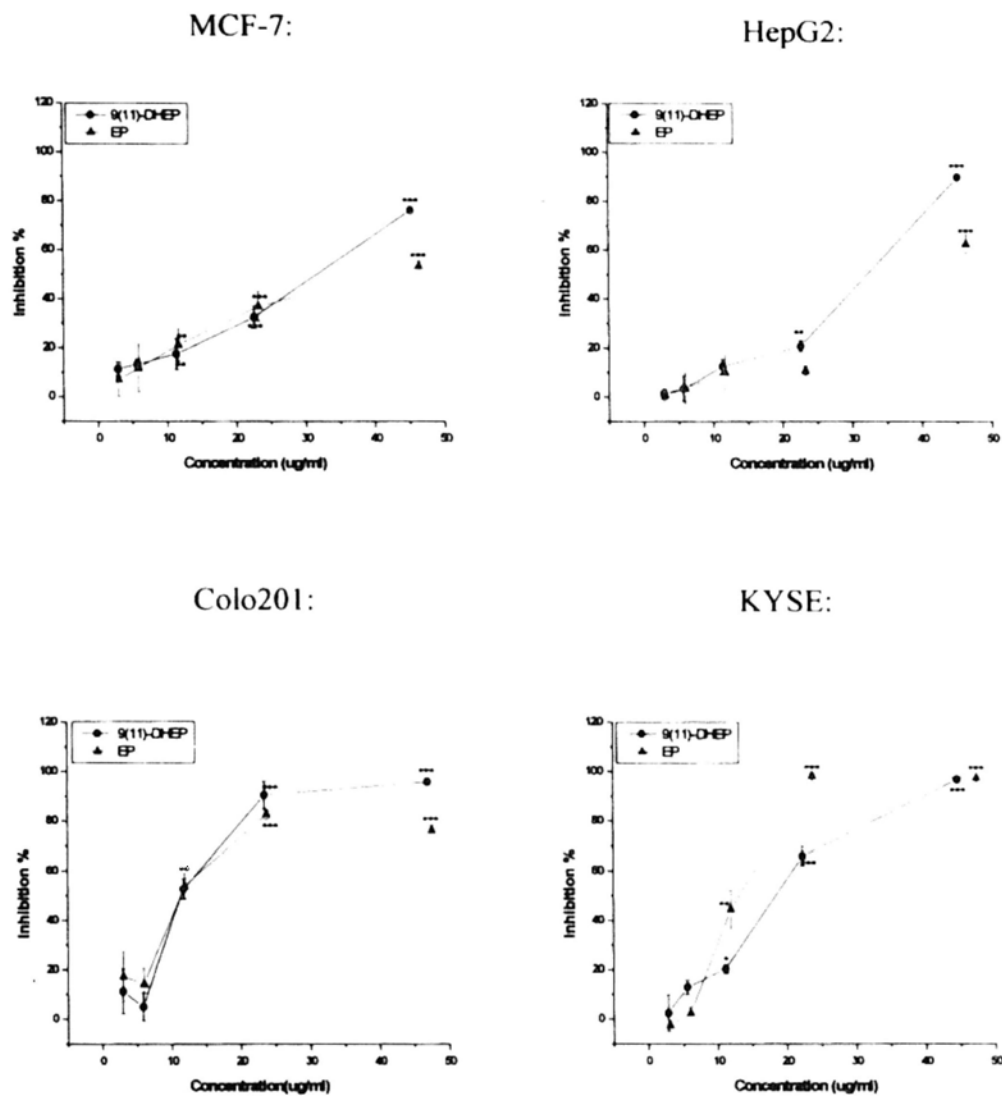


Figure 3.5. Inhibitory effects of 9(11)-DHEP and EP on different cancer cells in a dosage-dependent manner. Cells were treated with various concentrations of the two steroids for 72h; and cell proliferation was determined by the BrdU assay. Results are expressed as percentages of proliferation compared to the control (mean \pm SD, n=3). Differences with $P < 0.05$ (*), $P < 0.01$ (**), $P < 0.001$ (***) were considered significantly different.

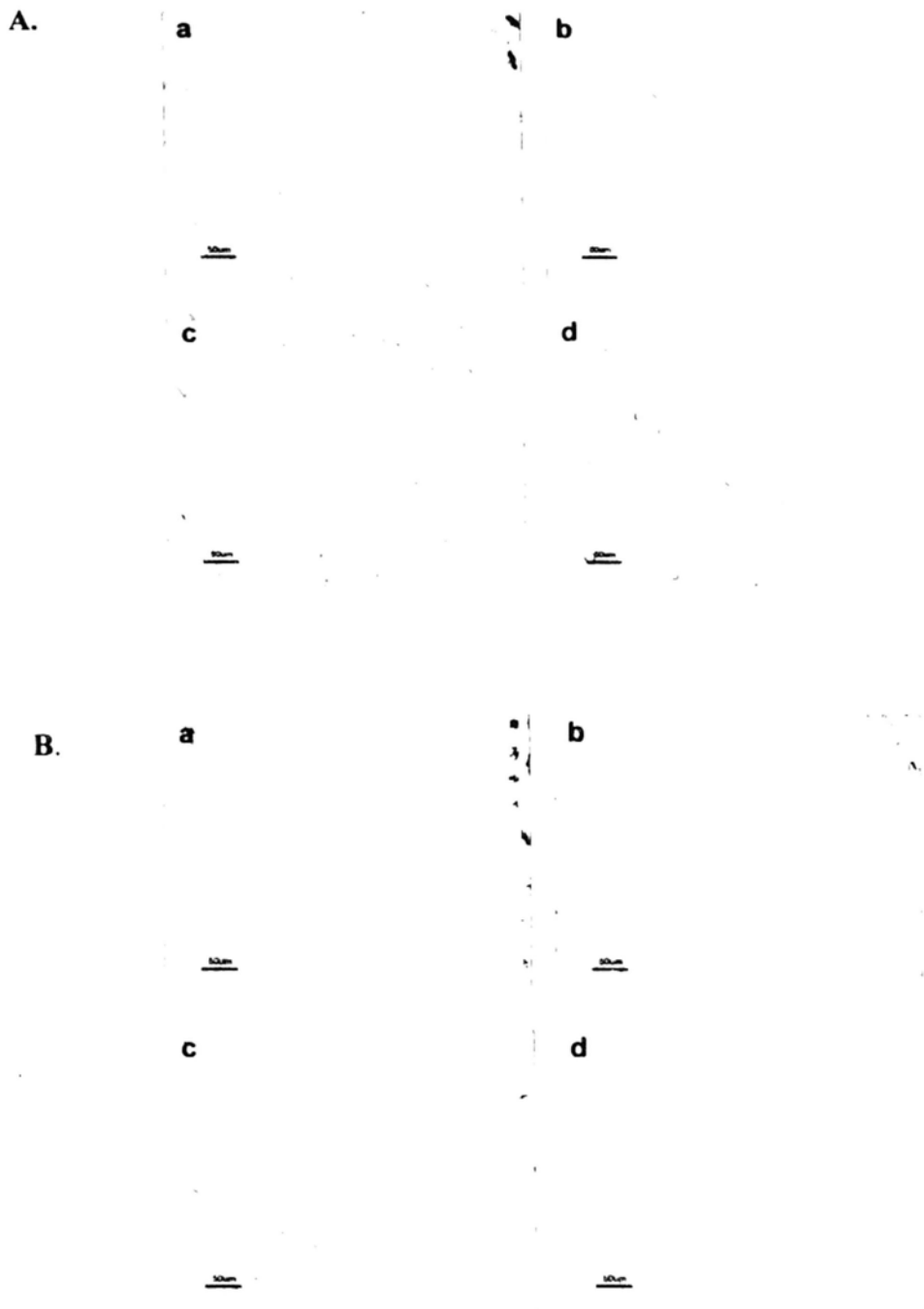


Figure 3.6 Effects of 9(11)-DHEP and EP treatment on the morphological changes of MCF-7 cells. MCF-7 cancer cells were treated with different concentrations of 9(11)-DHEP (A) and EP (B) for 72h. Light microscope photographs were obtained at 200× magnification. For each diagram, a.control; b. 10ug/ml; c. 20ug/ml; d.30ug/ml.

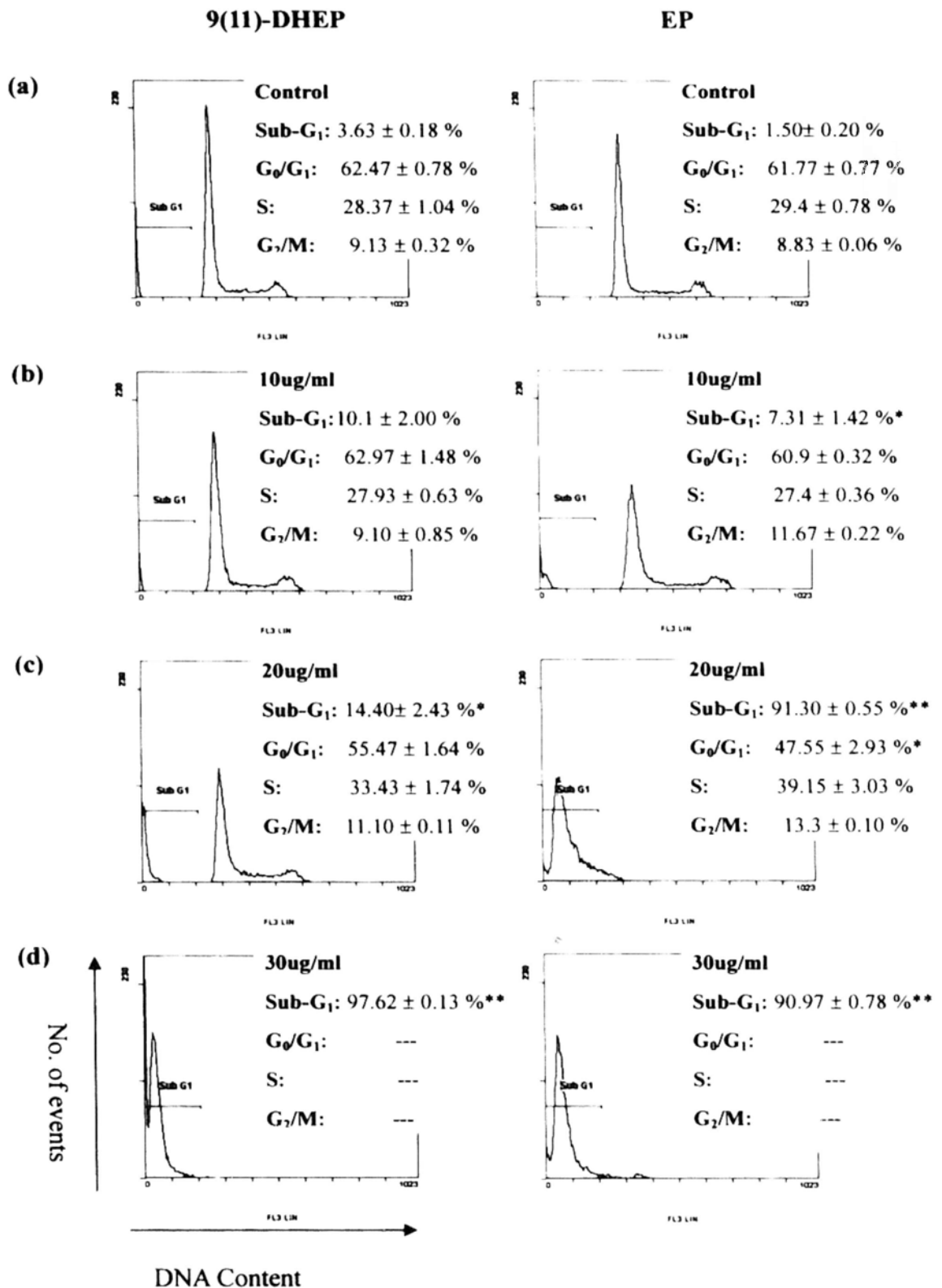


Figure 3.7. Fluorescence-activated cell sorting analysis of MCF-7 cancer cells after 72hr treatment with 9(11)-DHEP and EP at different concentration. Cell cycle phase distributions were quantified by staining cells with propidium iodide. (a) Control; (b) 10ug/ml; (c) 20ug/ml; (d) 30ug/ml. Results are expressed as percentage of cells in sub-G₁, G₀/G₀, S and G₂/M phase at each time point after exposure. Data are mean ± SD (n=3). Differences with P<0.05 (*), P<0.01 (**) were considered significantly different.

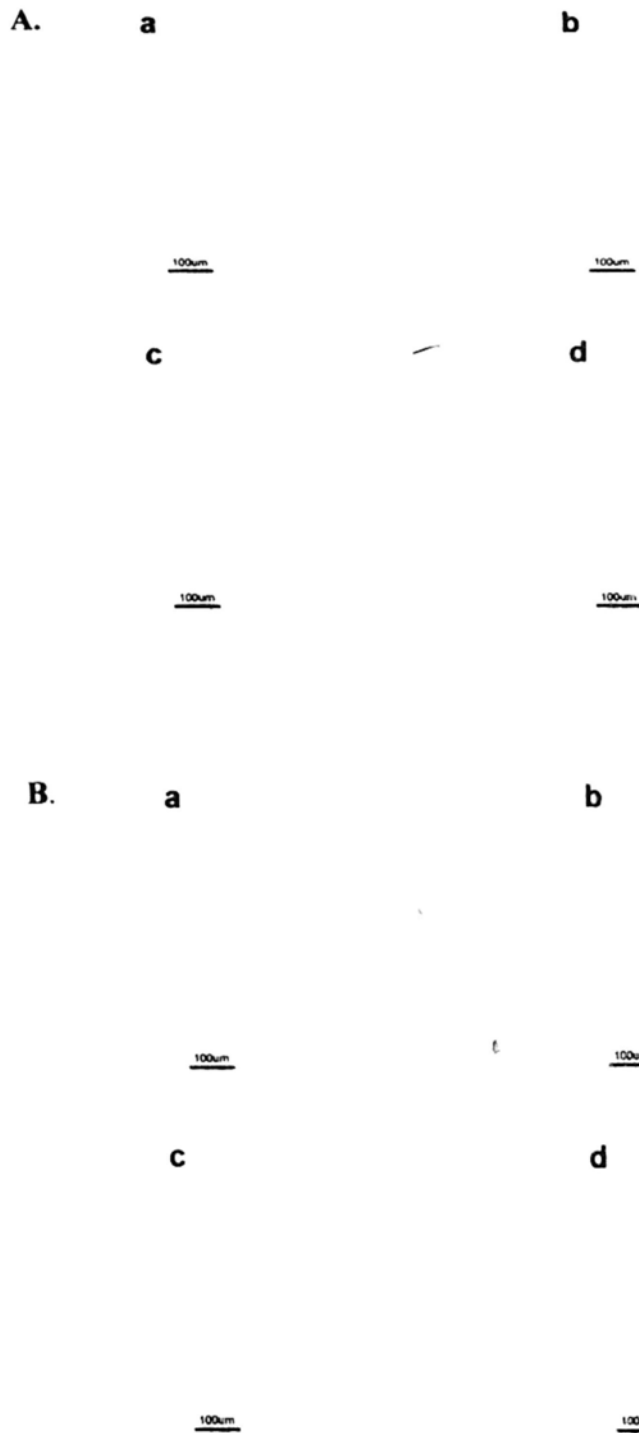


Figure 3.8. Effects of 9(11)-DHEP and EP treatment on the morphological changes of HepG2 cells. HepG2 cancer cells were treated with different concentrations of 9(11)-DHEP (A) and EP (B) for 72h. Light microscope photographs were obtained at 200× magnification. For each diagram, a.control; b. 10µg/ml; c. 20µg/ml; d.30µg/ml.

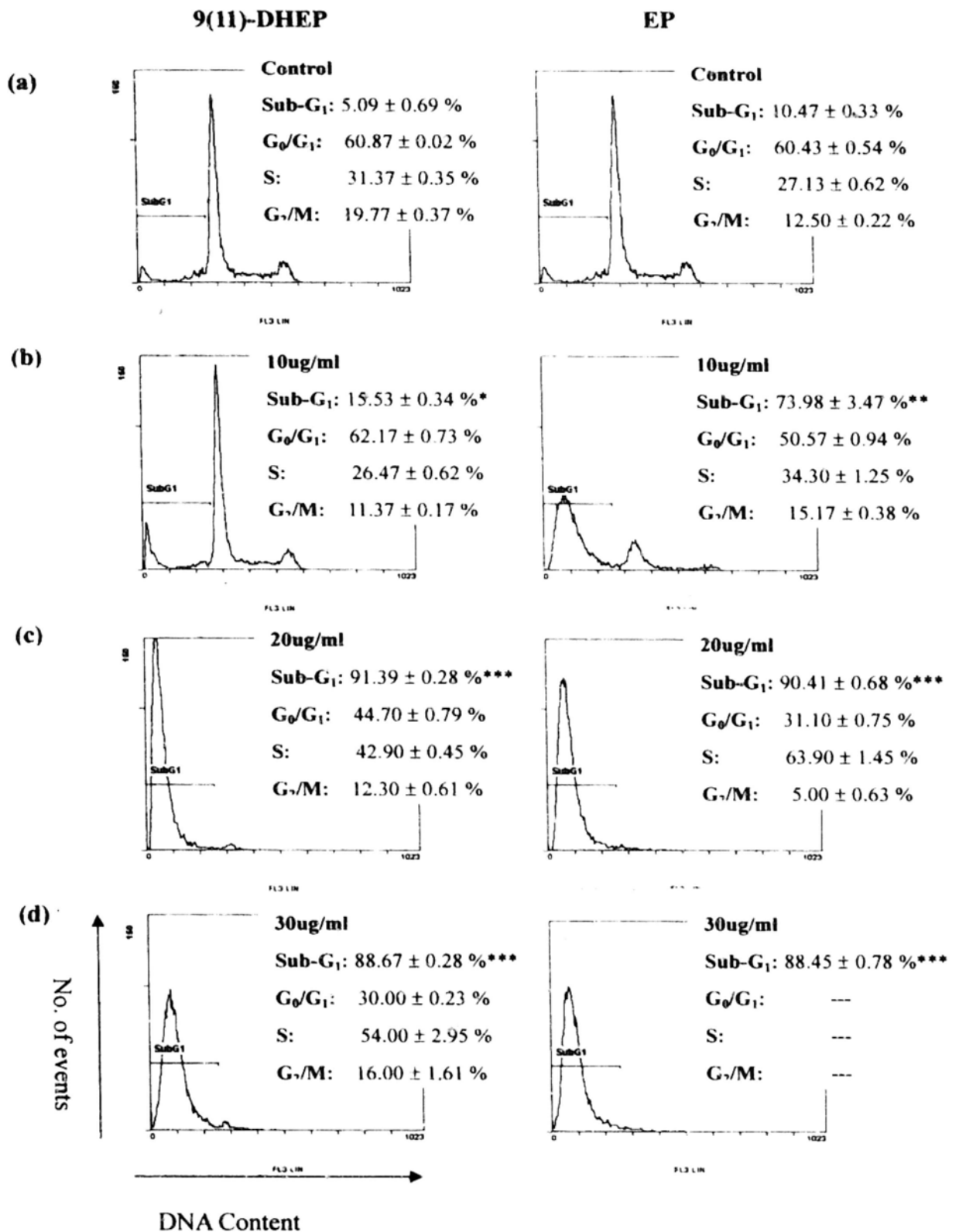
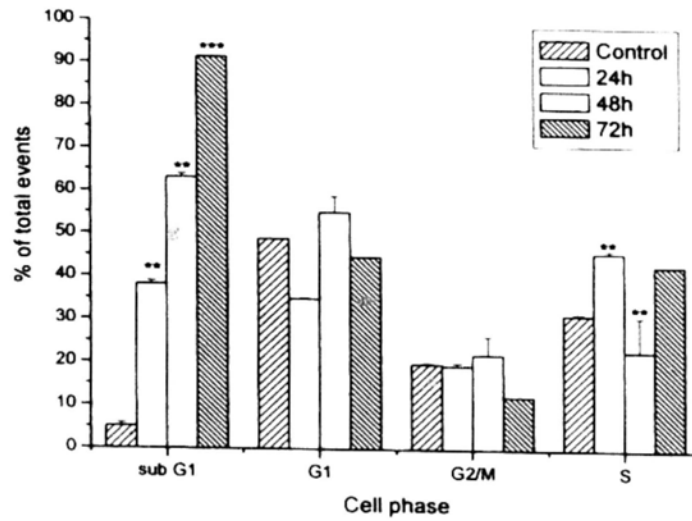


Figure 3.9 Fluorescence-activated cell sorting analysis of HepG2 cancer cells after 72hr treatment with 9(11)-DHEP and EP at different concentration. Cell cycle phase distributions were quantified by staining cells with propidium iodide. (a) Control; (b) 10ug/ml; (c) 20ug/ml; (d) 30ug/ml. Results are expressed as percentage of cells in sub-G₁, G₀/G₀, S and G₂/M phase at each time point after exposure. Data are mean ± SD (n=3). Differences with P<0.05 (*), P<0.01 (**), P<0.001 (***) were considered significantly different.

(a).



(b).

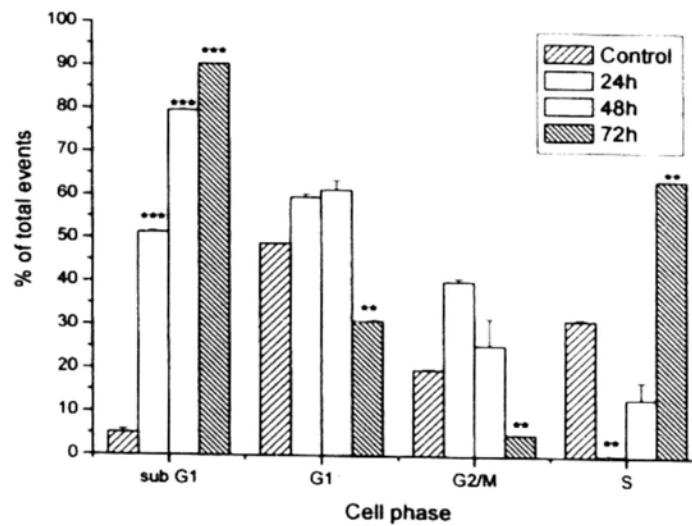


Figure 3.10 Effects of 20ug/ml 9(11)-DHEP (a) or EP (b) on cell cycle phase distribution in HepG2 cancer cells at different incubation times. Results are expressed as mean \pm SD (n=3). $P < 0.05$ (*), $P < 0.01$ (**), $P < 0.001$ (***) were considered significant difference comparing with the control.

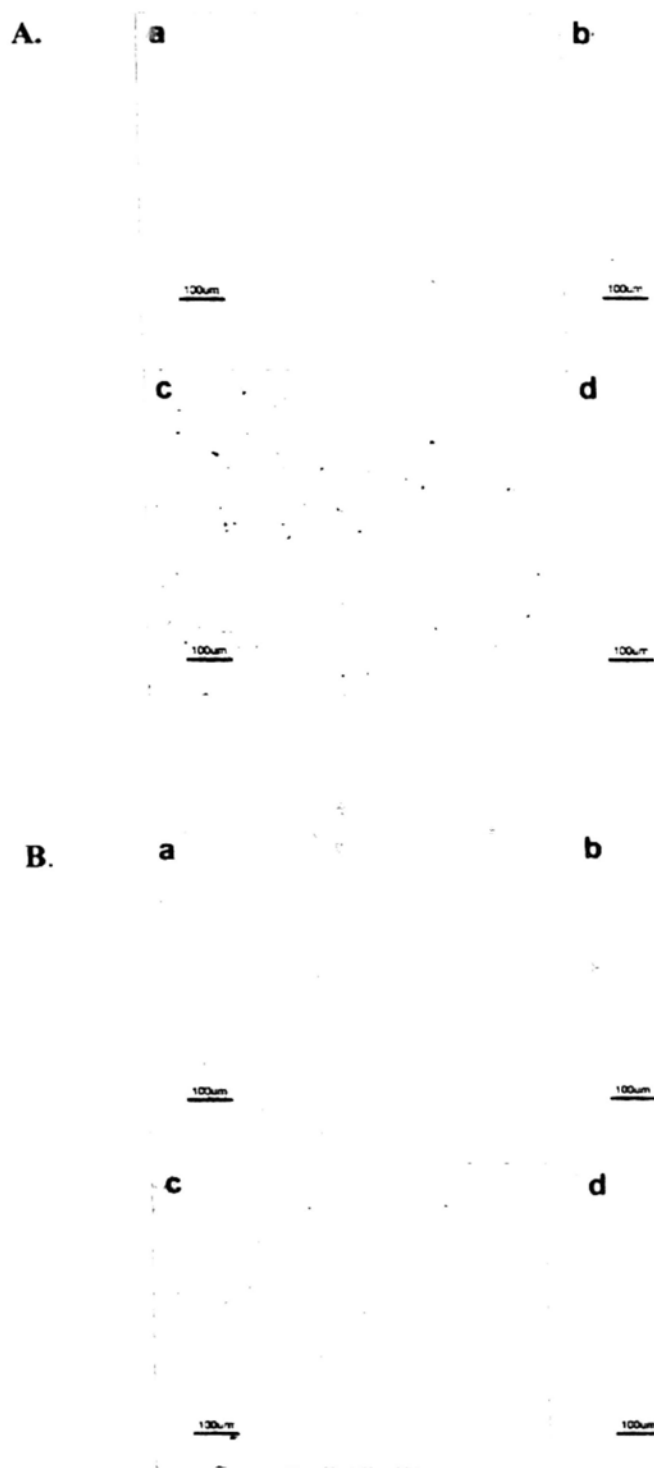


Figure 3.11 Effects of 9(11)-DHEP and EP treatment on the morphological changes of Colo201 cells. Colo201 cancer cells were treated with different concentrations of 9(11)-DHEP (A) and EP (B) for 72h. Light microscope photographs were obtained at 200 \times magnification. For each diagram, a.control; b. 10ug/ml; c. 20ug/ml; d.30ug/ml.

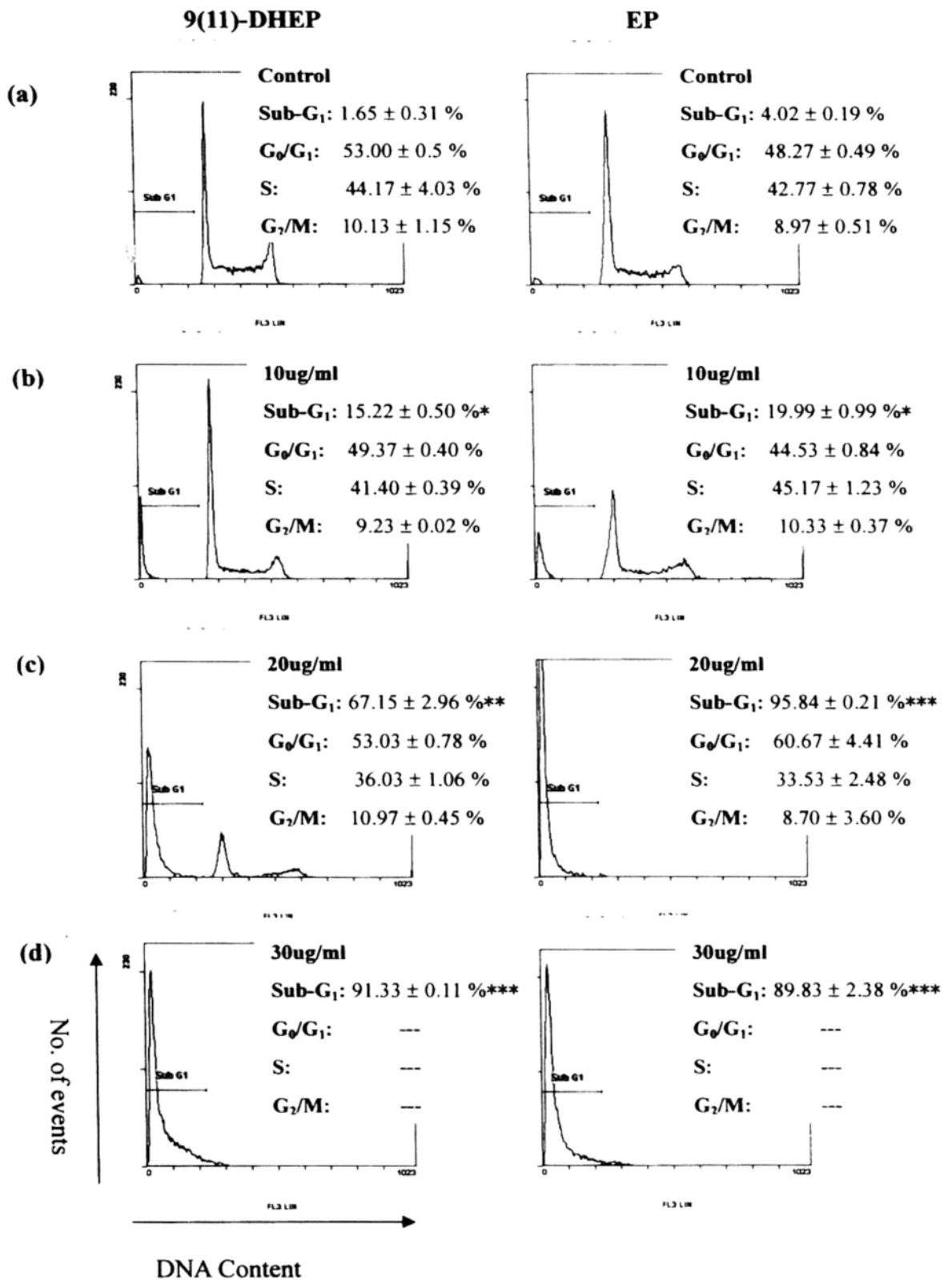


Figure 3.12 Fluorescence-activated cell sorting analysis of Colo201 cancer cells after 72hr treatment with 9(11)-DHEP and EP at different concentration. Cell cycle phase distributions were quantified by staining cells with propidium iodide. (a) Control; (b) 10ug/ml; (c) 20ug/ml; (d) 30ug/ml. Results are expressed as percentage of cells in sub-G₁, G₀/G₁, S and G₂/M phase at each time point after exposure. Data are mean ± SD (n=3). Differences with P<0.05 (*), P<0.01 (**), P<0.001 (***) were considered significantly different.

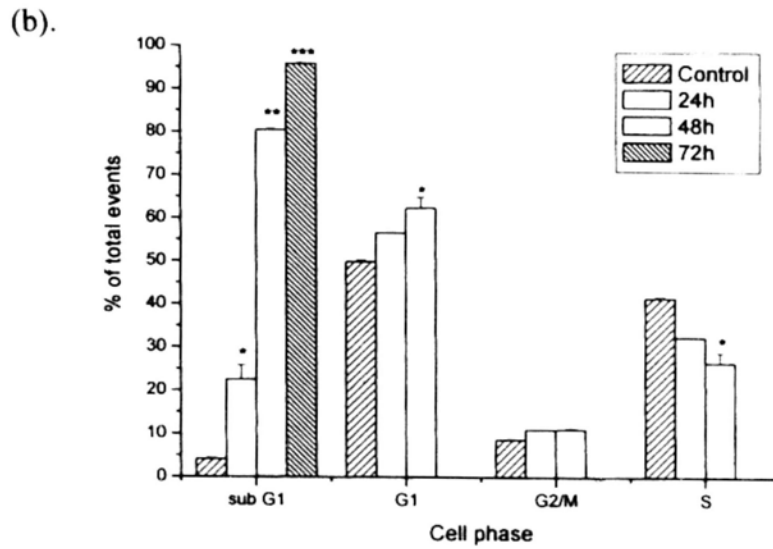
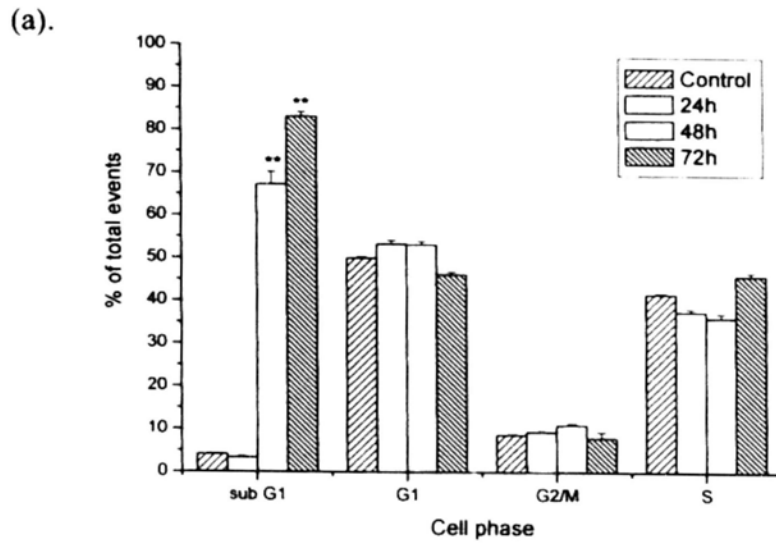
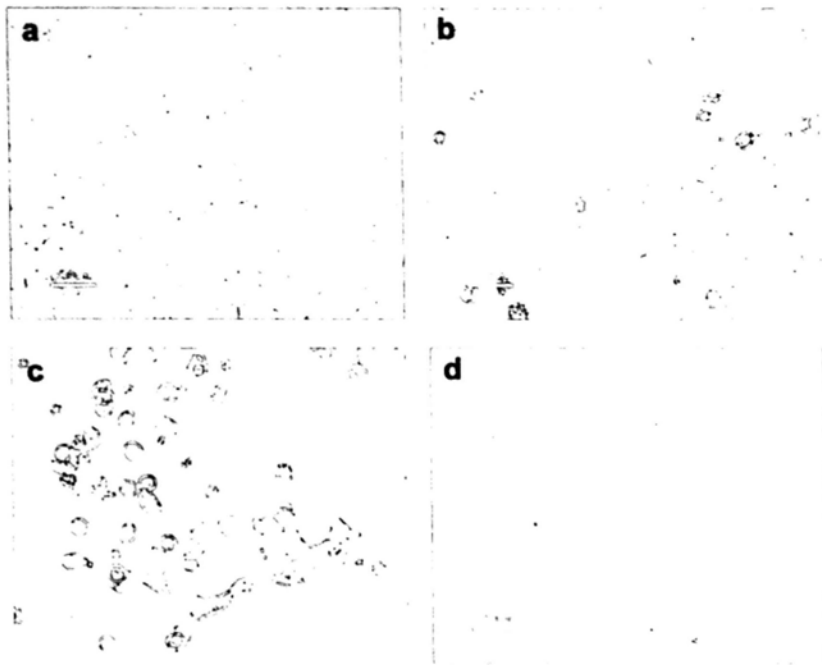


Figure 3.13 Effects of 20ug/ml 9(11)-DHEP (a) or EP (b) on cell cycle phase distribution in Colo201 cancer cells at different incubation times. Results are expressed as mean \pm SD (n=3). $P < 0.05$ (*), $P < 0.01$ (**), $P < 0.001$ (***) were considered significant difference comparing with the control.

A.



B.

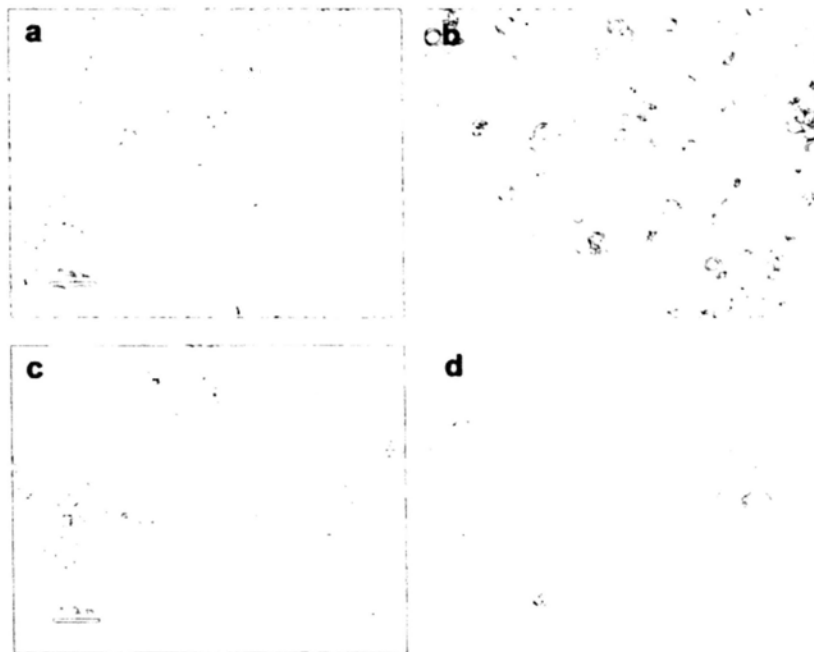


Figure 3.14 Effects of 9(11)-DHEP and EP treatment on the morphological changes of KYSE cells. KYSE cancer cells were treated with different concentrations of 9(11)-DHEP (A) and EP (B) for 72h. Light microscope photographs were obtained at 200 \times magnification. For each diagram, a.control; b. 10ug/ml; c. 20ug/ml; d.30ug/ml.

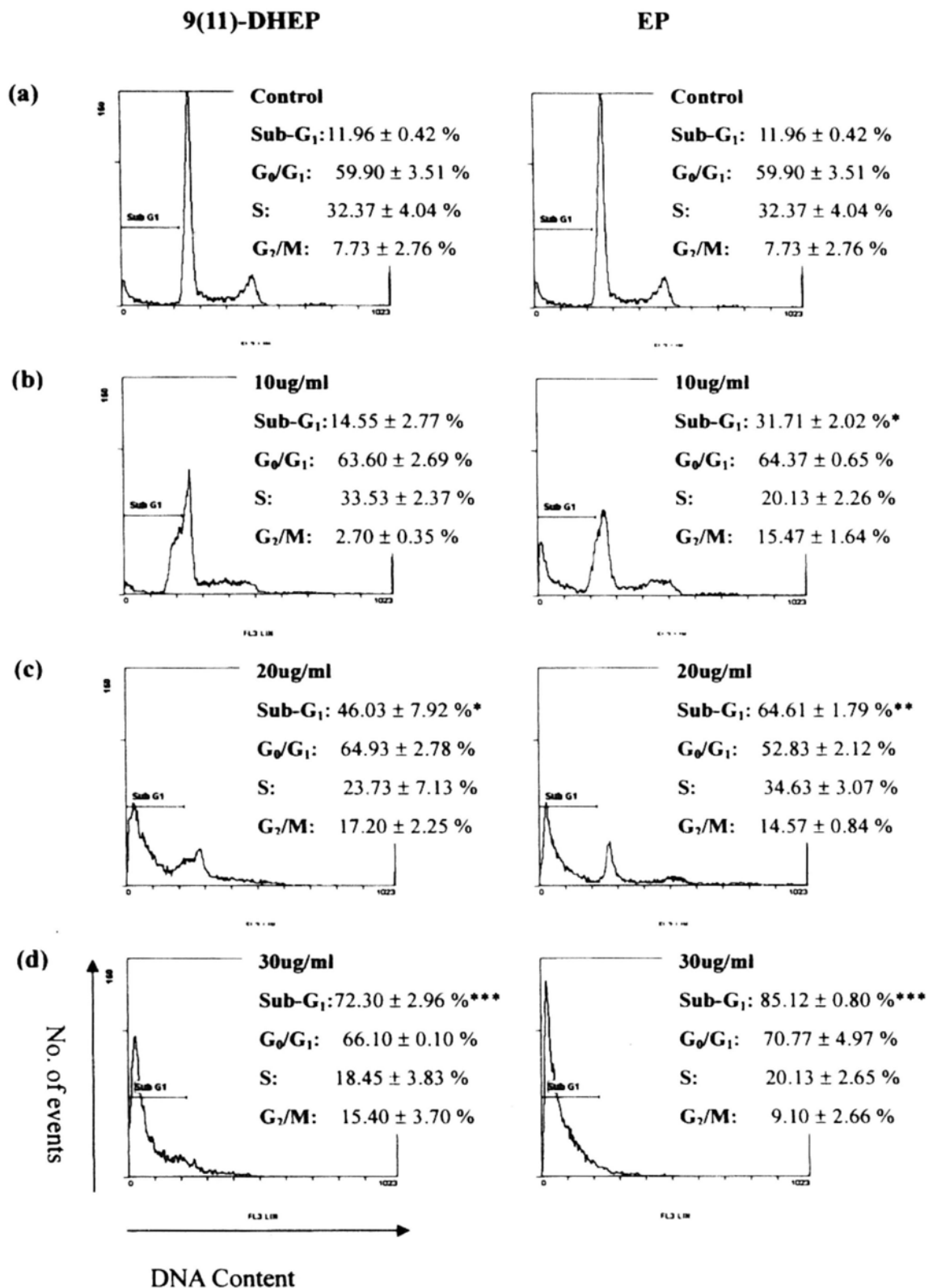


Figure 3.15. Fluorescence-activated cell sorting analysis of KYSE cancer cells after 72hr treatment with 9(11)-DHEP and EP at different concentration. Cell cycle phase distributions were quantified by staining cells with propidium iodide. (a) Control; (b) 10ug/ml; (c) 20ug/ml; (d) 30ug/ml. Results are expressed as percentage of cells in sub-G₁, G₀/G₁, S and G₂/M phase at each time point after exposure. Data are mean ± SD (n=3). Differences with P<0.05 (*), P<0.01 (**), P<0.001 (***) were considered significantly different.

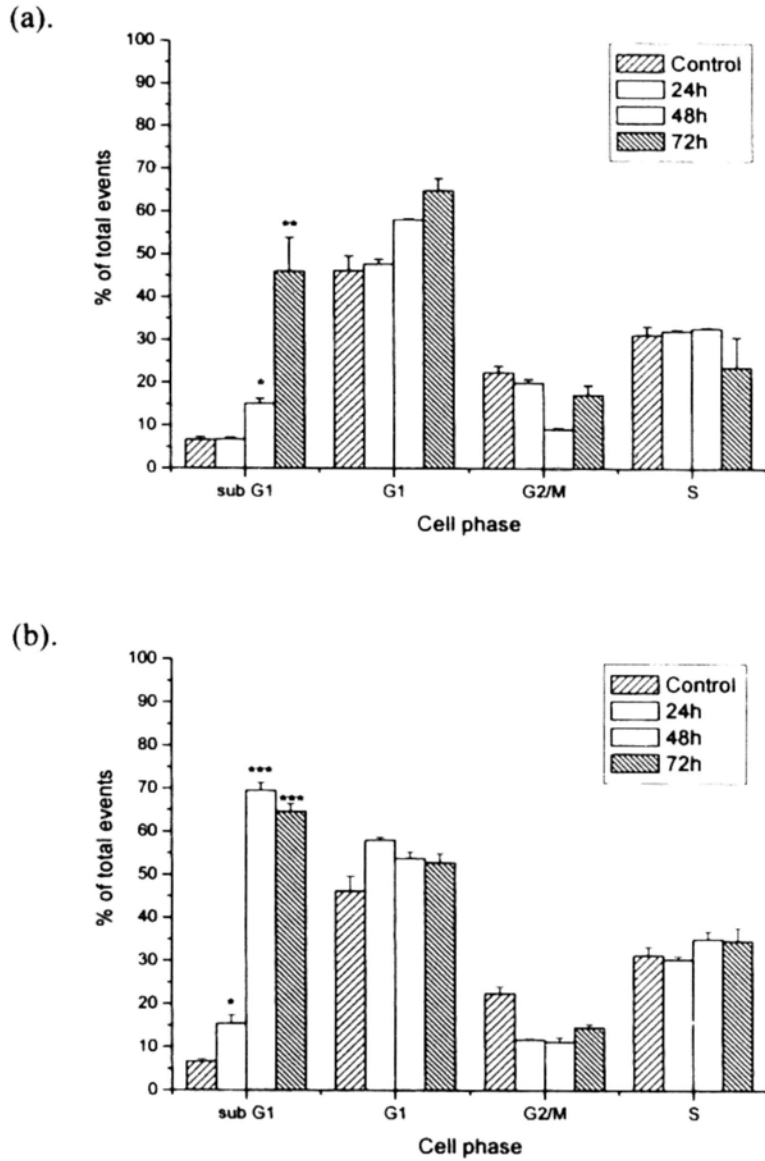


Figure 3.16 Effects of 20ug/ml 9(11)-DHEP (a) or EP (b) on cell cycle phase distribution in KYSE cancer cells at different incubation times. Results are expressed as mean \pm SD (n=3). $P < 0.05$ (*), $P < 0.01$ (**), $P < 0.001$ (***) were considered significant difference comparing with the control.

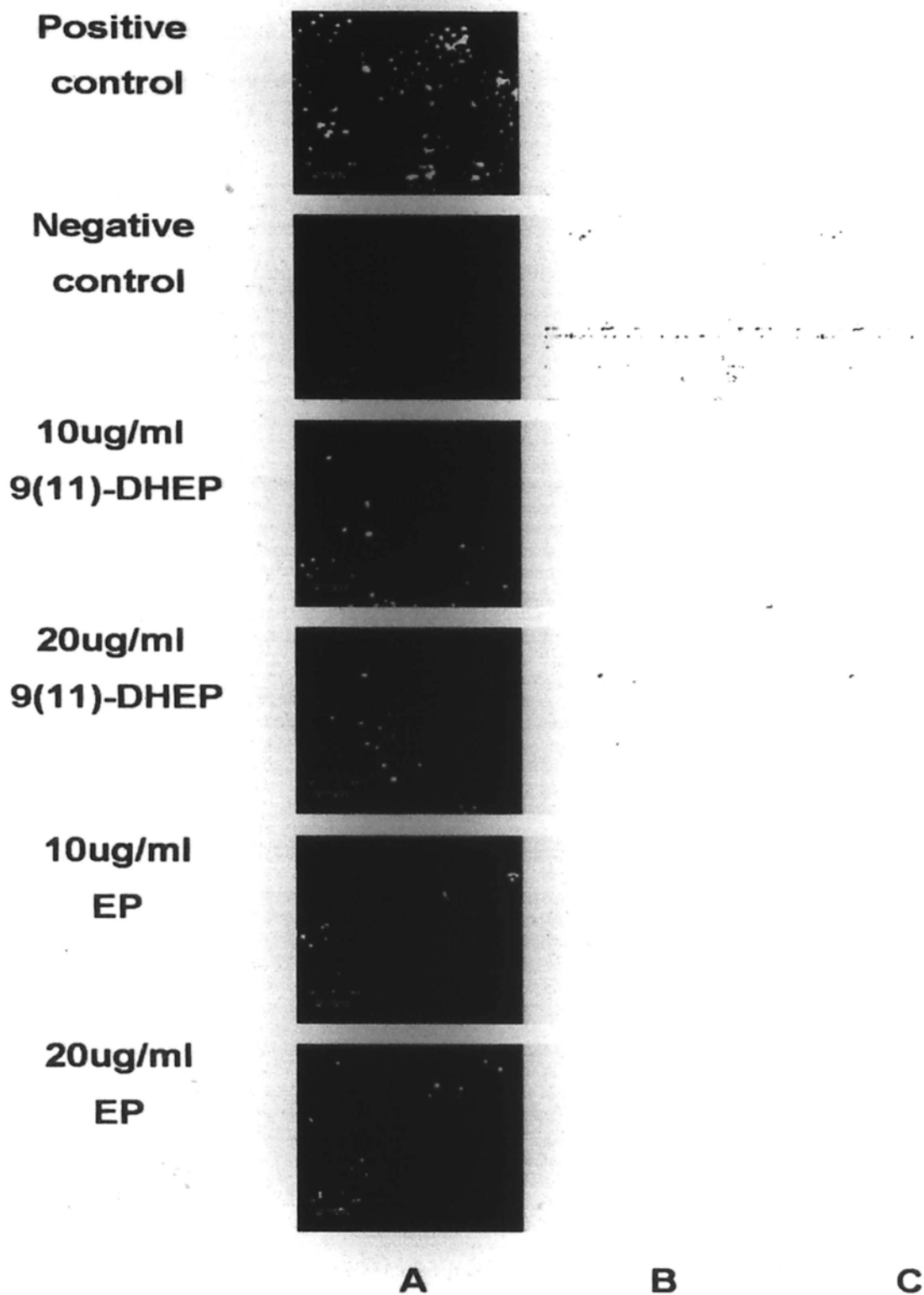


Figure 3.17. Effects of 9(11)-DHEP and EP on HepG2 cancer cells by confocal laser scanning microscopy using TUNEL assay. Cells were cultivated for 72h in the presence of different concentration sample. For the image, (A) single-parameter analysis by TUNEL treatment; (B) visible image of living cells. (C) dual-parameter analysis of TUNEL treatment and visible image of living cells. Cells of negative control were treated with 100% EtOH; cells of positive control were treated with DNaseI before TUNEL staining.

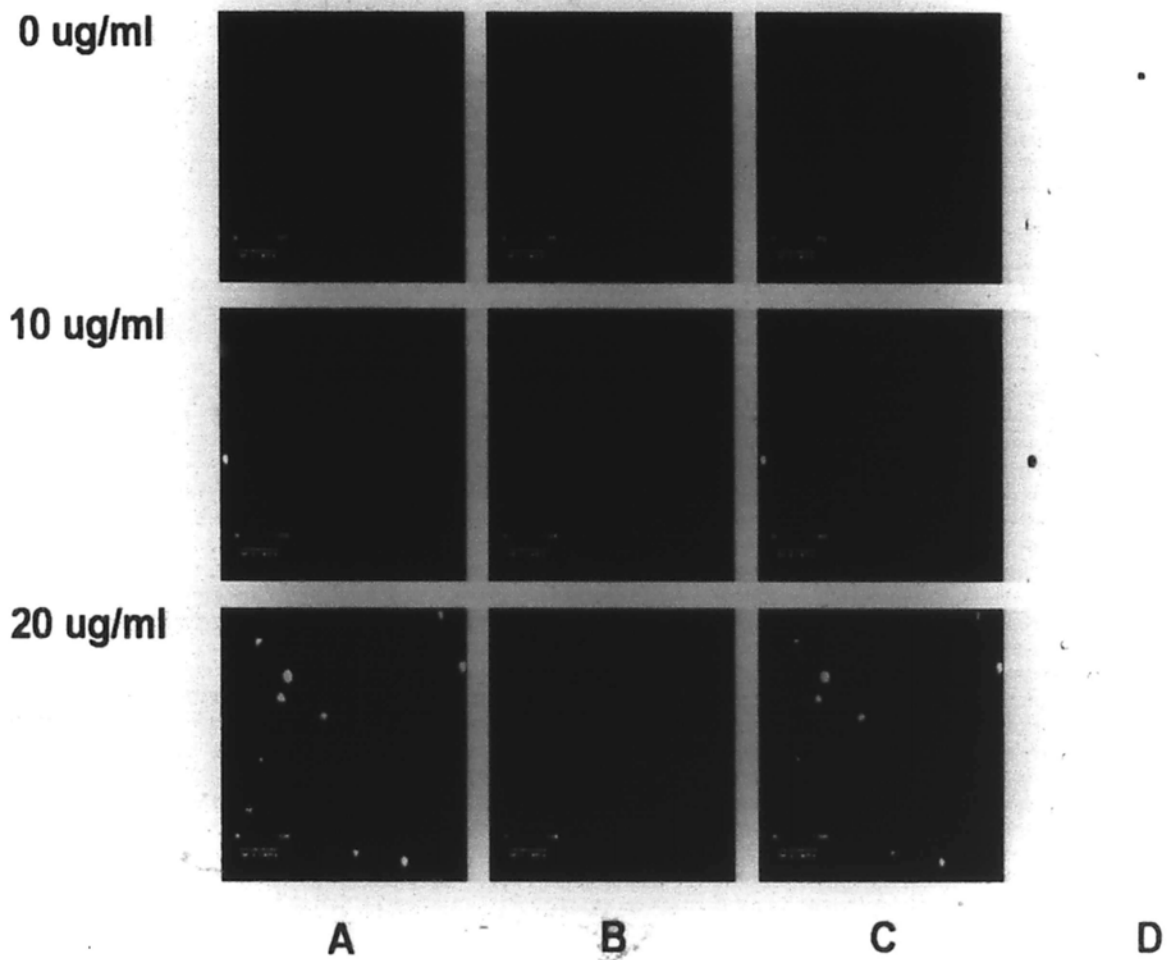


Figure 3.18. Effects of 9(11)-DHEP on HepG2 cancer cells by confocal laser scanning microscopy after staining with Annexin-V-FLUOS and propidium iodide. Cells were cultivated for 72h in the presence of different concentrations of samples. For the images, (A) single-parameter analysis staining with Annexin-V-FLUOS; (B) single-parameter analysis with propidium iodide; (C) dual-parameter analysis of TUNEL treatment and visible image of living cells; (D) visible image of living cells.

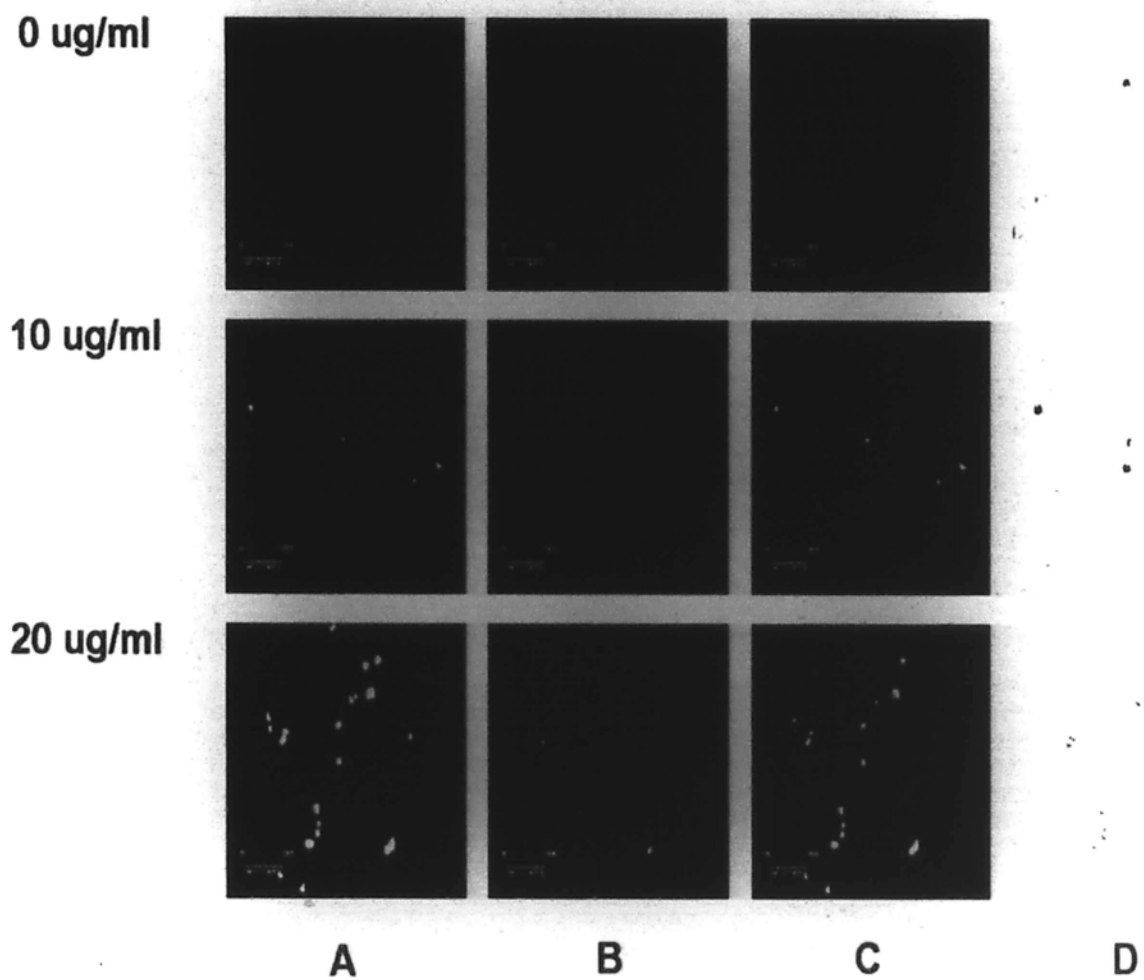


Figure 3.19. Effects of EP on HepG2 cancer cells by confocal laser scanning microscopy after staining with Annexin-V-FLUOS and propidium iodide. Cells were cultivated for 72h in the presence of different concentrations of samples. For the images, (A) single-parameter analysis staining with Annexin-V-FLUOS; (B) single-parameter analysis with propidium iodide; (C) dual-parameter analysis of TUNEL treatment and visible image of living cells; (D) visible image of living cells.

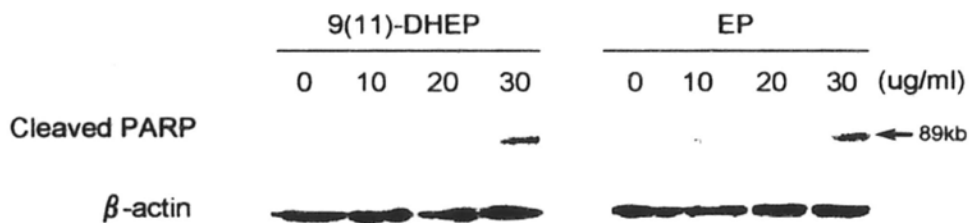


Figure 3.20 Dose-dependent effects of 9(11)-DHEP and EP on Colo201 cancer cells by western blot analysis using cleaved PARP(Asp214) antibody (human specific) 89Kb. Cells were treated with different concentrations of EP for 24h & 9(11)-DHEP for 48h. Total protein (60 μ g) was resolved in 10% SDS-PAGE and blotted on nitrocellulose membrane. The amount of protein was normalized to the densitometric units of β -actin.

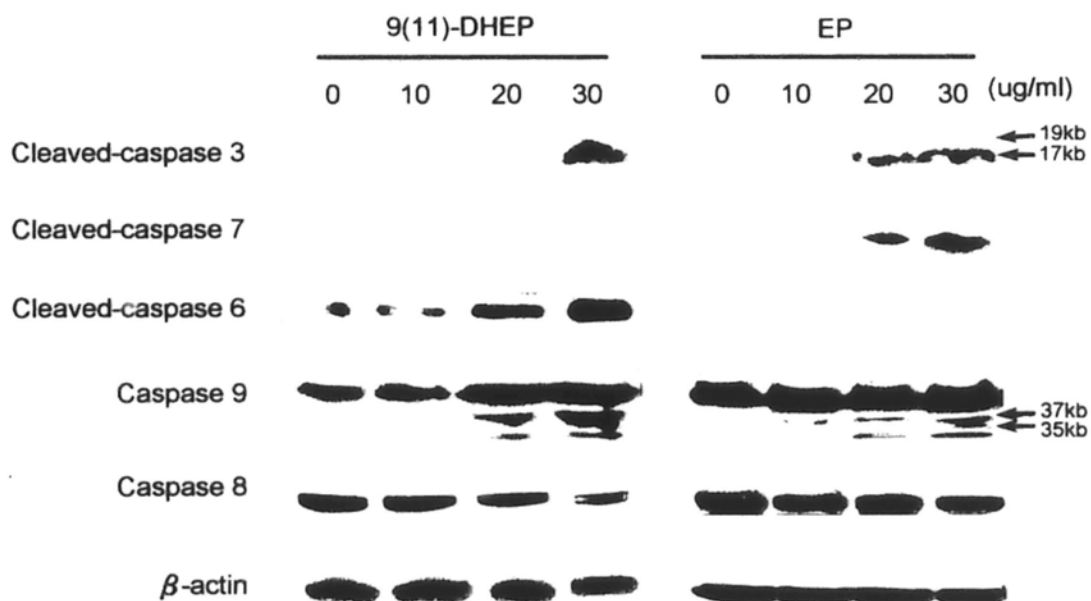


Figure 3.21. Dose-dependent effects of 9(11)-DHEP and EP on Colo201 cancer cells by Western blot analysis using cleaved caspase 3 antibody, cleaved caspase 7 antibody (human specific), cleaved caspase 6, caspase 9 and caspase 8. Cells were treated with different concentrations of EP for 24h & 9(11)-DHEP for 48h. Total protein (60-80 μ g) was resolved in 12% SDS-PAGE and blotted on nitrocellulose membrane. The amount of protein was normalized to the densitometric units of β -actin.

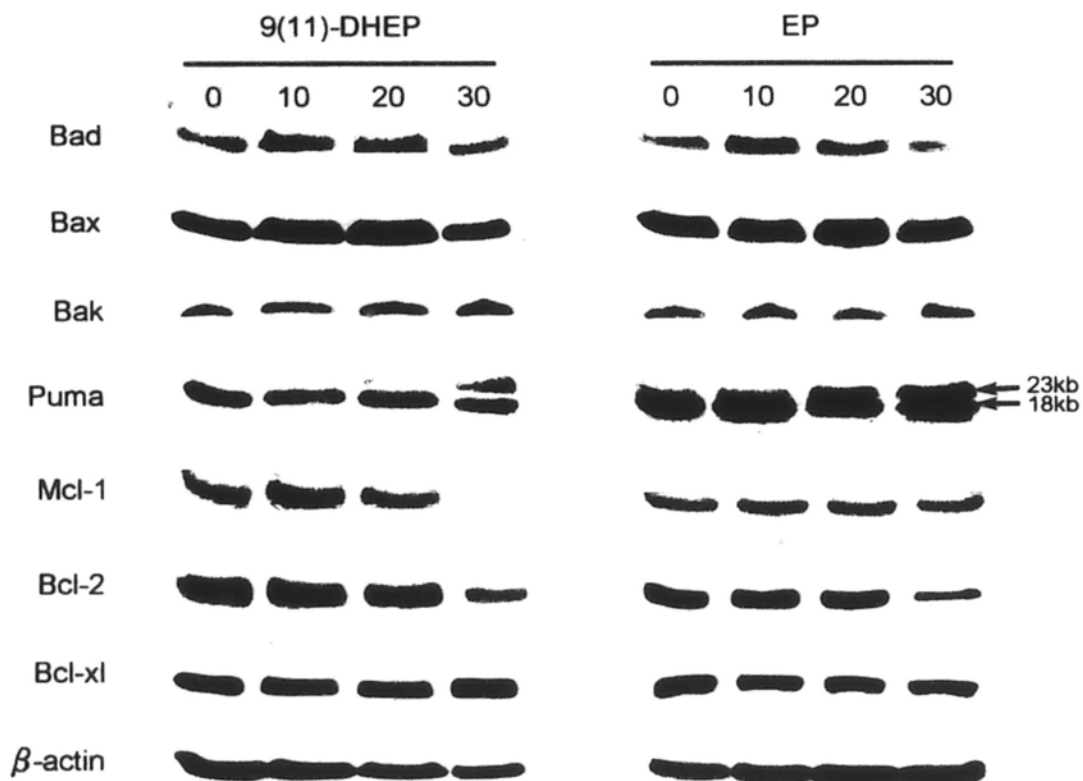


Figure 3.22. Dose-dependent effects of 9(11)-DHEP and EP on Colo201 cancer cells by western blot analysis using Bad, Bax, Bak, puma, Mcl-1, Bcl-2 and Bcl-xl antibodies. Cells were treated with different concentrations of EP for 24h & 9(11)-DHEP for 48h. Total protein (60-80 μ g) was resolved in 10-12% SDS-PAGE and blotted on nitrocellulose membrane. The amount of protein was normalized to the densitometric units of β -actin.

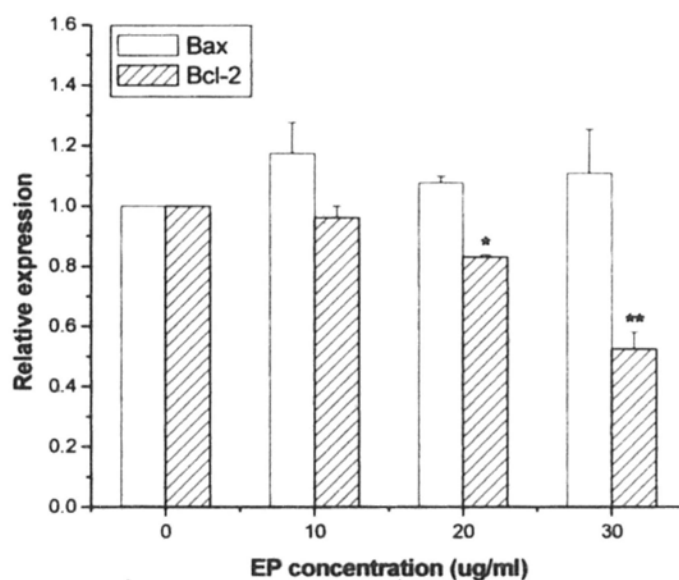
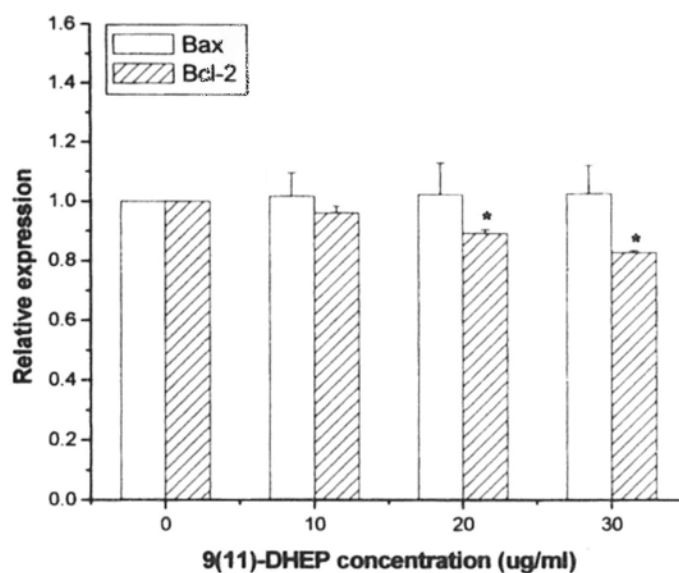


Figure 3.23 Dose-dependent effects of 9(11)-DHEP and EP on Bax/Bcl-2 expression in Colo201 cancer cells. Cells were treated with 9(11)-DHEP for 48h or EP for 24h. The density of the band is expressed as the relative density compared to that in untreated cells (control) that were taken as 1.0. Results are expressed as mean \pm SD (n=3). $P < 0.05$ (*), $P < 0.01$ (**) were considered significant difference comparing with the control.

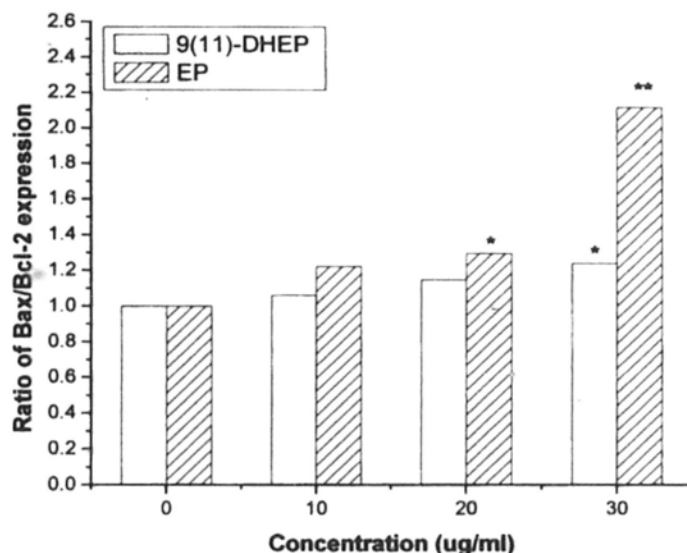


Figure 3.24 Dose-dependent effects of 9(11)-DHEP and EP on Bax/Bcl-2 expression ratio in Colo201 cancer cells. The density of the band is expressed as the relative density compared to that in untreated cells (control) that were taken as 1.0. Results are expressed as mean \pm SD (n=3). $P < 0.05$ (*), $P < 0.01$ (**) were considered significant difference comparing with the control

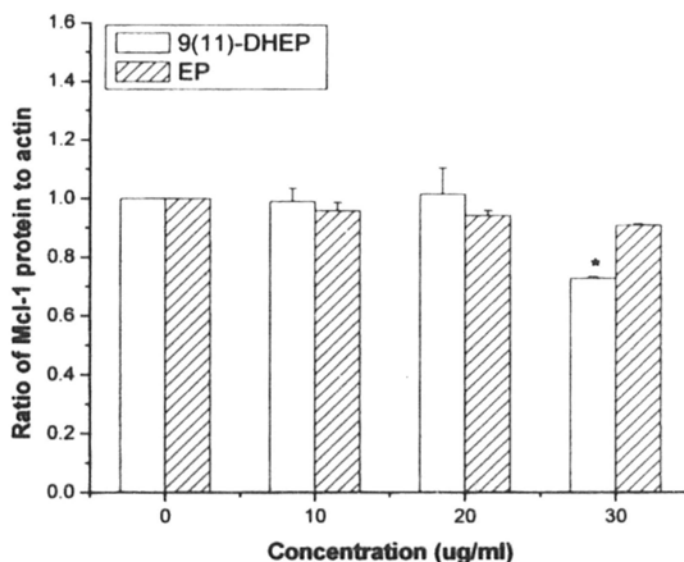


Figure 3.25 Dose-dependent effects of 9(11)-DHEP and EP on Mcl-1 expression in Colo201 cancer cells. Cells were treated with 9(11)-DHEP for 48h or EP for 24h. The density of the band is expressed as the relative density compared to that in untreated cells (control) that were taken as 1.0. Results are expressed as mean \pm SD (n=3). $P < 0.05$ (*) were considered significant difference comparing with the control.

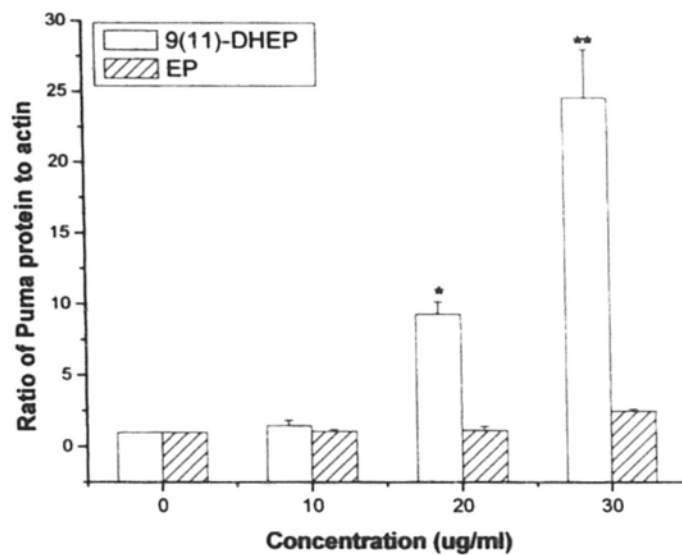


Figure 3.26 Dose-dependent effects of 9(11)-DHEP and EP on Puma expression in Colo201 cancer cells. Cells were treated with 9(11)-DHEP for 48h or EP for 24h. The density of the band is expressed as the relative density compared to that in untreated cells (control) that were taken as 1.0. Results are expressed as mean \pm SD (n=3). $P < 0.05$ (*), $P < 0.01$ (**), were considered significant difference comparing with the control.

3.4 Discussion

Induction of apoptosis is one of important anticancer strategy. Apoptosis, called programmed cell death, is a normal process involved in tissue remodelling and removal of damaged cells. Our studies found that both the two steroids can induce apoptosis in human breast cancer MCF-7 cells, hepatoma cancer HepG2 cells and colorectal carcinoma Colo201 cells but did not significantly inhibited growth of MCF-10-2A non-tumorigenic epithelial cells (they do not form tumors in immunosuppressed mice). Cells undergoing apoptosis show characteristic morphology and biochemical features. The biochemical hallmark of apoptosis is DNA fragmentation; this is an irreversible event that commits the cell to die. Flow cytometry results suggested that the two Ganoderma steroids can lead to the formation of subG1 cell on different cancer cells in a dosage- and time-dependent manner. In TUNEL assay, DNA strand breaks can be detected by enzymatic labeling the free 3'-OH termini with modified nucleotides. By using TUNEL method, the apoptosis induction effect of the two Ganoderma steroids which was revealed by cleavage of DNA strands was identified once again. Annexin V is a calcium-dependent phospholipids-binding protein; it has a high affinity for phosphatidylserine. They do not bind to normal and intact cells. Our results of Annexin V analysis showed that apoptosis is the major cause of HepG2 cancer cells death.

Phytosterols, structurally similar to dietary cholesterol, have been shown experimentally to inhibit colon cancer development, which act by competing with cholesterol at the luminal absorption site. Cholesterol is correlated etiologically to the incidence of colon cancer, to increase susceptibility to colon tumorigenesis (Rao AV, Janezic SA. 1992). The Colo201 cells are used as model to study the apoptosis molecular mechanisms of the two Ganoderma steroids on cancer cells. Apoptosis can

be divided into two classical pathways: the death receptor and mitochondrial pathway. In mitochondria-mediated pathway, the mitochondria stress will reduce the mitochondria membrane potential, which result in cytochrome C, released from the intermembrane space of the mitochondria into the cytosol. In turn, it binds to cytosolic procaspase-9 with oligomerized APAF-1 in an apoptosome complex, resulting in autoactivation and release of mature caspase-9. The latter enzyme activates caspase 3 and caspase 7, which in turn activate a downstream caspase cascade (Igney FH, et al., 2002).

Caspases are a ubiquitous family of cysteine proteases that include both upstream (initiator) and downstream effector caspases. Downstream effector caspases are cleaved and activated by initiator caspases. Initiator caspases (including 8, 9, 10 and 12) are closely coupled to proapoptotic signals. Once activated, these caspases cleave and activate downstream effector caspases (including 3 and 7), which in turn cleave cytoskeletal and nuclear proteins like PARP, α -Fodrin, DFF and Lamin A, and induce apoptosis. Our results indicated that both the two steroids could activate the caspase 3 and 7, which resulted in the cleavage of PARP. PARP, a 116 kDa nuclear poly (ADP-ribose) polymerase, appears to be involved in DNA repair predominantly in response to environmental stress. It is an important downstream protein in the apoptosis pathway and thought to be indicating protein of apoptosis. This indicated that apoptosis induced by the two Ganoderma steroids on colon cancer cell was caspase-dependent. In addition, the expression of caspase 8 and 9 were observed. The two caspase were considered as signaling and key caspase in extrinsic and intrinsic pathway, respectively. In our case, caspase 9 but not caspase 8 was involved in the EP/9(11)-DHEP-mediated apoptosis of colon cancer cells, which suggested that intrinsic pathway might be involved in the two steroids induced apoptosis.

Bcl-2 and related cytoplasmic proteins are key regulators of apoptosis, the cell suicide program critical for development, tissue homeostasis, and protection against pathogens. They govern mitochondrial outer membrane permeabilisation (MOMP) and can be divided into pro-apoptotic members (Bax, Bad, Bak and Bok among others) or anti-apoptotic members (including Bcl-2 proper, Bcl-xL, and Bcl-w, among an assortment of others). The relative ratios of mitochondrial proapoptotic and antiapoptotic mediators determine the ultimate release of cytochrome c. In our work, the decrease of Bcl-2 expression was observed whereas the expression of the pro-apoptotic members Bax, Bad and Bak was not changed. Moreover, 9(11)-DHEP could induce the down-regulation of Mcl-1 and up-regulation of Puma. Mcl-1, also called myeloid cell leukaemia-1, is an anti-apoptotic member of Bcl-2 family. It is thought to promote cell survival by involving in the suppression of cytochrome c release from mitochondria, possibly via heterodimerisation with and neutralisation of pro-apoptotic Bcl-2 family proteins, for example, Bim or Bak (Michels J, et al., 2005). Puma (p53 upregulated modulator of apoptosis) is a highly potent pro-apoptotic protein that induces the rapid and complete death of many malignant cell types. Abundant experimental evidence supported that Puma was a critical mediator of p53-dependent apoptosis (Karst AM and Li G, 2007). The protein was found to be exclusively located at mitochondria and initiated apoptosis through displacing Bax from Bcl-2, binding to Bcl-2 and Bcl-xL through a BH3 domain (Yu J, et al., 2001; Ming LH, et al., 2006). This work indicated the apoptosis under the two *Ganoderma* steroids was by regulating the ratio of Bax/Bcl-2 groups, which altered the mitochondria membrane permeabilization and released the cytochrome C and triggered the apoptotic pathway (Figure 3.27).

Taken together, based on the results obtained above and the current paradigms of apoptosis reported in the literature, we found that apoptosis induced by EP and

9,11-DHEP in Colo201 cancer cells was through the intrinsic pathway. Our work also suggested that both 9(11)-DHEP and EP might be natural potential apoptosis-inducing agent for colon cancer treatment. Therefore, they have a bright future in clinical application. Further investigation to explore their potential in tumor treatment may prove to be worthwhile. But the acting mechanism of the two steroids against other tumor cells is not clear, what the structure-activity relationship is between the EP and 9,11-DHEP is also unknown to us. All this will need further studies.

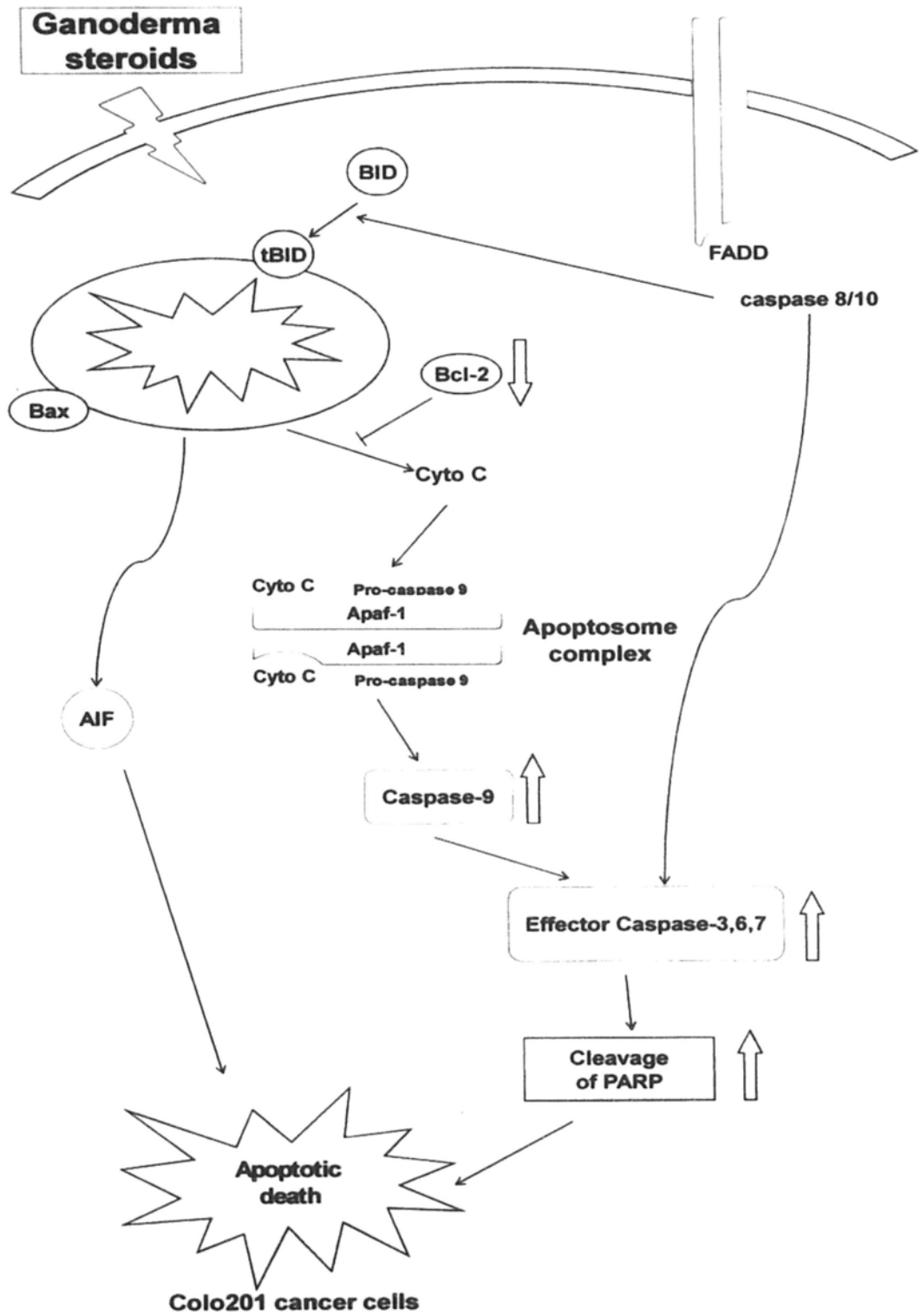


Figure 3.27 Mitochondria-mediated apoptosis induced by 9(11)-DHEP and EP in

Colo201 cancer cells

Chapter IV Mechanisms studies on the *in vitro* and *in vivo* antitumor activities of ergosterol peroxide and 9(11)-dehydroergosterol peroxide from *Ganoderma lucidum* mycelia against human A375 malignant melanoma

4.1 Introduction

According to their origin, there are three types of skin cancer: a. Basal cell carcinomas (BCC) are the most common type, accounting for about 90 % of all skin cancers. They arise from the skin cells at the bottom (or basal) layers of the skin; b. Squamous cell carcinomas (SCC) arise from the outer layers of the skin. They are less common than basal cell carcinomas, but are more dangerous because they can spread to other parts of the body. Both the basal cell carcinomas and squamous cell carcinomas belong to non-melanoma skin cancers. c. Malignant melanoma, although far less prevalent than non-melanoma skin cancers, is the major cause of death from skin cancer and is more likely to be reported and accurately diagnosed than non-melanoma skin cancers. Melanoma is a cancer of melanocytes – the melanin-producing cells in the skin, which is the least common type of skin cancer. Melanin is a dark pigment which absorbs the UV light and prevents it from doing damage to skin cells. The ultraviolet light in sunlight damages the DNA in skin, causing skin cells to mutate and grow into cancers. Studies showed that many important molecule are mutated in the melanoma cells. The mitogen-activated protein kinase (MAPK) pathway is activated in virtually all melanomas regardless of the status of the B-raf gene. Melanoma cells frequently lack endogenous raf inhibitors, and their absence contributes to MAPK activation

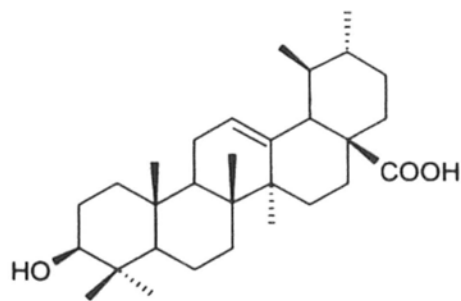
(Eisenmann KM, et al., 2003; Panka DJ, et al., 2006). So the melanoma is thought to be one of the most lethal cancers in the world.

Betulinic acid, oleanolic acid and ursolic acid (UA) are belonging to oleanane-type triterpene (Cragg GM and Newman DJ, 2005), which have very similar structure to the EP and 9(11)-DHEP. They were well studied to have unit function on the therapy for the skin cancer in Japan.

Betulinic acid (BetA) is a pentacyclic lupane-type triterpene derived from white birch trees that is widely distributed throughout the plant kingdom. A variety of biological activities have been ascribed to betulinic acid including anti-inflammatory and *in vitro* antimalarial effects. However, betulinic acid is most highly regarded for its anti-HIV-1 activity and specific cytotoxicity against a variety of tumor cell lines (Cichewicz RH and Kouzi SA, 2004). Betulinic acid is a prototype cytotoxic agent that triggers apoptosis by a direct effect on mitochondria (Fulda S, et al., 1998) and activates NF- κ B in a variety of tumor cell lines (Kasperczyk H, et al., 2005).

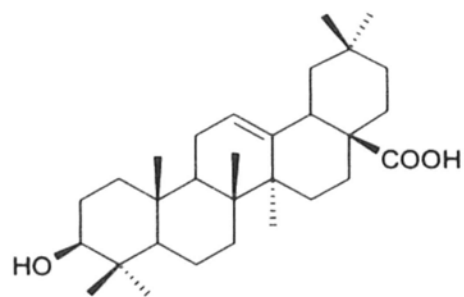
Oleanolic acid and ursolic acid are ubiquitous triterpenoids in plant kingdom, medicinal herbs, and are integral part of the human diet (Liu J, 2005). They were found to be important for anti-angiogenesis (Sohn KH, et al., 1995). UA blocked cell cycle progression in the G1 phase and also resulted in the triggering of apoptosis (Hsu YL, et al., 2004; Es-saadya D, et al., 1996). Both of them were recommended for skin cancer therapy in Japan (Muto Y, et al., 1990).

In this chapter, EP and 9(11)-DHEP induced apoptosis mechanism in A375 malignant melanoma *in vitro* and *in vivo* were studied. Meanwhile, the antitumor activities of the three positive control (betulinic acid, oleanolic acid and ursolic acid) were also documented.



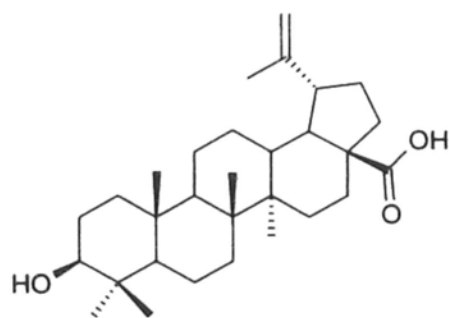
Ursolic acid (UA)
 (3b)-3-Hydroxyurs-12-en-28-oic acid

a.



Oleanolic acid (OA)
 (3b)-3-Hydroxyolean-12-en-28-oic acid

b.



Betulinic acid (BetA)
 3b-Hydroxy-lup-20(29)-en-28-oic acid

c.

Figure 4.1 The chemical structure of natural triterpenes: a. Ursolic acid; b. Oleanolic acid; c. Betulinic acid.

4.2 Materials and Methods

4.2.1 Chemicals and reagents

N-(2-Hydroxyethyl)piperazine-N'-(2-ethansulfonic acid) hemisodium salts (HEPES) solution, sodium bicarbonate, sodium pyruvate, trypsin, ethylenediaminetetraacetic acid (EDTA), bovine serum albumin (BSA), propidium iodide (PI), dimethylsulfoxide (DMSO), β -mercaptoethanol, glycerol, bromophenol blue and glycine were purchased from Sigma. Dulbecco's modified Eagle's (DMEM) medium, Leibovitz's L-15 medium, fetal bovine serum (FBS), fungizone (amphotericin B 250 μ g/ml), Triton X-100, phosphate buffered saline (PBS), penicillin (10,000unit/ml)-streptomycin (10,000 μ g/ml) and DNase (grade 1) were obtained from Invitrogen Chemical Co.. 3-(4,5-dimethyl-thiazoly-2-yl)-2,5-diphenyl tetrazolium bromide (MTT). SDS was bought from Bio-Rad. Culture flasks (25cm² and 75cm²) and 8-chamber polystyrene vessel (tissue culture treated glass slide) was obtained from Falcon. The lumi-film chemiluminescent detection film, cell proliferation ELISA-BrdU (chemiluminescence) assay kit, cytotoxicity detection kit (LDH), *in situ* cell death detection kit (fluorescein) and Annexin-V-FLUOS staining kit were bought from Roche Molecular Biochemicals. Ethanol, methanol, hydrochloric acid (HCl) and isopropanol were obtained from Merck. Sodium citrate, Tris-HCl, acrylamide/bis (37.5:1, 40%) solution was purchased from JT Baker. Antibody of β -actin was purchased from BD Biosciences Pharmingen, USA. Antibodies for anti-cleaved PARP (Asp214), anti-PARP, anti-cytochrome c, anti-Bax, anti-Bad, anti-Bak, anti-BID, anti-Bmf, anti-Bim, anti-puma, anti-Bcl-2, anti-Bcl-xl, anti-Mcl-1 and anti-cleaved caspase 3 (Asp175), anti-caspase 6, anti-cleaved caspase 7 (Asp198), anti-caspase 8, anti-caspase 9 and anti-caspase 10 were obtained from Cell signaling Co. (USA). Goat anti-rabbit IgG-conjugated to horseradish peroxidase (HRP) and goat anti-mouse IgG-conjugated to HRP were purchased from Biovision

(Mountain View, CA). Phototope[®]-HRP Western blot detection system was purchased from Cell Signaling Technology.

4.2.2 Sample preparation

EP and 9(11)-DHEP were freshly dissolved in 100% EtOH and filtered by a syringe filter with a 0.20 μ m PVDF membrane (Gelman Laboratory). In the subsequent assays, the two steroids were further diluted to desired concentrations. The final concentration of EtOH was 0.05% (v/v).

4.2.3 Cell culture

The human cell lines selected for this study included A375 malignant melanoma cells and normal skin fibroblast Hs68 cells. The cells of A375 malignant melanoma were obtained from American Type Culture Collection (ATCC) and the cells of Hs68 were kindly provided by Dr. Ngai of Biology Department in CUHK.

A375 malignant melanoma cells were cultured in DMEM medium supplemented with 2.01g/L sodium bicarbonate and 2mM L-glutamine. Hs68 fibroblast cells were cultured in DMEM with 1.5g/L sodium bicarbonate, 4.5g/L glucose and 4mM L-glutamine.

Cells were routinely cultured in appropriate essential medium supplemented with 10% heat-inactivated FBS, 1% penicillin and streptomycin solution and 0.1% fungizone. They were grown at 37°C in a humidified atmosphere with 5% CO₂. The cultured cells were propagated in cell culture flasks at desired density with three times a week.

Before each subsequent assay, cultured cells were seeded with desired cell density and pre-incubated for 24 hours at 37°C in a humidified atmosphere with 5% CO₂.

4.2.4 Analysis of anti-proliferative activities of EP and 9(11)-DHEP on A375 malignant melanoma cells

4.2.4.1 MTT assay

According to the method of Son *et al.* (2003) with some modifications, the 1×10^5 A375 human malignant melanoma cells/ml were plated in 96-well tissue culture plate and incubated for 24 h, then treated with different concentrations of the two steroids for different hours. Details were referred to 2.2.4.1 of Chapter II.

4.2.4.2 Cell proliferation ELISA-BrdU (chemiluminescence) assay

The 5-bromo-2'-deoxyuridine (BrdU) assay is a chemiluminescence immunoassay for the quantification of cell proliferation (Huong *et al.*, 1991; Porstmann *et al.*, 1985). This is based on the measurement of BrdU incorporation during DNA synthesis in proliferating cells. Details were referred to 3.2.4.2 of Chapter II.

4.2.4.3 Determination of 50% inhibitory concentration (IC₅₀)

A375 malignant melanoma cells and Hs68 fibroblast cells were treated with the two steroids of different concentrations. The IC₅₀ was determined in MTT assay and BrdU assays. It was defined as 50% of cell growth or cell proliferation was inhibited in relation to control, respectively. The IC₅₀ values were obtained from linear regression of analysis ($r^2 > 0.97$).

4.2.5 Cytotoxicity detection

4.2.5.1 Lactate dehydrogenase (LDH) assay

LDH assay is based on the measurement of cytoplasmic enzyme activity

released by damaged cells (Lobner, 2000) and is used for the quantification of cellular cytotoxicity. Using Cytotoxicity Detection Kit, LDH (Roche Molecular Biochemicals), cytotoxic potential of steroids on both human cancer cells and normal fibroblast cells were determined.

4.2.5.2 Optimal of cell density for LDH assay

Different cell types may contain different amount of LDH. In a preliminary experiment, the optimum cell concentration for specific cell lines should be determined for subsequent assay. In this cell concentration, the difference between the low and high control is at a maximum.

According to manufacturer's instruction, cell densities from 1.2×10^2 to 2×10^6 cells/ml were suspended in fresh medium. Aliquots of 100 μ l/well cells were seeded onto 96-multiwell plate. In each experimental setup, a background control, a low control and a high control were performed (Table 4.1). In the group of background control, 200 μ l/well culture medium was filled into triplicate wells. The absorbance value obtained in background control was subtracted from all other values, this provided information about the LDH activity contained in assay medium. For the low control, 100 μ l/well culture medium was added to triplicate wells containing 100 μ l of cells, this provided information about LDH activity released from the untreated normal cells. On the other hand, in high control, 100 μ l/well Triton X-100 solution (2% Triton X-100 in assay medium) was added to triplicate wells containing 100 μ l of cells, this provided information about the maximum releasable LDH activity in cells. After 72h incubation at 37°C in a humidified atmosphere with 5% CO₂, cells were removed from culture medium by centrifugation at 300g for 10min using a Beckman GS-15R centrifuge. To determine the LDH activity, 100 μ l/well of cell-free culture supernatant was removed from the plate and then added into 100 μ l

reaction mixture, which containing catalyst (Diaphorase/NAD⁺ mixture) and dye solution (INT and sodium lactate). After 30min incubation in darkness, absorbance at 490nm was taken using a microplate spectrophotometer (SpectroAmax™ 250).

4.2.5.3 Detection of LDH activity

After preliminary experiment, desired cell densities of each human cancer cells were determined. Aliquots of 100µl/well cell suspension with determined cell density were plated in 96-mutiwell and pre-incubated at 37°C for 24h. The cells were then re-incubated with a final concentration of steroids for 72h in a humidified incubator with 5% CO₂. In each experimental setup, the background control, the low control, the high control and the substance control were performed as mentioned in Table 4.1. The following steps of LDH detection were the same as optimal cell concentration in section 4.2.5.2. According to manufacturer's instructions, results were represented as percentage cytotoxicity (%). The average absorbance values of treatment were subtracted from corresponding absorbance value obtained in the background control. The resulting values were substituted in equation 4.1:

$$\text{Cytotoxicity (\%)} = \frac{(A_{\text{treatment}} - A_{\text{low control}})}{(A_{\text{high control}} - A_{\text{low control}})} \times 100\% \quad (4.1)$$

where $A_{\text{treatment}}$: absorbance of treatment group

$A_{\text{low control}}$: absorbance of low control

$A_{\text{high control}}$: absorbance of high control

4.2.5.4 Determination of 50% effective concentration (EC₅₀)

A375 malignant melanoma cells and Hs68 fibroblast cells were treated with the two steroids of different concentrations. The EC₅₀ was determined in LDH assay. It

was defined as 50% of the maximum cytotoxic response as compared with control group. The EC₅₀ concentration was obtained from linear regression of analysis ($r^2 > 0.95$).

4.2.6 Apoptosis detection

4.2.6.1 Terminal deoxynucleotidyl transferase-mediated biotinylated UTP nick end-labeling (TUNEL) enzymatic labeling assay

For TUNEL assay, cells density of 3×10^4 cells/chamber was suspended in fresh medium and then seeded onto chamber slide. After 24h pre-incubation, A375 malignant melanoma cells were treated with the two steroids at final concentration of 10, 20 μ g/ml. For the control group (negative control and positive control), 0.5% EtOH (v/v) was used instead of steroids. Details were referred to 3.2.5.1 of the Chapter III.

4.2.6.2 Annexin-V-FLUOS labeling assay

Detection of PS on outer leaflet of apoptotic cell membrane can be performed by using Annexin-V-FLUOS staining kit (Roche Molecular Biochemicals). For detection and quantification of apoptosis, both apoptotic cells and necrotic cells were stained by Annexin-V labeling, while propidium iodide (PI) only stained the DNA of leaky necrotic cells, this can help to discriminate between apoptosis and necrosis at single cell level. According to manufacturer's instruction, 3×10^4 A375 human melanoma cells was suspended in fresh medium and was seeded onto chamber slide for pre-incubation at 37°C. A375 human malignant melanoma cells were treated with the two steroids at final concentration of 5, 10, 20, 30 μ g/ml. For the control group (negative control and positive control), 0.05% EtOH (v/v) was used instead of steroids. Details were referred to 3.2.5.2 of the Chapter III.

4.2.7 Analysis of cell cycle progression by flow cytometry

With the use of flow cytometer and DNA specific fluorescence dye, DNA content can be measured at single cell level. Cells at different phases in cell cycle (G_0/G_1 , S, G_2/M) with difference of DNA content can be displayed in a flow cytometric diagram, these patterns give information on the cell cycle distribution and therefore the changes in cell cycle of a cell population can be analyzed. The cell cycle pattern can also be employed to confirm apoptosis.

Cell cycle distribution of A375 malignant melanoma cells after treatment with 9(11)-DHEP or EP was monitored by flow cytometry. Cell suspension of 6×10^5 cells was seeded in 75cm^2 culture flask. After pre-incubation for 24h, cells were treated in the absent or presence of 9(11)-DHEP or EP at the concentrations between 0 to $30\mu\text{g}$ and were incubated at desired time. Cell number of 2×10^6 cells was harvested and the proportion of cells in G_0/G_1 , S, G_2/M phases was represented as DNA histogram. Apoptotic cells with hypodiploid DNA content were observed in cell cycle pattern.

4.2.8 Western immunoblotting and detection

4.2.8.1 Preparation of protein lysates

Cells density of 6×10^5 A375 malignant melanoma cells was seeded in 75cm^2 culture flask. After pre-incubation for 24h, exponentially growing cells were treated with EP for 24h or 9(11)-DHEP for 48h at a concentration of 0,10,20 or 30 ug/ml . After harvesting, 2×10^6 cells was centrifuged at 1500rpm for 5min. Cell pellets were then resuspended with $50\mu\text{l}$ ice-cold lysis buffer (Cell signaling, USA) and incubated for at least 2hrs on ice. After centrifugation at 4°C for 30min at 14,000rpm, cell lysates were collected as supernatant and stored at -80°C until analysis.

4.2.8.2. Preparation of mitochondria-free cytosolic fraction and mitochondria fraction

A375 malignant melanoma cells (3×10^6 cells/dish) were grown in 75cm^3 culture flask for 24h and then treated with EP for 24h or 9(11)-DHEP for 48h at concentration of 0,20,30 $\mu\text{g/ml}$. We used the 0.05% EtOH treated cells as a control. Both adherent and floating cells were collected, cytosolic extracts were prepared by incubation for 30 min on ice in hypotonic buffer pH 7.5 (20 mM Hepes, 10 mM KCl, 1.5 mM MgCl_2 , 1 mM EDTA, 1 mM EGTA, 250 mM sucrose, 1 mM dithiothreitol, aprotinin, leupeptin and pepstatin 2 mg/ml each). Then cells were broken in and centrifuged at 1000g for 10 min at 4°C , to remove unbroken cells and nuclei. The homogenates were then centrifuged twice at 12,000g for 30 min at 4°C , and the mitochondria-free supernatants were frozen at -80°C until further analysis. The rest pellet were continuously extracted in the ice-cold lysis buffer (Cell signaling, USA) for 2h, and then centrifuged at 14,000g for 30min at 4°C , and the supernatants were collected as mitochondria control for further analysis.

4.2.8.3 Tricine-SDS-polyacrylamide gel (Tricine-SDS-PAGE)

Total cellular protein was determined by using the BCA assay kit (Sigma). Equal amounts of protein (50-100 μg) were mixed with 2X sample loading buffer (0.0625M Tris-HCl, pH6.8, 2% SDS, 1% β -mercaptoethanol, 10% glycerol and 0.01% bromophenol blue) and heated at 95°C for 10min. The samples were resolved in 10-12% Tricine-SDS-PAGE in electrode buffer (25mM Tris, 0.19M glycine and 0.1% SDS, pH 8.3) at 50V for 30min and followed at 100V for 90min (Schägger H, 2006). After electrophoresis, the gel was stained in colloidal Coomassie solution (0.1% coomassie brilliant blue G-250, 34% methanol, 17% ammonium sulfate and 3% phosphoric acid) for 24h or further proceed the procedure of Western blot

analysis in section 2.3.6.2.3.

4.2.8.4 Western blot analysis

Protein samples (in the gel) were blotted onto nitrocellulose membrane (Amesham bioscience, USA) using Mini Trans-Blot cell (Bio-Rad) and then transferred in transfer buffer (25mM Tris, 0.2M Glycine and 20% methanol) at 200A for 90min. After transfer, the blotted membrane was first blocked in 0.2% Aurora blocking (w/v) with TBS/T (0.1% Tween-20, 20mM Tris, 137mM NaCl, and 1M HCl) for 1hr and incubated with primary antibody in desired dilution for overnight at 4°C. The membranes were also probed with β -actin antibody in 1:5000 dilution to verify uniform protein loading across samples. This was followed by washing in TBS-T and then incubating with horseradish peroxidase (HRP)-conjugated secondary antibody (1:2000) and HRP-conjugated anti-biotin antibody (1:1000) (Cell signaling, Inc.) to detect biotinylated protein markers with gentle agitation for 1 hr at room temperature. After several washings, membranes were subjected to chemiluminescent Western detection with LumiGLO[®] reagent as described in the manual of Phototope[®]-HRP Western Blot detection system (Cell Signaling Technology, Inc.). The membranes were visualized by Digital Imaging System (Bio-Gene Technology Ltd.). Quantification was performed by densitometric analysis (Model GS-690 Imaging Densitometer) (Bio-Rad).

4.2.9 *In vivo* studies on the xenograft mice

4.2.9.1 Chemicals and reagents

Propylene glycol was purchased from Sigma. EP was filtered by a syringe filter with a 0.20 μ m PVDF membrane (Gelman Laboratory) before use.

4.2.9.2 Animals

5-to 6- weeks-old male nude athymic mice were obtained from Laboratory Animal Services Centre, the Chinese University of Hong Kong. Nude mice were housed in metabolic cages under a 12/12h light/dark cycle (light period from 8a.m. to 8p.m.). The mice were divided randomly into 2 groups, and each group includes 7 mice. The animals were subcutaneous injected with 2×10^6 cells/ml of A375 human malignant melanoma cells in 0.1 ml DMEM medium per mouse. When the size of solid tumor in tumor-bearing nude mice reached 100 mm^3 , the tumor-bearing nude mice were treated with ergosterol peroxide via celiac injection at the dosage of 25 mg/kg for 12 days, another group was given 20% propylene glycol instead of ergosterol peroxide to act as control group and then observed for another consecutive 5 days. At the end of the experiments, animals were euthanized with carbon dioxide inhalation, followed by cervical dislocation, and then the solid tumors were picked up. Data were statistically analyzed by solid tumor weight. Tumors were measured in two dimensions by using calipers at every 3 days intervals and the volume of the tumor was calculated according to the formula: $\text{Volume} = (\text{length} \times \text{width}^2)/2$. (Zhang YH, et al., 2006)

4.2.9.3 Analysis of protein expression in the tumor by western blotting

Total protein of solid tumor was extracted by blandering in liquid nitrogen with 1ml ice-cold lysis buffer (Cell signaling, USA). After centrifugation at 4°C for 30min at 14,000rpm, cell lysates were collected as supernatant and stored at -80°C until analysis.

Total protein content was detected by BSA assay and separated by tricine-SDS-polyacrylamide gel (Tricine-SDS-PAGE). Details was followed 4.2.8.3.

4.2.9.4 Analysis of gene expression in the tumor by real-time PCR

Total RNA from solid tumor was extracted using Trizol® Reagent (Invitrogen, Carlsbad, CA, USA) according to the manufacturer's instructions. 50-100mg solid tumor block of seven tumors from the control and treatment group was homogenized in 1ml Tri Reagent at room temperature. After mixing in chloroform, the mixture was centrifuged at 12,000 ×15min at 4°C. The supernatant was collected and 500µL isopropanol was added to precipitate the RNA. Then RNA pellet was collected and washed with 75% ethanol. Finally the pellet was dried and dissolved in 20µL of Diethyl pyrocarbonate (DEPC) water for further use. RNA concentration was determined by spectrophotometric measurement and the RNA sample quality was checked by formaldehyde agarose gel electrophoresis.

Before RT-PCR reaction, RNA sample was treated with DNase I (1U/µL) to remove DNA contaminant. The cDNA was synthesized from RNA samples using Superscript II Rnase H Reverse Transcriptase and oligo(dT) (Invitrogen, USA) according to the manufacturer's instructions. The treated RNA samples were incubated at 65°C for 5min after adding 200µM Oligo dT and 10 mM dNTPs. Then the mixture was cooled on ice and incubated in 42°C for 2min with reaction mixture of 5X first strand buffer, 0.1 M DTT and RNase OUT. Subsequently, Superscript II Reverse Transcriptase was added to the mixture and reacted at 42°C for 2hrs. Finally, the reaction was stopped by heating to 70°C for 15mins. The cDNA was diluted to desired concentration.

For quantitative analysis of caspase 7, Bcl-2 and Bax mRNA, the human GAPDH gene served as endogenous control. Primer pairs were designed according to the sequences in the GenBank. *Caspase 7*: forward 5'-GTCTCACCTATCCTGCCCTCAC-3'; reverse 5'- TTCTTCTCCTGCCTCAC TGTCC-3'. *BAX*: forward 5'-CCAGCTGCCTTGGACTGT-3'; reverse 5'-

ACCCCCTCAAGACCACTCTT-3'. *GAPDH*: forward 5'-CCAGGCGCCC AATACGA-3'; reverse 5'-GCCAGCCGAGCCACATC-3'. (Huand TC, et al., 2007; Bodzioch M, et al. 2005). Quantitative gene expression was performed with SYBR Green I (Bio-Rad) on Bio-Rad IQ5 Multicolor Real-Time PCR detection system with iCycler PCR machine. The reaction mixture (20 μ L) (5mM forward and reverse primers, cDNA, DEPC-water and 2X SYBR Green I) was added to Axygen PCR microplate with dot cap covered. The thermal cycling condition of the RT-PCR was done according to So et al. (2005) with some modification: comprised an initial denaturation step at 95°C for 10 min and 40 cycles at 95°C for 15 s and 60°C for 1 min. The fold change is given as a mean according to Livak KJ and Schmittgen TD, 2001. The fold change showed linear correlation with relative DNA copy numbers. Experiments were performed in triplicate for each data point. Multiple negative controls (water control and no template control) were included in each set of reaction. The signals were collected at the end of each cycle and data analysis was performed using Bio-Rad IQ 5 version 2.0 Standard edition.

4.2.10 Statistical analysis

β -Actin was used as the internal control in Western blot. The amount of protein was expressed as arbitrary densitometric units of β -actin. The data were expressed as the relative density compared to their respective controls (untreated cells), taken as 1.0. Dates were expressed as mean \pm standard deviation (SD) in three independently experiments. Statistical analysis was performed using a two-tailed Student's *t*-test. Differences with $p < 0.05$ were considered statistically significant.

Table 4.1 Overview of the experimental setup of cytotoxicity (LDH) assay

Contents	Background control	Low control	High control	Substance control	Treatment group
Assay medium	200µl	100µl	-	100µl	-
Cells	-	100µl	100µl	-	100µl
2% Triton X-100 solution	-	-	100µl	-	-
Test substance	-	-	-	100µl	100µl

4.3 Results

4.3.1 9(11)-DHEP and EP inhibited the A375 malignant melanoma cells proliferation

Effects of various concentrations (0-50ug/ml) of 9(11)-DHEP and EP on human skin cancer A375 malignant melanoma cell growth were examined by MTT assay. 9(11)-DHEP and EP mediated growth inhibition in a dose-dependent manner (Figure 4.2). IC_{50} after 72h treatment with the sample were 9.462ug/ml for 9(11)-DHEP and 9.147ug/ml for EP. The inhibitory effect also behaved in a time-dependent manner (Figure 4.3). Significant inhibition of both the two steroids on cell growth was observed at 24h for all the cancer cell lines. After 48h treatment, the viability of the two cancer cells was suppressed above 50%. Meanwhile, natural triterpenes were also documented. Results showed that ursolic acid and betulinic acid also inhibited the A375 malignant melanoma cells growth.

Furthermore, we investigated the effects of the two steroids on the DNA synthesis of A375 malignant melanoma cells evaluated by BrdU chemiluminescence assay. The maximum anti-proliferative response of different concentration (0-50ug/ml) 9(11)-DHEP and EP was observed after 72hr treatment. IC_{50} were used to interpret the result of the sample. As showed in Figure 4.4, 9(11)-DHEP and EP inhibited A375 malignant melanoma cells proliferation in a dose-dependent manner. Above 5 μ g/ml both the two steroids showed significant inhibitory effects. The concentration of EP and 9(11)-DHEP required to inhibit 50% of A375 malignant melanoma cells proliferation (IC_{50}) in BrdU assay is about for 12.57 μ g/ml and 15.89 μ g/ml, respectively.

4.3.2 The cytotoxicity of 9(11)-DHEP and EP on the A375 malignant melanoma cells and Hs68 normal fibroblast cells

Cellular membrane integrity was monitored using the permeability assay based on the determination of the release of LDH into the medium. This assay measured the conversion of tetrazolium salt into a red formazan product. Cells were treated with 9(11)-DHEP and EP in concentration ranging from 0 to 100 μ g/ml for 72h. The results were represented as cytotoxicity (%). Both the two steroids were found to be cytotoxic in A375 malignant melanoma cells; the effect was observed when concentration exceeded 10 μ g/ml (Figure 4.5).

On the other hand, in order to determine the cytotoxic effect on human normal cells, the EC₅₀ of 9(11)-DHEP and EP on skin fibroblast (Hs68) cells were illustrated in Table 4.2. 9(11)-DHEP and EP were observed to have less cytotoxic effect in Hs68 cells.

4.3.3 Cell cycle analysis on the A375 malignant melanoma cells by flow cytometry

To investigate the mechanism by which the two steroids inhibit cancer cells growth, cell cycle analysis was performed with flow cytometry. The A375 malignant melanoma cells were treated with different concentration of the two steroids for 72hrs (Figure 4.6). As shown in Figure 4.7, the number of the cells in subG1 phase increased gradually in a dosage-dependent manner after 72hr treatment with the steroids. These results suggested that the two steroids inhibited the cancer cells by inducing apoptosis. The cancer cells seemed to more sensitive to EP than to 9(11)-DHEP.

The A375 malignant melanoma cells were treated with 20 μ g/ml EP or

9(11)-DHEP for 24h, 48h. Results showed that both the two steroids could induce apoptosis of A375 malignant melanoma cells in a time-dependent manner (Figure 4.8). A significant increase on subG1 phase appeared after treatment with 20ug/ml EP. The subG1 cell increased from $1.03 \pm 0.11\%$ to $32.89 \pm 0.81\%$ on 24h, $3.97 \pm 0.09\%$ to $44.62 \pm 0.74\%$ on 48h and $1.14 \pm 0.10\%$ to $49.89 \pm 1.04\%$ on 72h. After different time inhibition, the apoptosis cell of 9(11)-DHEP-treated was increase dramatically. The subG1 cell increased from $1.03 \pm 0.11\%$ to $5.57 \pm 0.45\%$ on 24h, $3.97 \pm 0.09\%$ to $29.62 \pm 1.06\%$ on 48h and $1.14 \pm 0.10\%$ to $36.49 \pm 0.39\%$ on 72h.

In addition, the positive control betulinic acid and ursolic acid could also arrested the A375 malignant melanoma cells on subG1 phase in a dosage-dependent manner (Figure 4.9).

4.3.4 Analysis of apoptotic morphology in A375 malignant melanoma cells treated with 9(11)-DHEP and EP

To understand characteristic of the cytotoxic effect, the A375 malignant melanoma cells were subjected to apoptosis assays, including TUNEL enzymatic labeling assay (*In situ* Cell Death Detection Kit, Fluorescein) and Annexin-V-FLUOS assay. Cells were cultivated with 9(11)-DHEP and EP in concentration of 0ug/ml, 10ug/ml, and 20ug/ml for 72h. The results were represented as image under the confocal laser scanning microscope (CLSM).

In TUNEL assay, DNA strand breaks can be detected by enzymatic labeling of the free 3'-OH termini with modified nucleotides. Those apoptotic cells are intensely stained green and are easily visible under fluorescence microscopy. Compared with the negative control, apoptotic bodies were greatly induced in the A375 malignant melanoma cells by TUNEL staining treated with the two steroids above 10ug/ml as

the Figure 4.10 showed.

In this research of Annexin-V-FLUOS assay, the green dye, Annexin-V, is used and serves as a marker for apoptotic cells. Simultaneously, the red dye, propidium iodide, is used for DNA staining. This can help to discriminate between early phase, late phase apoptosis and necrosis at single cell level (Vermees I, et al., 1995; Koopman G, et al., 1994). The Annexin V-/PI- population was regarded as normal healthy cells, while Annexin V+/PI- cells were taken as a measure of early apoptosis, Annexin V+/PI+ as late apoptosis, and Annexin V-/PI+ as necrosis. These results show that the number of apoptotic cells increased concomitantly with dosage and that annexin V/PI double-positive cells also increased at 20µg/ml steroids. At 5ug/ml 9(11)-DHEP (Figure 4.11) or EP (Figure 4.12), A375 cancer cells were living and observed with low staining of annexin and PI. Nevertheless, late apoptotic cells with high annexin and high PI staining were shown at 20µg/ml 9(11)-DHEP (Figure 4.11), which suggested that apoptosis was the major reason of the A375 malignant melanoma cells death.

4.3.5 9(11)-DHEP and EP induced apoptosis of A375 malignant melanoma cells by mitochondria-mediated pathway

To study how the two steroids induce apoptosis of A375 malignant melanoma cells, the expressions of PARP, caspase family and Bcl-2 family were investigated in our work. PARP, a 116 kDa nuclear poly (ADP-ribose) polymerase, appears to be involved in DNA repair predominantly in response to environmental stress. It is an important downstream protein in the apoptosis pathway and thought to be labeling protein of apoptosis. Our results indicated that the significant increase expression of cleaved PARP fragments were observed in A375 malignant melanoma cells treated with 9(11)-DHEP and EP in a dosage-dependent manner (Figure 4.13), which

suggested that the two Ganoderma steroids can induce apoptosis on A375 malignant melanoma cells.

Caspases, a family of cysteine acid proteases, are central regulators of apoptosis. Several caspase expressions were detected in A375 malignant melanoma cells treated by the two steroids. The data are shown in Fig.4.15, both the two steroids noticeably stimulated the activities of caspase 3, 7, 9 in tumor cells in a dosage-dependent manner but not the caspase 6, 8, 10. The result suggested that the apoptosis of A375 malignant melanoma cells induced by the two steroids is caspase-dependent.

In addition, cytochrome C plays an important role in the mitochondria pathway. Here our results showed that cytochrome C in the cytosolic fraction significantly increased in a dosage-dependent manner after treated with both of the two steroids (Figure 4.14), while that in the mitochondria fraction decreased a little. These suggested that cytochrome C released from the mitochondria into the cytosol.

Meanwhile, the expressions of the Bcl-2 family of A375 malignant melanoma cell under the two Ganoderma steroids treatment were detected. Our result showed that the Mcl-1 protein was down-regulated (Figure 4.17) and Bak was slightly up-regulated (Figure 4.18) in a dosage-dependent manner, whereas the expressions of Bad, Bax, puma, BID, Bmf, Bim, Bcl-xl and Bcl-2 were no changed (Figure 4.16).

4.3.6 EP inhibited tumor growth in xenograft tumor-bearing nude mice

When the solid tumors in xenograft tumor-bearing nude mice were treated with 25mg/kg EP, the suppression of tumor growth was observed. As the Figure 4.21b showed, average tumor volume increased rapidly over the 18 days treatment period in control mice. In EP-treated mice, tumor volume almost did not increase during the first 10 days of treatment and then little increase in tumor volume between 12 to 20 days. The tumor volume was dramatically lower in the group treated with 25mg/kg

EP than in the control group, which decreased 53% compared with the control group. While for the final tumor weights, the EP-treated tumor decreased significantly by 47.7% of the control level (Figure 4.21c). But there is no significant difference between the control group and the treatment group on the body weights of nude mice after 20 days growth (Figure 4.21a). Our results suggested that EP could effectively inhibit tumor growth *in vivo*, but had little side effect on the body weight.

To further study the mechanism of tumor growth suppression of EP, RNA and crude protein were extracted from each solid tumor. Real time-PCR and Western blotting were used to study how EP affected the tumor cell on the transcription level and the translation level *in vivo*. Our results showed that cleaved PARP fragments significantly increased in the 25mg/kg EP-treated group compared with the control group (Figure 4.22). For the Real time-PCR analysis, EP greatly enhanced the effector *caspase 7* gene expression but not BAX gene in the treatment group (Figure 4.23). Gene expression of *caspase 7* in the tumor treated with 25mg/kg EP increased 74.39% compared to the control group. Both the above dates suggested that EP could inhibit the tumor growth by inducing the tumor cell apoptosis.

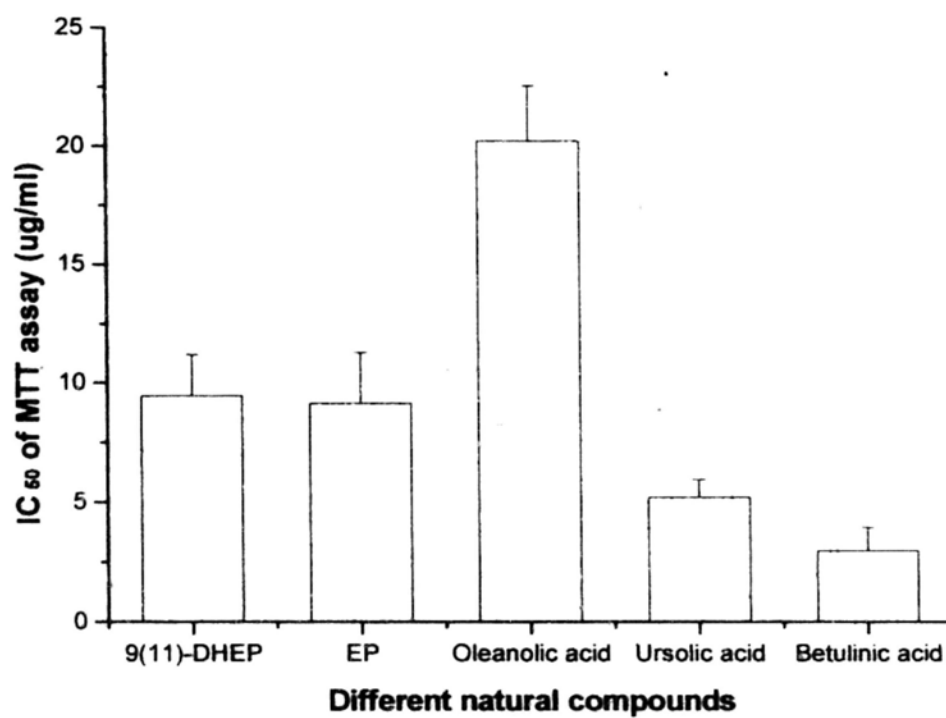


Figure 4.2 Inhibitory activities of different natural compounds on A375 malignant melanoma cells growth. Cells were treated with various concentrations of different fractions for 72h; and cell viability was determined by the MTT assay.

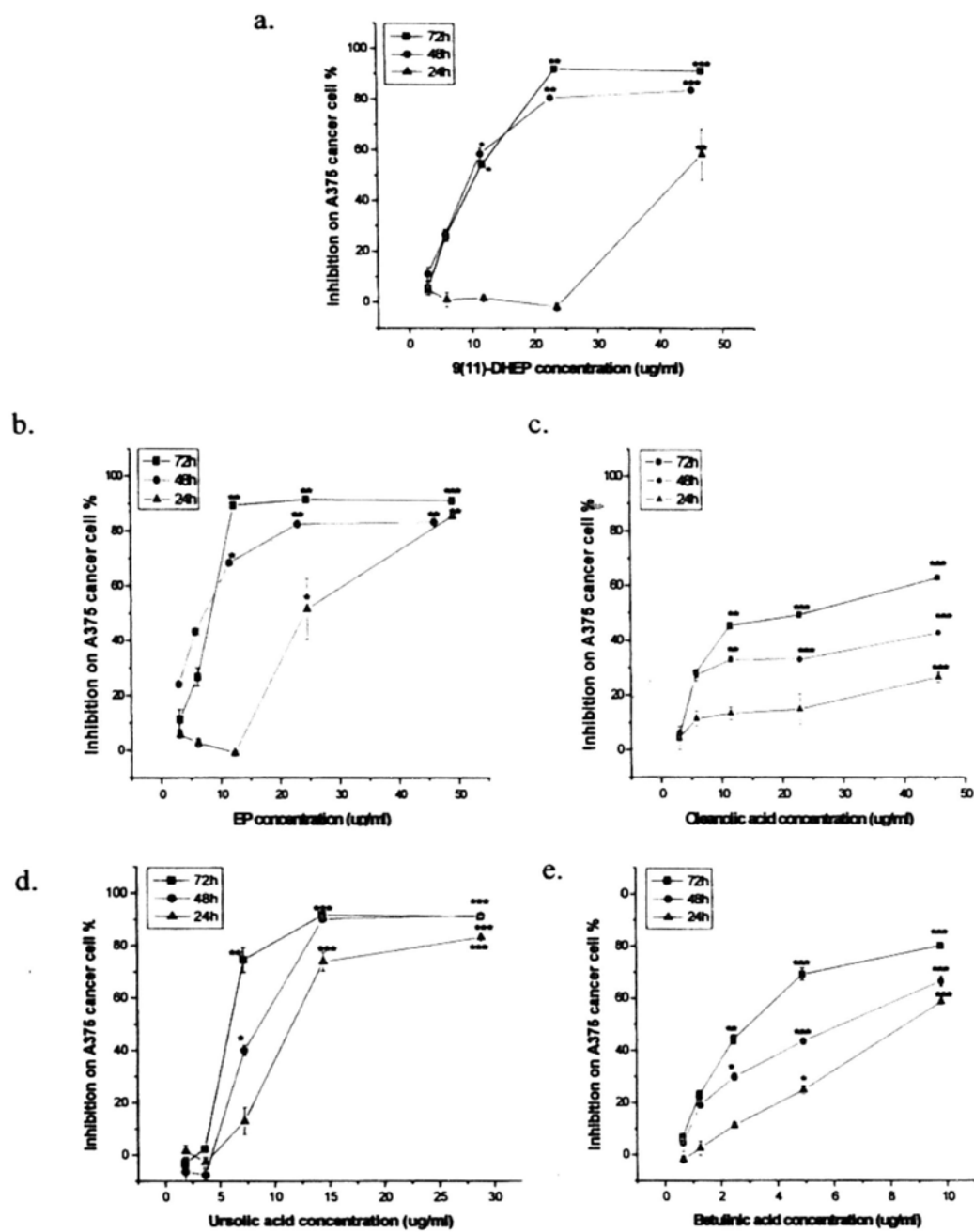


Figure 4.3 Inhibitory effects of natural compounds on A375 malignant melanoma cells in a time-dependent manner. Cells were treated with various concentrations of the two steroids for 24h, 48h, 72h; and cell viability was determined by the MTT assay. a. 9(11)-DHEP; b. EP; c. Oleanolic acid; d. Ursolic acid; e. Betulinic acid. Results are expressed as percentages of proliferation compared to the control (mean \pm SD, n=3). P<0.05 (*), P<0.01 (**), P<0.001 (***) were considered significantly different.

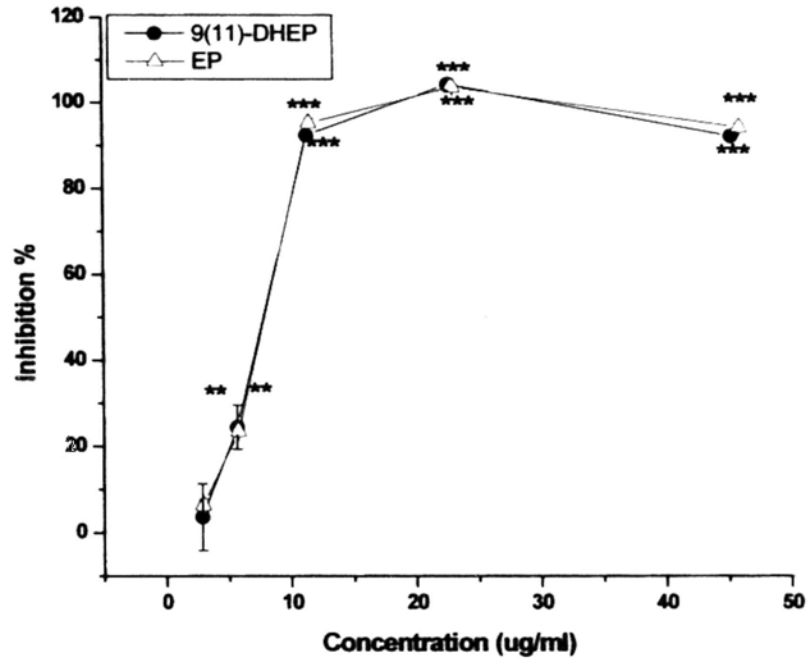


Figure 4.4. Inhibitory effects of 9(11)-DHEP and EP on A375 malignant melanoma cells in a dosage-dependent manner by BrdU assay. Cells were treated with various concentrations of the two steroids for 72h; and cell viability was determined by the BrdU assay. Results are expressed as percentages of proliferation compared to the control (mean \pm SD, n=3). $P < 0.05$ (*), $P < 0.01$ (**), $P < 0.001$ (***) were considered significantly different.

Table 4.2 The EC₅₀ values of 9(11)-DHEP and EP on different cell lines after 72h incubation as determined by LDH assay.

	EC ₅₀ (ug/ml)	
	9(11)-DHEP	EP
Hs68	65.61±3.08	39.74±1.79
A375	30.79±1.76	15.43±2.45

The EC₅₀ concentrations are calculated graphically and represented the concentration which results in 50% cytotoxicity after incubation. Results are expressed as mean value of three independent experiments.

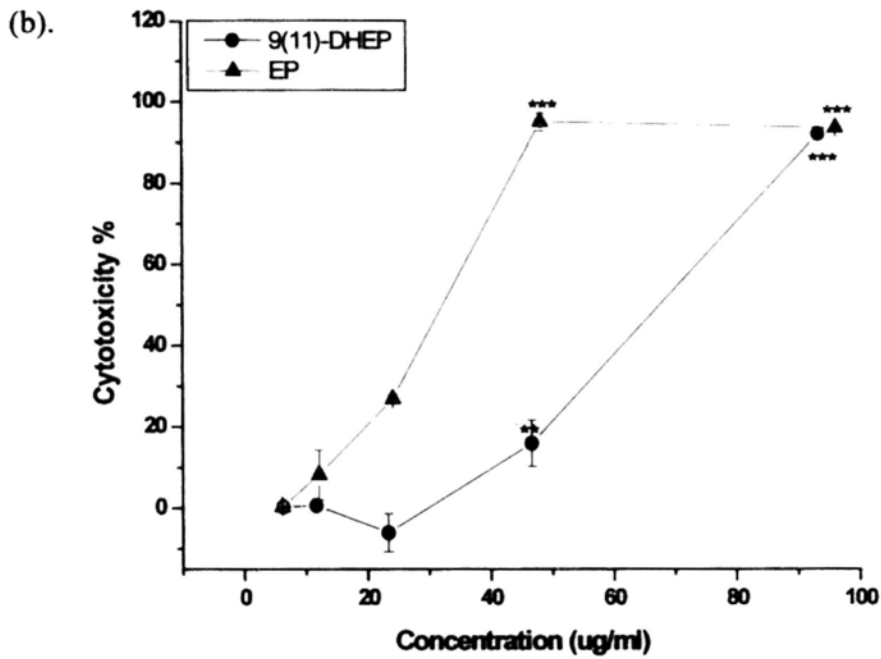
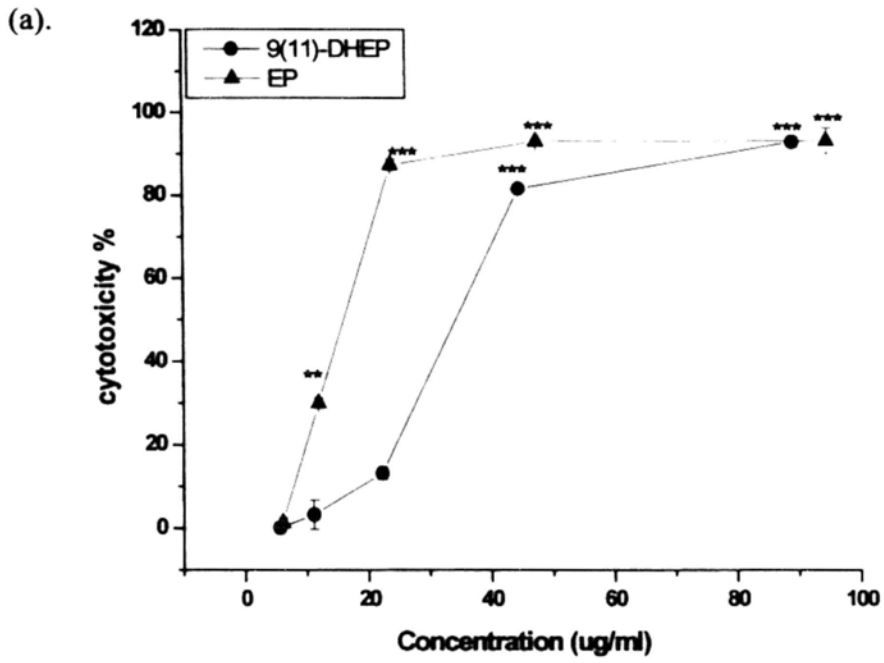


Figure 4.5 The cytotoxicity of 9(11)-DHEP and EP on different cells as determined by LDH assay after 72h incubation. (a) A375 malignant melanoma cells; (b) Hs68 normal cells. Results are expressed as mean \pm SD (n=3). $P < 0.05$ (*), $P < 0.01$ (**), $P < 0.001$ (***) were considered significantly different.

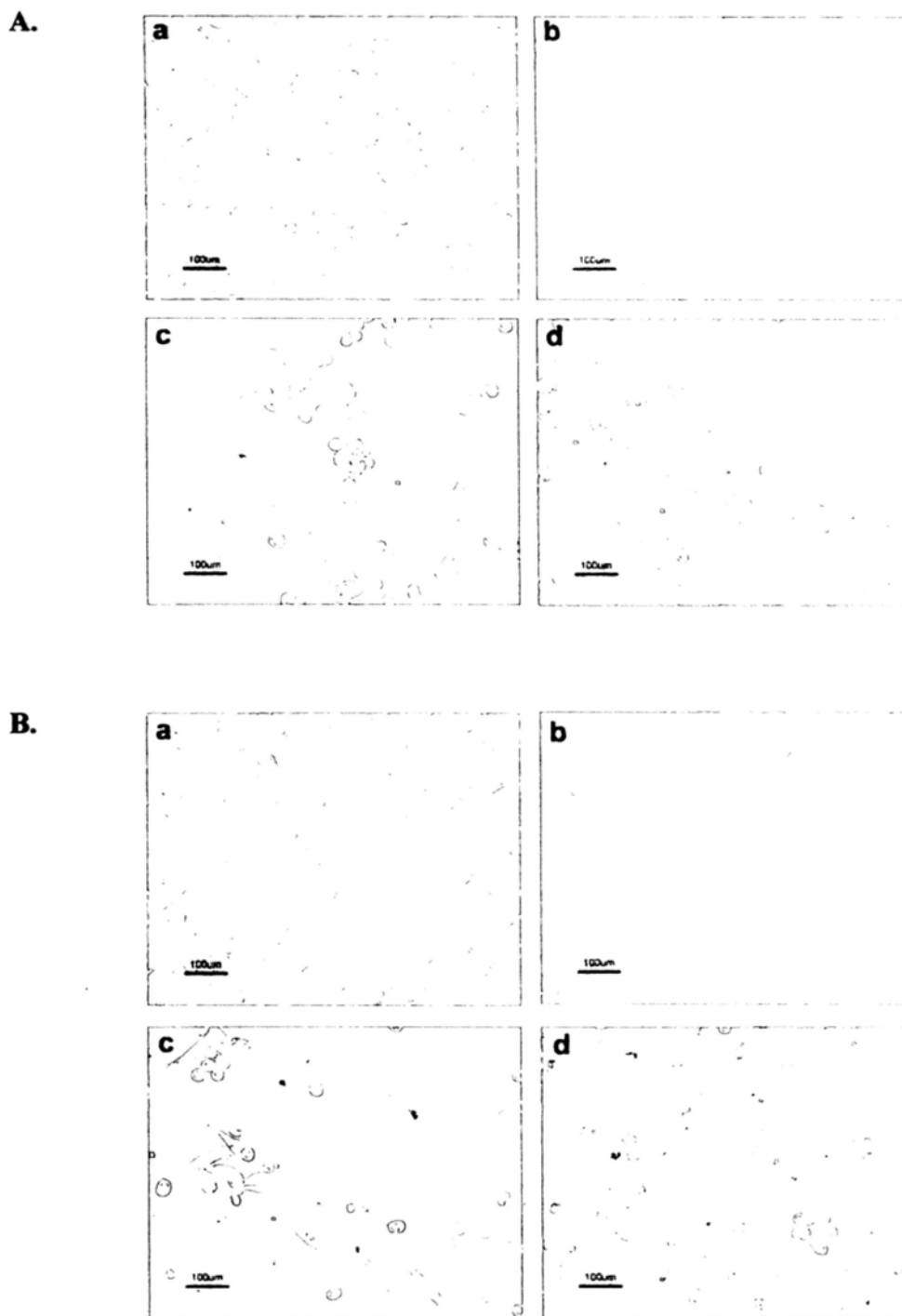


Figure 4.6 Effects of 9(11)-DHEP and EP treatment on the morphological changes of A375 cells. A375 cancer cells were treated with different concentrations of 9(11)-DHEP (A) and EP (B) for 72h. Light microscope photographs were obtained at 200× magnification. For each diagram, a.control; b. 10ug/ml; c. 20ug/ml; d.30ug/ml.

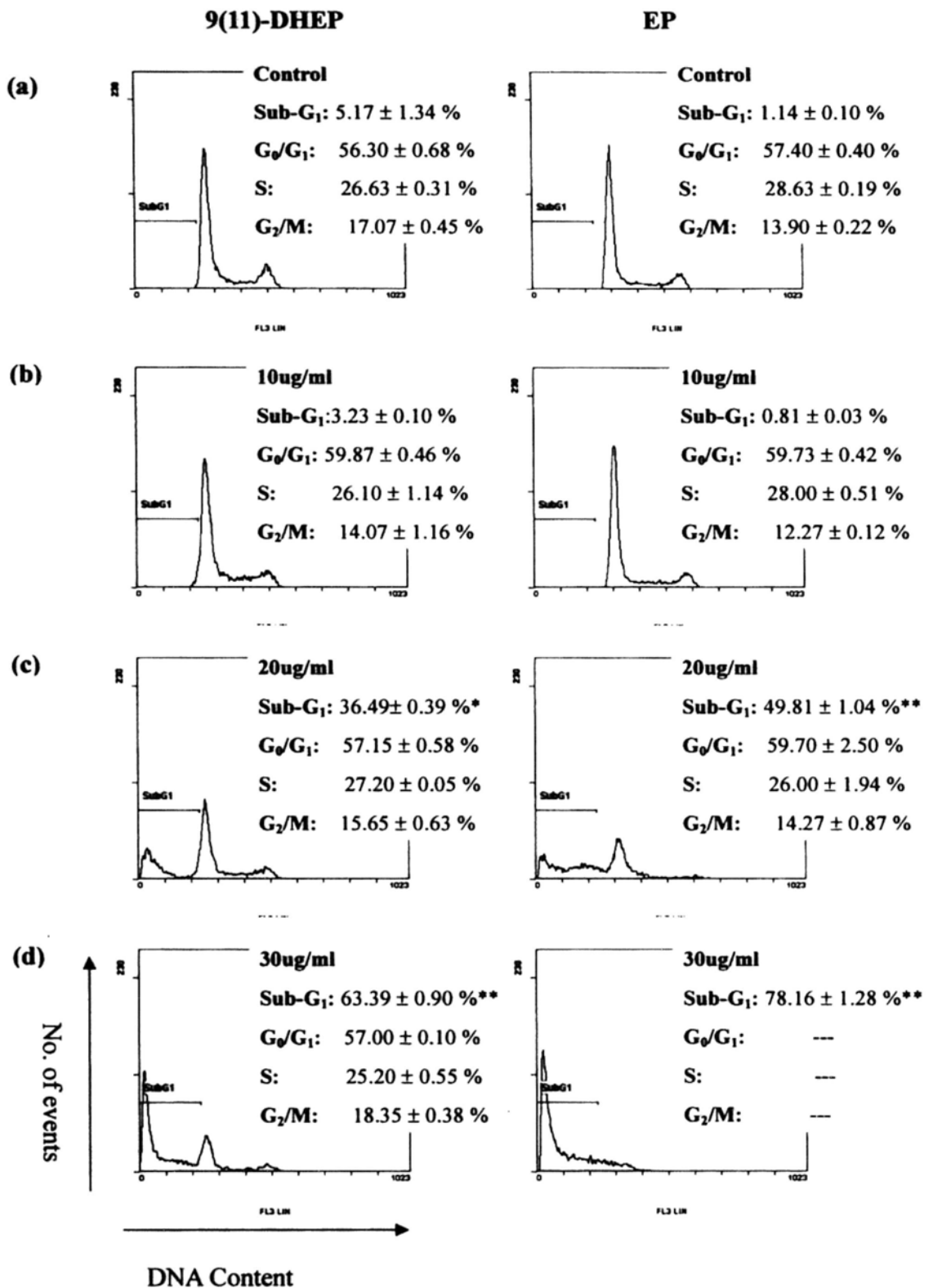


Figure 4.7 Fluorescence-activated cell sorting analysis of A375 malignant melanoma cells after 72hr treatment with 9(11)-DHEP and EP at different concentration. Cell cycle phase distributions were quantified by staining cells with propidium iodide. (a) Control; (b) 10ug/ml; (c) 20ug/ml; (d) 30ug/ml. Results are expressed as percentage of cells in sub-G₁, G₀/G₀, S and G₂/M phase at each time point after exposure. Data are mean ± SD (n=3). P<0.05 (*), P<0.01 (**), were considered significantly different.

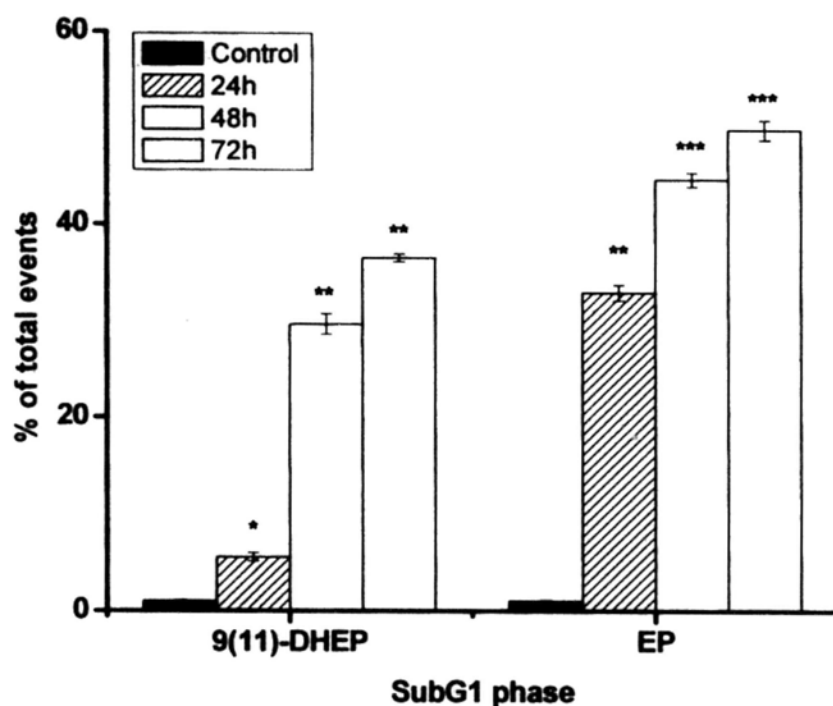


Figure 4.8 Effects of 20ug/ml 9(11)-DHEP and EP on cell cycle phase distribution in A375 cancer cells at different incubation times. Results are expressed as mean \pm SD (n=3). $P < 0.05$ (*), $P < 0.01$ (**), $P < 0.001$ (***) were considered significant difference comparing with the control.

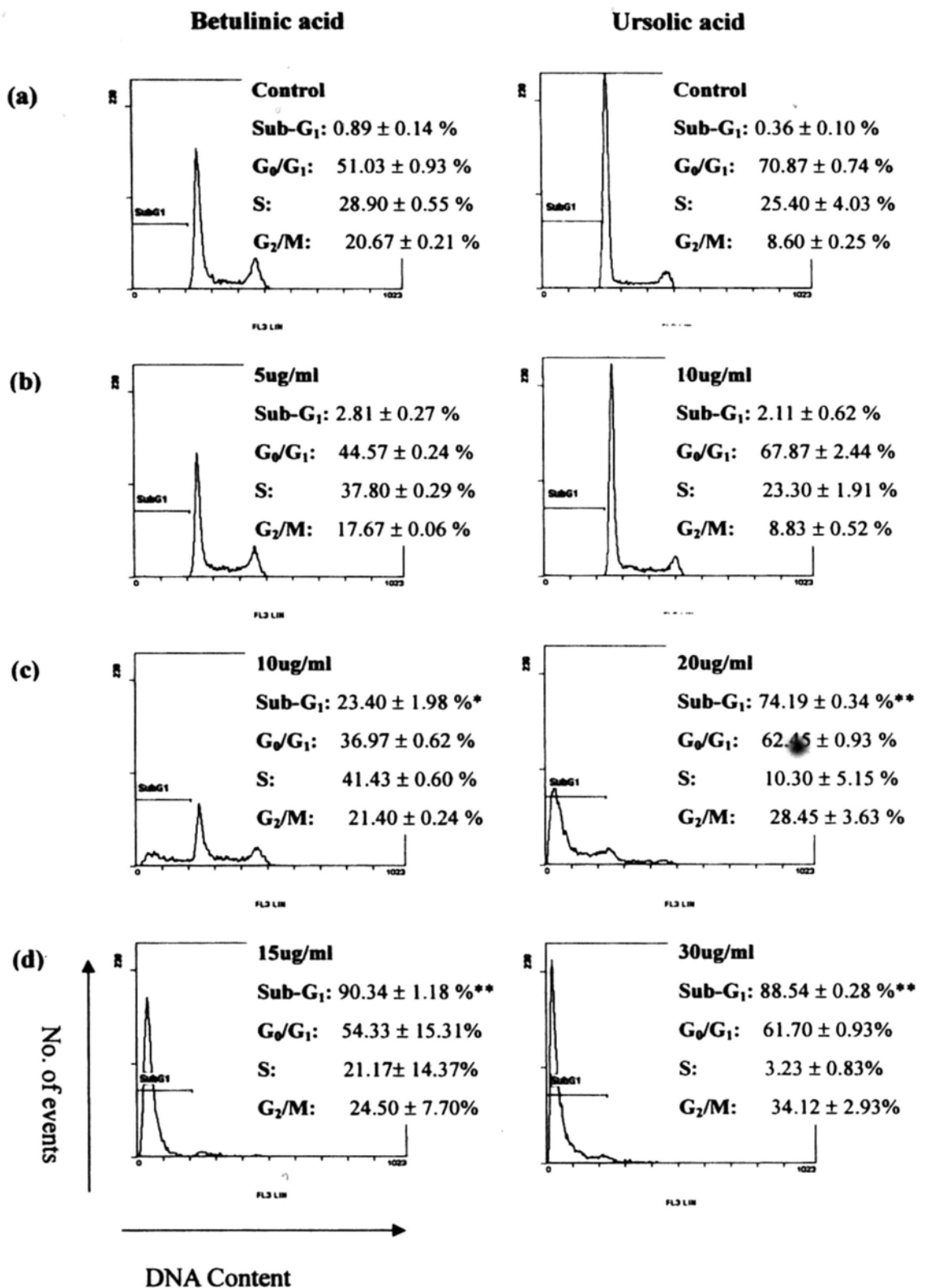


Figure 4.9 Fluorescence-activated cell sorting analysis of A375 malignant melanoma cells after 72hr treatment with natural triterpenes at different concentration. Cell cycle phase distributions were quantified by staining cells with propidium iodide. (a) Control; (b) 10ug/ml; (c) 20ug/ml; (d) 30ug/ml. Results are expressed as percentage of cells in sub-G₁, G₀/G₀, S and G₂/M phase at each time point after exposure. Data are mean ± SD (n=3). P<0.05 (*), P<0.01 (**) were considered significantly different.

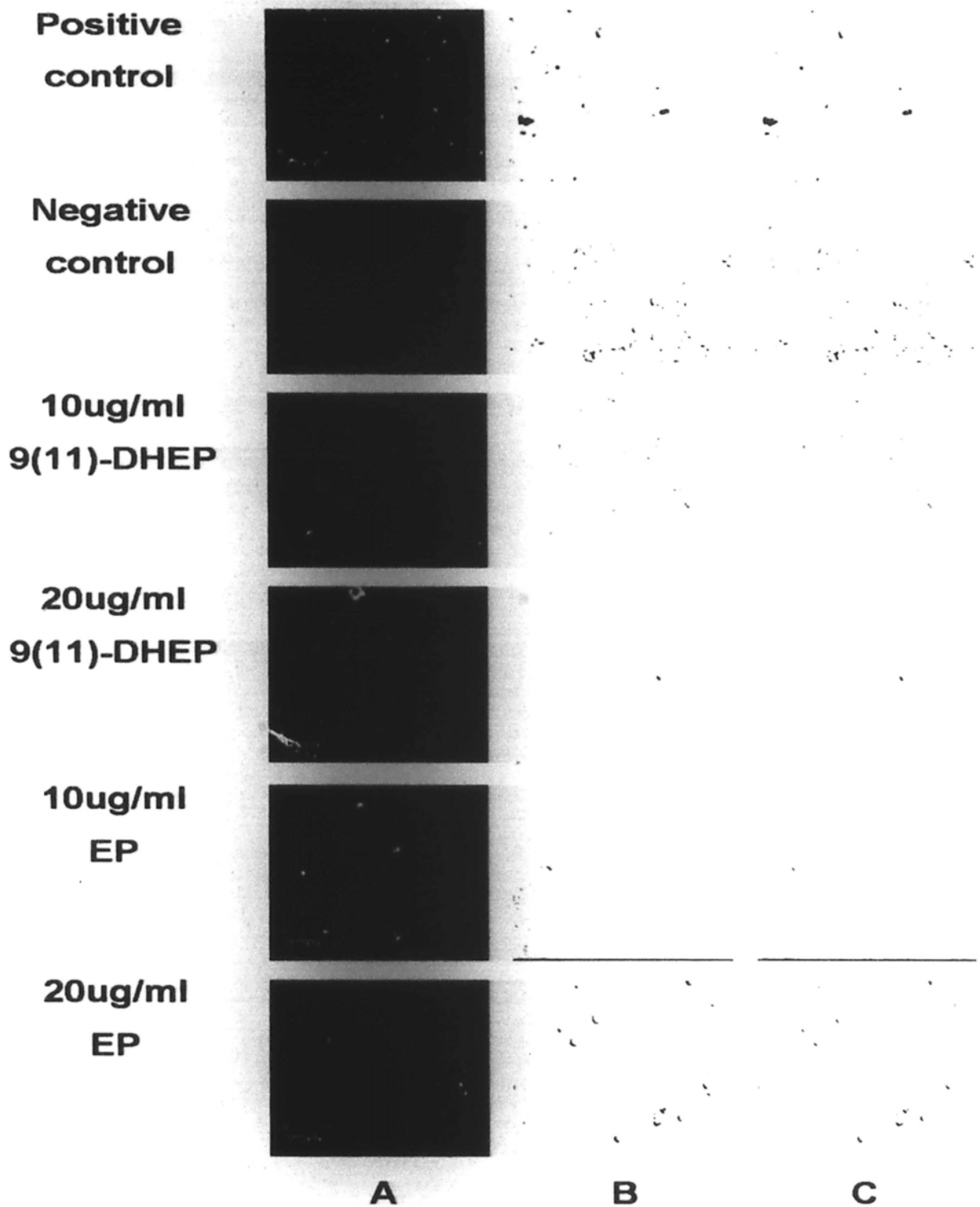


Figure 4.10. Effects of 9(11)-DHEP and EP on A375 malignant melanoma cells by confocal laser scanning microscopy using TUNEL assay. Cells were cultivated for 72h in the presence of different concentration EP and 9(11)-DHEP. (A) single-parameter analysis by TUNEL treatment; (B) visible image of living cells. (C) dual-parameter analysis of TUNEL treatment and visible image of living cells. Cells of negative control were treated with EtOH; cells of positive control were treated with DNaseI before TUNEL staining.

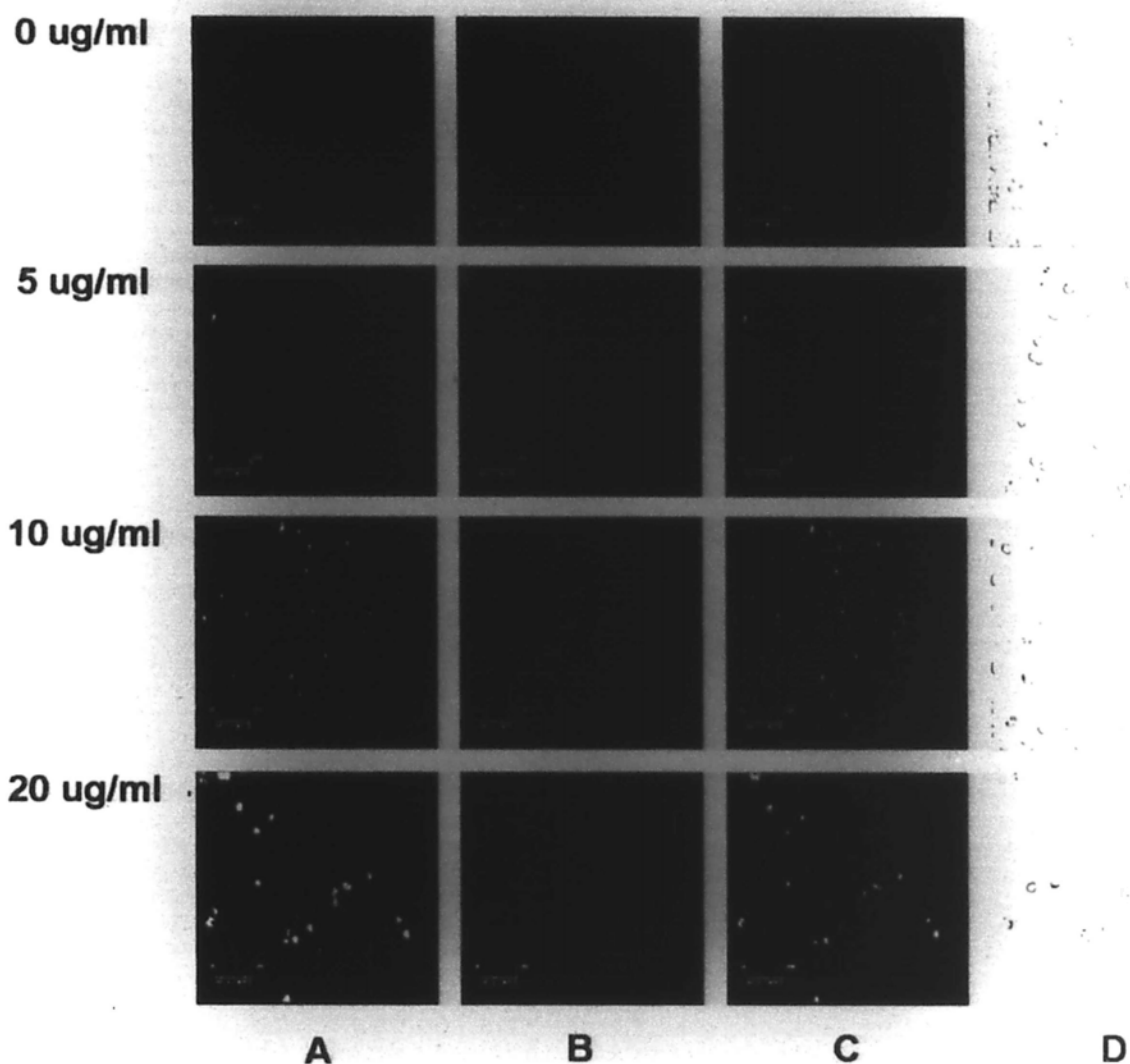


Figure 4.11. Effects of 9(11)-DHEP on A375 malignant melanoma cells by confocal laser scanning microscopy after staining with Annexin-V-FLUOS and propidium iodide. (A) single-parameter analysis staining with Annexin-V-FLUOS; (B) single-parameter analysis with propidium iodide; (C) dual-parameter analysis of TUNEL treatment and visible image of living cells; (D) visible image of living cells.

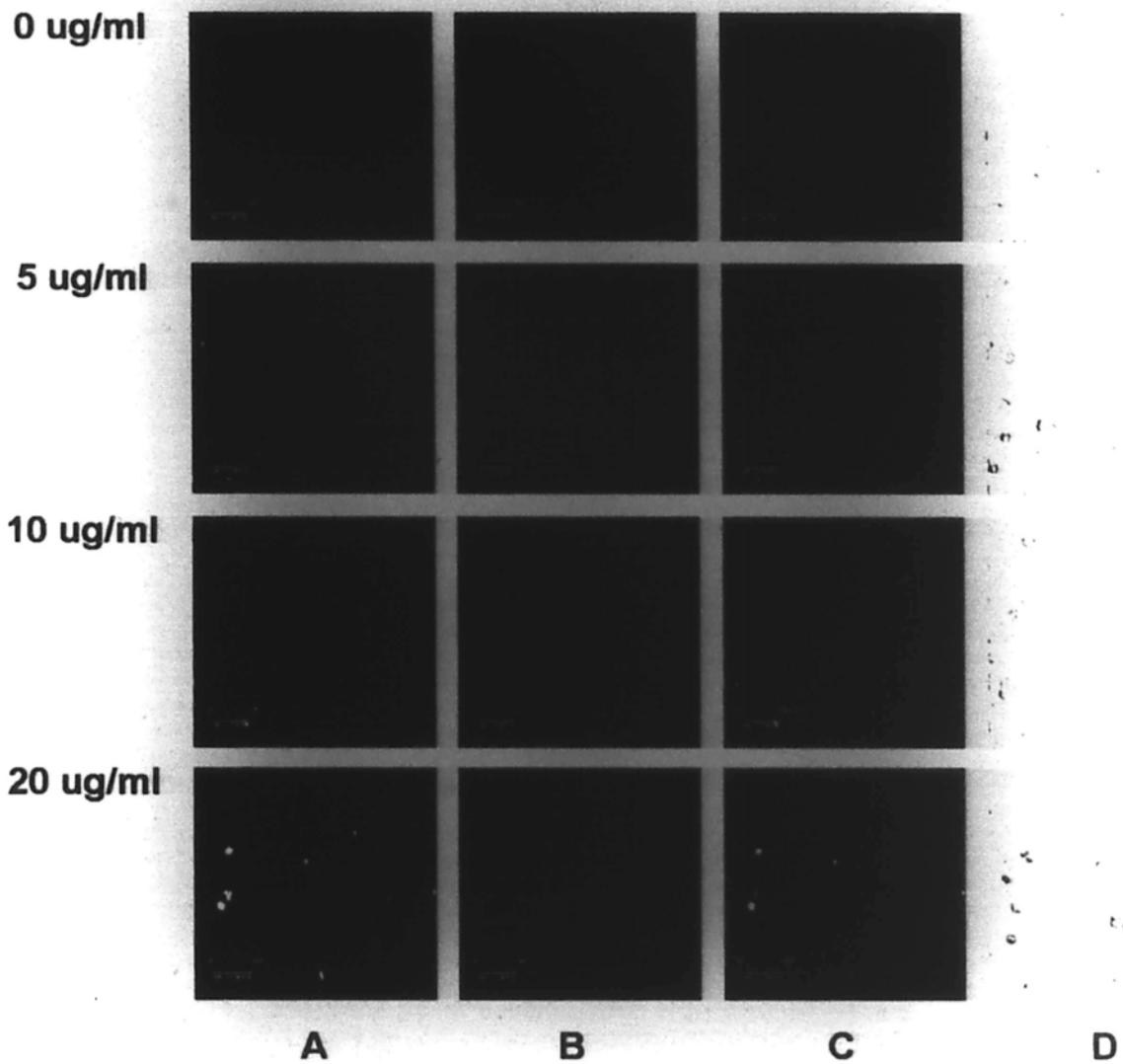


Figure 4.12. Effects of EP on A375 malignant melanoma cells by confocal laser scanning microscopy after staining with Annexin-V-FLUOS and propidium iodide. (A) single-parameter analysis staining with Annexin-V-FLUOS; (B) single-parameter analysis with propidium iodide; (C) dual-parameter analysis of TUNEL treatment and visible image of living cells; (D) visible image of living cells.

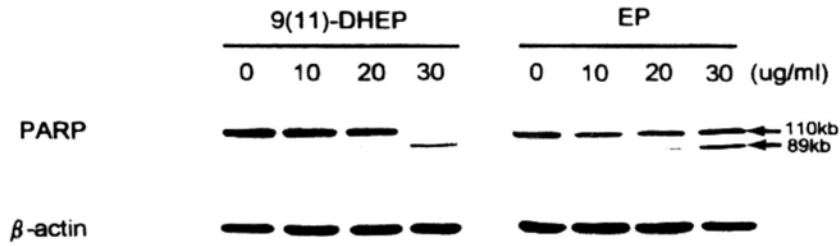


Figure 4.13 Dose-dependent effects of 9(11)-DHEP and EP on A375 malignant melanoma cells by western blot analysis using total PARP antibody (human specific). Cells were treated with different concentrations of EP for 24h & 9(11)-DHEP for 48h. Total protein (60 μ g) was resolved in 10% Tricine-SDS-PAGE and blotted on nitrocellulose membrane. The amount of protein was normalized to the densitometric units of β -actin.

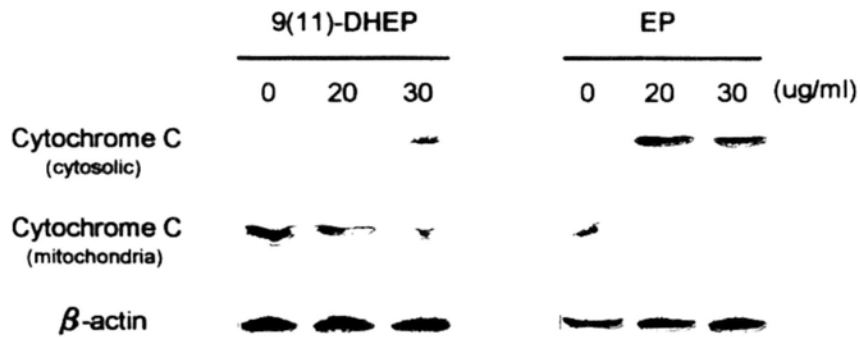


Figure 4.14. Dose-dependent effects of 9(11)-DHEP and EP on A375 malignant melanoma cells by western blot analysis using an anti-cytochrome c antibody. Cells were treated with different concentrations of 9(11)-DHEP for 48h & EP for 24h. Both cytosolic and nuclear protein (50ug) were separated by 12% Tricine-SDS-PAGE and blotted on nitrocellulose membrane. The amount of protein was normalized to the densitometric units of β -actin.

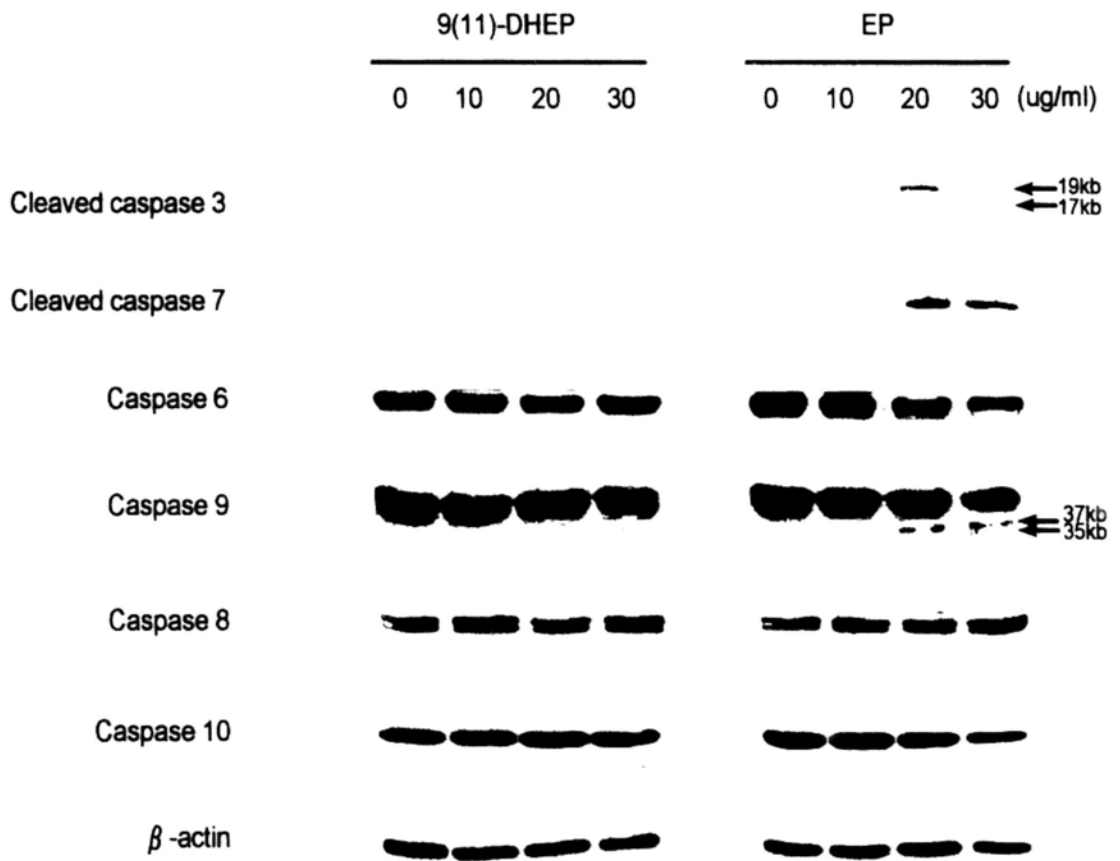


Figure 4.15. Dose-dependent effects of 9(11)-DHEP and EP on A375 malignant melanoma cells by western blot analysis using cleaved caspase 3 antibody, cleaved caspase 7 antibody (human specific), caspase 6, caspase 9, caspase 8 and caspase 10. Cells were treated with different concentrations of 9(11)-DHEP for 48h & EP for 24h. Total protein (60-80 μ g) was resolved in 10% Tricine-SDS-PAGE and blotted on nitrocellulose membrane. The amount of protein was normalized to the densitometric units of β -actin.

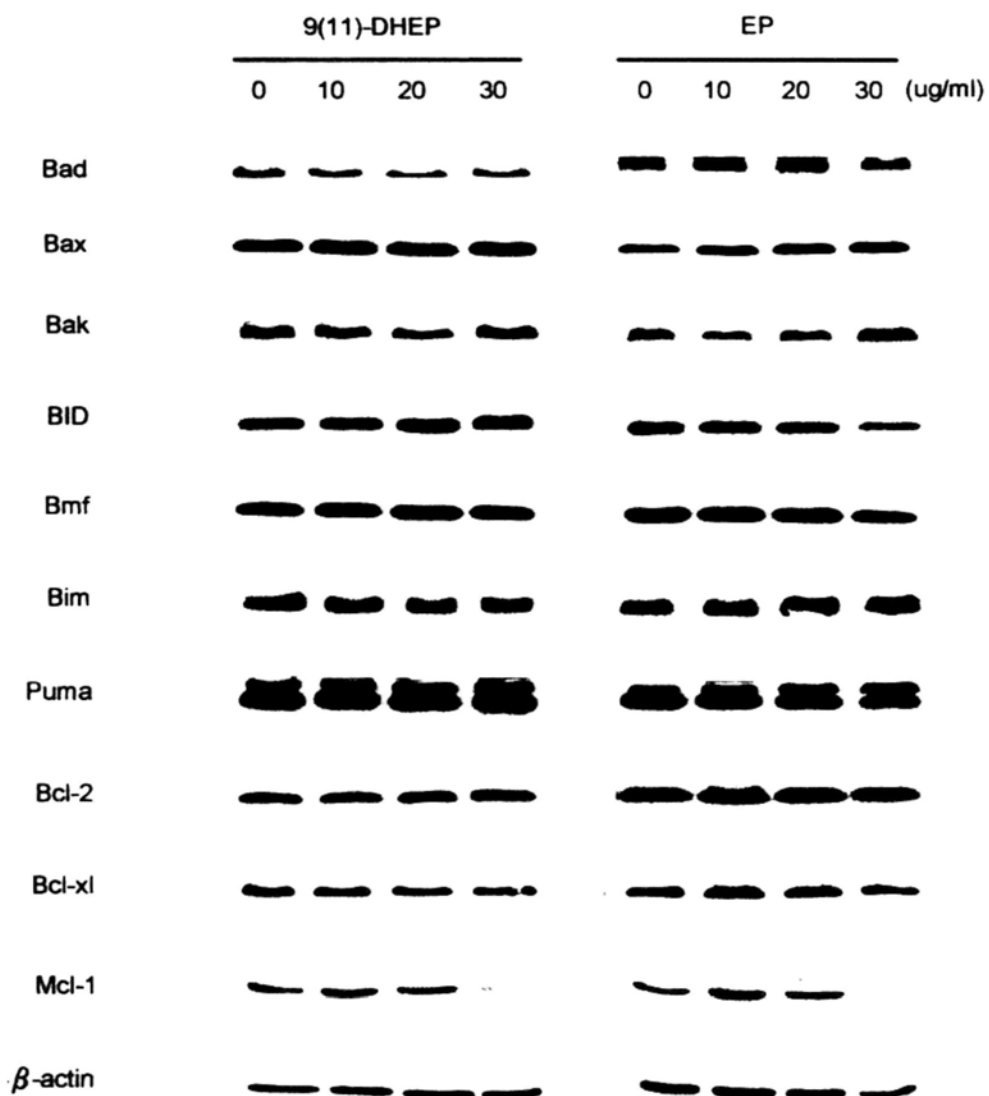


Figure 4.16. Dose-dependent effects of 9(11)-DHEP and EP on A375 malignant melanoma cells by western blot analysis using Bad, Bax, Bak, puma, Mcl-1, Bcl-2 and Bcl-xl antibodies. Cells were treated with different concentrations of 9(11)-DHEP for 48h & EP for 24h. Total protein (60-80 μ g) was resolved in 10-12% Tricine-SDS-PAGE and blotted on nitrocellulose membrane. The amount of protein was normalized to the densitometric units of β -actin

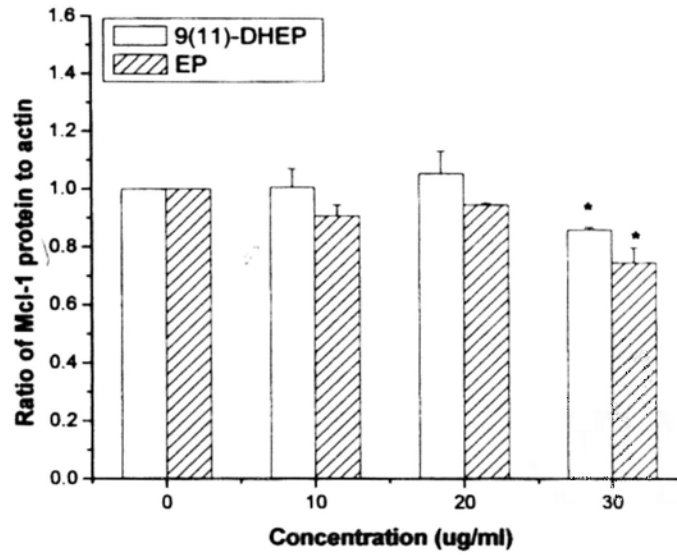


Figure 4.17 Dose-dependent effects of 9(11)-DHEP and EP on Mcl-1 expression in A375 malignant melanoma cells. Cells were treated with 9(11)-DHEP for 48h or EP for 24h. The density of the band is expressed as the relative density compared to that in untreated cells (control) that were taken as 1.0. Results are expressed as mean \pm SD (n=3). $P < 0.05$ (*) were considered significantly different compared with the control.

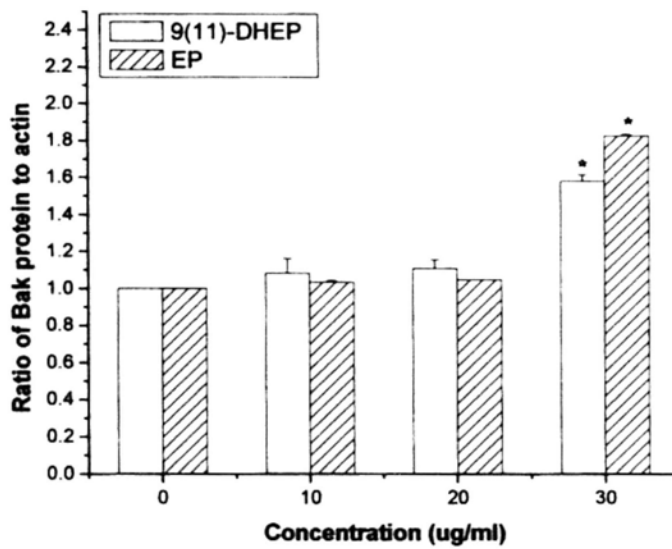
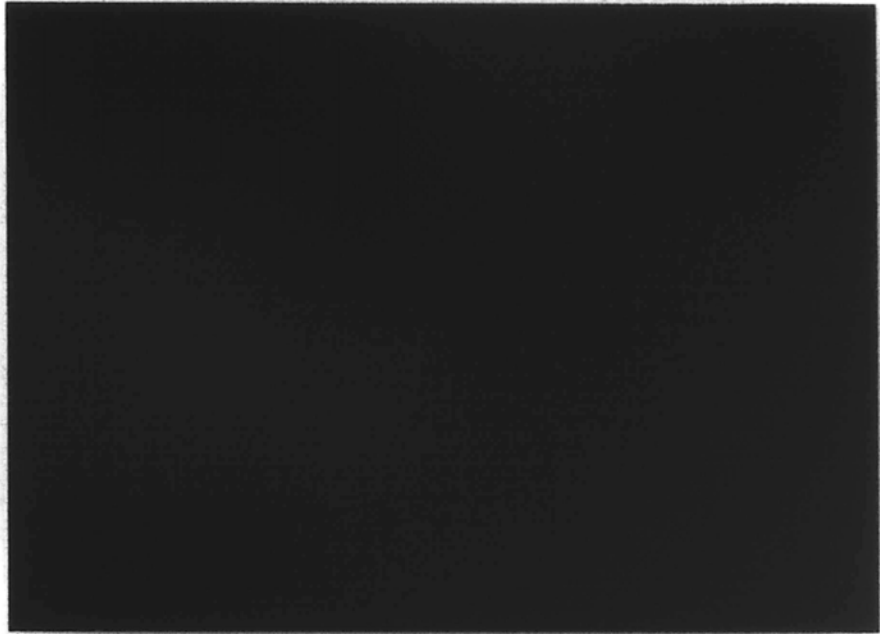


Figure 4.18 Dose-dependent effects of 9(11)-DHEP and EP on Bak expression in A375 malignant melanoma cells. Cells were treated with 9(11)-DHEP for 48h or EP for 24h. The density of the band is expressed as the relative density compared to that in untreated cells (control) that were taken as 1.0. Results are expressed as mean \pm SD (n=3). P<0.05 (*) were considered significantly different compared with the control.

Control



25 mg/Kg



Figure 4.19 Nude mice with A375 malignant melanoma solid tumor. Two groups of the tumor-bearing mice each received 0, 25 mg/kg of EP respectively for 12 consecutive days.

Control

25 mg/kg

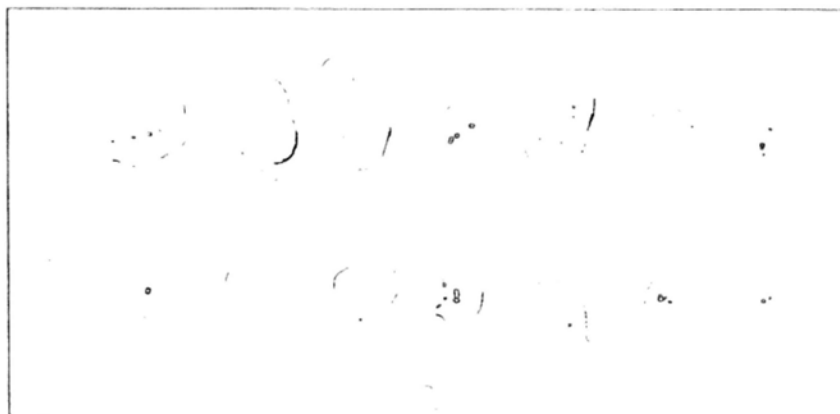


Figure 4.20 A375 malignant melanoma solid tumor excised from EP-treated and control group of xenograft tumor-bearing nude mice. Two groups of the tumor-bearing mice each received 0, 25 mg/kg of EP respectively for 12 consecutive days. The solid tumors were then enucleated, the longest and shortest dimensions were measure, the final weight was detected. Numeric dates are shown in Fig 4.21.

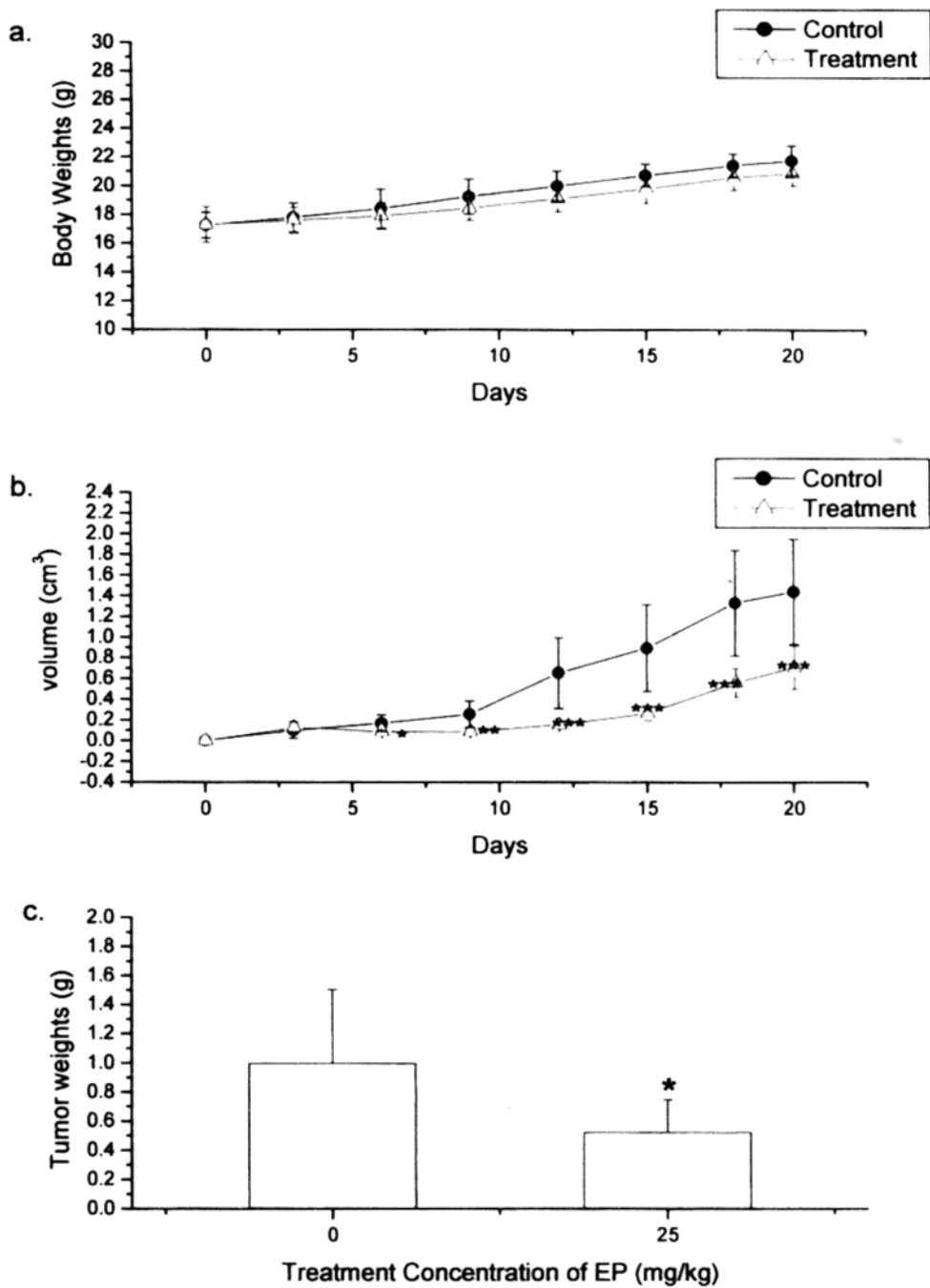


Figure 4.21. The inhibitory effect of EP on A375 malignant melanoma cells in xenograft tumor-bearing nude mice. a. the change of body weights of the nude mice; b. the change of tumor volumes; c. the change of the final tumor weight. Significance was assessed by t-test. $P < 0.05$ (*), $P < 0.01$ (**), $P < 0.001$ (***) were considered significantly different compared with the control.



Figure 4.22 Effect of EP on A375 malignant melanoma tumor by Western blot analysis using cleaved PARP(Asp214) antibody (human specific) 89kb. Nude mice with tumor were treated with 25mg/kg of EP for 12 days. Total protein (100 μ g) was extracted from seven solid tumor of both control and treatment group, resolved in 10% SDS-PAGE and blotted on nitrocellulose membrane. The amount of protein was normalized to the densitometric units of β -actin. The number means the individual mice.

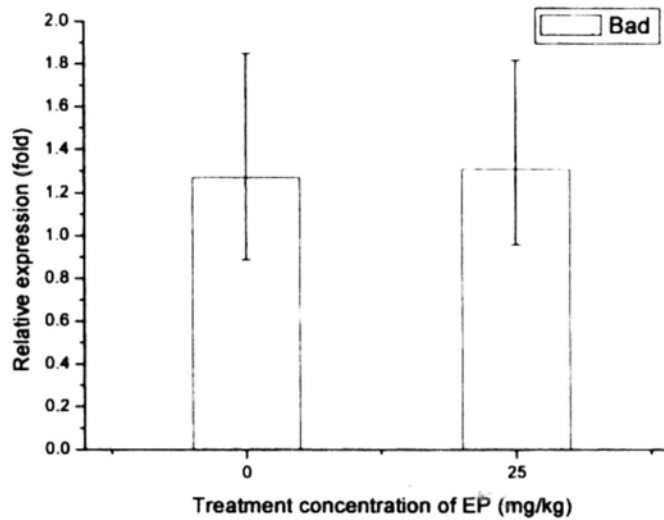
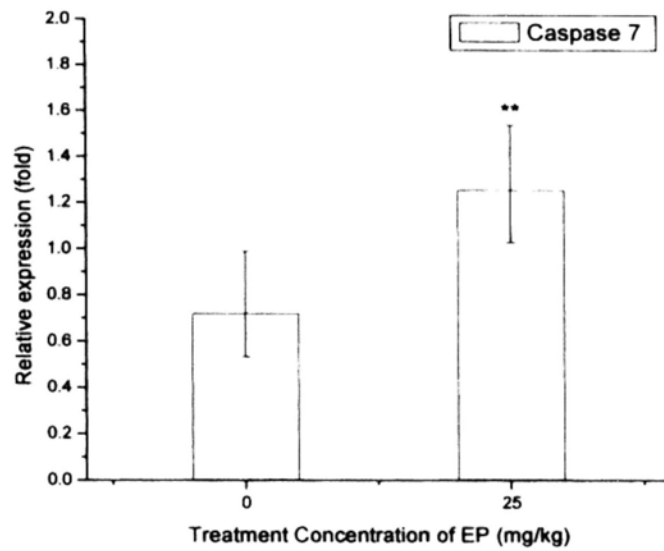


Figure 4.23 EP induced gene expression changes in A375 malignant melanoma tumor. RNA was extracted from every tumors of each group and Real time PCR was then performed. Caspase 7 and BAX expression levels normalized to GAPDH and plotted relative to those of the control group. Values shown are the means±S.D. of seven tumors of each group. $P < 0.05$ (*), $P < 0.01$ (**) were considered significantly different compared with the control.

4.4 Discussion

Chemopreventive agents of natural origin, often a part of our daily diet, may provide a cheap, effective way of preventing and controlling cancer. A wide range of studies in recent years has shown that triterpenoids and steroids hinder carcinogenesis by intervening in pathways such as carcinogen activation, DNA repair, cell cycle arrest, cell differentiation and the induction of apoptosis in cancer cells. This is the first study to investigate the molecular mechanisms of the anti-tumoral and pro-apoptotic effects of EP and 9(11)-DHEP in A375 malignant melanoma cells.

Apoptosis, called programmed cell death, is a normal process involved in tissue remodelling and removal of damaged cells. Cells undergoing apoptosis show characteristic morphology and biochemical features. The biochemical hallmark of apoptosis is DNA fragmentation; this is an irreversible event that commits the cell to die. Flow cytometry results suggested that the A375 malignant melanoma cells treated with the two Ganoderma steroids could be stopped in subG1 phase in a dosage- and time-dependent manner. By using TUNEL assay and Annexin-V-FLUOS analysis, the apoptosis induction effect of the two Ganoderma steroids which was revealed by cleavage of DNA strands was identified once again. In TUNEL assay, DNA strand breaks can be detected by enzymatic labeling the free 3'-OH termini with modified nucleotides. Annexin V is a calcium-dependent phospholipids-binding protein; it has a high affinity for phosphatidylserine. They do not bind to normal and intact cells, which can be used to differentiate early apoptotic cell from late apoptotic cell. In our studies, the morphology of cancer cells treated with the two steroids have been observed in TUNEL and Annexin V assay and results suggested that both of the two steroids could inhibit the growth of A375 malignant melanoma cell by inducing apoptosis. Meanwhile, betulinic acid and ursolic acid, which have similar chemical structure with EP and 9(11)-DHEP, could also induce apoptosis on A375 malignant

melanoma cell.

Apoptosis can be divided into two classical pathways: the exogenous death receptor pathway and the endogenous mitochondrial pathway. In the endogenous mitochondria-mediated pathway, the mitochondria stress will reduce the mitochondria membrane potential, which results in cytochrome *c*, released from the intermembrane space of the mitochondria into the cytosol. In turn, it binds to cytosolic procaspase-9 with oligomerized APAF-1 in an apoptosome complex, resulting in autoactivation and release of mature caspase-9. The latter enzyme activates caspase 3 and caspase 7, which in turn activate a downstream caspase cascade (Igney FH, et al., 2002). One key mechanism in the process involved in the function of antitumoral drugs is the activation of the mitochondrial apoptotic pathway. Triterpenoids such as betulinic acid, ursolic acid, and CDDO (2-cyano-3,12-dioxoolean-1,9-dien-28-oic acid) have been reported to produce apoptosis by activating this pathway (Wick W, et al., 1999; Gopal DVR, et al., 2004 & 2005; Harmand PO, et al., 2005; Konopleva M, et al., 2004).

Caspases are a ubiquitous family of cysteine proteases that include both upstream (initiator) and downstream effector caspases are cleaved and activated by initiator caspases. Initiator caspases (including 8, 9, 10 and 12) are closely coupled to proapoptotic signals. Once activated, these caspases cleave and activate downstream effector caspases (including 3, 6 and 7), which in turn cleave cytoskeletal and nuclear proteins like poly(ADP-ribose polymerase) (PARP), α -Fodrin, DFF and Lamin A, and induce apoptosis. Our results indicated that both the two steroids could activate the caspase 3, 6 and 7 in a dosage-dependent manner. Caspase 3 cleaved PARP, which responded to DNA fragmentation, and eventually led to A375 cancer cells apoptosis. This suggested that apoptosis induced by the two *Ganoderma* steroids on A375 cancer cell was caspase-dependent. In addition, the expression of caspase 8, 9

and 10 were observed. The three caspase were considered as signaling and key caspase in extrinsic and intrinsic pathway, respectively. In our case, caspase 9 but not caspase 8 and caspase 10 was involved in the EP/9(11)-DHEP-mediated apoptosis of A375 cancer cells.

In order to elucidate if mitochondria are an important target for the apoptotic induction by 9(11)-DHEP and EP, cytochrom *c* content were detected in both the cytosolic and mitochondria fraction. Our results showed that both the two steroids could induce the release of cytochrome *c* into the cytosol, which hinted that apoptosis induced by the two steroids might be via the mitochondria pathway.

In our work, the decrease of Mcl-1 and a slight increase Bak expression was observed whereas the expression of the other members Bcl-2, Bcl-xl, Bax, Bad, Bim, BID, Bmf and puma was not changed. Mcl-1, also call myeloid cell leukaemia-1, is an anti-apoptotic member of Bal-2 family. It is thought to promote cell survival by involving in the suppression of cytochrome *c* release from mitochondria, possibly via heterodimerisation with and neutralisation of pro-apoptotic Bcl-2 family proteins, for example, Bim or Bax (Michels J, et al., 2005). The Mcl-1 protein is often overexpressed in melanoma and has been shown to affect the susceptibility of melanoma cells to apoptotic stimuli in other system (Thallinger C, et al., 2003). So the Mcl-1 was supposed to be one of important diagnostic target in the melanoma cell line (Panka DJ, et al., 2008). Proapoptotic multidomain proteins (prototypes: Bax, Bak) contain three BH domains. In healthy cells, the protein Bak is associated with the outer mitochondria membrane, whereas the other protein Bax resides in the cytosol. Once activated, the motichondria potential may result from a conformational change of Bax or Bak (with exposure of their NH2 terminus), their full insertion into mitochondrial membranes as homooligomerized multimers, and formation of giant protein-permeable pores by binding to components of the permeability transition

pore complex (PTPC). The resulting heterooligomers may provide intermembrane space (IMS) proteins (Cty C etc.) with a route for release (Kroemer G, et al., 2007; Kuwana T, et al., 2002; Nechushtan A, et al., 2001;) This work proposed the apoptosis under the two Ganoderma steroids was by regulating the ratio of Bax/Bcl-2 groups.

We recently demonstrated that some extracts of *G. lucidum* mycelia proved to have great antitumor activities which implicated *G. lucidum* mycelia as a potential chemopreventive and/or therapeutic natural product. Further studies are necessary to confirm this preventative/therapeutic potential of *G. lucidum* mycelia *in vivo*. EP was found to be one of the major steroids of *G. lucidum* mycelia and was responsible for the antitumor activity of chloroform extract of *G. lucidum* mycelia. Previous studies found that EP markedly inhibited tumor promotion by DMBA and TPA in two-stage carcinogenesis in mouse skin (Yasukawa K, et al., 1996). The inhibition of tumor growth of A375 melanoma subcutaneous xenografts in nude athymic mice further supported the antitumor property of EP. In the present study, untreated tumors volume increased 15-fold (0.1cm^3 to 1.5cm^3), whereas a significantly delay of tumor growth was seen after EP treatment. EP also demonstrated a growth inhibitory activity of decreasing 47% to the control group in the tumor weight. Furthermore, the results suggested that cleaved PARP and caspase 7 gene expressions were greatly enhanced in the EP-treated tumor. Caspase-7 is highly related to caspase-3, and these two caspases are activated by both death receptor- and mitochondria-induced apoptosis. Caspase-7 might be involved in the development of human cancers (Soung, YH et al., 2003). These result suggested that EP could inhibit the tumor growth by inducing apoptosis, which provided *in vivo* evidence that EP could provide therapeutic benefit as potential anti-cancer drug.

Taken together, based on the results obtained above and the current paradigms

of apoptosis reported in the literature, we could identify that the apoptosis of A375 malignant melanoma cells induced by EP and 9(11)-DHEP was through intrinsic pathway. Our work also suggested that both of the two Ganoderma steroids might be natural potential apoptosis-inducing agents for malignant melanoma treatment. But the structure-activity relationship of EP and 9(11)-DHEP is also unknown to us. All this will need further studies.

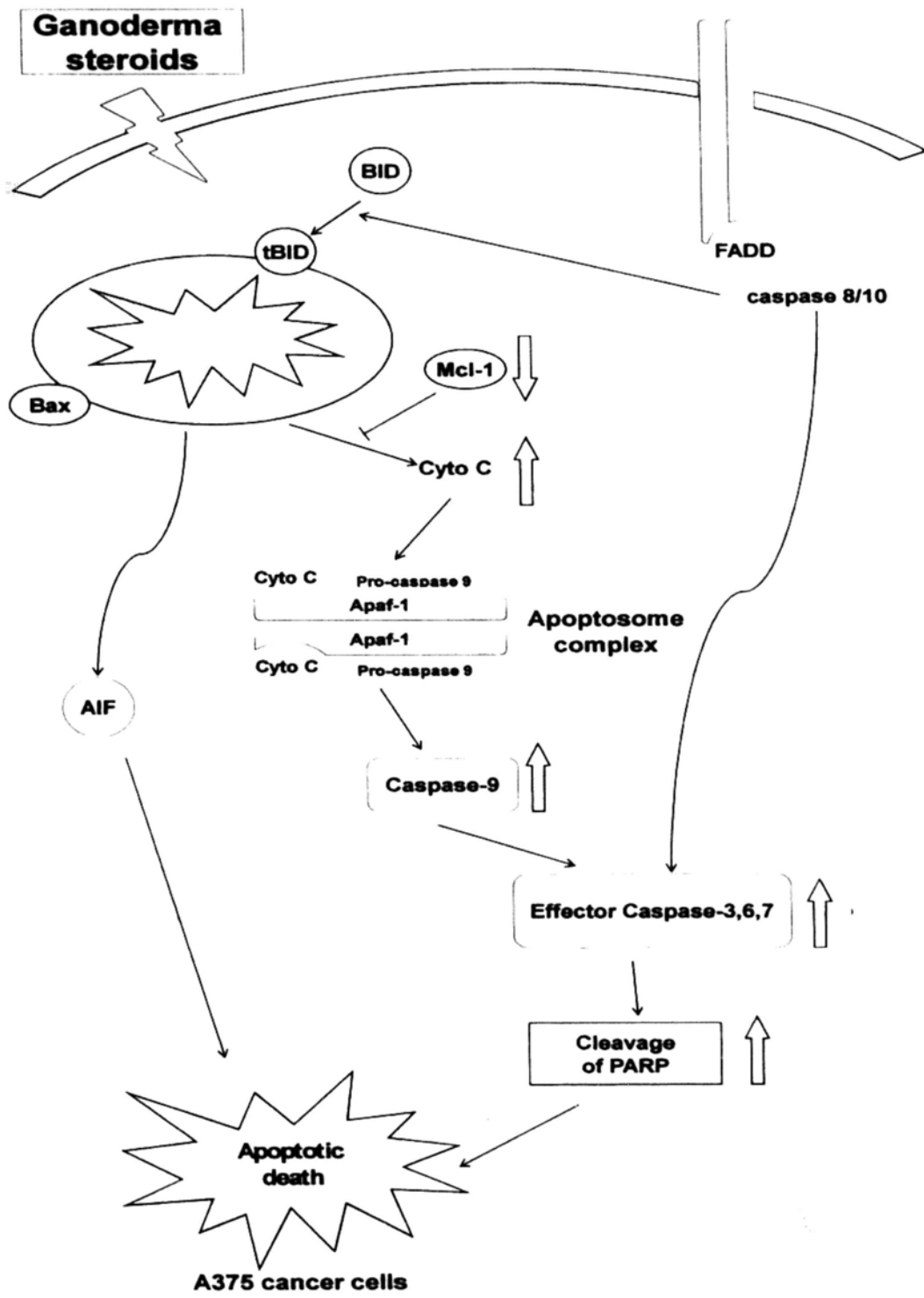


Figure 4.24 Mitochondria-mediated apoptosis induced by EP and 9(11)-DHEP in A375 cancer cells

Chapter V Conclusion

Ganoderma lucidum is a popular medicinal mushroom, which has been used for the treatment of a variety of diseases in traditional Chinese medicine. Great interest is currently being paid to bioactive compounds from this mushroom. They are known to be anti-proliferative and may play an important role in cancer chemoprevention. In our studies, two steroids 5 α ,8 α -epidioxy-22*E*-ergosta-6,22-dien-3 β -ol (ergosterol peroxide (EP)) and 5 α ,8 α -epidioxy-22*E*-ergosta-6,9(11),22-trien-3 β -ol (9,11-dehydroergosterol peroxide (9(11)-DHEP)) were purified from *Ganoderma lucidum* on submerged culture using activity-guided purification procedures against human breast adenocarcinoma MCF-7 cells. The yields of EP and 9(11)-DHEP were 101.23mg and 69.07mg from 413g of *Ganoderma lucidum* dried mycelia, which were found to reach 0.024% and 0.017% in *Ganoderma lucidum* mycelia, respectively. Our result showed that the two compounds are the major fractions responsible for antitumor activities of *Ganoderma lucidum* mycelia. The results obtained in this study are very useful for the simultaneous, highly efficient production of *Ganoderma* steroid on a large scale. Meanwhile, it was hoped to be developed into the quality control marker and nutrition parameter of mycelium production.

The anti-proliferative effects of EP and 9(11)-DHEP were observed in a dose- and time-dependent manner by MTT assay and BrdU assay. In the study of *in vitro* cytotoxicity, EP and 9(11)-DHEP were found to exert cytotoxic effect on A375 cells but with less effect on the viability of normal cells (human normal skin fibroblast cells Hs68). Different cancer cell lines showed selectively susceptibility when exposed

to EP and 9(11)-DHEP. EP was found to have a stronger anti-proliferative activity than 9(11)-DHEP in HepG2, MCF-7 and Colo201 cells. Meanwhile, we compared the anti-proliferation activities of EP and 9(11)-DHEP extracted from different fungi source on different cancer cells (table 5.1). Studies documented that both of the steroids had greater inhibitory effects on human colon carcinoma cells, such as HT29, Caco-2. It may be due to their structure similarity with the dietary cholesterol. Dietary cholesterol is correlated etiologically to the incidence of colon cancer, with changes in serum cholesterol levels and fecal bile acid profiles suggested to increase susceptibility to colon tumorigenesis (Rao AV, Janezic SA. 1992). It was suggested that they can act by competing with cholesterol at the luminal absorption site. Therefore, they have a bright future in clinical application (Radtke & Clevers, 2005).

As reported to have stronger anti-proliferative activities on human cancer cells, EP and 9(11)-DHEP was further investigated for their possible mechanisms. Cell cycle analysis indicated that both of the two Ganoderma steroids could stop different cancer cells on subG1 phase in a dose- and time-dependent manner. Furthermore, the two steroids induced apoptosis on HepG2 hepatoma cancer cells and A375 malignant melanoma cells by TUNEL assay and Annexin-V-FLUOS assay. All of the above results suggested that the anti-proliferative activities of EP and 9(11)-DHEP were mediated via inducing apoptotic.

Results demonstrated that apoptosis induced by EP and 9(11)-DHEP in the human colon carcinoma Colo201 cells and malignant melanoma A375 cells involved the activation of caspase 3, 7 and 9, which were followed the cleavage of PARP. The ratio of expression levels of Bcl-2/Bax family member were changed after different concentration EP and 9(11)-DHEP treatment in human colon carcinoma Colo201 cells. In A375 human malignant melanoma cells, the two steroids-induced apoptosis resulted in release of mitochondria cytochrome *c*. In addition, Mcl-1 protein was

down-regulated and Bak was little up-regulated in a dosage-dependent manner. These indicated that the mitochondria-mediated pathway was involved in the apoptosis signal pathways of Colo201 cancer cells and malignant melanoma A375 cells induced by the two steroids.

Moreover, EP greatly suppressed the growth of A375 human malignant melanoma tumor in an A375 xenograft model, which inhibited 49% tumor weight growth compared with the control group. Further studies showed that EP could result in the PARP cleavage and total caspase 7 gene expression enhancement in the tumor cells, which suggested that EP might be inhibiting solid tumor growth through inducing apoptosis.

According to these results we proposed an intrinsic mechanism for the induction of apoptosis by EP and 9(11)-DHEP in cancer cells. This mechanism is regulated via the inhibition of Bcl-2 family protein expression, producing mitochondrial disruption and the release of cytochrome-c, which leads finally to the activation of caspases 9 and 3. Triterpenoids such as betulinic acid, ursolic acid, and CDDO (2-cyano-3,12-dioxoolean-1,9-dien-28-oic acid), which have similar chemical structure with EP and 9(11)-DHEP, have been reported to produce apoptosis by similar mechanisms. The following events have been proposed in the apoptosis induced by steroids and triterpenoids: (a) participation of the Bcl-2 protein family; (b) increase in mitochondrial membrane permeability; (c) cytochrome-c release and (d) caspase-9 and -3 activation.

In conclusion, EP and 9(11)-DHEP are novel natural compounds and they are able to induce caspase-dependent apoptosis in human cancer cells via the intrinsic mitochondrial pathway. But the precise mechanisms by which EP and 9(11)-DHEP triggers mitochondria permeability remains to be identified. Many cancer cells exhibit a disturbed intracellular redox balance. Some tumors, such as solid lung

carcinoma, are hypoxic, and its cells are therefore more reducing than normal, while others, such as the ones of breast and prostate cancer, proliferate under oxidative stress (OS). These biochemical differences between normal and tumor tissue are significant, which provide new target for the cancer treatment (Fry FH and Jacob C, 2006). Previous studies found that ergosterol peroxide showed potent antioxidant activities (Kim SW, et al. 1999). It is possible that the two steroids inhibited cancer cell growth but not MCF-10A-2 and Hs68 cells through changing its redox status, which result in the mitochondria potential change and induce cancer cell apoptosis. Nevertheless, our data could contribute to the development of EP and 9(11)-DHEP and related drugs for use as cancer chemotherapeutic or chemopreventive agents.

Chapter V Conclusion

Table 5.1 Inhibitory effects of EP and 9(11)-DHEP extracted from different mushroom on different cancer cells

Fungi Source	Cell type	Cell source	IC50(μ M)	Reference
EP	HT29	Human colorectal adenocarcinoma cells	12.00	Kobori M, 2007
	Caco-2	Human colorectal adenocarcinoma cells	14.00	
<i>Paecilomyces tenuipes</i>	SNU-1	Human gastric adenocarcinoma cells	18.70	Nam KS, 2001
	SNU-354	Human hepatocellular carcinoma cells	158.20	
	SNU-C4	Human colorectal adenocarcinoma cells	84.60	
	Sarcoma-180	Mouse solid tumor	74.10	
<i>Sarcodon aspratus</i>	HL60	Human promyelocytic leukemia cells	11.00	Kobori M, 2007; Takei T, 2005
	MCF-7	Human breast adenocarcinoma cells	39.43	In this study
<i>Ganoderma lucidum</i>	Colon201	Human colorectal adenocarcinoma cells	30.19	
	SW620	Human colorectal adenocarcinoma cells	25.14	
	HepG2	Human hepatocellular carcinoma cells	32.78	
	KYSE	Esophageal squamous cell carcinoma cells	10.33	
	A375	Human malignant melanoma cells	21.36	
9(11)-DHEP	HL60	Human promyelocytic leukemia cells	4.00	Takei T, 2004

<i>Ganoderma lucidum</i>	Cell Line	Human colorectal adenocarcinoma cells	Kobori M, 2007
	HT29	Human colorectal adenocarcinoma cells	7.00
	MCF-7	Human breast adenocarcinoma cells	40.39
	Colon201	Human colorectal adenocarcinoma cells	30.54
	SW620	Human colorectal adenocarcinoma cells	77.09
	HepG2	Human hepatocellular carcinoma cells	32.81
	KYSE	Esophageal squamous cell carcinoma cells	18.51
	A375	Human malignant melanoma cells	22.19

The IC50 concentrations represented the concentration which results in 50% inhibition of cell growth after 72hr or 120hr incubation in MTT assay. Results are expressed as mean value of three independent experiments.

Reference

- Adams JM and Cory S. 1998 The Bcl-2 protein family: arbiters of cell survival. *Science*, 281: 1322–1326.
- Akihisa T, Nakamura Y, Tagata M, Tokuda H, Yasukawa K, Uchiyama E, Suzuki T, Kimura Y. 2007 Anti-inflammatory and anti-tumor-promoting effects of triterpene acids and sterols from the fungus *Ganoderma lucidum*. *Chemistry & Biodiversity*, 4(2):224-31
- Arisawa M, Fujita A, Saga M, Fukumura H, Hayashi T, Shimizu M and Morita N. 1986 Three new lanostanoids from *Ganoderma lucidum*. *Journal of Natural Products*, 49(4): 621-625.
- Bates ML, Reid WW, White JD. 1976 Duality of pathways in the oxidation of ergosterol to its peroxide *in vivo*. *Journal of the Chemical Society. Chemical communications*, 4445.
- Bergeron L, Perez GI, Macdonald G, Shi L, Sun Y, Jurisicova A, Varmuza S, Latham KE, Flaws JA, Salter JC, Hara H, Moskowitz MA, Li E, Greenberg A, Tilly JL, Yuan J. 1998 Defects in regulation of apoptosis in caspase-2-deficient mice. *Genes & Development*, 12: 1304–1314.
- Black S, Kadyrov M, Kaufmann P, Ugele B, Emans N, Huppertz B. 2004 Syncytial fusion of human trophoblast depends on caspase 8. *Cell Death & Differentiation*, 11: 90–98.
- Bodzioch M, Dembinska-Kiec A, Hartwich J, Lapicka-Bodzioch K, Banas A, Polus A, Grzybowska J, Wybranska I, Dulinska J, Gil D, Laidler P, Placha W, Zawada M, Balana-Nowak A, Sacha T, Kiec-Wilk B, Skotnicki A, Moehle C, Langmann T and Schmitz G. 2005 The microarray expression analysis identifies BAX as a mediator of β -carotene effects on apoptosis. *Nutrition and Cancer*, 51(2), 226–235
- Boh B, Berovic M, Zhang JS and Lin ZB 2007 *Ganoderma lucidum* and its pharmaceutically active compounds. *Biotechnology Annual Review*, 13: 265-301
- Borner C. 2003 The Bcl-2 protein family: sensors and checkpoints for life-or-death

decisions. *Molecular Immunology*, 39: 615–47.

Bortman P, Folgueira MAAK, Katayama MLH, Snitcovsky IML and Brentani MM. 2002 Antiproliferative effects of 1,25-dihydroxyvitamin D₃ on breast cells - A mini review. *Brazilian Journal of Medical and Biological Research*, 35: 1-9

Bradford PG and Awad AB. 2007 Phytosterols as anticancer compounds. *Molecular Nutrition & Food Research*, 51, 161 – 170

Butler M. 1996 Cell line and culture monitoring. *Animal Cell Culture and Technology*. pp. 33-45. Oxford University press, New York

Cao LZ, Lin ZB 2002 Regulation on maturation and function of dendritic cells by *Ganoderma lucidum* polysaccharides. *Immunology Letter*, 83(3):163-169.

Cao LZ, Lin ZB 2003 Regulatory effect of *Ganoderma lucidum* polysaccharides on cytotoxic T-lymphocytes induced by dendritic cells *in vitro*, *Acta Pharmacologica Sinica*, 24 (4): 312-326

Chaudhary PM, Eby MT, Jasmin A, Kumar A, Liu L, Hood L. 2000 Activation of the NF-kappaB pathway by caspase 8 and its homologs. *Oncogene*, 19: 4451–4460.

Chen HS, Tsai YF, Lin S, Lin CC, Khoo KH, Lin CH, Wong CH. 2004. Studies on the immunomodulating and anti-tumor activities of *Ganoderma lucidum* (Reishi) polysaccharides. *Bioorganic & Medicinal Chemistry*, 12:5595–5601.

Cheng KC, Huang HC, Chen JH, Hsu JW, Cheng HC, Ou CH, Yang WB, Chen ST, Wong CH and Juan HF 2007 *Ganoderma lucidum* polysaccharides in human monocytic leukemia cells: from gene expression to network construction, *BMC Genomics*, 8:411

Chien CM, Cheng JL, Chang WT, Tien MH, Tsao CM, Chang YH, Chang HY, Hsieh JF, Wong CH and Chen ST 2004 Polysaccharides of *Ganoderma lucidum* alter cell immunophenotypic expression and enhance CD56+ NK-cell cytotoxicity in cord blood. *Bioorganic & Medicinal Chemistry*, 12: 5603–5609

Chipuk JE, Bouchier-Hayes L and Green DR 2006 Mitochondrial outer membrane permeabilization during apoptosis: the innocent bystander scenario. *Cell Death and Differentiation*, 13, 1396–1402

- Chiu CM, Kong KL and Ooi EC. 2003 Antiproliferative effect of chlorophyllin derived from a traditional Chinese medicine *Bombyx mori excreta* on human breast cancer MCF-7 cells. *International Journal of Oncology*, 23: 729-735.
- Cichewicz RH, Kouzi SA. 2004 Chemistry, biological activity and chemotherapeutic potential of betulinic acid for the prevention and treatment of cancer and HIV infection. *Medicinal Research Reviews*, 24 (1): 90-114.
- Cory S and Adams JM. 2002 The Bcl-2 family: regulators of the cellular life-or-death switch. *Nature Reviews Cancer*, 2: 647-656.
- Costa MA, Pellerito L, Izzo V, Fiore T, Pellerito C, Melis M, Musmeci MT, Barbieri G. 2006 Diorganotin(IV) and triorganotin(IV) complexes of meso-tetra (4-sulfonatophenyl)porphine induce apoptosis in A375 human melanoma cells. *Cancer Letters*, 238: 284-294.
- Cragg GM, Newman DJ. 2005 Plants as a source of anti-cancer agents. *Journal of Ethnopharmacology*, 100: 72-79.
- Cui YL, Hou S, Qi AD, Wang XH, Wang H, Cai KY and Yin YJ. 2003 Biomimetic surface modification of poly (L-lactic acid) with gelatin and its effects on articular chondrocytes *in vitro*. *Biomimetic Surface Modification*, 66A: 770-778.
- Czub J and Baginski M. 2006 Comparative molecular dynamics study of lipid membranes containing cholesterol and ergosterol. *Biophysical Journal*, 90: 2368-2382.
- De Botton S, Sabri S, Daugas E, Zermati Y, Guidotti JE, Hermine O, Kroemer G, Vainchenker W, Debili N. 2002 Platelet formation is the consequence of caspase activation within megakaryocytes. *Blood*, 100: 1310-1317.
- Deb TB, Su L, Wong L, Bonvin E, Wells A, Davids M and Johnson GR. 2001. Epidermal growth factor (EGF) receptor kinase-dependent signaling by EGF. *The Journal of Biological Chemistry*, 276: 15554-15560.
- Eckhart L, Declercq W, Ban J, Rendl M, Lengauer B, Mayer C, Lippens S, Vandenabeele P, Tschachler E. 2000 Terminal differentiation of human

keratinocytes and stratum corneum formation is associated with caspase-14 activation. *Journal of Investigative Dermatology*, 115: 1148–1151.

Eguchi R, Toné S, Suzuki A, Fujimori Y, Nakano T, Kaji K, Ohta T. 2009 Possible involvement of caspase-6 and -7 but not caspase-3 in the regulation of hypoxia-induced apoptosis in tube-forming endothelial cells. *Experimental Cell Research*, 315: 327 – 335.

Eisenmann KM, VanBrocklin MW, Staffend NA, Kitchen SM, Koo H-M. 2003 Mitogen-activated protein kinase pathway-dependent tumor-specific survival signaling in melanoma cells through inactivation of the proapoptotic protein Bad. *Cancer Research*, 63:8330–8337.

El-Mekawy S, Meselhy MR, Nakamura N, Tezuka Y, Hattori M, Kakiuchi N, Shimotohno K, Kawahata T, Otake T. 1998 Anti-HIV-1 and anti-HIV-1-protease substances from *Ganoderma lucidum*. *Phytochemistry*, 49: 1651-1657.

Es-saadya D, Simona A, Ollierb M, Maurizisb JC, Chuliaa AJ, DelageN C. 1996 Inhibitory effect of ursolic acid on B 16 proliferation through cell cycle arrest. *Cancer Letters*, 106: 193- 197.

Evans AC, Ireland JL, Winn ME, Lonergan P, Smith GW, Coussens PM, Ireland JJ. 2004 Identification of genes involved in apoptosis and dominant follicle development during follicular waves in cattle. *Biology of Reproduction*, 70(5):1475-84.

Fang QH and Zhong JJ 2002 Two-Stage Culture Process for Improved Production of Ganoderic Acid by Liquid Fermentation of Higher Fungus *Ganoderma lucidum*. *Biotechnology Progress*, 18:51-54

Fernando P, Brunette S, Megeney LA. 2005 Neural stem cell differentiation is dependent upon endogenous caspase 3 activity. *Journal of the Federation of American Societies for Experimental Biology/ FASEB J*, 19: 1671–1673

Franchi L, Amer A, Body-Malapel M, Kanneganti TD, Ozören N, Jagirdar R, Inohara N, Vandenabeele P, Bertin J, Coyle A, Grant EP, Núñez G. 2006 Cytosolic flagellin requires Ipaf for activation of caspase-1 and interleukin 1beta in salmonella-infected macrophages. *Nature Immunology*, 7: 576–582.

- Fry FH and Jacob C 2006 Sensor/effector drug design with potential relevance to cancer. *Current Pharmaceutical Design*, 12: 4479-4499
- Fujimoto H, Nakayama M, Nakayama Y, Yamazaki M. 1994 Isolation and characterization of immunosuppressive components of three mushrooms, *Pisolithus tinctorius*, *Microporus flabelliformis* and *Lenzites betulina*. *Chemical & Pharmaceutical Bulletin (Tokyo)*, 42(3):694-7.
- Fulda S, Scaffidi C, Susin SA, Krammer PH, Kroemer G, Peter ME and Debatin KM. 1998 Activation of mitochondria and release of mitochondrial apoptogenic factors by betulinic acid. *The Journal of Biological Chemistry*, 273 (51): 33942–33948.
- Gao JJ, Min BS, Ahn EM, Nakamura N, Lee HK and Hattori M 2002 New triterpene aldehydes, lucialdehydes A—C, from *Ganoderma lucidum* and their cytotoxicity against murine and human tumor cells. *Chemical & Pharmaceutical Bulletin (Tokyo)*, 50:837-840
- Gao JJ, Nakamura N, Min BS, Hirakawa A, Zuo F and Hattori M 2004 Quantitative determination of bitter principles in specimens of *Ganoderma lucidum* using high-performance liquid chromatography and its application to the evaluation of Ganoderma products. *Chemical & Pharmaceutical Bulletin (Tokyo)*, 52(6): 688—695.
- Gao JM, Dong ZJ and Liu JK 2000 The constituents of the basidiomycetes *Russula cyanoxantha*. *Acta Botanica Yunnanica*, 22(1): 85—89.
- Gao JM, Zhang AL, Yao HY, Shen J. 2003 A study on the chemical constituents from *Polyporus ellissi*. *Zhong guo Zhong Yao Za Zhi*. 28(10):943-6.
- Gao Y, Gao H, Chan E, Tang W, Xu A, Yang H, Huang M, Lan J, Li X, Duan W, Xu C, Zhou S. 2005 Antitumor activity and underlying mechanisms of ganopoly, the refined polysaccharides extracted from *Ganoderma lucidum*, in mice. *Immunological investigations*, 34(2):171-98.
- Gavrieli Y, Sherman Y and Ben-Sasson SA. 1992 Identification of programmed cell death in situ via specific labeling of nuclear DNA fragmentation. *The Journal of Cell Biology*, 119 (3):493-501

Ghayur T, Banerjee S, Hugunin M, Butler D, Herzog L, Carter A, Quintal L, Sekut L, Talanian R, Paskind M, Wong W, Kamen R, Tracey D, Allen H. 1997 Caspase-1 processes IFN-gamma-inducing factor and regulates LPS-induced IFN-gamma production. *Nature*, 386: 619–623.

Gorczyca W, Bigman K, Mittelman A, Ahmed T, Gong J, Melamud MR and Darzynkiewicz Z. 1993. Induction of DNA strand breaks associated with apoptosis during treatment of leukemia. *Leukemia*. 7: 659–670.

Gold EJ, Francis RJB, Zimmermann A, Mellor SL, Cranfield M, Risbridger GP, Groome NP, Wheatley AM and Fleming JS. 2003. Changes in activin and activin receptor subunit expression in rat liver during the development of CCl₄-induced cirrhosis. *Molecular and Cellular Endocrinology*. 201: 143-153.

Gopal DVR, Narkar AA, Badrinath Y, Mishra KP, Joshi DS, 2004 Protection of Ewing's sarcoma family tumour (ESFT) cell line SK-NMC from betulinic acid-induced apoptosis by alpha-DL-tocopherol. *Toxicology Letters*, 153: 201–212.

Gopal DVR, Narkar AA, Badrinath Y, Mishra KP, Joshi DS, 2005 Betulinic acid induces apoptosis in human chronic myelogenous leukemia (CML) cell line K-562 without altering the levels of Bcr-Abl. *Toxicology Letters*, 155: 343–351.

Gross A, McDonnell JM, and Korsmeyer SJ. 1999 Bcl-2 family members and the mitochondria in apoptosis. *Genes & Development*, 13: 1899–1911.

Guan SH, Yang M, Wang XM, Xia JM, Zhang ZM, Liu X and Guo DA 2007 Structure elucidation and complete NMR spectral assignments of three new lanostanoid triterpenes with unprecedented $\Delta^{16,17}$ double bond from *Ganoderma lucidum*. *Magnetic Resonance Chemistry*, 45: 789–791

Gunatilaka AA Leslie, Gopichand Y, Schmitz FJ and Djerassi C. 1981 Minor and trace sterols in marine invertebrates. 26.' isolation and structure elucidation of nine new 5a,8a-epidioxy sterols from four marine organisms. *Journal of Organic Chemistry*, 46:3860-3866

Güçlü-Ustündağ Ö and Mazza G 2007 Saponins: Properties, Applications and Processing. *Food Science and Nutrition*, 47:231–258

Hajjaj H, Macé C, Roberts M, Niederberger P and Fay LB 2005 Effect of 26-Oxygenosterols from *Ganoderma lucidum* and their activity as cholesterol synthesis inhibitors. *Applied and Environmental Microbiology*, 71(7): 3653–3658

Hansen CM, Binderup L, Hamberg KJ and Carlberg C 2001 Vitamin D and cancer: effects of 1,25(OH)₂D₃ and its analogs on growth control and tumorigenesis. *Frontiers in Bioscience*, 6:820-848.

Harmand PO, Duval R, Delage C, Simon A, 2005 Ursolic acid induces apoptosis through mitochondrial intrinsic pathway and caspase-3 activation in M4Beu melanoma cells. *International Journal of Cancer*, 114:1–11.

Hitomi J, Katayama T, Eguchi Y, Kudo T, Taniguchi M, Koyama Y, Manabe T, Yamagishi S, Bando Y, Imaizumi K, Tsujimoto Y, and Tohyama M 2004 Involvement of caspase-4 in endoplasmic reticulum stress-induced apoptosis and A β -induced cell death, *The Journal of Cell Biology*, 165(3): 347--356

Hong JK, Dumn DM, Shen CL, Pence BC. 2004 Effects of *Ganoderma lucidum* on apoptotic and anti-inflammatory function in HT-29 human colonic carcinoma cells. *Phytotherapy Research*, 18: 768-770.

Hsu CL, Yu YS and Yen GC 2008 Lucidenic acid B induces apoptosis in human leukemia cells via a mitochondria-mediated pathway. *Journal of Agricultural and Food Chemistry*, 56, 3973–3980

Hsu HY, Hua KF, Lin CC, Lin CH, Hsu J and Wong CH 2004 Extract of reishi polysaccharides induces cytokine expression via TLR4-modulated protein kinase signaling pathways. *The Journal of Immunology*, 173: 5989–5999

Hsu HY, Hua KF, Wu WC, Hsu J, Weng ST, Lin TL, Liu CY, Hseu RS and Huang CT 2008 Reishi immuno-modulation protein induces interleukin-2 expression via protein kinase-dependent signaling pathways within human T cells. *Journal of Cellular Physiology*, 215: 15–26.

Hsu MJ, Lee SS, Lee ST, Lin WW. 2003. Signaling mechanisms of enhanced neutrophil phagocytosis and chemotaxis by the polysaccharide purified from *Ganoderma lucidum*. *British Journal of Pharmacology*, 139:289–298.

- Hsu YL, Kuo PL, Lin CC. 2004 Proliferative inhibition, cell-cycle dysregulation, and induction of apoptosis by ursolic acid in human non-small cell lung cancer A549 cells. *Life Sciences*, 75: 2303–2316.
- Hu H, Ahn NS, Yang X, Lee YS, Kang KS. 2002 *Ganoderma lucidum* extract induces cell cycle arrest and apoptosis in MCF-7 human breast cancer cell. *International Journal of Cancer*, 102:250-253.
- Huang TC, Huang HC, Chang CC, Chang HY, Ou CH, Hsu CH, Chen ST and Juan HF 2007 An apoptosis-related gene network induced by novel compound-cRGD in human breast cancer cells. *FBES Letters*, 581(18): 3517-3522
- Hua KF, Hsu HY, Chao LKP, Chen ST, Yang WB, Hsu J and Wong CH 2007 *Ganoderma Lucidum* polysaccharides enhance CD14 endocytosis of LPS and promote TLR4 signal transduction of cytokine expression. *Journal of Cellular Physiology*, 212: 537–550.
- Igney FH, Krammer PH 2002 Death and anti-death: tumor resistance to apoptosis. *Nature Reviews: Cancer*, 2: 277-288
- Jiang JH (a), Slivova V, Harvey K, Valachovicova T, Sliva D. 2004 *Ganoderma lucidum* suppresses growth of breast cancer cells through the inhibition of Akt/NF- κ B signaling. *Nutrition and Cancer*, 49(2): 209-216
- Jiang JH (b), Slivova V, Valachovicova T, Harvey K, Sliva D. 2004 *Ganoderma lucidum* inhibits proliferation and induces apoptosis in human prostate cancer cells PC-3. *International Journal of Oncology*, 24(5):1093-9
- Jiang JH, Slivova V and Sliva D 2006 *Ganoderma lucidum* inhibits proliferation of human breast cancer cells by down-regulation of estrogen receptor and NF- κ B signaling. *International Journal of Oncology*, 29: 695-703.
- Jiang J, Grieb B, Thyagarajan A, Sliva D 2008 Ganoderic acids suppress growth and invasive behavior of breast cancer cells by modulating AP-1 and NF-kappaB signaling. *International Journal of Molecular Medicine*, 21(5):577-84
- Jun JI, Chung CW, Lee HJ, Pyo JO, Lee KN, Kim NS, Kim YS, Yoo HS, Lee TH, Kim E, Jung YK. 2005 Role of FLASH in caspase-8-mediated activation of NF-

kappaB: dominant-negative function of FLASH mutant in NF-kappaB signaling pathway. *Oncogene*, 24(4): 688–696.

Kang TB, Ben-Moshe T, Varfolomeev EE, Pewzner-Jung Y, Yogev N, Jurewicz A, Waisman A, Brenner O, Haffner R, Gustafsson E, Ramakrishnan P, Lapidot T, Wallach D. 2004 Caspase-8 serves both apoptotic and nonapoptotic roles. *Journal of Immunology*, 173: 2976–2984.

Kao YH, Yu CL, Chang LW. 2003 Low concentrations of arsenic induce vascular endothelial growth factor and nitric oxide release and stimulate angiogenesis *in vitro*. *Chemical Research in Toxicology*, 16:460–468.

Karst AM and Li G. 2007 BH3-only proteins in tumorigenesis and malignant melanoma. *Cellular and Molecular Life Sciences*, 64:318 – 330.

Kasperczyk H, La Ferla-Brühl K, Westhoff MA, Behrend L, Zwacka RM, Debatin KM and Fulda S. 2005 Betulinic acid as new activator of NF-κB: molecular mechanisms and implications for cancer therapy. *Oncogene*, 1–12

Kaufmann T, Schinzel A, Borner C. 2004 Bcl-w(edding) with mitochondria. *Trends Cell Biology*, 14:8–12.

Kim DH, Shim SB, Kim NJ, Jang IS. 1999. β-Glucuronidase inhibitory activity and hepatoprotective effect of *Ganoderma lucidum*. *Biological & Pharmaceutical Bulletin*, 22:162–164.

Kim SW, Park SS, Min TJ, and Yu KH 1999 Antioxidant activity of ergosterol peroxide (5,8-epidioxy-5a,8a-ergosta-6,22E-dien-3b-ol) in *Armillariella mellea*. *Bulletin of the Korean Chemical Society*, 20(7): 819-823

Kimura Y, Taniguchi M, Baba K. 2002 Antitumor and antimetastatic effects on liver of triterpenoid fractions of *Ganoderma lucidum*: mechanism of action and isolation of an active substance. *Anticancer Research*, 22:3309-3318.

Ko HH, Hung CF, Wang JP, Lin CN 2008 Antiinflammatory triterpenoids and steroids from *Ganoderma lucidum* and *G. tsugae*. *Phytochemistry*, 69:234–239

Kobori M, Yoshida M, Ohnishi-Kameyama M, Shinmoto H. 2007 Ergosterol peroxide from an edible mushroom suppresses inflammatory responses in

RAW264.7 macrophages and growth of HT29 colon adenocarcinoma cells. *British Journal of Pharmacology*, 150:209–219.

Komoda Y, Shimizu M, Sonoda Y, Sato Y. 1989 Ganoderic acid and its derivatives as cholesterol synthesis inhibitors. *Chemical & Pharmaceutical Bulletin (Tokyo)*, 37:531-533.

Konopleva M, Tsao T, Estrov Z, Lee RM, Wang RY, Jackson CE, McQueen T, Monaco G, Munsell M, Belmont J, Kantarjian H, Sporn MB, Andreeff M, 2004 The synthetic triterpenoid 2-cyano-3, 12-dioxooleana-1, 9-dien-28-oic acid induces caspase-dependent and -independent apoptosis in acute myelogenous leukaemia, *Cancer Research*, 64:7927–7935.

Koopman G, Reutelingsperger CPM, Kuijten GAM, Keehnen RMJ, Pals ST and van Oers MHJ. 1994 Annexin V for flow cytometric detection of phosphatidylserine expression on B cells undergoing apoptosis. *Blood*, 84 (5):1415-1420.

Koyama K, Imaizumi T, Akiba M, Kinoshita K, Takahashi K, Suzuki A, Yano S, Horie S, Watanabe K, Naoi Y. 1997 Antinociceptive components of *Ganoderma lucidum*. *Planta Medicine*, 63:224-227.

Kohoda H, Tokumoto W, Sakamoto K, Fuji M, Hirai Y, Yamasaki K, Komoda Y, Nakamura H, Ishihara S, Uchida M. 1985 The biologically active constituents of *Ganoderma lucidum* (Fr.) Karst. histamine release-inhibitory triterpenes. *Chemical & Pharmaceutical Bulletin (Tokyo)*, 33:1367-1374.

Kritchevsky D and Chen SC. 2005 Phytosterols—health benefits and potential concerns: a review. *Nutrition Research*, 25:413–428

Kroemer G, Galluzzi L and Brenner C. 2007 Mitochondrial membrane permeabilization in cell death. *Physiology Review* 87: 99–163.

Kubota T and Kubo I. 1969 Bitterness and Chemical Structure. *Nature*, 223: 97-98.

Kumazawa T, Kashiwayanagi M and Kurihara K. 1985 Neuroblastoma cell as a model for a taste cell: mechanism of depolarization in response to various bitter substances. *Brain Research*, 333, 27-33.

- Kuo MC, Weng CY, Ha CL, Wu MJ 2006 *Ganoderma lucidum* mycelia enhance innate immunity by activating NF- κ B. *Journal of Ethnopharmacology*, 103: 217–222
- Kuwana T, Mackey MR, Perkins G, Ellisman MH, Latterich M, Schneiter R, Green DR, Newmeyer DD. 2002 Bid, Bax, lipids cooperate to form supramolecular openings in the outer mitochondrial membrane. *Cell*, 111: 331–342.
- Kwon NS, Nathan CF, Gilker C, Griffith OW, Matthews DE, Stuehr DJ 1990 L-Citrulline production from L-arginine by macrophage nitric oxide synthase: the ureido oxygen derives from dioxygen. *Journal of Biology Chemistry*, 265:13442-13445.
- Lagarda MJ, García-Llatas G, Farré R 2006 Analysis of phytosterols in foods. *Journal of Pharmaceutical and Biomedical Analysis*, 41:1486–1496.
- Lakshmanan U, Porter AG. 2007 Caspase-4 interacts with TNF receptor-associated factor 6 and mediates lipopolysaccharide-induced NF-kappaB-dependent production of IL-8 and CC chemokine ligand 4 (macrophage-inflammatory protein-1). *Journal of Immunology*, 179(12):8480-90.
- Lamkanfi M, D'Hondt K, Vande Walle L, Van Gorp M, Denecker G, Demeulemeester J, Kalai M, Declercq W, Saelens X, Vandenabeele P. 2005 A novel caspase-2 complex containing TRAF2 and RIP1. *Journal of Biological Chemistry*, 280:6923–6932
- Lamkanfi M, Festjens N, Declercq W, Vanden Berghe T and Vandenabeele P. 2007 Caspases in cell survival, proliferation and Differentiation. *Cell Death and Differentiation*, 14:44–55
- Lamkanfi M, Kalai M, Saelens X, Declercq W, Vandenabeele P. 2004 Caspase-1 activates NF-kappa B independent of its enzymatic activity. *Journal of Biological Chemistry*, 279: 24785–24793.
- Lee SH, Shim SH, Kim JS, Kang SS. 2006 Constituents from the fruiting bodies of *Ganoderma applanatum* and their aldose reductase inhibitory activity. *Archives of Pharmaceutical Research*, 29(6):479-83.
- Li C, Yin J, Guo F, Zhang D, Sun HH. 2005 Ganoderic acid Sz, a new lanostanoid from the mushroom *Ganoderma lucidum*. *Natural Products Research*, 19(5):461-5.

- Li CH, Chena PY, Chang UM, Kan LS, Fang WH, Tsai KS, Lin SB. 2005 Ganoderic acid X, a lanostanoid triterpene, inhibits topoisomerases and induces apoptosis of cancer cells. *Life Sciences*, 77: 252-265
- Li P, Allen H, Banerjee S, Franklin S, Herzog L, Johnston C, McDowell J, Paskind M, Rodman L, Salfeld J. 1995 Mice deficient in IL-1 beta-converting enzyme are defective in production of mature IL-1 beta and resistant to endotoxic shock. *Cell*, 80: 401–411.
- Lin KI, Kao YY, Kuo HK, Yang WB, Chou A, Lin HH, Yu AL, and Wong CH 2006 Reishi polysaccharides induce immunoglobulin production through the TLR4/TLR2-mediated induction of transcription factor Blimp-1. *The Journal of Biological Chemistry*, 281 (34): 24111–24123
- Lin SB, Li CH, Lee SS, Kan LS. 2003 Triterpene-enriched extracts from *Ganoderma lucidum* inhibit growth of hepatoma cells via suppressing protein kinase C, activating mitogen-activated protein kinases and G2-phase cell cycle arrest. *Life Sciences*, 72: 2381-90.
- Lin ZB 2005 Cellular and Molecular Mechanisms of immuno-modulation by *Ganoderma lucidum*, *Journal of Pharmacological Sciences*, 99: 144 – 153.
- Lin ZB, Zhang HN 2004 Anti-tumor and immunoregulatory activities of *Ganoderma lucidum* and its possible mechanisms. *Acta Pharmacologica Sinica*, 25 (11): 1387-1395
- Ling WH and Jones PJH. 1995 Dietary phytosterols: a review of metabolism, benefits and side effects. *Life Sciences*, 57(3): 195-206
- Lippens S, Kockx M, Knaapen M, Mortier L, Polakowska R, Verheyen A, Garmyn M, Zwijsen A, Formstecher P, Huylebroeck D, Vandenabeele P, Declercq W. 2000 Epidermal differentiation does not involve the pro-apoptotic executioner caspases, but is associated with caspase-14 induction and processing. *Cell Death & Differentiation*, 7: 1218–1224.
- Livak KJ and Schmittgen TD. 2001 Analysis of relative gene expression data using real-time quantitative PCR and the $2^{-\Delta\Delta CT}$ method. *Methods*, 25, 402–408.

- Liu J. 2005 Oleanolic acid and ursolic acid: research perspectives. *Journal of Ethnopharmacology*, 100: 92–94.
- Liu J, Kurashiki K, Shimizu K and Kondo R 2006 Structure–activity relationship for inhibition of 5 α -reductase by triterpenoids isolated from *Ganoderma lucidum*. *Bioorganic & Medicinal Chemistry*, 14: 8654–8660
- Liu J, Shimizu K, Konishi F, Kumamoto S and Kondo R 2007 The anti-androgen effect of ganoderol B isolated from the fruiting body of *Ganoderma lucidum*. *Bioorganic & Medicinal Chemistry*, 15:4966–4972
- Liu J, Shimizu K, Konishi F, Noda K, Kumamoto S, Kurashiki K, Kondo R. 2007 Anti-androgenic activities of the triterpenoids fraction of *Ganoderma lucidum*. *Food Chemistry*, 100:1691–1696
- Lly C, Lly Y and Sun HH. 2006 New ganoderic acids, bioactive triterpenoid metabolites from the mushroom *Ganoderma lucidum*. *Natural Product Research*, 20(11): 985–991
- Lobner D. 2000 Comparison of the LDH and MTT assays for quantifying cell death: validity for neuronal apoptosis? *Journal of Neuroscience Methods*, 96: 147-152.
- Lochman J and Mikes V. 2005 Activation of different defence-related genes expression by ergosterol. *FEBS Journal*, 272:470-470.
- Lu QY, Jin YS, Zhang QF, Zhang ZF, Heber D, Go VLW, Li FP, Rao JY. 2004 *Ganoderma lucidum* extracts inhibit growth and induce actin polymerization in bladder cancer cells *in vitro*. *Cancer Letters*, 216: 9-20
- Ma C, Guan SH, Yang M, Liu X and Guo DA 2008 Differential protein expression in mouse splenic mononuclear cells treated with polysaccharides from spores of *Ganoderma lucidum*. *Phytomedicine*, 15 (4): 268-276
- Mariathasan S, Weiss DS, Dixit VM, Monack DM. 2005 Innate immunity against *Francisella tularensis* is dependent on the ASC/caspase-1 axis. *The Journal of Experimental Medicine*, 202: 1043–1049.
- Martin SJ, Reutelingsperger CEM, McGahon AJ, Rader JA, van Schie RCAA, LaFace DM and Green DtL. 1995 Early Redistribution of plasma membrane phosphatidylserine is a general feature of apoptosis regardless of the initiating

- stimulus: inhibition by overexpression of Bcl-2 and Abl. *Journal of Experimental Medicine*, 182: 1545-1556
- Martinon F, Burns K, Tschopp J. 2002 The inflammasome: a molecular platform triggering activation of inflammatory caspases and processing of proIL-beta. *Molecular Cell*, 10: 417-426.
- Martinon F, Tschopp J. 2007 Inflammatory caspases and inflammasomes: master switches of inflammation. *Cell Death & Differentiation*, 14(1):10-22.
- Michels J, Johnson WMP, Packham G. 2005 Mcl-1. *The International Journal of Biochemistry & Cell Biology*, 37: 267-271
- Min BS, Gao JJ, Hattori M, Lee HK, Kim YH. 2001 Anticomplement activity of terpenoids from the spores of *Ganoderma lucidum*. *Planta Medicines*, 67:811-814.
- Min BS, Nakamura N, Miyashiro H, Bae KH, Hattori M. 1998 Triterpenes from the spores of *Ganoderma lucidum* and their inhibitory activity against HIV-1 protease. *Chemical & Pharmaceutical Bulletin (Tokyo)*, 46:1607-1612.
- Min BS, Gao JJ, Nakamura N, Hattori M. 2000 Triterpenes from the spores of *Ganoderma lucidum* and their cytotoxicity against meth-A and LLC tumor cells. *Chemical & Pharmaceutical Bulletin (Tokyo)*, 48: 1026-1033.
- Ming LH, Wang P, Bank A, Yu J and Zhang L. 2006 PUMA dissociates Bax and Bcl-XL to induce apoptosis in colon cancer cells. *The Journal of Biological Chemistry*, 281(23): 16034-16042.
- Miura M, Chen XD, Allen MR, Bi Y, Gronthos S, Seo BM, Lakhani S, Flavell RA, Feng XH, Robey PG, Young M, Shi S. 2004 A crucial role of caspase-3 in osteogenic differentiation of bone marrow stromal stem cells. *The Journal of Clinical Investigation*, 114:1704-1713.
- Mizushima Y, Watanabe I, Togashi H, Hanashima L, Takemura M, Ohta K, Sugawara F, Koshino H, Esumi Y, Uzawa J, Matsukage A, Yoshida S and Sakaguchi K. 1998 An ergosterol peroxide, a natural product that selectively enhances the inhibitory effect of linoleic acid on DNA polymerase β . *Biological & Pharmaceutical Bulletin*, 21(5): 444-448

- Moreau RA, Whitaker BD, Hicks KB. 2002 Phytosterols, phytostanols, and their conjugates in foods: structural diversity, quantitative analysis, and health-promoting uses. *Progress in Lipid Research*, 41:457–500
- Muto Y, Ninomiya M and Fujiki H 1990 Present status of research on cancer chemoprevention in Japan. *Japan Journal of Clinical Oncology*, 20: 219–224.
- Nechushtan A, Smith CL, Lamensdorf I, Yoon SH, Youle RJ. 2001 Bax and Bak coalesce into novel mitochondria-associated clusters during apoptosis. *Journal of Cell Biology*, 153: 1265–1276.
- Nishitoba T, Sato H and Sakamura S. 1986 New terpenoids, ganolucidic acid D, ganoderic acid L, lucidone C, and lucidenic acid G from the fungus *Ganoderma lucidum*. *Agricultural and Biological Chemistry*, 50: 809-811.
- Nishitoba T, Sato H and Sakamura S 1988 Bitterness and Structure Relationship of the Triterpenoids. *Agricultural and Biological Chemistry*, 52 (7), 1791-1795.
- Nonaka Y, Ishibashi H, Nakai M, Shibata H, Kiso Y and Abe S. 2008 Effects of the antlered form of *Ganoderma lucidum* on tumor growth and metastasis in cyclophosphamide-treated mice. *Bioscience, Biotechnology, and Biochemistry*, 72:70607-1–10.
- Ostlund RE Jr. 2002 Phytosterols in human nutrition. *Annual Review of Nutrition*, 22:533–49
- Ovesná Z, Vachálková A, Horváthová K 2004 Taraxasterol and beta-sitosterol: new naturally compounds with chemoprotective/chemopreventive effects. *Neoplasma*, 51(6):407-14
- Pajak B, Gajkowska B, Orzechowski A 2009 Sodium butyrate sensitizes human colon adenocarcinoma COLO 205 cells to both intrinsic and TNF- α -dependent extrinsic apoptosis. *Apoptosis*,
- Panka DJ, Atkins MB and Mier JW. 2006 Targeting the mitogen-activated protein kinase pathway in the treatment of malignant melanoma. *Clinical Cancer Research*, 12(7 Suppl):2371-2375
- Panka DJ, Cho DC, Atkins MB and Mier JW. 2008 GSK-3 β inhibition enhances

sorafenib-induced apoptosis in melanoma cell lines. *The Journal of Biological Chemistry*, 283(2): 726–732.

Paterson RR 2006 Ganoderma – A therapeutic fungal biofactory. *Phytochemistry*, 67:1985–2001

Plat J and Mensink RP. 2005 Plant stanol and sterol esters in the control of blood cholesterol levels: mechanism and safety aspects. *The American Journal of Cardiology*, 96(suppl):15D–22D

Rao AV, Janezic SA. 1992 The role of dietary phytosterols in colon carcinogenesis. *Nutrition and Cancer*, 18(1):43-52.

Reichrath J, Rech M, Moeini M, Meese E, Tilgen WG, Seifert M. 2007 *In Vitro* comparison of the vitamin D endocrine system in 1,25(OH)₂D₃-responsive and -resistant melanoma cells. *Cancer Biology & Therapy*, 6(1): 48-55

Roy S, Sharom JR, Houde C, Loisel TP, Vaillancourt JP, Shao W, Saleh M, Nicholson DW. 2008 Confinement of caspase-12 proteolytic activity to autoprocessing. *The Proceedings of the National Academy Sciences USA*, 105(11):4133-8.

Ryan E, Galvin K, O'Connor TP, Maguire AR and O'Brien NM. 2007 Phytosterol, squalene, tocopherol content and fatty acid profile of selected seeds, grains, and legumes. *Plant Foods for Human Nutrition*, 62:85–91

Saikumar P, Dong Z, Mikhailov V, Denton M, Weinberg JM, Venkatachalam MA. 1999 Apoptosis: definition, mechanisms, and relevance to disease. *The American Journal of Medicine*, 107:489 –506

Salami S and Karami-Tehrani F. 2003 Biochemical studies of apoptosis induced by tamoxifen in estrogen receptor positive and negative breast cancer cell lines. *Clinical Biochemistry*, 36: 247-253.

Saleh M, Vaillancourt JP, Graham RK, Huyck M, Srinivasula SM, Alnemri ES, Steinberg MH, Nolan V, Baldwin CT, Hotchkiss RS, Buchman TG, Zehnbaauer BA, Hayden MR, Farrer LA, Roy S, Nicholson DW. 2004 Differential modulation of endotoxin responsiveness by human caspase-12 polymorphisms. *Nature*, 429: 75–79.

- Saleh M, Mathison JC, Wolinski MK, Bensinger SJ, Fitzgerald P, Droin N, Ulevitch RJ, Green DR, Nicholson DW. 2006 Enhanced bacterial clearance and sepsis resistance in caspase-12-deficient mice. *Nature*, 440: 1064–1068.
- Salmena L, Lemmers B, Hakem A, Matysiak-Zablocki E, Murakami K, Au PY, Berry DM, Tamblyn L, Shehabeldin A, Migon E, Wakeham A, Bouchard D, Yeh WC, McGlade JC, Ohashi PS, Hakem R. 2003 Essential role for caspase 8 in T-cell homeostasis and T-cell-mediated immunity. *Genes & Development*, 17(7): 883–895.
- Salo P and Wester I 2005 Low-fat formulations of plant stanols and sterols. *The American Journal of Cardiology*, 96(suppl):51D–54D
- Santambrogio L, Potoicchio I, Fessler SP, Wong SH, Raposo G, Strominger JL. 2005 Involvement of caspase-cleaved and intact adaptor protein 1 complex in endosomal remodeling in maturing dendritic cells. *Nature Immunology*, 6: 1020–1028.
- Schägger H. 2006 Tricine-SDS-PAGE. *Nature Protocols*, 1(1): 16-22.
- Schinzl A, Kaufmann T, Schuler M, Martinalbo J, Grubb D, Borner C. 2004 Conformational control of Bax localization and apoptotic activity by Pro168. *Journal of Cell Biology*, 164:1021–1032.
- Sgarbi DB, da Silva AJ, Carlos IZ, Silva CL, Angluster J and Alviano CS. 1997. Isolation of ergosterol peroxide and its reversion to ergosterol in the pathogenic fungus *Sporothrix schenckii*. *Mycopathologia*, 139: 9–14.
- Sgonc R, Dietrich GH, Gruber J, Recheis H and Wick G. 1994. Simultaneous determination of cell surface antigens and apoptosis. *Trends in Genetics*. 10: 41-42.
- Shao BM, Dai H, Xua W, Lin ZB, Gao XM 2004 Immune receptors for polysaccharides from *Ganoderma lucidum*. *Biochemical and Biophysical Research Communications*, 323:133–141
- Shia YL, Sunb J, Hea H, Guoa H, Zhang S 2008 Hepatoprotective effects of *Ganoderma lucidum* peptides against d-galactosamine-induced liver injury in mice. *Journal of Ethnopharmacology*, 117:415–419

- Sliva D. 2003 *Ganoderma lucidum* (Reishi) in Cancer Treatment. *Integrative Cancer Therapies*, 2(4): 358-364
- Slominski A, Semak I, Zjawiony J, Wortsman J, Gandy MN, Li JH, Zbytek B, Li W, Tuckey RC. 2005 Enzymatic metabolism of ergosterol by cytochrome P450_{scc} to biologically active 17R,24-dihydroxyergosterol. *Chemistry & Biology*, 12: 931-939.
- Smith JE, Rowan NJ, Sullivan R. 2002. Medicinal mushrooms: a rapidly developing area of biotechnology for cancer therapy and other bioactivities. *Biotechnology Letter*, 24, 1839–1845.
- So WK, Kwok HF and Ge W. 2005 Zebrafish gonadoreopins and their receptors: II. Cloning and characterization of zebrafish follicle-stimulating hormone and luteinizing hormone subunits—their spatial-temporal expression patterns and receptor specificity. *Biology of Reproduction*, 72: 1382-1396.
- Sohn KH, Lee HY, Chung HY, Young HS, Yi SY, Kim KW. 1995 Anti-angiogenic activity of triterpene acids. *Cancer Letters*, 94: 213-218
- Song YS, Kimb SH, Sa JH, Jin C, Limd CJ, Park EH. 2004 Anti-angiogenic and inhibitory activity on inducible nitric oxide production of the mushroom *Ganoderma lucidum*. *Journal of Ethnopharmacology*, 90:17–20
- Sonoda Y, Sekigawa Y, Sato Y. 1988 *In vitro* effects of oxygenated lanosterol derivatives on cholesterol biosynthesis from 24,25-dihydrolanosterol. *Chemical & Pharmaceutical Bulletin (Tokyo)*, 36: 966-973.
- Soung YH, Lee JW, Kim HS, Park WS, Kim SY, Lee JH, Park JY, Cho YG, Kim C J, Park YG, Nam SW, Jeong SW, Kim SH, Lee JY, Yoo NJ and Lee SH. 2003 Inactivating mutations of CASPASE-7 gene in human cancers. *Oncogene*, 22:8048–8052
- Stanley G, Harvey K, Slivova V, Jiang JH, Sliva D. 2005 *Ganoderma lucidum* suppresses angiogenesis through the inhibition of secretion of VEGF and TGF- β 1 from prostate cancer cells. *Biochemical and Biophysical Research Communications*, 330: 46-52

- Su CY, Shiao MS, and Wang CT 1999 Differential effects of Ganodermic acid S on the thromboxane A₂-signaling pathways in human platelets. *Biochemical Pharmacology*, 58: 587-595.
- Su CY, Shiao MS, and Wang CT 2000 Potentiation of Ganodermic acid S on prostaglandin E₁-induced cyclic AMP elevation in human platelets. *Thrombosis Research*, 99:135-145
- Su H, Bidère N, Zheng L, Cubre A, Sakai K, Dale J, Salmena L, Hakem R, Straus S, Lenardo M. 2005 Requirement for caspase-8 in NF-kappaB activation by antigen receptor. *Science*, 307: 1465–1468.
- Takahashi K, Kawai T, Kumar H, Sato S, Yonehara S, Akira S. 2006 Cutting edge: roles of caspase-8 and caspase-10 in innate immune responses to double-stranded RNA. *Journal of Immunology*, 176: 4520–4524.
- Takei T, Yoshida M, Ohnishi-kameyama M and Kobori M. 2005 Ergosterol peroxide, an apoptosis-inducing component isolated from *Sarcodon aspratus* (Berk.) S. Ito. *Bioscience, Biotechnology, and Biochemistry*, 69(1): 212-215
- Tang YJ, Zhong JJ 2002 Fed-batch fermentation of *Ganoderma lucidum* for hyperproduction of polysaccharide and ganoderic acid. *Enzyme and Microbial Technology*, 31:20–28.
- Tang YJ and Zhong JJ 2003 Scale-up of a liquid static culture process for hyperproduction of ganoderic acid by the medicinal mushroom *Ganoderma lucidum*. *Biotechnology Progress*, 19:1842-1846
- Tang W, Liu JW, Zhao WM, Wei DZ, Zhong JJ. 2006 Ganoderic acid T from *Ganoderma lucidum* mycelia induces mitochondria mediated apoptosis in lung cancer cells. *Life Science*, 80:205–211.
- Thallinger C, Wolschek MF, Wacheck V, Maierhofer H, Günsberg P, Poltrauer P, Pehamberger H, Monia BP, Selzer E, Wolff K, Jansen B. 2003 Mcl-1 antisense therapy chemosensitizes human melanoma in a SCID mouse xenotransplantation model. *Journal of Investigative Dermatology*, 120:1081–6.
- Thompson GR and Grundy SM. 2005 History and development of plant sterol and stanol esters for cholesterol-lowering purposes. *The American Journal of Cardiology*, 96(suppl):3D–9D
- Thyagarajan A, Jiang JH, Hopf A, Adamec J and Sliva D 2006 Inhibition of oxidative stress-induced invasiveness of cancer cells by *Ganoderma lucidum* is mediated through the suppression of interleukin-8 secretion. *International Journal of*

Thyagarajan A, Zhu JS and Sliva D 2007 Combined effect of green tea and *Ganoderma lucidum* on invasive behavior of breast cancer cells. *International Journal of Oncology*, 30: 963-969.

Tong MH, Chien PJ, Chang HH, Tsai MJ and Sheu F 2008 High processing tolerances of immunomodulatory proteins in Enoki and Reishi mushrooms. *Journal of Agriculture and Food Chemistry*, 56:3160–3166

Townsend K, Banwell CM, Guy M, Colston KW, Mansi JL, Stewart PM, Campbell MJ, and Hewison M 2005 Autocrine metabolism of vitamin D in normal and malignant breast tissue. *Clinical Cancer Research*, 11(9): 3579-3586

Vermes I, Haanen C, Steffens-Nakken H, Reutelingsperger C 1995 A novel assay for apoptosis flow cytometric detection of phosphatidylserine early apoptotic cells using fluorescein labeled expression on Annexin V. *Journal of Immunological Methods*, 184: 39-51

Wagner R, Mitchell DA, Sasaki GL, Maria Angela Lopes de Almeida Amazonas 2004 Links between morphology and physiology of *Ganoderma lucidum* in submerged culture for the production of exopolysaccharide. *Journal of Biotechnology*, 114:153-164

Wang G, Zhao J, Liu JW, Huang YP, Zhong JJ, Tang W 2007 Enhancement of IL-2 and IFN- γ expression and NK cells activity involved in the anti-tumor effect of ganoderic acid Me *in vivo*. *International Immunopharmacology*, 7: 864–870

Wang MY, Liu Q, Che QM, Lin ZB. 2000. Effects of triterpenoids from *Ganoderma lucidum* (Leyss. Ex fr.) karst on three different experimental liver injury models in mice. *Acta Pharmaceutica Sinica* 35, 326–329.

Wang YY, Khoo KH, Chen ST, Lin CC, Wong CH, Lin CH. 2002. Studies on the immunomodulating and antitumor activities of *Ganoderma lucidum* (Reishi) polysaccharides: Functional and proteomic analyses of a fucose-containing glycoprotein fraction responsible for the activities. *Bioorganic & Medicinal Chemistry*, 10:1057–1062.

Wang S, Miura M, Jung YK, Zhu H, Li E, Yuan J. 1998 Murine caspase-11, an ICE-interacting protease, is essential for the activation of ICE. *Cell*, 92: 501–509.

- Wang SY, Hsu ML, Hsu HC, Tzeng CH, Lee SS, Shiao MS and Ho CK. 1997 The antitumor effect of *Ganoderma Lucidum* is mediated by cytokines released from activated macrophages and tymphocytes. *International Journal of Cancer*, 70:699-705
- Wasser SP, Weis AL 1999 The therapeutic effects of substances occurring in higher basidiomycetes mushroom: a modern perspective. *Critical Reviews in Immunology*, 19: 65-69
- Wendt KU, Schulz GE, Corey EJ, Liu DR 2000 Enzyme mechanisms for polycyclic triterpene formation. *Angewandte Chemie International Edition*, 39:2812-2833.
- Weng CJ, Chau CF, Chen KD, Chen DH and Yen GC 2007 The anti-invasive effect of lucidenic acids isolated from a new *Ganoderma lucidum* strain. *Molecular Nutrition & Food Research*, 51, 1472 – 1477
- Weng CJ, Chau CF, Hsieh YS, Yang SF and Yen GC 2008 Lucidenic acid inhibits PMA-induced invasion of human hepatoma cells through inactivating MAPK/ERK signal transduction pathway and reducing binding activities of NF-kB and AP-1. *Carcinogenesis*, 29(1): 147–156.
- Wick W, Grimm C, Wagenknecht B, Dichgans J, Weller M, 1999 Betulinic acid-induced apoptosis in glioma cells: a sequential requirement for new protein synthesis, formation of reactive oxygen species, and caspase processing, *The Journal of Pharmacology and Experimental Therapeutics*, 289: 1306–1312.
- Won SJ, Lee SS, Ke YH and Lin MT. 1989 Enhancement of splenic NK cytotoxic activity by extracts of *Ganoderma lucidum* mycelium in mice. *Journal of Biomedical Laboratory Science*, 2: 201–213.
- Woo M, Hakem R, Furlonger C, Hakem A, Duncan GS, Sasaki T, Bouchard D, Lu L, Wu GE, Paige CJ, Mak TW. 2003 Caspase-3 regulates cell cycle in B cells: a consequence of substrate specificity. *Nature Immunology*, 4: 1016–1022.
- Wu TS, Shi LS and Kuo SC. 2001 Cytotoxicity of *Ganoderma lucidum* triterpenes. *Journal of Nature Product*, 64: 1121-1122

- Xie JT, Wang CZ, Wicks S, Yin JJ, Kong J, Li J, Li YC, Yuan CS. 2006 *Ganoderma lucidum* extract inhibits proliferation of SW480 human colorectal cancer cells. *Experimental Oncology*, 28(1): 25–29
- Xie YZ, Li SZ, Yee A, La Pierre DP, Deng ZQ, Lee DY, Wu QP, Chen Q, Li C, Zhang Z, Guo J, Jiang Z, Yang BB 2006 *Ganoderma lucidum* inhibits tumour cell proliferation and induces tumour cell death, *Enzyme and Microbial Technology*, 40 : 177–185
- Yang FC, Ke YF, Kuo SS. 2000 Effect of fatty acids on the mycelial growth and polysaccharide formation by *Ganoderma lucidum* in shake flask cultures. *Enzyme and Microbial Technology*, 27: 295-301
- Yasukawa K, Akihisa T, Kanno H, Kaminaga T, Izumida M, Sakoh T, Tamura T, Takido M. 1996 Inhibitory effects of sterols isolated from *Chlorella vulgaris* on 12-0-tetradecanoylphorbol-13-acetate-induced inflammation and tumor promotion in mouse skin. *Biological & Pharmaceutical Bulletin*. 19(4):573-6.
- Yu J, Zhang L, Hwang PM, Kinzler KW and Vogelstein B. 2001 PUMA induces the rapid apoptosis of colorectal cancer cells. *Molecular Cell*, 7: 673–682.
- Yuan JP, Wang JH, Liu X, Kuang HC and Huang XN 2006 Determination of ergosterol in *Ganoderma* spore lipid from the germinating spores of *Ganoderma lucidum* by high-performance liquid chromatography. *Journal of Agriculture and Food Chemistry*, 54:6172-6176.
- Yuan JP, Wang JH and Liu X 2007 Distribution of free and esterified ergosterols in the medicinal fungus *Ganoderma lucidum*. *Applied Microbiology and Biotechnology*, 77:159–165
- Yuan JP, Zhao SY, Wang JH, Kuang HC, and Liu X 2008 Distribution of nucleosides and nucleobases in edible fungi. *Journal of Agriculture and Food Chemistry*, 56, 809–815
- Yue GG, Fung KP, Tse GM, Leung PC, Lau CB. 2006 Comparative studies of various *Ganoderma* species and their different parts with regard to their antitumor and immunomodulating activities *in vitro*. *The Journal of Alternative and Complementary Medicine*, 12(8):777–789

- Yuen JWM, Gohel MDI. 2008 The dual roles of Ganoderma antioxidants on urothelial cell DNA under carcinogenic attack. *Journal of Ethnopharmacology*, 118(2):324-30.
- Zaidman BZ, Yassin M, Mahajna J, Wasser SP. 2005 Medicinal mushroom modulators of molecular targets as cancer therapeutics. *Applied Microbiology and Biotechnology* 67: 453-468
- Zhang GL, Wang YH, Ni W, Teng HL, Lin ZB 2002. Hepatoprotective role of Ganoderma lucidum polysaccharide against BCG-induced immune liver injury in mice. *World Journal of Gastroenterology*, 8: 728-733
- Zhang HN, He JH, Yuan L, Lin ZB 2003 *In vitro* and *in vivo* protective effect of Ganoderma lucidum polysaccharides on alloxan-induced pancreatic islets damage. *Life Sciences*, 73:2307-2319
- Zhang YH, Gu JF, Zhao LL, He LF, Qian WB, Wang JH, Wand YG, Qian QJ, Cheng Q, Wu J and Liu XY. 2006 Complete elimination of colorectal tumor xenograft by combined manganese superoxide dismutase with tumor necrosis factor-related apoptosis-inducing ligand gene virotherapy. *Cancer Research*, 66(15): 4291-4298.
- Zhou CY, Jia W, Yang Y, Bai YQ. 2002. Experimental studies on prevention of several kinds of fungi polysaccharides against alcohol-induced hepatic injury. *Edible Fungi*, 24: 36-37.
- Zhao HB, Wang SZ, He QH, Yuan L, Chen AF, Lin ZB 2005. Ganoderma total sterol (GS) and GS1 protect rat cerebral cortical neurons from hypoxia/reoxygenation injury. *Life Sciences*, 76, 1027-1037.
- Zhao MW, Liang WQ, Zhang DB, Wang N, Wang CG, Pan YJ 2007 Cloning and characterization of squalene synthase (SQS) gene from *Ganoderma lucidum*. *Journal of Microbiology Biotechnology*, 17(7):1106-12.
- Zhivotovsky B, Orrenius S. 2005 Caspase-2 function in response to DNA damage. *Biochemical and Biophysical Research Communications*, 331: 859-867.

Zhu HS, Yang XL, Wang LB, Zhao DX, Chen L. 2000 Effects of extracts from sporoderm-broken spores of *Ganoderma lucidum* on HeLa cells. *Cell Biology Toxicology*, 16: 201-206.

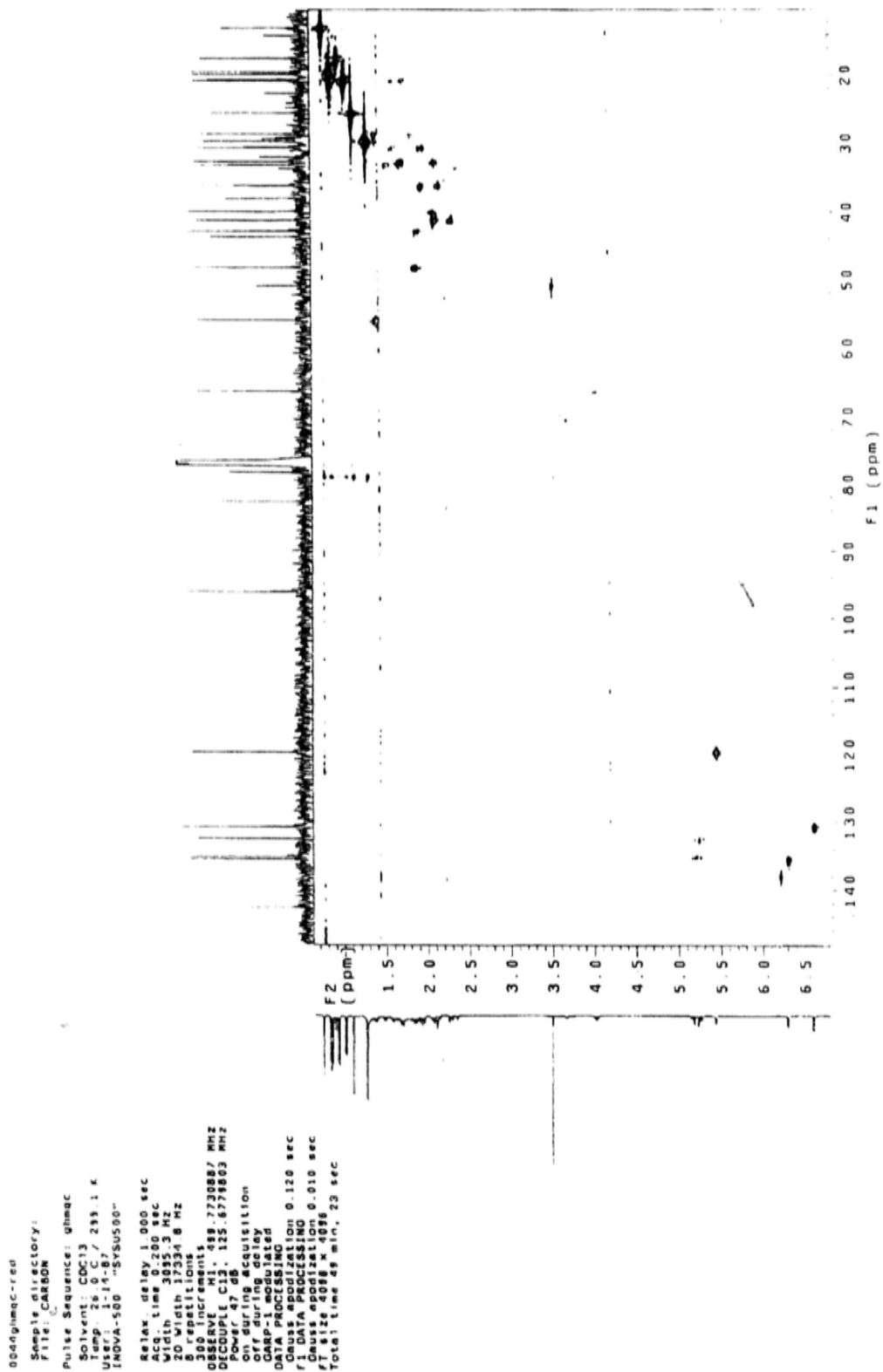
Zhu XL, Lin ZB 2005 Effects of *Ganoderma lucidum* polysaccharides on proliferation and cytotoxicity of cytokine-induced killer cells. *Acta Pharmacologica Sinica*, 26 (9): 1130–1137

Zhu XL, Chen AF and Lin ZB 2007 *Ganoderma lucidum* polysaccharides enhance the function of immunological effector cells in immunosuppressed mice. *Journal of Ethnopharmacology*, 111 (2): 219-226

Ziegenbein FC, Hanssen HP, König WA. 2006 Secondary metabolites from *Ganoderma lucidum* and *Spongiporus leucomallellus*. *Phytochemistry*, 67: 202–211

Appendix

Appendix 1. Two dimensions NMR analysis of 9(11)-DHEP: C-H relation in CDCl_3 , 500MHz

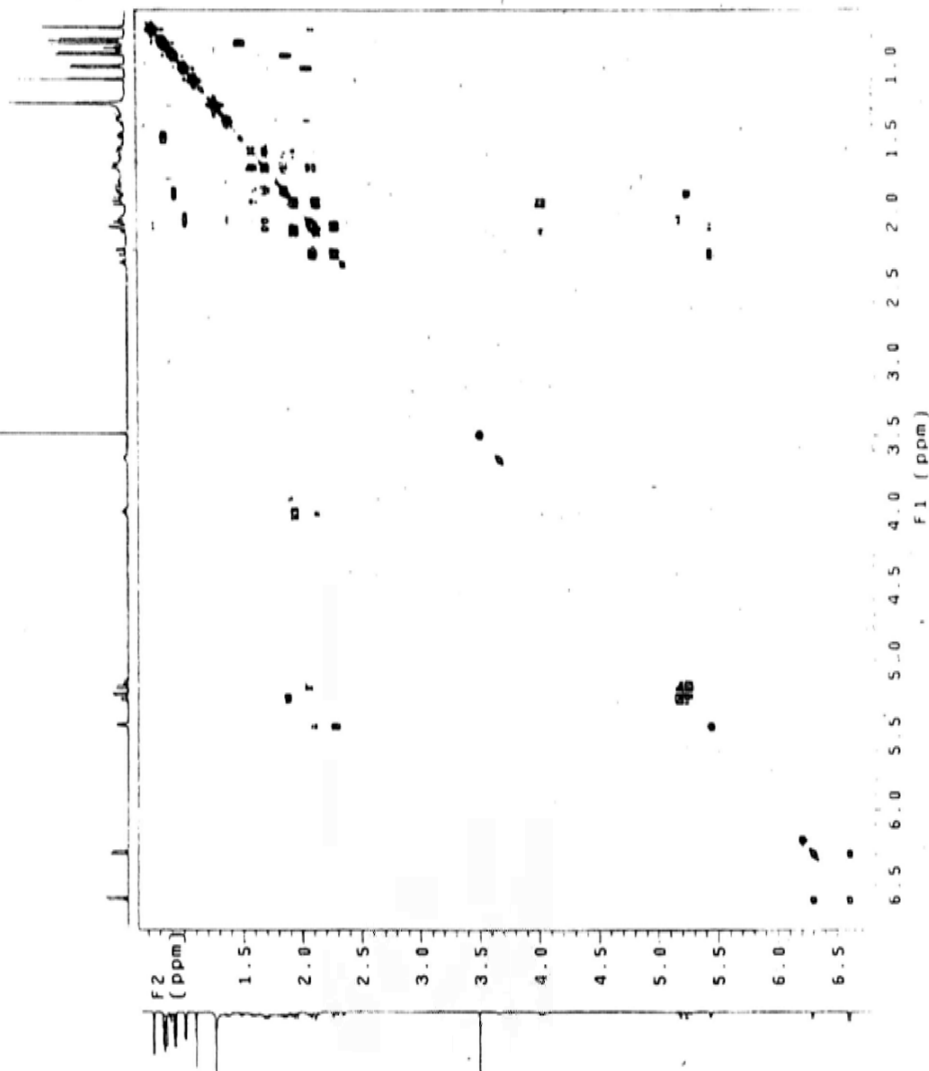


Appendix 3. Two dimensions NMR analysis of 9(11)-DHEP: H-H relation in CDCl₃, 500MHz

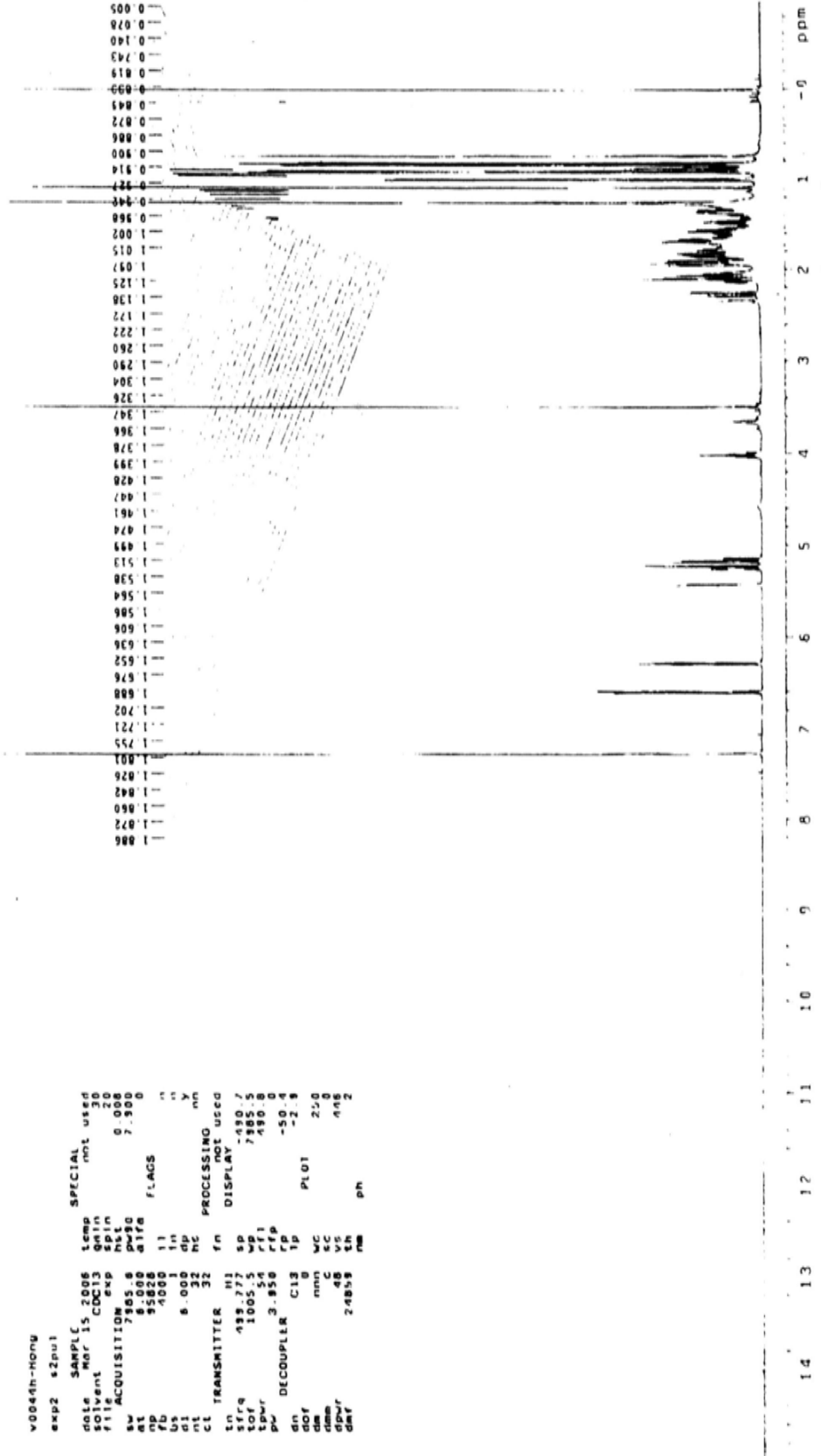
```

000gpcosy-rem
Archive directory: /export/home/pub/vnmr/sys/data
Sample directory:
File: PROTON
Pulse Sequence: gpcosy
Solvent: CDCl3
Temp: 26.0 C / 299.1 K
INDVA=500 --SYSUS00"
Relax. delay: 1.000 sec
Acq. time: 30.25 sec
NUC1: 13C
20 Width: 3085.3 Hz
4 repetitions
256 increments
DATA PROCESSING: 7.730822 MHz
Sine bell: 0.116 sec
F1 DATA PROCESSING
Sine bell: 0.00106 sec
Time: 0.000000 sec
Total time: 22 min. 0 sec

```



Appendix 4. H-NMR analysis of 9(11)-DHEP in CDCl₃, 500MHz



```

V0044h-NONG
EXP2  S2PUL
=====
DATE  SAMPLE  TEMP  SPECIAL  INT  USED
MOR 15 2006  CDC13  30
SOLVENT  CDC13  GAIN  20
FILE  EXP  SPIN  0.20
=====
SW ACQUISITION  EXP  7.900
AT  7.905  8  0.430
SI  8.000  8178  FLAGS
NP  95828  11
PB  4000  11
DI  8.000  11  Y
NI  32  11  Y
CL TRANSMITTER  32  FN  PROCESSING  NN
LN  TRANSMITTER  N1  FN  DISPLAY  NOT USED
SFRQ  499.777  SP  490.7
TQF  1005.5  WP  7985.5
TPI  54  F11  490.8
PULPROG  3.958  F1P  -50.4
DECOUPLER  C13  TP  -2.9
DOF  0  WC  250
DM  0  VC  495
DPR  48  TH  495
DWT  24858  RM  PH
=====

```

14 13 12 11 10 9 8 7 6 5 4 3 2 1 -0 ppm

1.10 1.11 1.10 1.17 0.73 0.95 1.32 26.31 3.26 96

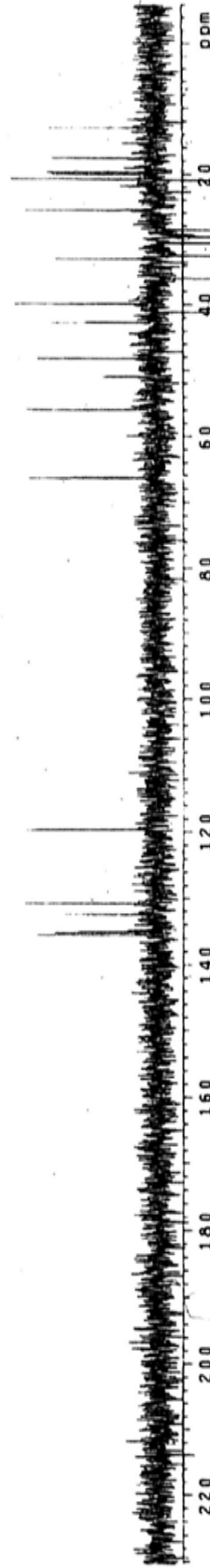
Appendix 5. DEPT analysis of 9(11)-DHEP in CDCl₃, 500MHz

12.954
17.535
19.619
19.922
20.694
20.875
25.528
28.601
29.668
30.578
32.561
33.045
36.046
39.877
41.175
42.755
48.151
50.849
55.856
66.323

119.207
130.730
132.418
135.095
135.441

```

0049sept135-red
EXPI DEPT
DATE SAMPLE MAR 24 2006 111W DEPT 140.0
SOLVENT CDCl3 mult SPECIAL 1 5
SAMPLE
SW ACQUISITION temp 26.0
gt 29706.6 gain 54
ns 0.400 spin NOT USED
ds 23786 PROCESSING 3.00
di -4 f0 SPECTRUM 65530
nl 1.000 W0 29705.7
ct 200 W1 -761.9
   200 W2 -64.3
   200 W3 42.3
tn TRANSMITTER C13 1p
lof 2182.0 a1 PH
tpwr 8.85 f1 REFERENCE 782.8
pw DECOUPLER M1 PLOT
dn -45.6 WC 250
dof 43 EC 0
dpr 111V VS 5460
dm 100V hzmm 118.82
den 10592 th
def 27.800
ppiv1
pp
  
```



Appendix 6. C-NMR analysis of EP in CDCl₃, 500MHz

0045-132
exp2 s2p01

```

SPECIAL 25.0
date Mar 23 2006 temp
solvent Mar 23 2006 CDC13 gain not used
file ACQUISITION exp not used
kw ACQUISITION exp not used
at 290.05 4 net 0.000
np 23766 0178 8.800
rb 18000 13
ds 1.80 1n
dl 30000 1p
ct 1772 1772
CT TRANSMITTER fb 3.00
lv 105 23 fn
lpr 2182 50 DISPLAY 65536
tdw 28705.7 50
pw DECOUPLER 2.200 rf1 10438.2
dn -45 1p rf2 8676.4
dm YXY ip -153.1
dmm WC 250
dpr CC 423
dmr 10582 56
AT 6
  
```

```

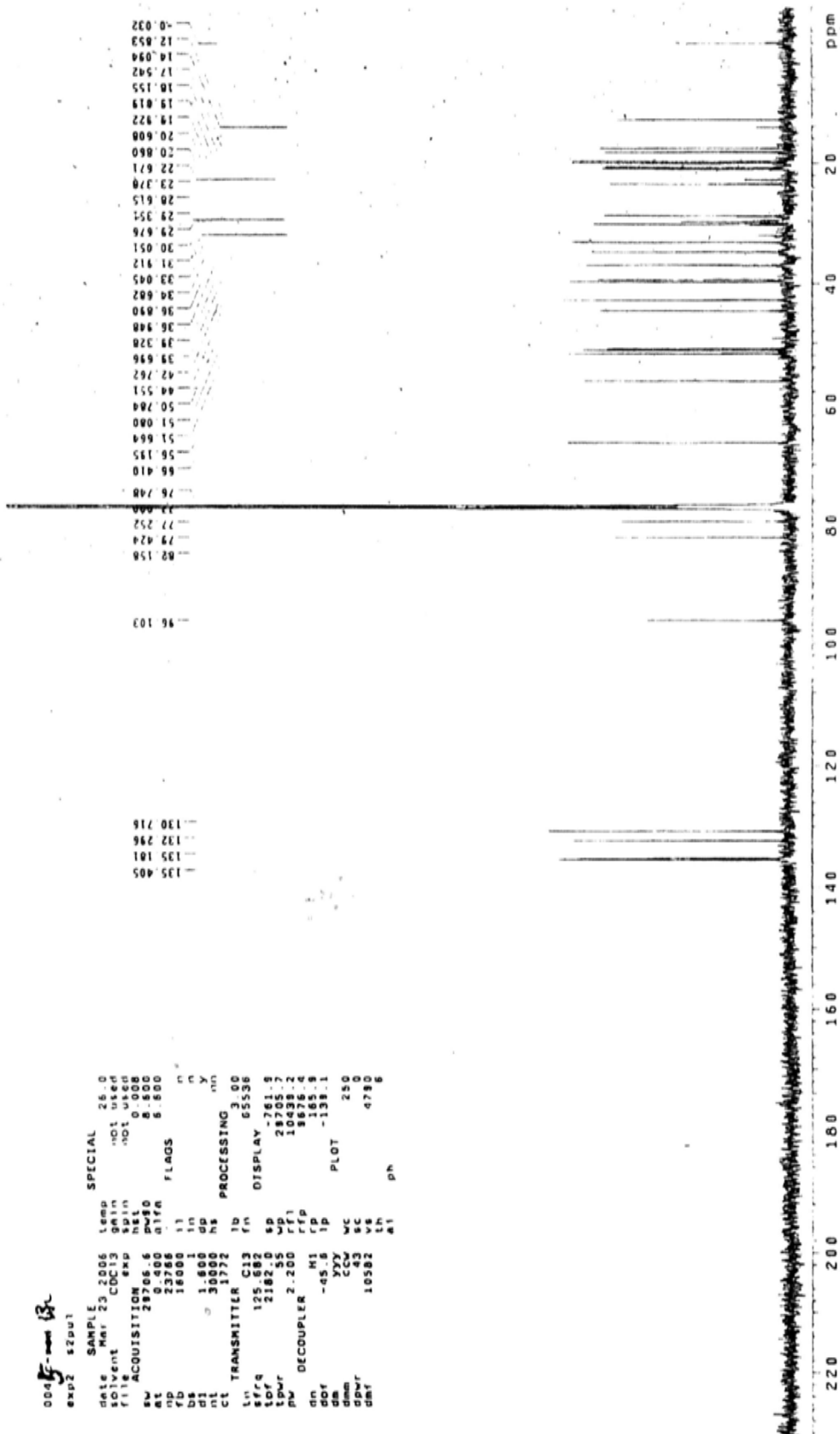
SPECIAL 25.0
temp not used
gain not used
net 0.000
8.800
  
```

```

SPECIAL 25.0
temp not used
gain not used
net 0.000
8.800
  
```

135.405
133.296
130.718

76.748
66.410
56.185
51.684
51.080
50.784
44.551
42.762
39.948
39.328
38.690
34.682
33.045
31.912
30.051
29.676
29.351
28.615
23.370
22.671
20.860
19.822
19.019
18.155
17.542
14.094
12.853
-0.023



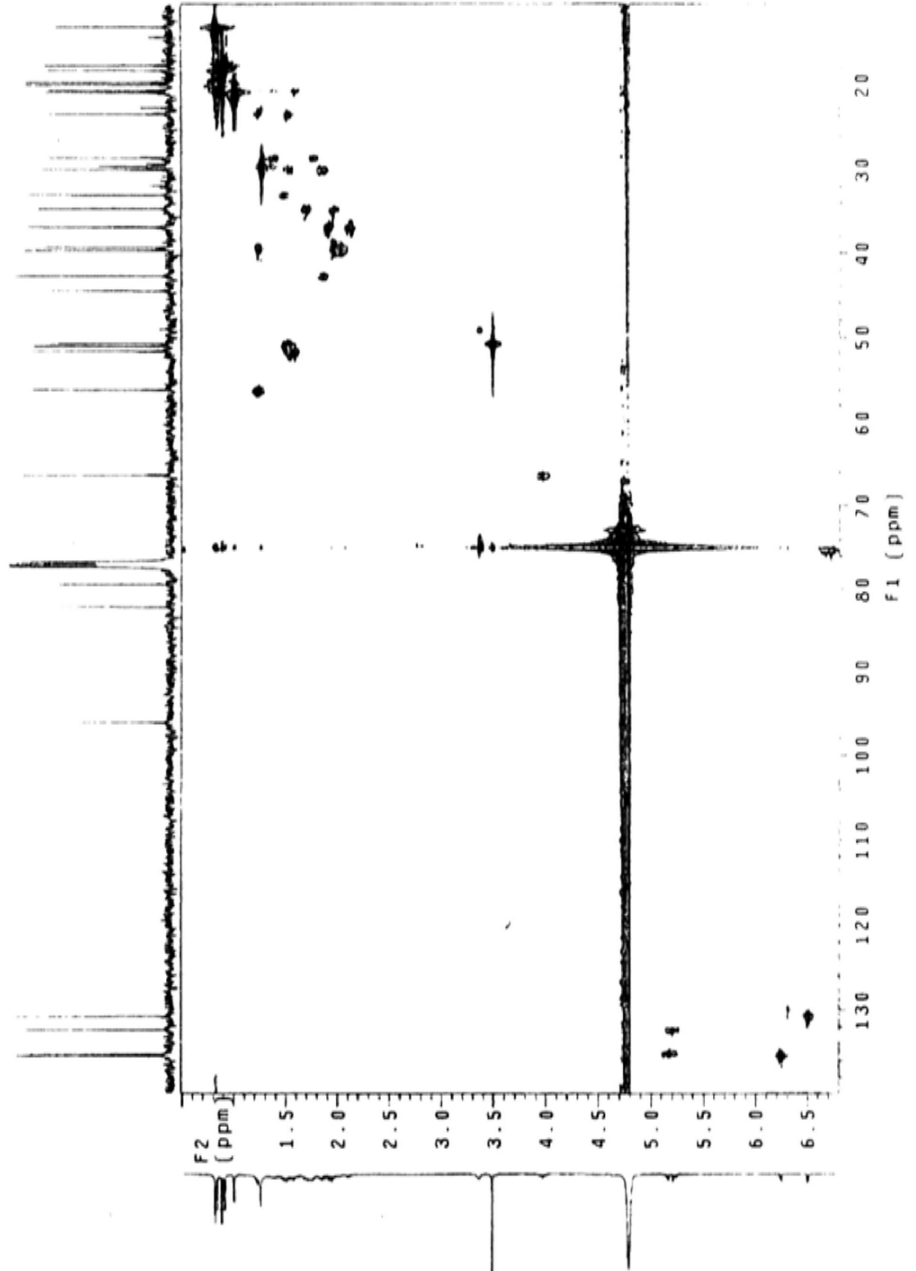
Appendix 8. Two dimensions NMR analysis of EP: C-H relation in CDCl_3 , 500MHz

0045ghmc-green

Sample directory:
File: CARBON

Pulse Sequence: ghmc
Solvent: CDCl_3
Temp: 26.0 C / 289.1 K
User: 1-14-87
INDVA-500 "SYNUS100"

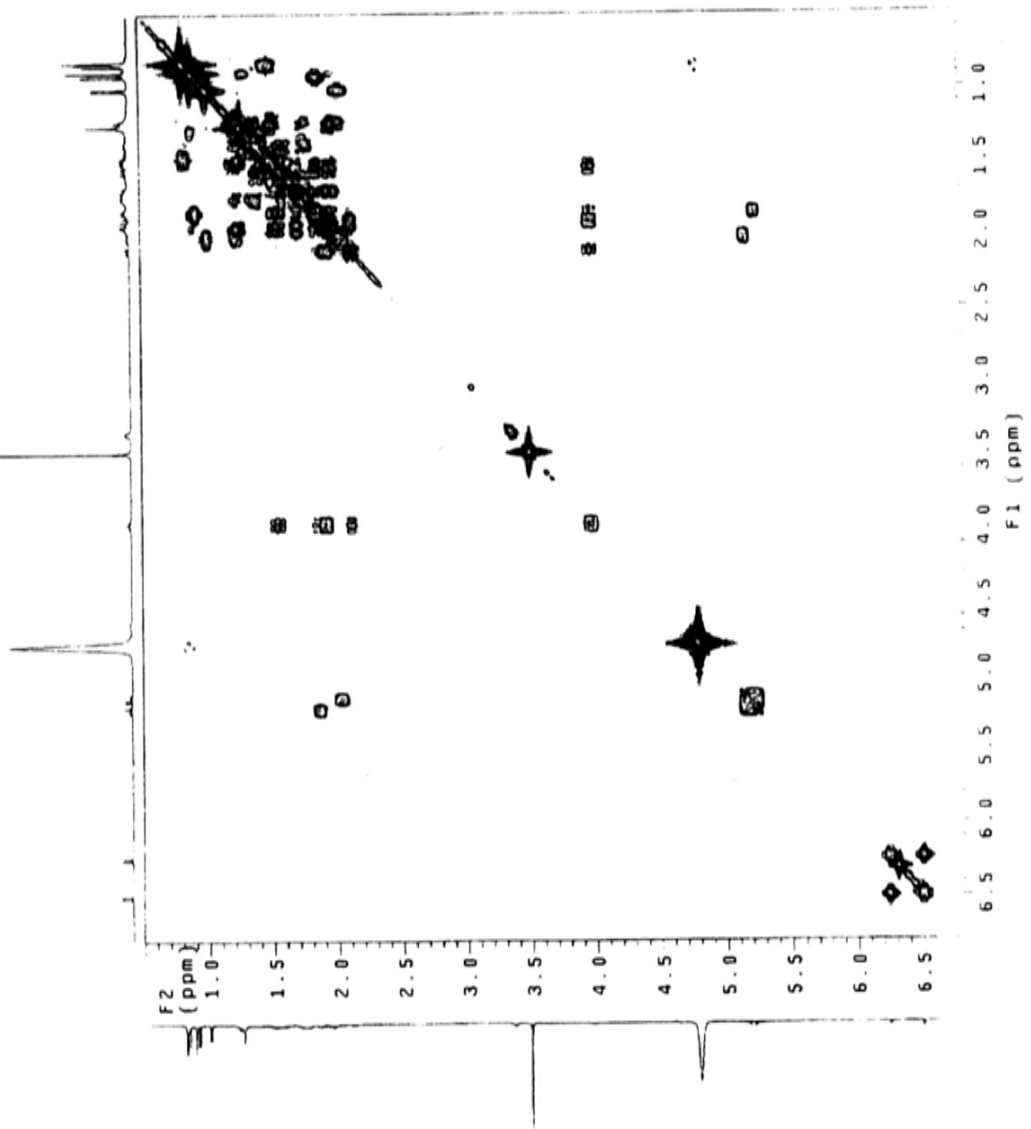
Relax. delay 1.000 sec
Acq. time 0.200 sec
Width 3151.2 Hz
2D Width 16319.9 Hz
16 repetitions
300 increments
DECUPLE C13: 125.672729 MHz
Power 47.08, 125.672729 MHz
on during acquisition
off during delay
GARP-1 modulated
DATA PROCESSING
Gauss optimization 0.120 sec
F2 DATA PROCESSING 0.011 sec
F1 size 2048
F2 size 2048
Total time 1 hr, 38 min, 39 sec



Appendix 9. Two dimensions NMR analysis of EP: H-H relation in CDCl_3 , 500MHz

```

00459c0sy-green
Archive directory: /export/home/pub/vnmrSYS/data
Sample directory:
File: PROTON
Pulse Sequence: gcosy
Solvent:  $\text{CDCl}_3$ 
Temp: 26.0 C / 299.1 K
INOVA-500 "SYSUS500"
Relax. delay 1.000 sec
Acq. time 0.232 sec
Width 3151.2 Hz
2D Width 3151.2 Hz
4 repetitions
Observer:
Date:
Data processing: 189.7730836 MHz
Sine bell 0.041 sec
F1 Data processing
Sine bell 0.041 sec
F1 size 2048 x 2048
Total time 21 min., 59 sec
  
```



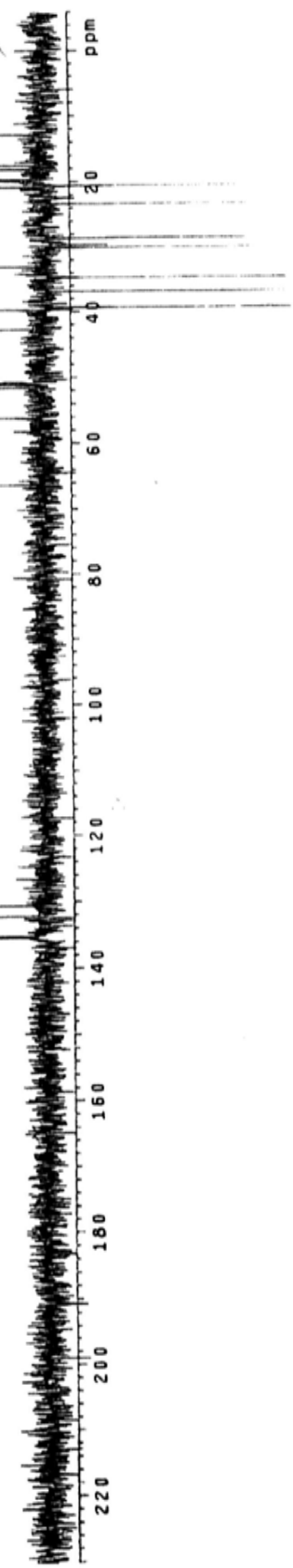
Appendix 10. DEPT analysis of EP in CDC13, 500MHz

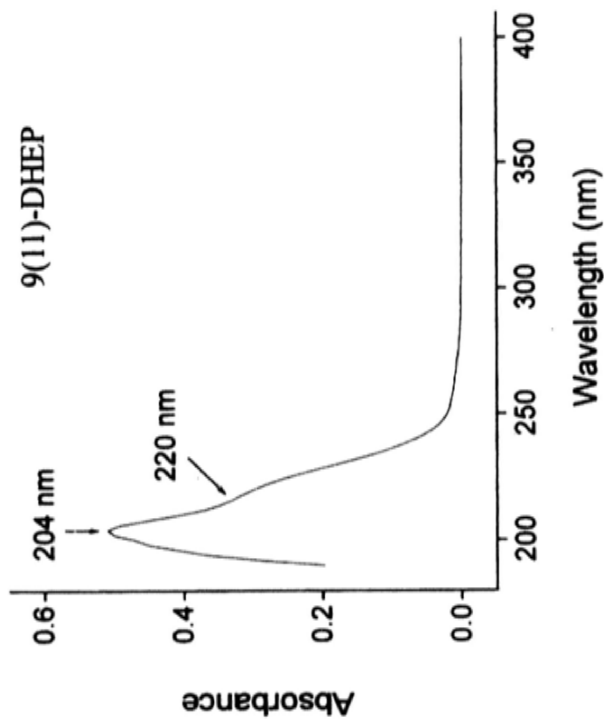
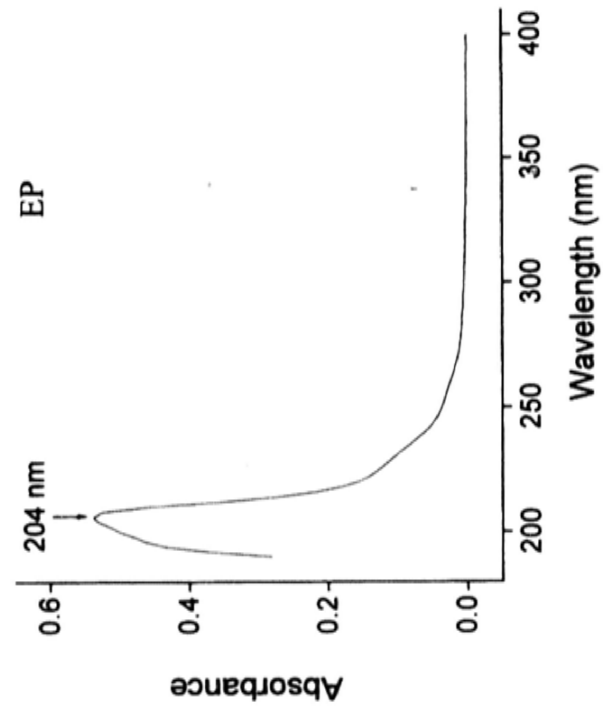
66 356
56 137
51 614
51 029
50 741
42 712
39 653
39 278
38 838
34 632
33 002
30 000
29 633
28 565
23 335
20 810
20 557
19 879
18 105
18 105
17 491
20 802

135 354
135 131
132 242
130 669

```

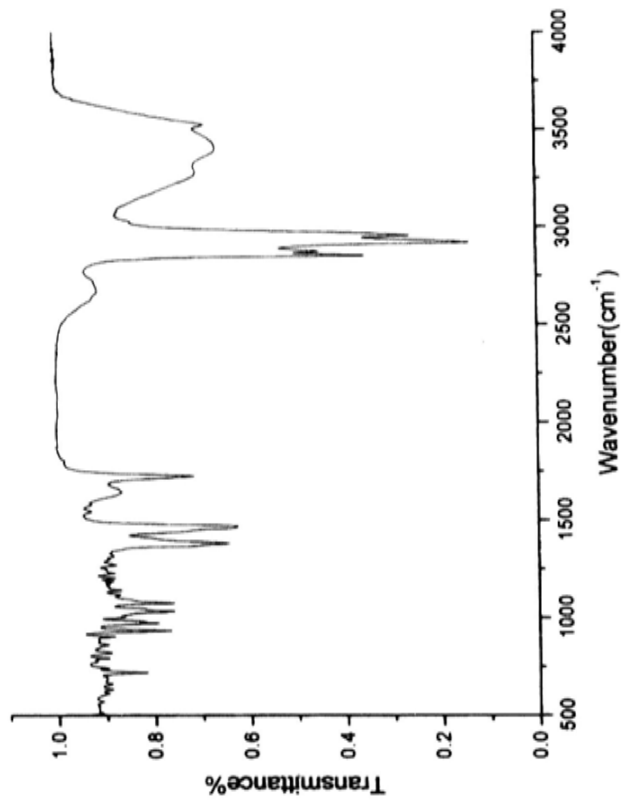
0045dept135-green
exp1 DEPT
date SAMPLE DEPT 140.0
solvent Mer 23.006 11th
mult CDC13 mult SPECIAL 1 1 5
ACQUISITION temp 26.0
sw 29780.6 gain 54
at 0.400 spin not used
np 23766 PROCESSING
ds 1 1b 3500
ss 1.000 fn 85536
sl 200 wp 28705.7
cl 131 sp -768.2
CI TRANSMITTER C13 1d ph -30.4
tof 2182.0 ei ph 37.6
tpwr 8.55 REFERENCE 768.1
pw DECOUPLER M1 PLOT
ds -45.6 WC 250
dof 43 SC 0
dpar nny VE 4517
dm CCW hzmm 118.82
dss 10582 th
def pp1v1
pp 27.800
    
```



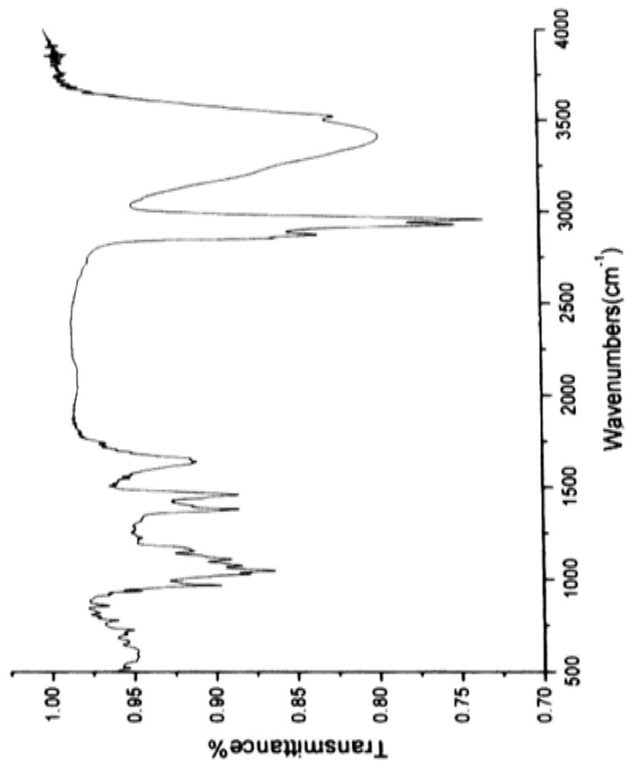


Appendix 11. UV analysis of 9(11)-DHEP and EP in CDCl_3 , 500MHz

9(11)-DHEP



EP



Appendix 12. IR spectrum analysis of 9(11)-DHEP and EP in CDCl₃, 500MHz